Efficient Methods for Robust Shape Optimisation for Crashworthiness

Submitted in partial fulfillment of the requirements of the Degree of

Doctor of Philosophy

Milan Rayamajhi
School of Engineering and Materials Science
Queen Mary University of London

October 2014

Abstract

Recently complex geometry and detailed Finite Element (FE) models have been used to capture the true behaviour of the structures for crashworthiness. Such model complexity, detailed FE model, high non-linearity of crash cases and high number of design variables for crashworthiness optimisation add to the required computational effort. Hence, engineering optimisation problems are currently highly restricted in exploring the entire design space and including the desired number of design parameters. Hence it is advantageous to reduce the computational effort to fully explore the design alternatives and also to study even more complex and computationally expensive problems.

This thesis presents an efficient robust shape optimisation approach via the use of physical surrogate models, i.e. sub-models and models derived for the Equivalent Static Loads Method (ESLM). The classical simultaneous robust design optimisation (RDO) approach (where robustness analysis of each design is assessed) is modified to make use of the physical surrogate models. In the proposed RDO approach, design optimisations are made using sub-models and robustness analyses are made using either non-linear dynamic analysis or ESLM.

The general idea is to approximate the robustness of designs at the start of the optimisation (using ESLM) and use accurate robustness evaluations (via non-linear dynamic analysis) towards the end of the optimisation where the optimisation has already found interesting regions of the design space. The approach is validated on crashworthiness design cases.

Acknowledgements

A PhD thesis does not reflect an individual's sole achievement. Behind the success lies the contributions from other individuals that have supported the completion of the thesis. Whether this support be technical, financial or emotional it has a direct or indirect influence on the course of the PhD completion. I would like to thank everyone involved in this thesis at any stage but some contributors need special mention.

First and foremost I would like to thank Professor Fabian Duddeck for offering me the PhD position. His support, confidence and patience towards me was key to the completion of this thesis. My second supervisor Dr Jens Müller for administrative support. In the research group, I would like to thank Stephan for guiding me with his experience in the research field. This would not have been possible without your support considering the overseas supervision situation. The sponsors, PSA Peugeot and Citroën and EPSRC for the research fund. At Peugeot and Citroën, I would like to thank Malek and Federic for their technical support. I would also like to acknowledge the software support from Dynardo (optiSLang) and SFE GmbH (SFE CONCEPT).

Researchers who shared the PhD office at any point during the PhD: Neveen, Henry, Percy, Faidon, Andrei, Shenren, Jerome, Hassan, Wei and Yang. Also Ahmed for joining us sometimes. It was great to exchange ideas, jokes, food and some form of support between us.

In the family, my parents Juddha and Indira. My dad, the first person to put the idea of pursuing a PhD in my head. My wife Prapti for her patience and encouragement. Sisters Sabita and Sunita and brother-in-laws Suraj and Mahesh for their support and encouragement. My in-laws for their patience and support.

Last but not the least, I would like to thank the Saturday football group for helping me to release the week long stress.

*** * * To my Family * * ***

Table of Contents

List of Figures

List of Tables

List of Abbreviations

ALHS Advanced Latin Hypercube Sampling

ARSM Adaptive Response Surface Method

BIW Body-in-white

BL Base Line

BS Base section

CAE Computer Aided Engineering

CPUs Central Processing Units

DFSS Design for Six-Sigma

DOE Design of Experiments

EA Evolutionary Algorithm

ES Evolutionary Strategy

ESL Equivalent Static Load

ESLM Equivalent Static Loads Method

FE Finite Element

FEA Finite Element Analysis

FMVSS Federal Motor Vehicle Safety Standards

GA Genetic Algorithm

ICs Interface Conditions

IP Influence Point

IRSM Iterative Response Surface Method

LHS Latin Hypercube Sampling

MCS Monte Carlo Sampling

MDB Moving Deformable Barrier

NHTSA National Highway Traffic Safety Administration

NVH Noise, Vibration and Harshness

OEM Original Equipment Manufacturer

PCA Principal Component Analysis

PDF Probability Density Function

PDP Product Development Process

RBDO Reliability Based Design Optimisation

RBF Radial Basis Function

RDO Robust Design Optimisation

RSM Response Surface Method

SRSM Successive Response Surface Method

TI Target Interval

TWB Tailored-welded Blank

UNECE United Nations Economic Commission for Europe

PART I
Background

Chapter 1

Introduction

1.1 Problem Area

Due to issues such as fuel economy and vehicle emissions, the automotive industry is currently searching for new concepts and methods for lightweight structures. Besides the standard requirements for new car bodies - such as high energy absorption for passive safety, low injury risks to occupants and vulnerable road users (pedestrians and cyclists), low repair costs or appropriate stiffness with respect to torsion or bending modes for comfort - the reduction of mass becomes increasingly important. The best compromise between all these conflicting goals can only be derived via advanced Computer Aided Engineering (CAE) methods based on Finite Element (FE) simulations and numerical optimisation. The conflicting goals are treated via a multi-criteria optimisation.
Current FE models represent the complexity of the geometry and the non-linearities of material behaviour, contact and large deformations. This results in high numerical effort, which is increased in numerical optimisations due to the necessity to consider a high number of design variables and design variants to cover the design space sufficiently well. Hence it is very attractive to look for approaches to reduce this computational effort.
There have been several studies to reduce the computational effort for structural optimisation, e.g. Averill (2004); Park (2011); Redhe and Nilsson (2006); Sousa et al. (2008); Takada and Abramowicz (2006). However, the proposed methods are rarely applied in industrial cases and there is hence a need for further investigations in efficient approaches for crash optimisation.

1.2 Motivation

Especially for crashworthiness studies, the consideration of uncertainties in material, geometry and load cases is very important. In addition, the product development process itself has its inherent lack of knowledge. At the beginning of the design

process the engineers have to decide without having the full picture available at the end. Hence an optimal design without the knowledge of its performance in uncertain conditions is of little value in engineering. Therefore, designs that are insensitive to these variations are of huge interest and robustness studies should be performed. However the inclusion of robustness studies into the design process and in particular the realisation of robust design optimisation (RDO) for crashworthiness is challenging due to the additional numerical effort. Hence, in this thesis a special approach based on physical surrogate models is presented to reduce the computational effort to enable RDO for crashworthiness even for larger industrial cases.

1.3 Research Aim and Objectives

This study aims to develop first a procedure for sub-model optimisation for cases where the optimisation, i.e. the changes of design variables, is restricted to the sub-model area. For such cases, the coupling of the remaining model and the sub-model has to be taken into consideration during the optimisation. The implementation and the update of this coupling behaviour is of interest and will be investigated here.
To extend the sub-model approach to RDO, additional methods for reduction of the numerical effort are needed. Hence the classical simultaneous RDO (where robustness analysis of each design is assessed) approach is modified to make use of the physical surrogate approaches. Here physical surrogate models are low fidelity FE models that approximate the behaviour of the computationally expensive high fidelity FE models. Physical surrogate models considered in this thesis include (i) **sub-models** and (ii) linear static models used in the **Equivalent Static Loads Method** (**ESLM**). The main application will be on shape and size optimisations although it could also include aspects of topology optimisation.

1.4 Thesis Overview

This thesis is structured into four different parts which include chapters within them. A short summary of each chapter is provided below.

Part I - Background This part contains the **current chapter** (Introduction) and **Chapter 2**, which starts with some accident statistics followed by the most relevant legislation and consumer tests. A general insight into the vehicle structures for crashworthiness and their requirements is presented. The chapter concludes with a discussion of crash simulation characteristics.

Part II - Literature Review In this part **Chapter 3** provides a rough overview of the principles of structural optimisation. Some optimisation algorithms and optimisation types, relevant to this thesis, are discussed. **Chapter 4** presents approaches, tools and challenges for shape optimisation in crashworthiness design. The importance of design robustness in crashworthiness design is discussed in **Chapter**

5. The RDO approaches in the context of this thesis are presented and their challenges discussed.

Part III - Methods and Validations This part includes the author's contribution, presenting the tools and methods investigated in this thesis. Four different approaches are considered in the thesis hence these approaches are separated into four different chapters. In each chapter, where relevant, first a literature review is presented followed by the author's proposed approach and its implementation.
Chapter 6 presents a shape parameterisation approach to avoid geometrical conflicts during shape modifications. This approach is used for two industrial optimisation cases.
A sub-model optimisation approach is presented in **Chapter 7** to reduce the computational effort during optimisation. This approach is validated on a simple design case and an industrial design case.
A RDO approach is presented in **Chapter 8** where the number of design evaluations required for the RDO is reduced. This approach is tested by various analytical and physical test cases.
Finally in **Chapter 9** an ESLM is presented to replace the expensive non-linear dynamic robustness analysis with linear static robustness analysis of designs. This approach is used to further enhance the RDO approach presented in **Chapter 8**.

Part IV - Overall Approach This part includes **Chapter 10** which combines all the approaches presented in **Part III** to one efficient RDO loop. The applicability of the overall approach is also tested with two validation cases. **Chapter 11** summarises the work presented in this thesis with some proposals for further improvement of the overall RDO approach.

1.5 Author's Main Contributions

This section summarises the author's main contributions (**PART III**) in the thesis. Here first a shape parameterisation approach, based on a mapping technique, is presented to avoid shape parameter conflicts during shape optimisation. This is followed by a sub-model optimisation approach, based on an IRSM, to reduce the computational effort of large industrial models. Finally a RDO approach is presented where the computational effort is reduced via the use of physical surrogate models ; sub-modelling and ESLM. First the sub-modelling and ESLM are validated separately. Then an efficient RDO approach is proposed where sub-models are used for design optimisation whereas robustness analyses of designs are made either via non-linear dynamic analysis or ESLM. The robustness analysis method (via non-linear dynamic or ESLM) depends on the location of the optimisation design from the feasible design space boundary. The approaches are validated by various crash cases.

Chapter 2

Vehicle Crashworthiness Design

2.1 Introduction

The automotive industry is under immense pressure from the government bodies to reduce the CO_2 emissions from vehicles. This can be achieved through reduced fuel consumption which is also an issue due to its rising prices. However to reduce fuel consumption by more efficient engines is not sufficient. Hence one of the options that vehicle manufacturers are currently looking into is to reduce the total mass of the vehicle.
Also, due to the high number of injuries and fatalities of occupants and pedestrians in vehicle crashes, government legislations and consumer test organisations have forced the automotive industry to design for safety. Because of these requirements and the rising competition worldwide, Original Equipment Manufacturers (OEMs) are forced to look for ways to design lightweight vehicles without compromising the safety of occupants and pedestrians. The automotive industry is currently fulfilling these requirements through the use of alternative materials, improved manufacturing processes and better design concepts for vehicle components assisted by various CAE tools.
This chapter outlines the importance of vehicle safety for crash through the assessment of injuries and fatalities sustained by the occupants and pedestrians. The effort from the automotive industry to design safer vehicles to reduce and limit these injuries and fatalities is also discussed.

2.2 Vehicle Crashworthiness

Vehicle crashworthiness is a field that assesses the ability of the vehicle structures to protect the occupant in survivable crashes. The capability of vehicle crash structures to absorb the impact energy and to reduce the deceleration of the occupants determine the safety of the occupants. The impact energy absorption by the vehicle structures involves a controlled structural deformation while maintaining a

survivable space for the occupants. This is derived by various aspects of the vehicle structures such as structural design features (structural shape), material and manufacturing processes etc.
Going back to the history, the origin of the term "crashworthiness" came from the aerospace industry in the early 1950s Tho (2006). Following the first vehicle fatality, the need of vehicle safety for passengers and the occupants was realised to be important. This led to several crashworthiness standards such as in the USA ; Federal Motor Vehicle Safety Standards (FMVSS, www.nhtsa.gov) by National Highway Traffic Safety Administration (NHTSA, www.nhtsa.gov) and in Europe ; United Nations Economic Commission for Europe (UNECE, www.unece.org). Since the introduction of these regulatory tests, crashworthiness has been the driving criteria in vehicle design. Hence the automotive industry has seen the evolution of innovative safety features in vehicles through both active and passive safety, as discussed in Section 2.2.3.

2.2.1 Accident Statistics

Vehicle accidents claim thousands of lives every year worldwide. With the increase in the use of automobiles, road traffic accidents have been a major issue. Due to the lack of knowledge of vehicle crash safety before 1960-70s the number of fatalities increased dramatically until then. After the 1970s the fatality figures declined due to the introduction of vehicle safety features (mainly the seat belt) and crash safety regulations.
Figure 2.1 shows the number of cars per 100 people worldwide in the year 2002. It can be seen that the Western European countries dominate the top ten list with about 47 cars per 100 people followed by Japan and North America. The relation between the developed countries and the reduced number of road accidents is obvious from the data. The strict enforcement of vehicle safety regulations, better roads and engineering in the developed countries have an influence on the lower number of casualties in comparison to the underdeveloped countries. In Western Europe the road casualties in 2002 were 10 per 100,000 people in comparison to developing countries where the number of casualties were 20 per 100,000 people Dorling et al. (2010).
Although the traffic accident trend shows an improvement in comparison to the previous years, in 2009 there were a total of 222,146 reported accident casualties worldwide of which 2,222 people were killed in Great Britain Department for Transport (2010). These figures reveal the importance of improving the traffic safety even further to reduce the number of casualties in the coming years.

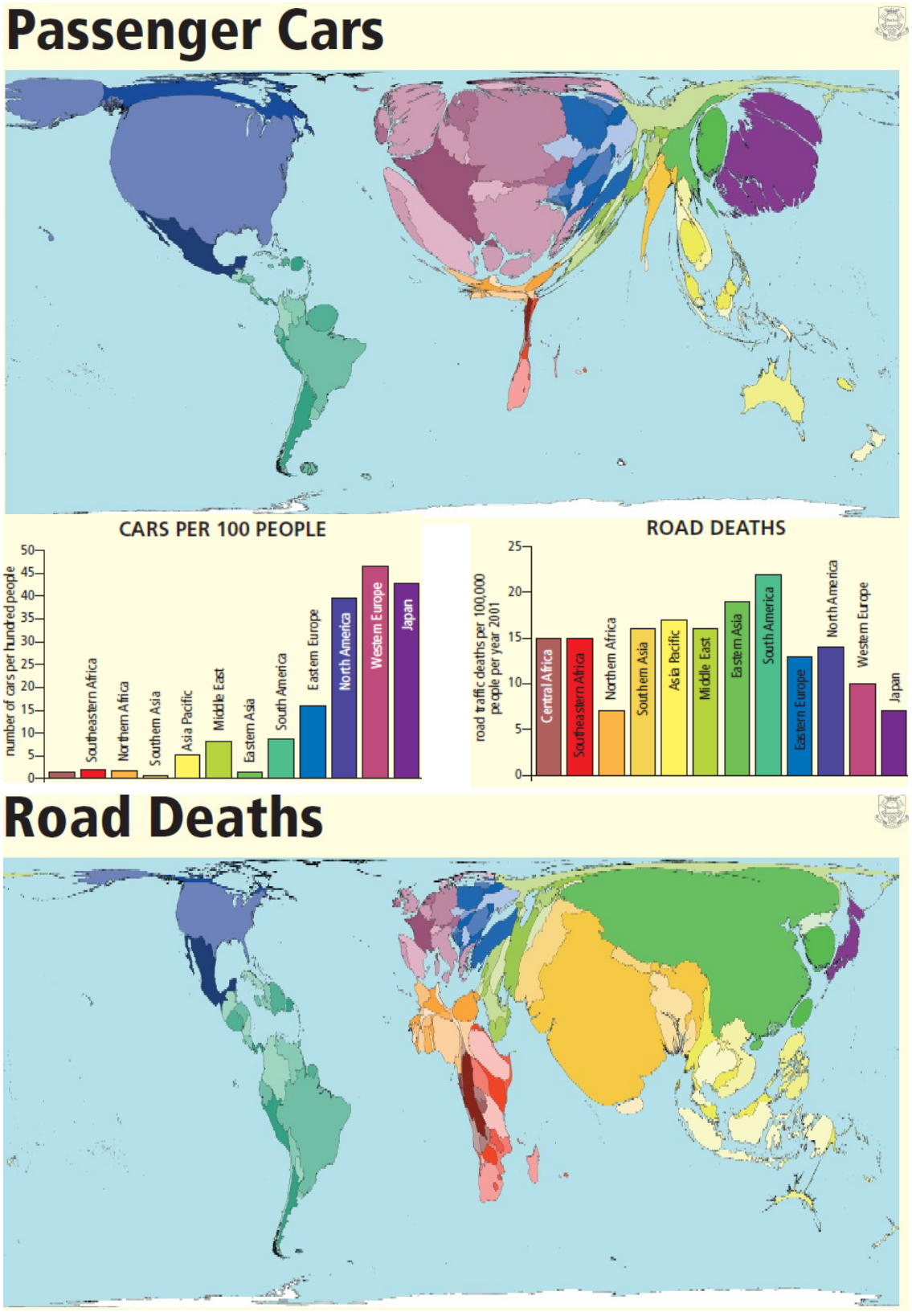

FIGURE 2.1 – World statistics on passenger car use and casualties, Dorling et al. (2010).

2.2.2 Regulatory and Consumer Tests

To further reduce casualties worldwide, vehicle manufacturers are forced to consider occupant and pedestrian safety in their design by various government regulations. Moreover, the safety standards that vehicle manufacturers are required to fulfil are getting more stringent in the recent years. Hence vehicle designs are hugely determined by different occupant and pedestrian safety standards imposed by the regulatory testing bodies, see Figure 2.2. The most frequently addressed vehicle crash tests are briefly discussed here.

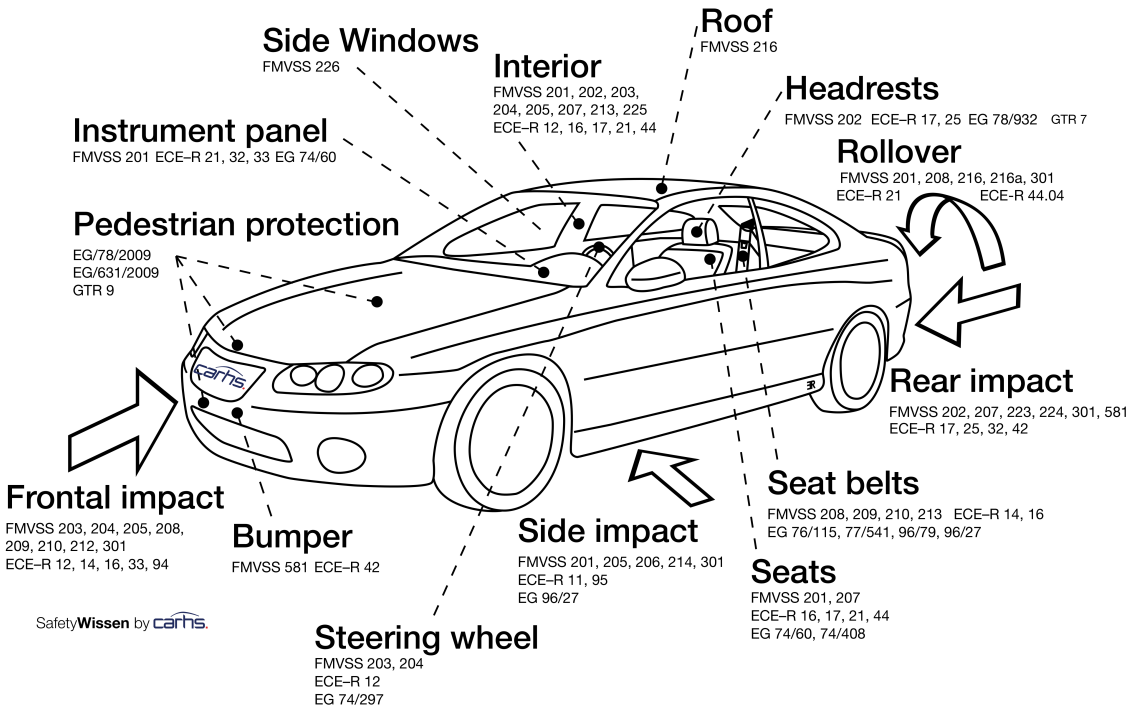

FIGURE 2.2 – Major crash safety regulations in Europe and USA, CARHS GmbH (2012).

Frontal Impact

Two main frontal impact tests are generally considered ; 40% offset impact to a deformable barrier and full width impact to a rigid wall. In the first test the vehicle impacts the deformable barrier with a velocity of 64 kph. The aim here is to assess the intrusion of the front structures. In the second test a velocity of 56 kph is used for the impact test. This test case assesses the performance of the restraint systems in the vehicle. In addition to the structural criterion, the injuries to the occupants are also assessed via dummy injury criteria, see European Commission (1996) for more details.

Lateral Impact

Although the occurrence of lateral crash is less frequent, statistics show that almost 35% of these crashes are fatal Nohr and Blume (2009). The unavailability of crumpling zones and limited space between the structure and occupants make lateral crashes more severe. In EuroNCAP two lateral impact tests are considered. In the first test the vehicle is propelled with a velocity of 29 kph towards a fixed pole with 254 mm diameter. In the second test a Moving Deformable Barrier (MDB) impacts a stationary vehicle with a velocity of 50 kph, see EuroNCAP (www.euroncap.com) for further information.

Pedestrian Protection

This test considers the impact between pedestrian and vehicle and is associated with the safety of the pedestrians. Generally front impact is considered where impact velocity of 40 kph is used. A series of test are carried out, which include the lower leg form, upper leg form and head form. The impact areas ; bumper and bonnet for lower and upper leg injuries and bonnet for head injury, are assessed to rate the performance of the vehicle.

2.2.3 Active and Passive Safety

Occupant and pedestrian safety can be divided into active and passive safety. Passive safety is a term which encompasses all the features that mitigate the consequences of accidents whereas active safety relates to the avoidance of the crashes. The most important developments in these two fields of vehicle safety will be presented in the following paragraphs. A more extensive survey on vehicle safety device is given in Rekveldt and Labibes (2003).

Passive Safety

The most essential feature for passive safety is still the seat belt ; the modern version, the three-point belt, was introduced by Nils I. Bohlin and realised in Volvo cars from 1957 onwards. This invention was regarded by the German patent office as one of the eight most important patents for humanity Linzmeier (2006).
The use of seat-belts on their own for occupant safety was later realised as insufficient. In 1981 Mercedes S-Class was integrated with an airbag system. The use of airbag and the seat-belt together improved occupant safety significantly Linzmeier (2006).
In-terms of pedestrian safety by passive protection, the structural characteristics itself have been changed. An important field of ongoing research looks into the interaction of the pedestrian and the vehicle bumper and hood structures Dietrich (2013).

Active Safety

The driver has a big influence on vehicle collisions. Factors such as the driver condition, age and experience plays an important role. It is estimated that the driver behaviour (human error) contributes to more than 85% of all the traffic accidents Statistisches Bundesamt Deutschland (2011) . Hence the present developments of some active safety systems assist the driver for a better control of the vehicle. Some of these systems include Anti-lock Breaking System (ABS), Electronic Stability Programme (ESP) and pedestrian detection systems Linzmeier (2006). Because this thesis is focused on structural optimisation for passive safety, active safety is not discussed further.

2.2.4 Vehicle Crashworthiness Structures

Automotive body structures are manufactured to withstand both static and dynamic loads throughout its life cycle while providing good shape for low aerodynamic drag and comfortable space for occupants. In addition, automotive structures are required to fulfil additional safety criteria for both the occupants and the pedestrians. Hence vehicle structures have to be designed to provide sufficient protection in survivable crashes and also minimise injuries to pedestrians. An example of typical crashworthiness structures in a vehicle is shown in Figure 2.3. Vehicle body structures are mainly divided into two categories: body-over-frame structure or unit-body structure.

FIGURE 2.3 – Typical vehicle crashworthiness structures in red, Fradin (2004).

The body-over-frame Structure

The body-over-frame structure includes vehicle frame, body and front end. The vehicle body provides an occupant cell to keep the injury levels to a minimum in the event of crash and additionally contributes to the vehicle stiffness in torsion and bending. The chassis supports the engine, suspension, transmission, powertrain and other units Braess and Seiffert (2005).

Unit-body or Body-in-white (BIW)

BIW is the main framework of the vehicle structure that provides some required performance (bending, torsion, ...) and also the necessary housing of structures such as enclosures, rear/front axle etc. It is constructed by assembling stamped metal sheets using the required type of fasteners e.g. laser weld spot. This type of vehicle structure is known to reduce the vehicle mass Braess and Seiffert (2005). A BIW structure is shown in Figure 2.4.

FIGURE 2.4 – A body-in-white structure, Breidenbach et al. (2009).

2.3 Lightweight Design

As mentioned in Section 2.1, the interest in lightweight automotive design is of ever growing interest for vehicle manufacturers. Some main strategies to achieve the lightweight vehicle architecture are presented here.
A SuperLightCar project, for example, has been set up to develop and deliver design concepts and technologies that would reduce the mass of a car by upto 30% while respecting constraints on the cost SuperLIGHT-CAR (2011). Here the materials and manufacturing processes are studied which could be used for the design of a lightweight vehicle while respecting the performance requirements. The aim of this European project is to reduce the mass of the vehicle which as a result reduces fuel

consumption and hence the reduction in CO_2 emission, SuperLIGHT-CAR (2011). WorldAutoSteel, World Auto Steel (2011b), is also working on a comparable project, called the FutureSteelVehicle, to develop a steel intensive design for electric vehicles, World Auto Steel (2011a). Also see Breidenbach et al. (2009) for similar research.
These projects develop new improved structures through the use of various materials and manufacturing technologies. From the use of traditional mild steel (tensile strength 250 to 400 MPa) to the currently used pinnacle boron steel (tensile strength 1500 MPa), the automotive industry has seen the evolution of different grades of steel SAE International (2008). The ability to use these materials have highly been assisted by the manufacturing processes. Innovative ideas such as tailored rolled blanks, tailored tempering have also been implemented in the automotive industry, see Breidenbach et al. (2009); Chuang et al. (2008); Xu et al. (2013).
In the projects above, development of new design concepts in-terms of shape, size and topology of structures were not sufficiently considered. Although some optimisations were realised, a concise study including robustness of the concepts is missing. Methods to realise this are presented in this thesis and discussed in detail in Chapters 3 - 5.

2.3.1 Crash Characteristics and Simulation

Crash cases exhibit large deformations which changes the contact characteristics during crash events. To fully represent this behaviour ; small element sizes (currently 5 mm), several detailed material models, different element types and sophisticated contact algorithms are used in FE models. This increases the size and complexity of FE models and hence the computational time. However it is necessary to use these finer models to accurately capture the physical crash behaviour.
Furthermore due to the highly non-linear behaviour of crash, bifurcation characteristics are also encountered. Bifurcations are two totally different deformation characteristics shown by the similar design in the same impact conditions, see Duddeck (2008). It is important to identify and avoid these designs with bifurcation characteristics for robust behaviour.
To deal with the size and complexity of the FE models, parallel computing approaches have been used. Here a decomposition of the full model into several domains is realised. Then these domains are computed in parallel using different CPUs. The communication between the CPUs is critical to ensure continuity between the different domains. Hence the computational advantage may be reduced when a high number CPUs is used due to the communication requirement.
Since the use of parallel computing crash simulations are known to be non-repeatable Duddeck (2007). Results may vary due to different numerical rounding and the ordering of summation of results from one run to another in parallel computing. To encounter this situation consistency options are introduced in FE codes that pro-

vide similar results independent of the number of CPUs used, Paik et al. (2004). However this slows the computation by about 30% and the bifurcation designs are also unidentified. Readers are referred to Duddeck (2007); Paik et al. (2004); Thole and Mei (2003) for further information.

PART II
Literature Review

Chapter 3

Structural Optimisation for Crashworthiness

3.1 Introduction

Structural optimisation searches for the best set of design parameters to define a structure with improved performance. Whether it is the design of a new system or improvement of the existing systems, design optimisation studies are performed regularly by OEMs. The reason being that by optimisation the best compromise between the different functionalities and the associated cost can be identified. This is usually achieved through reduction of materials used, manufacturing time, product assembly time and so on. Hence design optimisation at present has become one of the compulsory tools in many industrial sectors such as mechanical, aerospace, civil and automotive engineering.

In the recent years the optimisation tasks have been assisted by the accelerated advances in computers and various CAE software packages. Engineers are now able to solve complex and bigger problems to seek for improved designs. Intensive use of structural optimisation have been utilised in automotive engineering for crash. Structural optimisation for crashworthiness is often challenged due to factors such as lightweight, low cost, structural performance and aesthetics requirements from the consumers and regulations. These requirements are addressed by the design optimisation by searching for structures with good crash performance characteristics but without the loss of other secondary criteria.

This chapter starts with a brief introduction to engineering optimisation in order to familiarise the notations and terminology used in structural optimisation. A brief overview of structural optimisation types and various algorithms to solve these structural optimisation problems is presented, for detailed discussion see Antoniou and Lu (2007); Jurecka (2007). In this chapter more emphasis is put on topics relevant to this thesis.

3.2 Fundamentals of Engineering Optimisation

3.2.1 Optimum Design and Optimum Conditions

In literature usually the term "optimum design" is used for the result of an optimisation study. However there is no certainty that the achieved result is an (global) optimum design due to various characteristics of an optimisation problem (multi-modal, non-linear, non-convex etc.). Depending on the type of problem, a function may have several local minima, see Figure 3.1.
Due to the high complexity, in industrial examples, the focus is here less on the identification of the global optimum than on design improvement. Hence in this thesis "optimum" refers to an improved design. In addition, because optimisation drives designs more to the limits of the design space, the robustness of the design becomes much more important, as discussed in Chapter 5.

In an optimisation case for minimisation, design x^* is said to be optimum if it

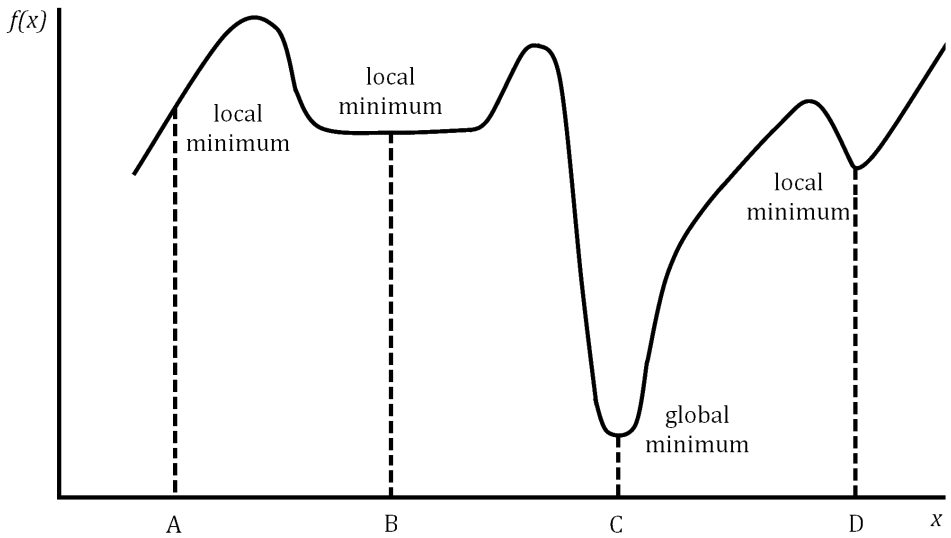

FIGURE 3.1 – A function with different types of minima, Antoniou and Lu (2007).

satisfies all the constraints and gives a minimum value for the objective function $f(x^*)$ in comparison to the objective value $f(x)$ of designs x in its neighbourhood, N.

$$\forall x \in N; f(x) \geq f(x^*). \tag{3.1}$$

Design Variables

In engineering optimisation, design variables are a set of parameters that an engineer can alter to optimise the performance of a structure within some given restrictions. Typically the design variables are expressed as a vector with notation $\mathbf{x} = [x_1, x_2, ...x_n]^T$. The optimal design for a given set of design variables or the design vector $\mathbf{x}$ is given by x^*, see Equation (3.1).

Design variables are categorised into categorical (binary, discrete etc.) and continuous. Binary design variables, or zero/one variables, are used in optimisation problems where yes or no decisions have to be made. In engineering optimisation this could be the existence or non-existence of a part. Discrete design variables take only the integer values e.g. number of weld points. In comparison, the continuous design variables can take any real value within the restriction defined by lower and upper limits, also called side constraints e.g. beam length. Usually material thickness variable is also taken as continuous variables although in real life it is a discrete variable due to manufacturing possibilities.

Objective Function

An optimisation problem is formulated by considering the n parameters $x_1, x_2, ..., x_n$ of a design. The objective function, as a performance criterion, is derived in dependency to the design variables and eventually further parameters. In simple cases it is given by mathematical functions, on more realistic problems it is often based on the results of a numerical simulation. The performance of each design has to be evaluated in the optimisation process to compare and rank the designs to find the optimum. For this purpose an objective function f has to be defined. It is a scalar quantity and can take different forms such as mass of a product or manufacturing cost. The optimisation problems are normally subjected to equality and inequality constraint functions that restrict the design space for the objective function to search for the optimum design.
The most basic optimisation problem is to arrange the design variables in such a manner that the objective function $f(\mathbf{x})$ is minimised or maximised, as required. In theory for optimisation, minimisation is normally analysed without loosing generality because maximisation can be constructed by simply transforming the objective by

$$f_{min}(\mathbf{x}) = -f_{max}(\mathbf{x}). \tag{3.2}$$

Optimisation with several objective functions $f(\mathbf{x}) = [f_1(\mathbf{x}), f_2(\mathbf{x}), ..., f_p(\mathbf{x})]^{\mathrm{T}}$ are referred to as multi-objective optimisation problems. In such problems the conflicts between objective functions can make it difficult to find the general optimal solution, see Section 5.5.1. Multi-objective optimisation problems are addressed in Branke et al. (2008); Rudenko et al. (2002); Syberfeldt (2009); Yin et al. (2011).

Constraints

Since this thesis is focused on shape optimisation, constraints are only discussed in this context. Optimisation constraints can usually be categorised into side constraints and performance constraints.

Side Constraints The side constraints are normally the upper, x^U, and lower bounds, x^L, of the design variables. The decision on the design variable bounds has to consider both the geometrical compatibility and also the design variable conflict. The side constraints define the design space, D, of the optimisation problem, see Section 3.2.2. A conservative form of side constraints would restrict the exploration of the full design space. Hence, it is ideal to have a design space as big as possible for full exploration and increased chance of finding the best solution. This is further discussed in Chapter 6.

Performance Constraints Performance constraints define the requirements that have to be fulfilled by a design solution to be feasible. These differentiate between feasible and infeasible solution regions of a design space. The performance constraints define the feasible design space within which the optimum design is to be found. Examples of performance constraints, related to the work at hand, include ; deformation, energy, force etc. Generally the j^{th} optimisation constraint can be formulated in an inequality form:

$$\text{Inequality constraint}: \; g_j(\mathbf{x}) \leq 0. \tag{3.3}$$

where j represents the number of inequality constraint.

Design Parameterisation

One of the important aspects of optimisation is the way the parameters are defined since the type of parameterisation used leads to different results from the optimisation. This is specially vital in the case of shape optimisation, as inappropriate parameter definition leads to physically infeasible designs with surface penetrations and overlap.

In the past, for shape optimisation, studies that considered parameter conflicts usually included parameter constraints within the optimisation constraints or the parameter ranges. For this, boundaries were defined in a way that the parameter conflicts were removed. However the drawback of such an approach is that the design space is reduced and hence is not fully explored, reducing the probability of finding a better optimum. Further discussion on this is given in Section 6.4. To deal with some of these aspects and achieve accurate parameterisation, offset mapping technique (implicit parameterisation) provided by SFE CONCEPT is implemented, see Section 6.4.2. A different approach for dealing with the geometrical conflicts is given in Hilmann (2009).

3.2.2 General Optimisation Formulation

A general mathematical formulation of an optimisation problem can be written as,

$$\text{find} : \mathbf{x};\ \ \mathbf{x}\ \epsilon\ D, \tag{3.4}$$

$$\text{to}\quad \text{minimise} : f(\mathbf{x}), \tag{3.5}$$

$$\text{subject}\quad \text{to} : g_i(\mathbf{x}) \leq 0\ \ (i = 1, 2, ..., l), \tag{3.6}$$

$$x_k^L \leq x_k \leq x_k^U\ \ (k = 1, 2, ..., n). \tag{3.7}$$

Where, D is the n dimensional design space and x_i is a design variable. The design space, D, is formed by the limits of design variables, Equation (3.7).

$$D = \left\{\mathbf{x}\ \epsilon\ D \mid x_k^L \leq x_k \leq x_k^U\right\}. \tag{3.8}$$

Feasible Region

Combination of the constraints, Equation (3.6), and variable upper and lower bounds, Equation (3.7), form the feasible region denoted by C.

$$C = \left\{\mathbf{x}\ \epsilon\ D \mid g_j(\mathbf{x}) \leq 0 \bigwedge x_k^L \leq x_k \leq x_k^U\right\}. \tag{3.9}$$

This is a region in the design space where all designs satisfy the inequality constraints. A design within this region is said to be a feasible solution of the optimisation problem. The optimum point found must be within this feasible region C. Any point lying outside C is an infeasible point and cannot be a solution to the optimisation problem, Jurecka (2007).

3.3 Fields of Structural Optimisation

Structural optimisation can be categorised into three different optimisation disciplines depending on the types of design variables considered, Figure 3.2 Forsberg (2002).

Sizing optimisation For sizing optimisation the design variables are the cross-section dimensions ; the topology and the structural geometry remain unchanged. Examples include plate thickness, beam section parameters and truss members cross-sectional area.

Shape optimisation The system performance is optimised by geometrical parameters of the structure and the topology of the system remains unchanged. Typical examples of design variables in shape optimisation usually consist of dimensions

of beams and beam cross-section shape describing the shape of a part, curvature, angles etc.

Topology optimisation The structural configuration of a system is defined through topology optimisation. Here the design space is normally filled with material and the algorithm operates by removing materials from the design space where it is not required. Topology optimisation is used in the early stages of structural design.

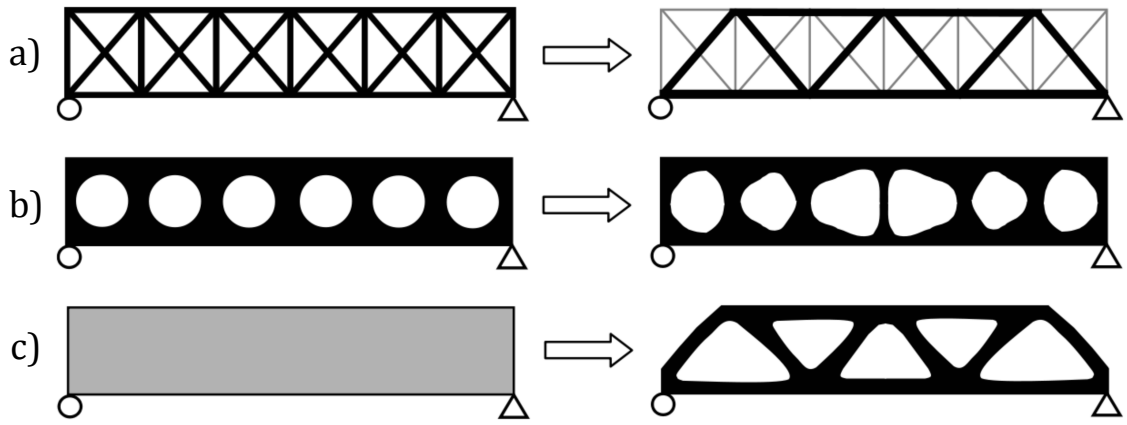

FIGURE 3.2 – Classification of structural optimisation: (a) sizing optimisation, (b) shape optimisation and (c) topology optimisation, Bendsoe and Sigmund (2003).

Other structural optimisation types include ; material optimisation, topography optimisation and topometry optimisation, see Hilmann (2009) and Leiva et al. (2007). Usually in engineering optimisation these different optimisation cases appear in combination with each rather than separately.

3.4 Crashworthiness Optimisation

In crashworthiness optimisation it is almost impossible to optimise all components of a vehicle due to the huge number of parts. Thus structures that are important for crash performance are often optimised separately such as B-pillar and door structures for lateral crash.
In the past most of the structural optimisation for crashworthiness were limited to metal sheet thickness (Delcroix et al. (2007); Redhe et al. (2004); Sun et al. (2011); Will et al. (2006)). More advanced thickness optimisation (Tailored-welded Blank (TWB), tailor rolled blank) studies are presented in Chuang et al. (2008); Xu et al. (2013). Only recently crashworthiness optimisation has been extended to shape and topology optimisation aided by CAE tools and methods such as morphing and SFE CONCEPT (Georgios and Dimitrios (2009); Volz et al. (2007); Zimmer et al. (2009)). Yet the number of realised shape optimisations for crash is still limited. This remains

therefore one of the open research fields for structural engineering. Shape optimisation is further discussed in Chapter 4. In Chapter 6, a parameterisation approach for shape optimisation is presented to avoid geometrical conflicts.

3.5 Optimisation Approaches for Crashworthiness

Contributions have been made from different research communities such as engineering, computer science and mathematics to deal with optimisation problems. Hence there are various algorithms in relation to their use in different applications. Due to this reason there is no standard or particular algorithm that fits all the optimisation tasks. It is therefore beneficial to match the optimisation algorithm according to the problem features. Some of the distinctive features of problems in crashworthiness are the problem size (number of design variables), multi-modality and non-convexity of the objectives, the existence of large number of constraints, high computational effort, stability and repeatability of the simulations etc. Jurecka (2007). Here optimisation approaches, frequently addressed in crashworthiness studies and in the context of this thesis, are briefly discussed.

Deterministic Optimisation Approaches Deterministic algorithms use a defined pattern to search for regions of interest. Here the randomness of the search approach is eliminated. Deterministic algorithms are normally not appropriate for crashworthiness optimisations except when used on response surfaces. This is due to the characteristics of crash optimisation problems listed above. A widely used group of algorithms is based on gradient calculations (gradient-based optimisation) to indicate search directions. Gradient-based optimisation use the derivative information of the objective and constraint functions to determine the direction of search to find the optimum.

Non-deterministic Optimisation Approaches Crashworthiness optimisation problems are highly non-linear, multi-modal and contain often a large number of variables. Non-deterministic approaches use random exploration of the design space to find regions of extrema. Although the probability of finding the global optimum is very small, these methods can successfully find improved designs with relatively few runs. The following sections present the basic ideas behind some of the most interesting algorithms used in crashworthiness optimisation.

3.5.1 Stochastic Methods

In stochastic methods, designs are randomly generated within the available design space. The performance of each design is evaluated in terms of the improvement

of the objective function or the degree of violation of the constraints. Here the representation on the overall design space with the generated sample points is very critical. A straight forward solution would be to generate many sample points to fill the design space. However crashworthiness simulations are very expensive and hence it is essential to reduce the number of simulation runs and yet represent the design space sufficiently well. Some interesting sampling techniques are presented below.

Stochastic Sampling Techniques

The ability to efficiently explore the design space through reduced number of support points and yet successfully represent the design space is very important. This is even more significant for crashworthiness problems, to reduce the number of simulation points, as the computational effort is very high. Frequently used stochastic sampling techniques include Monte Carlo Sampling (MCS) and Latin Hypercube Sampling (LHS).

MCS uses completely random approach to fill the design space based on the probability distribution function and without the influence of already available sample points. This results in duplicated designs. Here the sample points allocation is unsystematic and hence regions of the design space may be missed. This creates uneven distribution of the design space specially when fewer sample points are used, Figure 3.3(a). Hence the number of sample points required to represent the entire design space is very high.

LHS In LHS the design space is stratified into equal non-overlapping groups. For this each variable k range is subdivided into m intervals with equal probability, i.e. bigger width at the tails of a normally distributed variable. Then from each interval one value is generated at random based on the probability distribution within the interval. The m values of all the variables k are paired randomly. This gives $m \times k$ sampling matrix, where k columns represent the level of each variable and m rows represent design variable setting, see Figure 3.3(b). For crashworthiness studies the Latin Hypercube sampling is of interest since fewer sample points are required to efficiently represent the design space Mckay et al. (1979); Ryberg (2013).

For the LHS procedure described above it is required that the input variables are mutually independent. For mutually dependent variable the generated sample points are not well distributed due to input variable correlation. To consider the dependent variables, further modification to the LHS has been made to reduce the correlation between the sample points. This is done through the use of an internal optimisation procedure where the minimum distance between the generated sample points - sample points generated via LHS - are maximised, see Looss et al. (2010); Owen (1992). This modified LHS is generally termed as Advanced Latin Hypercube Sampling (ALHS) or Improved Latin Hypercube Sampling (ILHS), Hilmann (2009).

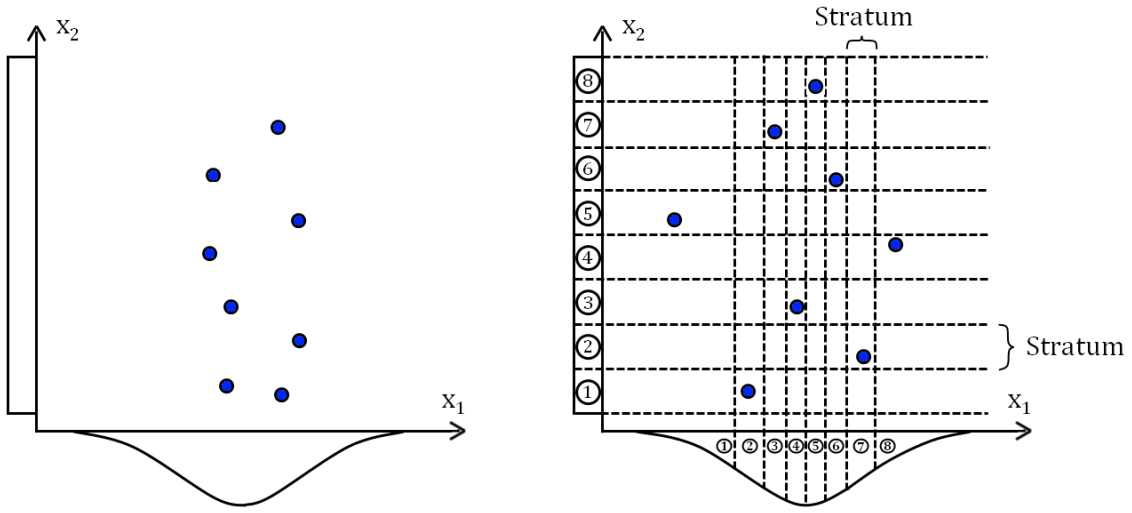

(a) Monte Carlo sampling. (b) Latin Hypercube sampling.

FIGURE 3.3 – Stochastic sampling approaches, Jurecka (2007).

The discussions on stochastic sampling presented here are in the context of the thesis. There are many variants of sampling methods, see for example Johnson et al. (1990) for maximin and minimax designs, Kalagnanam and Diwekar (1997) for Hammersley Sequence Sampling (HSS), see also overviews presented in Giunta et al. (2003); Wang and Shan (2007). Since the focus here is on robustness rather than reliability, discussions on sampling methods to estimate smaller probabilities are eliminated. Sampling approaches used in the reliability field include importance sampling, subset simulation and these are addressed in Au and Beck (2001); Zhang et al. (2010). For detailed review of reliability based optimisation techniques see Frangopol and Maute (2003).

3.5.2 Evolutionary Algorithms (EA)

Normally Evolutionary Algorithms (EA) start with an initial population that aims to explore the full design space to search for promising regions. Evaluation of the individuals, in the population, is made to rate and rank the individuals according to their fitness values. Selection operators are then used to choose individuals, for reproduction, that are fit and can improve the following generations[1]. The reproduction of individuals depend on the algorithm settings used and hence the reproduction operator. Recombination (Genetic Algorithm (GA)) and mutation (Evolutionary Strategy (ES)) are the two mechanics used for reproduction. Here two or more parent individuals are selected for reproduction. Crossover operator is used to rearrange the genes of the parents to produce the offsprings. Diversity within a population is achieved through the use of mutation operator. Mutation modifies each individual separately by simply introducing small variations to the

1. Reproduce individuals that perform even better than the parents.

genes of the individuals. In general, a combination of these operators is used. The new population is then evaluated again and hence the optimisation continues until a termination criterion is fulfilled. The particularities of EA are detailed in Bäck (1996) and Steer et al. (2009).
EA have the ability to explore various regions of the search space at the same time. They are able to handle a variety of problem features such as discrete and continuous variables, noisy and discontinuous objective functions and multi-modal problems. Hence EA are considered to be robust optimisation algorithms and are applied in crashworthiness Duddeck (2008); Rudenko et al. (2002). A state-of-the-art survey on evolutionary computation is presented in Kicinger et al. (2005). However EA are known to have a slow convergence and are expensive due to the high number of evaluations required before convergence. Some other population-based algorithms include Particle Swarm Optimisation (PSO), Eberhart and Kennedy (1995), Bee Colony Method Tereshko and Loengarov (2005) etc.

3.5.3 Response Surface Methods

Response Surface Methods (RSM) were introduced in the 1950s Gustafsson and Strömberg (2008). Since then response surface methods have been applied to a wide variety of problems such as crashworthiness Forsberg and Nilsson (2006), manufacturing Gustafsson and Strömberg (2008), Noise, Vibration and Harshness (NVH) Craig et al. (2002) etc. within the automotive industry.
RSM are used in crashworthiness optimisation to reduce the computational effort by approximating the objectives and constraints. In RSM, a set of support points is generated using a sampling method. The sampling strategy is hugely important and influences the accuracy of the approximations made, further discussed in Sections 3.5.1 and 3.5.3. Each of these support points are evaluated and the required responses extracted. The objective and constraint functions are then replaced by approximate surfaces created using the support point evaluations, Figure 3.4. The standard response surfaces are either based on linear functions or on higher order polynomials depending on the complexity of the problem, number of design variables and the available computational resources. Hence the number of evaluation (support points) required depends on the above mentioned factors Forsberg (2002). The optimisation is then performed on the smooth surfaces, that have replaced the original objective and constraint functions, which might noisy, have sudden jumps and bifurcations. Classical optimisation methods such as Gradient-based, EA etc. can be used on the surfaces. Since the response surfaces are available, various design configurations can be solved without the need to perform additional computations hence reducing the number of evaluations required. The process ends with a validation check of the approximated optimum value on the response surface with the actual optimum value of the function. Other response surface approaches include

kriging and Radial Basis Functions (RBF) , see Cavazzuti (2013a); Jurecka (2007); Kitayama and Yamazaki (2014); Picheny et al. (2013).

Some of the drawbacks of RSM include restriction in the number of design va-

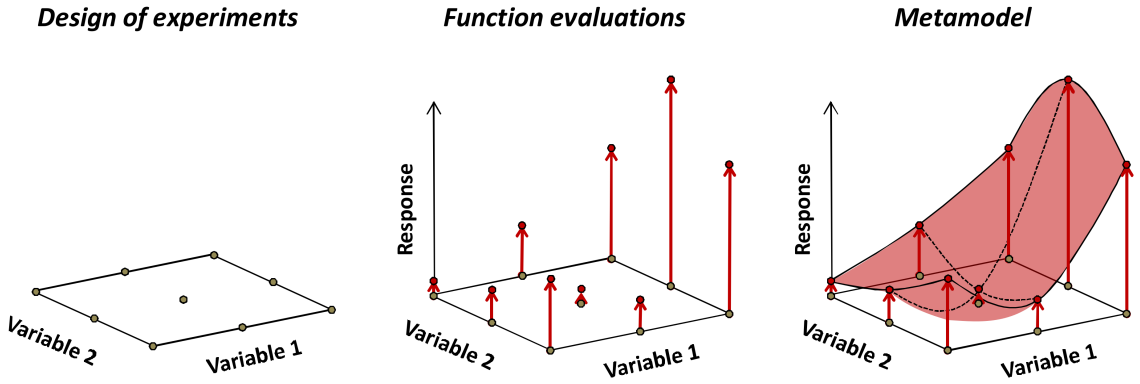

FIGURE 3.4 – Response surface generation considering two design variables, Ryberg (2013).

riables - generally less than 20 parameters, Duddeck (2008) - and the accuracy of the generated response surfaces. Also in cases where the optimisation is made on designs which are already pre-optimised (using engineering knowledge and experience), the determination of a good approximation model is complicated. This is because the pre-optimised models are already pushed to the boundaries of the design space which may be highly non-linear. Hence although the approximated designs may be deemed as feasible, due to the quality of the response surface at these highly non-linear regions, the design may actually be infeasible. To avoid this accurate approximations are required in these regions, Duddeck (2008). An iterative approximation approach could be applied to better approximate at the boundaries of the design space. The approximation from single response surfaces generally fails in problems such as crashworthiness due to their complexity. Consequently Iterative Response Surface Methods (IRSM) have been developed where the accuracy is increased through the use of successive local response surfaces, discussed later. A detailed discussion on RS can be found in Myers et al. (2008); Ryberg (2013).

Systematic Sampling Techniques

Also known as Design of Experiments (DOE), these techniques systematically generate the sample points in a given design space. They are more appropriate for response surface generation since they better represent the design space compared to stochastic samplings presented in Section 3.5.1. The DOE discussed here are exemplary and are only discussed in the context of this thesis. Other DOE include factorial, central composite designs, Box-Behnken designs, see Cavazzuti (2013b); Myers et al. (2008) for further reading.

Koshal Designs require a minimum number of evaluation points and use a one-factor-at-a-time approach. For linear designs they generate $N = n+1$ points to fit a linear approximation function. Similarly, for quadratic designs $N = n(n+1)/2+n+1$ points are used to fit a quadratic approximation function, where n is the number of design variables. Although a minimum number of support points is required, this however affects the quality of the responses surfaces, Koshal (1933); Cavazzuti (2013b).

D-optimal The support points increase significantly with the increasing number of design variables in the above presented DOE. D-optimal sampling reduces this effect in an optimised manner. Generally, the distances between the support points are optimised to improve the representation of the design space. For this, first a factorial DOE creates all possible design point candidates (see Cavazzuti (2013b) for factorial designs). Then from this, the required number of support points is determined such that it reduces the response surface approximation error. For crashworthiness this DOE approach is favourable to reduce the number of support points required for response surfaces Cavazzuti (2013b).

Variable Screening

The required number of sample points to generate a good response surface approximation depends on the number of design variables. This is one of the drawbacks of RSM and hence several approaches have been used to reduce the number of design variables. The idea is to identify and avoid the use of variables that do not influence the design responses. Some approaches include Principal Component Analysis (PCA), sensitivity analysis and analysis of variance, see Hilmann (2009); Ryberg (2013).
To understand the influence of each design variable on the responses and to identify the most important parameters, generally a global sensitivity analysis is made. For this a sampling approach is used to generate the required number of samples within the global design space. Then the correlations between the design variables and the responses are evaluated. From the full set of design variables, the most influential design variables can be chosen using the correlation analysis results. The reduced set of design variables can then be used to build the response surfaces.

3.5.4 Iterative Response Surface Method (IRSM)

The requirement to fully represent the global design space with a single response surface significantly increases the number of required sample points. Hence an iterative approach to the RSM is more appropriate where small sub-regions of the global design space are explored successively. The quality of the response surface approximation increases by fitting the surfaces into the smaller sub-regions. The idea here

is to start with a sub-region within the entire design space and progress successively towards better regions of the design space.

Generally in an IRSM [2], the algorithm starts by taking a sub-region of the global design space or the global design space itself. Within this sub-region, the sample points are generated and evaluated, Figure 3.4. Then a response surface is created in this sub-region using the support point responses and optimisation is performed on this response surface to find an optimum of the sub-region. The next iteration then starts with the previously found optimum point and the new sub-region is obtained by scaling (zooming) or shifting (panning) of the design space, around the previously found optimum. The panning and zooming of the design space is shown in Figure 3.5. In Figure 3.5 green dot represents the optimum in the first iteration, k, which is the centre point of the new sub-region in iteration, $k+1$, and the arrow shows the panning direction, Kurtaran et al. (2002). The response surface approximation improves as the algorithm advances. This is because the sample point density increases as the sub-region size reduces. The optimisation terminates when a stop criterion is fulfilled such as sub-region size, objective value change from one iteration to another.

Successive exploration of the design space was addressed in Toropov (1989); Stander (2001). Toropov (1989) used a move limits strategy to search for promising regions of the design space. Similarly trust region approach is used by Rodriguez et al. (2000) for the exploration of the designs space and approximation at local regions of the design space. A successive exploration using domain reduction approach is presented in Stander and Craig (2002).

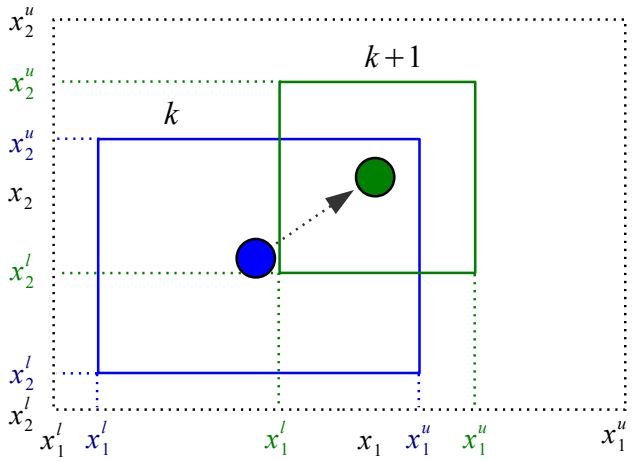

FIGURE 3.5 – IRSM sub-region adaptation: panning and zooming, Stander and Craig (2002).

2. Also referred to as Successive Response Surface Method (SRSM) or Adaptive Response Surface Method (ARSM).

Response Surfaces Applied to Crashworthiness

Due to the expensive nature of crashworthiness problems it is attractive to approximate and solve crashworthiness problems using response surfaces. In Myers et al. (2008) various aspects of RSM are presented and discussed. A comparison of polynomial based RSM and kriging is made in Forsberg and Nilsson (2006). The methods were applied to analytical function and industrial frontal impact problems. The paper concludes by recommending the use of kriging at the beginning of the optimisation followed by the use of polynomial response surfaces at the final iterations of the optimisation. This is because in kriging the response function interpolates through all the support points in the design space. Hence at the start of the optimisation kriging gives a good global approximation. However for local approximations, towards the end of the optimisation, kriging can create an over-fitted approximation surface, see Figure 3.6. Due to this overfitting, the optimisation algorithm could converge to a local optima too early.

In a study by Duddeck (2008), a comparison was made to assess the quality of

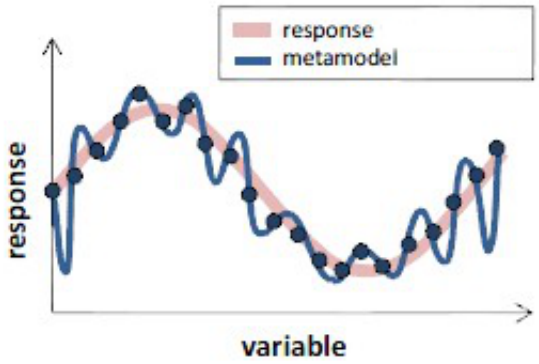

FIGURE 3.6 – Response surface over-fitting.

approximation models such as linear response surface, kernel smoother and kriging for high speed frontal, lateral and rear impacts. The approximation models were created from 150 support points for each case. The author concluded that the lateral impact behaviour was captured by the approximate models while it failed for the other impact cases. This was because in frontal impact the front members are subjected to bifurcation behaviour whereas in lateral crash the structures are subjected mainly to bending. In general, RSM can handle bending cases much better than cases with bifurcations due to stability or near-contact situations. The application of RSM for both crashworthiness and metal forming is presented in Jansson et al. (2003). Further applications of RSM in crashworthiness are presented in Avalle et al. (2002); Kurtaran et al. (2002); Redhe et al. (2002); Stander and Craig (2002).

3.5.5 Multi-fidelity Optimisation Approach

An approach to reduce the computational effort of large optimisation problems includes multi-fidelity approaches. In this approach many coarse model evaluations are used for optimisation and a few fine model evaluations are made for correction of the responses. Here coarse model refers to low-fidelity models that are faster to compute but are less accurate. Similarly fine model refers to high fidelity models that are accurate but take longer to compute. These different fidelity models can be physical (sub-models, simplified models) or analytical response surfaces.
An approach where a coupling of RSM and space mapping technique is implemented and tested for crash is presented in Redhe and Nilsson (2006). A mapping function is used which minimises the error in responses between the different models. Here the mapping of the input parameters are performed to get the correspondence between the two models, see Bakr et al. (2001). A two-stage multi-fidelity approach is presented by Sun et al. (2010) where different fidelity of FE models are used. A correction response surface is then used to approximate the responses of the high fidelity model. The general aspects of multi-fidelity approach is also used in this thesis. Different fidelity (ESLM and sub-modelling) of FE models are used at different levels of RDO to reduce the computation time, see Chapter 10.

Chapter 4

Crashworthiness Shape Optimisation

4.1 Introduction

In addition to already well established methods to optimise the thickness of different components, new approaches based on shape modifications of structural components are recently introduced. For parametric shape optimisation, a special challenge lies on the appropriate parameterisation of the geometry of a car body. The design space should be made as big as possible allowing for many design configurations. This may then lead to geometrical conflicts during optimisation. To establish a parameterisation fulfilling both requirements is therefore challenging.
Alternatively, parameter free shape optimisations can be used. Here the shape modifications are realised by changing directly the nodes of the FE mesh. The use of FE node coordinates as design variables, where movement of each node is made independently, allows for the freedom of shape modifications. However, this approach is limited to small geometrical changes to avoid numerical instability due to mesh quality. Hence in this case the challenge to avoid geometrical conflicts is not so high.
In this chapter first a general overview of the existing methods is given followed by a new shape parameterisation technique. In particular a special offset mapping approach is proposed to avoid geometrical conflicts. Via this approach, it is possible to define a large range of design variables without the need to restrict it artificially to avoid geometrical conflicts. Hence this approach is superior to the standard parameterisation of geometries where the parameters are directly linked to the structures. To demonstrate this technique, a bumper beam and a B-pillar reinforcement shape optimisation are presented.

4.2 Shape Parameterisation Techniques

4.2.1 Explicit Parameterisation

In explicit parameterisation changes are made directly to the entities which are topologically independent of other entities, such as points, lines etc. Hence via an explicit parameterisation approach it is a priori difficult or even impossible to assure geometrical or topological compatibility. In Figure 4.1 the difference between explicit and implicit parameterisation is shown when the position of the rocker is modified. In the explicit parameterisation case, Figure 4.1 (left), the cross beams, floor and joint do not follow the change in the rocker. This is because the topological connection between the objects is missing after the modification which results in geometrical discontinuity, see in Figure 4.1 (left) the highlighted zone in red.

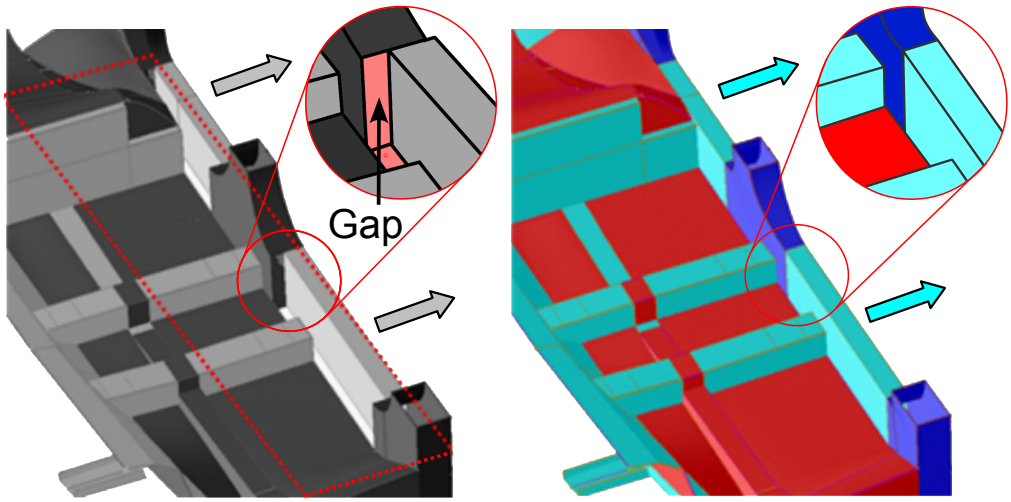

FIGURE 4.1 – Comparison between implicit and explicit parameterisation, inspired from Zimmer (2006).

4.2.2 Implicit Parameterisation

In implicit parameterisation the topological connection between different objects is defined. Since the model features are topologically connected, any changes made to one entity will lead to modifications of all other related components. Hence implicit parameterisation is a preferred parameterisation technique since the parameterisation is accurate and also the geometrical and topological compatibility is retained. In Figure 4.1 (right), the cross beams, floor and joint follow the change in the location of rocker, this retains the geometrical compatibility, see in Figure 4.1 (right) highlighted zone in red [1].

1. Please note, the figures show the geometrical models and not the FE models; the latter is generated after geometry modifications.

4.3 State-of-the-art

4.3.1 Shape Modification Techniques

This section presents the typical shape modification techniques used in crashworthiness optimisation. Shape modifications are made on either the geometry models, defined with CAD tools, or on the FE models. In CAD-based approaches, the shape modifications are made using directly the geometrical design features whereas in CAE-based approaches, the shape modifications are made using the mesh nodal locations or mesh-related parameters (handles). Most frequently used geometry-based shape modifications include the use of CAD, CAE and spline based approaches. For FEM model based approaches, mesh morphing is commonly used.

Parametric modelling is well established for CAD software, e.g. CATIA or NX (Siemens). The corresponding parameters are until now rarely used directly in computational mechanics where the studies are based on CAE tools like finite element software. Recent studies can be found to connect these two different modelling areas, but a one-to-one transfer of the CAD parameterisation to the CAE world is still in its infancy, Dietrich (2013); Suhrer (2013).

Chiandussi and his co-workers, see Avalle et al. (2002); Chiandussi and Avalle (2002), were among the first to publish on shape optimisation for crashworthiness using a CAD-based geometry representation. A tapered beam is optimised in Chiandussi and Avalle (2002) and a crash box is additionally considered in Avalle et al. (2002) while Farkas et al. (2010) looked at a CAD-embedded optimisation of a bumper. Regarding CAE, some commercially available tools offer their tool-specific parametric description, e.g. ANSYS Parametric Design Language APDL, e.g. Zhang et al. (2009) but without supporting a conflict-free choice of parameters. Coupled CAD-CAE integration approaches can be found in Dietrich (2013); Suhrer (2013). In between a purely CAD and a purely CAE approach, parameterisations using SFE CONCEPT are proposed, see 6 for SFE CONCEPT. For example, in Hunkeler et al. (2013), Hunkeler et al. optimised the cross-sectional geometry of a front rail using four shape parameters and in Duddeck (2008) and Zeguer et al. (2008) simple design parameters such as beam height and width are used as shape parameters.

Other studies propose splines for geometrical representation, e.g Brecher et al. (2010). In this approach, the control points are linked to the design geometry. The geometrical design features can then be defined by moving the spline control points. The geometric continuity from one spline to another is of importance here. However the definition of parameters can be tedious depending on the geometrical complexity. In Zhang et al. (2009) the optimisation of an interior reinforcement (arc-like rib) of a hollow cross-section is described by a spline curve and modified via the corresponding control points.

In addition to the geometry-based methods (presented above), approaches that use

the FE mesh to change the geometry are available; these so-called morphing techniques are studied e.g. in Sharma et al. (2010). Here morphing handles or parameters are created that are linked to the structural shape modifications, see Figure 4.2. The definition of morphing boxes and the corresponding morphing parameters/handles is not always easy and it is difficult to include adaptation of joints or assembled structures. To realise the full flexible design maintaining connectivity and avoiding geometrical conflicts is to the author's point of view not always achievable.
In Georgios and Dimitrios (2009) morphing boxes are used to parameterise the front

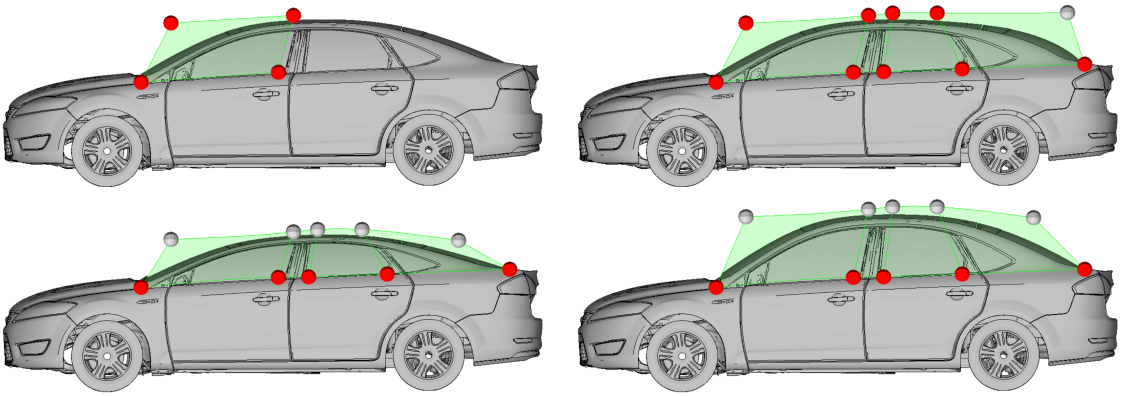

FIGURE 4.2 – Roof structure (height) modification via morphing handles, Hilmann (2009). Here the grey handles are chosen to modify the shape.

rails and their beads. The front rail height and width along with their bead depth are parameterised. A geometrical sub-frame part of a vehicle subjected to static load is parameterised using morphing boxes in Georgios (2007). The design variables are the depth, slope angle and opening of the holes in the model. Similarly the width of the upper part of a door trim is parameterised using morphing boxes in Meissner and Thiele (2009) for side crash.
A mesh-based optimisation like in Arnout et al. (2012) may be employed where the coordinates of the FE nodes are used directly as shape parameters. This is currently not feasible for crash because first a gradient-based approach is required due to the high number of variables. Second it is difficult to assure mesh quality for larger geometrical changes, due to independent movements of nodes. And third, this approach is difficult to realise for structures built by many assembled components. This is because changes in one component should be followed by other connected components, see for example Figure 4.1.

4.3.2 Crashworthiness Shape Optimisation

Regarding optimisation for crashworthiness, there is a recent shift from simple size optimisation where the thicknesses of the components are taken as design parameters, e.g. Duddeck (2008), to more advanced problems addressing the improvements of the shape or even topology of car body structures, e.g. Zimmer et al.

(2009). Size optimisation is more appropriate for later development stages while shape/topology optimisation may be used earlier in the product development process (PDP). In the literature, studies for crash shape optimisation consider either cross-section parameters, non cross-section parameters or both. Some of the work in these two categories are presented in the following sections.

Cross-section optimisations

In the literature, most studies on shape optimisation parameterised only the cross-section, which can be regarded as a two-dimensional design problem. Here analytical reference solutions are partially available, e.g. Jones (1997); Lu and Yu (2003), and the simulation models can often be reduced using sub-models or direct component-only optimisation. The literature ranges from quasi-static crush to truly dynamic problems for different materials and structures looking at single or multi-cell, foam-filled and honeycomb structures, e.g. Kim et al. (2002); Yin et al. (2011); Zarei and Kröger (2008). The complexity in shape parameterisation is in most of these studies limited; often the height or width of the total cross-section is used, which makes the optimisation closer to a size or scale optimisation than to a real shape optimisation where more freedom is given to the cross-sectional shape, e.g. Lanzi and Castelletti (2004); Lee et al. (2002).

More challenging is a shape optimisation with more flexible definitions of shape variations either based on the location of characteristic points of the cross-section or on corresponding control points. Eby et al. Eby et al. (2002) defined a set of points and varied them in a hierarchic manner first as a group on a coarse level and then as single points on the refined level using an agent-based optimisation scheme. One of the challenges they have solved lies in the requirement that shape changes should not oscillate too much assuring a smooth transition between adjacent sections (this is more discussed in Chiandussi et al. (2010)). A similar approach is used for the Future Steel Car project World Auto Steel (2011a).

Investigating carefully the examples discussed so far, one of the main question arises immediately; all these parameterisations are limited because they have to carefully avoid geometrical conflicts. In Eby et al. (2002) the points are only allowed to move outwards, an overlapping or crossing of sectional parts can therefore be avoided to the cost of flexibility and a smaller design space. For example, Park et al. Park et al. (2010) defined modifications of a bumper only in the outward direction. The morphing approach in Feuerstein et al. (2008) uses the four corners of a rectangular and restricts itself to small shape modifications only. Again the design space is smaller than desirable. Finally, Farkas et al. (2010) employed 9 shape parameters of a bumper cross-section also with limitations to avoid overlapping.

To exploit the full potential in shape optimisation, the design space should be as large as possible. This restriction discussed above means that the better design

configuration may be missed during optimisation. It can be summarised that the avoidance of geometrical conflicts, without reducing the design space, allows for the exploration of a bigger design space and hence a greater possibility to find improved solutions. This is because the expected potential for improvement of designs is directly proportional to the magnitude of allowed design changes. Thus the design space should be made as big as possible which is primarily limited by the allowed change in the side constraint. An approach to avoid these geometrical conflicts will be presented in the Chapter 6.

Non-cross-section optimisations

One step more complex are shape optimisations where design variables are also defined in axial direction of the members. This is realised in some studies, but the approaches are again limited by the necessity to avoid geometrical conflicts. Normally the design variables are relatively simple and do not exploit once more the full potential of shape optimisation, for example Wu and Xin (2009) optimises not only the height and weight but also the angle of an S-bend. Often crash initiators are optimised (possible variables are depth, length, number and position of either beads or holes), e.g. Cho et al. (2006). Again, with the parameterisations chosen in these formulations, it is difficult to obtain a large range of design variables and avoid geometrical clashes. A comparable bead optimisation is performed in Kaya and Öztürk (2010); Redhe et al. (2005); Wang et al. (2005). Finally Volz Volz (2011) looked at shape optimisation for the complex problem of the frontend of an industrial vehicle optimising shape and thickness of several components using the implicit parameterisation technique of SFE CONCEPT. All these studies defined carefully their parameterisations and had to avoid geometrical conflicts which ended up in a reduced design space and less optimal result. Regarding the last example it becomes clear, that the question of conflict-free definition of shape alterations for the optimisation becomes more important in cases where several components are assembled to a more realistic structure. A shape modification of one component might affect via the connection points the other parts and their optimisation as well. This problem does not become apparent in single component optimisation as discussed in most of the work mentioned above. The connectivity should not be lost due to a change in variables, no gaps or overlappings should occur. This becomes even more important where standard joining techniques are included like spot welding. Number and location of the joints should follow the shape modifications even in cases when one component is moved over another one, which is illustrated in Figure 4.3 where the blue seat cross-member moves during the shape optimisation over the red part. A special mapping technique is required to maintain the connection information, which is realised here via the implicit parameterisation technique (SFE CONCEPT) discussed for example in Zimmer and Prabhuwaingankar (2005); Zimmer et al. (2009).

A very flexible definition of the design variables is possible because the components "know" implicitly how they are connected.

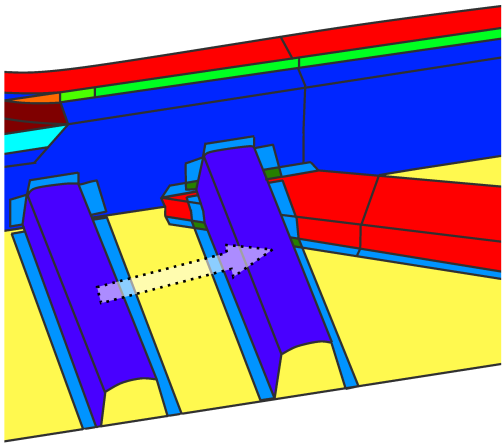

FIGURE 4.3 – Automatic adaptation of connection between components, inspired from Zimmer (2006). Here, the connection should follow automatically the modification even in cases where the shape modification swaps from a two-component to a three-component connection or flange.

4.4 Geometrical Conflicts

The general idea to avoid geometrical compatibility issues depends on the interdependency of shape parameters, the available design space for shape modification and also the topological relation between the neighbouring parts. Geometrical conflicts may occur when two or more design variables are defined independently with the aim to realise the largest possible design space. This is advantageous to obtain the best possible design but it might lead to clashes between the variations of the parameters. To avoid this, an easy approach is to reduce the design space but this is not desirable because a large part of the design space is lost. Also generally, a structural component used has other components around it which limits the possible changes. Both of the issues, mentioned above, can be solved by careful selection of parameters and their bounds. Additionally, it is also important to consider the topological compatibility between the structural parts while modifying the geometry. Improper or missing definition of topological connections lead to unwanted gaps or penetrations in the structure during shape modifications. Hence ideally any shape modification made to a structural part should be followed by the other parts connected to it, see Figure 4.1 (right).
Geometrical incompatibility can either be removed through careful definition of the upper and lower bounds of each design variable or it can be accepted in the definition of the optimisation problem but penalised during the optimisation. If bounds are used then the design space is restricted and eventually too small. Furthermore if incompatible designs are allowed to appear during the optimisation,

they normally do not satisfy the specified requirements and are hence withdrawn during optimisation. Nevertheless the simulation of the designs that are defective or non-manufacturable waste computational time. Also when there are many unacceptable designs, the algorithm could head in the unwanted direction. Hence it is best to either remove the occurrence of the incompatible designs in the first place without reducing the design space or avoid solving them during the optimisation.
The evaluation of designs that are incompatible add to the already high computational effort for crash optimisation. Hence incompatible designs can be neglected for evaluations during the optimisation to save computational time. However the optimisation algorithm used in this case is important since the algorithm should be able to continue without the performance responses of some designs. Also the reduced number of design evaluations means that the required information for certain types of optimisation algorithm may be missing. An Iterative Response Surface Method (IRSM) for example rejects certain incompatible design points, will suffer by low quality of the meta-model. Similarly, in GA the number of designs in one generation may be reduced and hence the information to create a new population for the next generation may not be enough.
Literature relevant to this approach include Brecher et al. (2010) and Hilmann (2009). In Brecher et al. (2010), an Evolutionary Algorithm is used as the optimisation algorithm where both recombination and mutation operators are used. The geometrical compatibility of designs is checked after recombination and mutation before handing the design to the FE solver for evaluation. If a design does not satisfy the compatibility rule then a new design is generated until the required size of the population is achieved. This approach is beneficial as the number of designs per generation is always constant and there is no absence of design evaluation responses. However there may be very few designs that satisfy the compatibility rules after both the recombination and mutation. A similar approach is presented in Hilmann (2009) applied to crashworthiness optimisation of crash box triggers. For a simple design case the position of the triggers are modified along the crash can. The limits of the location of each triggers are defined in such a way that there may occur an overlap in some of the cases, see Figure 4.4. This is done to cover a wide range of trigger configurations. The overlap occurs when the rear trigger is moved to the most forward position and the front trigger moved to the most rearward position. A small module is implemented to separate the compatible and incompatible designs. This check is performed before the handover of the designs for simulation. Here only the designs that satisfy the compatibility rules are simulated. The designs that are incompatible are rated as poor during the optimisation. GA is used for optimisation which learns the design variable settings that do not produce acceptable designs and hence these settings should be withdrawn after few generations. This compatibility issue between the two triggers could be easily

solved using the advanced parameterisation technique proposed later in this thesis. Since the geometrical incompatibility issue is already avoided by a more advanced parameterisation, the prerequisite for an adapted algorithm such as in Brecher et al. (2010) is avoided.

To overcome the drawbacks in shape parameterisation, presented in the sections

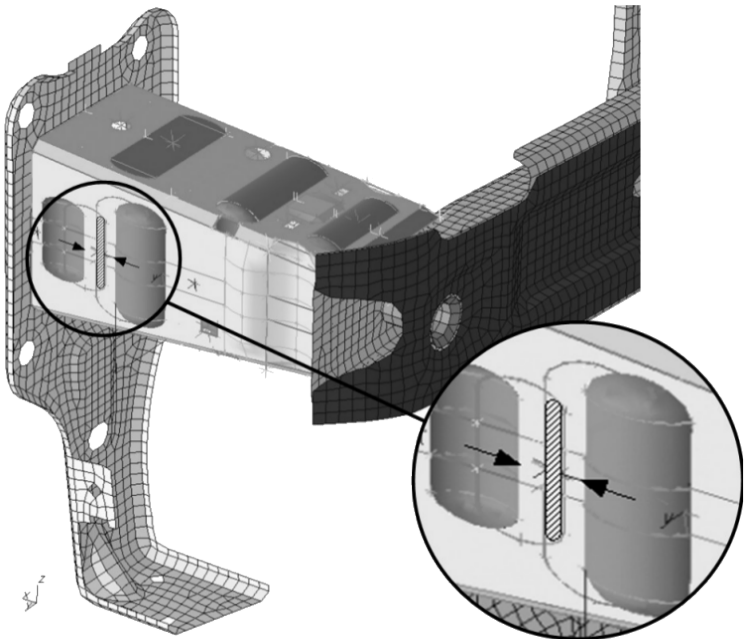

FIGURE 4.4 – Incompatible design: overlap between triggers, Hilmann (2009).

above, a parametric approach using SFE CONCEPT, see SFE CONCEPT (2009), but extended here by a special offset mapping technique is presented in Chapter 6. The special implicit definition of the parameters of allows to include such a mapping, which then leads to parameterisations without geometrical conflicts enabling to explore the full potential of shape optimisation. In addition topological changes may be included, for example the number of beams, holes, beads, reinforcements, spotwelds etc.

Chapter 5

Robust Design Optimisation for Crashworthiness

5.1 Introduction

As discussed above, optimisation for crashworthiness is already addressed in several studies. Nevertheless, robustness (insensitivity with respect to inevitable fluctuations) is rarely included. The latter is necessary because optimisation drives the design to the limits and robustness may be not assured. There are two main reasons for this. First the numerical effort is already high for the optimisation and inclusion of robustness makes this situation worse. Second, an appropriate modelling and sufficient data are often not available. The consideration of uncertainties in early design phases helps to reduce costs by avoiding decisions for designs with a narrow bandwidth to react to changes occurring later in development. In the latter design stages, uncertainties account for variations due to manufacturing or due to scatter in load cases. Here robustness reduces the cost with respect to failure during the full life cycle. The first category may be considered as some kind of epistemic uncertainty (e.g. lack of knowledge), see Möller and Beer (2008), while the second is related to aleatoric uncertainty (fluctuations/variability in the system). For a more detailed discussion see e.g. Möller and Beer (2008). In this thesis, epistemic uncertainties are not considered.

The scatter in the performance not only reduces the structural quality but also adds to the maintenance, repair and service costs. In contrast a high quality structure consistently performs even in the presence of inevitable variations throughout its service time. These requirements have given rise to yet another optimisation field, the so called Robust Design Optimisation (RDO), that considers and reduces the effect of uncertainties on the structural responses, Figure 5.1. Some of the frequently addressed uncertainties in crashworthiness are discussed in Section 5.2.

In previous design approaches, uncertainties in design were very often neglected and a deterministic approach was taken. A deterministic model of a structural system

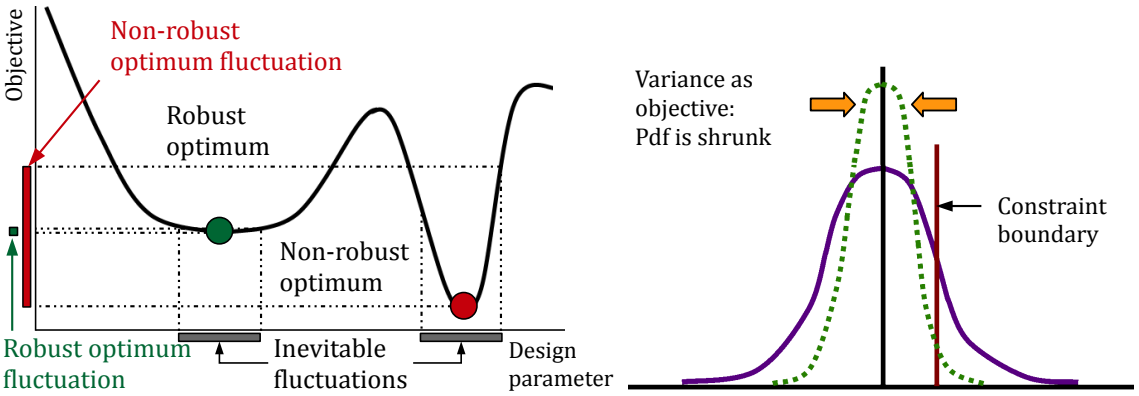

(a) Global (red) and robust optimum (green), Sun et al. (2011).

(b) Robust design optimisation, Delcroix et al. (2007).

FIGURE 5.1 – Characteristics of Robust design optimisation.

is obtained by considering only the nominal values of the parameters. This means that the objective functions and the constraints are also calculated using these nominal values. The system variation that causes the variability in the performance was considered only in terms of safety factors. Which means that the larger the uncertainty the larger the safety factor. Due to the lack of knowledge of the scatter in the structural performance, the safety factors specified could have been too conservative or too dangerous.

The optimum design from deterministic optimisation performs well under ideal conditions however in presence of uncertainties the design may actually exhibit poor performance. While another design with non-optimal performance in the ideal case may be less sensitive to variations in parameters, Figure 5.1(a). Therefore the latter design would be more robust than the optimal design. Due to such reason the deterministic approach does not yield the best design solution in the presence of uncertainties. Also in structural engineering, the interest should be on an improved design that exhibits robust characteristics in all conditions rather than an optimal design which performance deteriorates with changing conditions. Hence a robust design approach has to be implemented to search for designs that are less sensitive to uncertainties Kang (2005).

Design robustness can be achieved by either reducing or eliminating the scatter in the input parameter, this however is costly or impossible ; or by creating designs that are less sensitive to the scatter in parameters without actually eliminating the cause of scatter, see Figures 5.1(b). The latter is achievable by performing design under uncertainty. The next section starts with the sources of uncertainty in crashworthiness design followed by the modelling of these uncertainties.

5.2 Sources of Uncertainties

The concept of non-determinism is discussed in literature via different categorisations. Non-determinism means no clear definition of a system ; such as load case magnitude, angle etc. In Duddeck (2007) the distinction is made between uncertainty and variability. There, variability is related to variation from physical and environmental sources such as impact angle etc. In contrast uncertainty is referred to lack of knowledge of a problem definition. In Wynn et al. (2011) the uncertainty and variability are categorised as epistemic uncertainty and aleatory uncertainty respectively. In addition to these further categories are also presented. The uncertainty in a design process is categorised in Padulo (2009) into two main categories ; uncertainties about the problem and uncertainty within the problem. A list of uncertainties within these two levels and their propagation is also explained. In Duddeck (2007) the authors categorise the uncertainties into manufacturing, environmental and operating conditions and lists the most relevant sources for each of these uncertainties. The uncertainties in the parameter design in Beyer and Sendhoff (2007) are distinguished in four categories ; (*i*) *changing environmental and operating conditions*, (*ii*) *production tolerances and actuator imprecision*, (*iii*) *uncertainties in the system output* and (*iv*) *feasibility uncertainties* - Uncertainty concerning the fulfilment of constraints, i.e. design space uncertainty. Here some of the frequently addressed uncertainties in structural design for crashworthiness are discussed.

The product development process in engineering design is generally exposed to various uncertainties. Such uncertainties can exist since the start of the design process where the problem is only vaguely known. In structural design, uncertainties occur due to the scatter and fluctuations of material properties, environmental conditions, geometrical parameters, boundary conditions and loading conditions. The other aspect of uncertainty in engineering design is brought about by numerical scatter. This is because crash simulations are not repeatable, see Duddeck (2007) for further details.

Furthermore, uncertainties within a structural design may be concerned with different stages of its life cycle. These stages are conceptual design, manufacturing process, service time and the ageing process, see Figure 5.2. Uncertainty is inherited into the structural design due to unclear knowledge about the system and its modelling errors. For example during the conceptual stage no detailed knowledge of a design may be known (e.g. what a part thickness should be) and also the concept designs are subject to change as the designs evolve during the design process. Similarly, material and tolerance scatter introduce uncertainty in manufacturing processes which results in the unit-to-unit variation. Also the non-uniformity of the process by which the units are manufactured introduces uncertainty to manufacturing and assembly. During the service time of a structural system, uncertainties are introduced due to

operating environment (temperature, pressure etc.), loads and boundary condition changes and human errors. The changes in material properties due to material deterioration affects the performance of a system as it ages.

Depending on the type of problem, there may exist various uncertainties associated

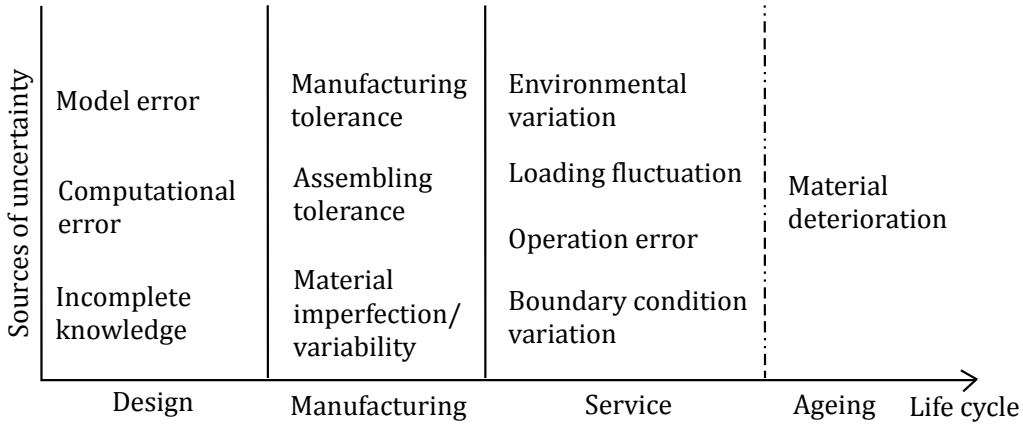

FIGURE 5.2 – Sources of uncertainty in a product life cycle, Kang (2005).

with the design. It is then difficult to consider all the uncertainties in the optimisation, one of the approaches could be to choose the most important uncertainty parameters either by experience or by sensitivity analysis. Some of the frequently addressed uncertainty parameters in crashworthiness robustness analysis include material parameters, thickness parameters and load parameters, Delcroix et al. (2007); Redhe et al. (2004); Will et al. (2006). However in these studies, the influence of the shape parameter uncertainty (a type of manufacturing uncertainty) is not considered. Shape parameter uncertainty is addressed in Zeguer et al. (2008).

In this thesis mainly manufacturing and environmental uncertainties are considered. Since the main aim here is to test approaches for RDO, these are taken as standard as they are also the most frequently addressed in the literature. It is also reasonable to first consider these uncertainties and extend to other uncertainty sources in the future. Here manufacturing uncertainties include thickness and shape tolerances. The information regarding their distribution is easily obtainable from steel manufacturing companies such as Corus, see Corus (2006). Environmental uncertainties are considered in-terms of crash test conditions. These include impactor velocity, impactor mass, impact angle and impact position. The variation data are easily available in various crash test protocol such as EuroNCAP (2012).

5.3 Uncertainty Modelling

Various models of uncertainty exist for structural design problems. These are dependent on the types of uncertainty considered in the study. The modelling of the uncertainties determines the problem formulation for design under uncertainty. In Kang (2005) the modelling of uncertainty is categorised as possibilistic and proba-

bilistic modelling.

Commonly used possibilistic uncertainty modelling include fuzzy approaches. They are used to model epistemic uncertainties which are vaguely defined. In this approach the design solution is assigned a membership value to the feasible design space. In contrast to probabilistic approach, where design $\mathbf{x}$ is either feasible or infeasible, it is assigned to a membership function $\mu_D(\mathbf{x}) \in [0,1]$. Here $\mu_D(\mathbf{x})$ is the degree of membership to the feasible set where $\mu_D = 1$ means a feasible solution and $\mu_D = 0$ means an infeasible solution, see Möller and Beer (2008) for further details.

Currently the most commonly used tool to model uncertainty is based on probability theory. This is due to the high computational complexity of other approaches, such as fuzzy approach, specially for industrial design cases Beyer and Sendhoff (2007); Padulo (2009). Also, since the uncertainties considered in this thesis (manufacturing and environmental) are well defined, probabilistic approach is more suited. Hence in this thesis the focus is set on probabilistic approach from this point onwards, although it seems to be interesting to extend the studies to fuzzy approaches in the future.

A frequently used approach to model uncertainties in structural design is stochastic randomness, Kang (2005). Since most of the uncertainties in structural problems are random in nature, their occurrences are modelled using Probability Density Function (PDF) and Cumulative Distribution Function (CDF). Often a normal distribution is assumed, which is described by its first two statistical moments, mean (μ) and standard deviation (σ). In this approach an assumption is made that the complete knowledge about the design and its modelling are known. However the accurate information on the probability distributions of the uncertainties is not always available or non-existent.

A common approach is to use standards and norms to model the uncertainties. For environmental and operational uncertainties such as loads, velocity, impact angle, impact location, regulatory test protocols can be used, e.g. EuroNCAP (2012). Similarly for thickness parameter uncertainties, information from manufacturing bodies such as Corus is available Corus (2006). The uncertainties can then be assumed to have either uniform distribution with a given range or normal distribution. Commonly used distributions in structural engineering include, normal, uniform, Weibull and lognormal. Other approaches to uncertainty modelling are presented in Zhang et al. (2010); Kang (2005); Beyer and Sendhoff (2007); Zaman et al. (2011). The following section focuses on probability based approaches for design under uncertainty.

5.4 Probability Based Design Under Uncertainty

Two main classes of design under uncertainty via probabilistic approaches include Robust Design Optimisation (RDO) and Reliability Based Design Optimisa-

tion (RBDO). These two fields are however different in some fundamental aspects presented in the following section.

5.4.1 Structural RDO and RBDO

In RDO the assessment of robustness is performed by measuring the variation of performance around the mean value. It is concerned with everyday fluctuations of the performance rather than extreme cases. Hence the performance variation is usually measured taking 2 sigma levels around the mean ($\pm 2\sigma$), see Figure 5.3, the extreme events ($> 2\sigma$) are not considered. RDO aims to find a set of design variables that realise both the improved performance and reduced sensitivity to the uncertainties within some constrained conditions Kang (2005). The main idea here is to keep the design near optimal even in changing conditions due to uncertainties. RBDO in contrast is concerned with the probability of failure of a structure and takes into account extreme events (variations), tails of a Gaussian distribution for example $> 2\sigma$, that lead to often catastrophic failure, see Figure 5.3(a). The failure probability should not exceed a certain limit. Hence the tails of the PDF are investigated in this approach. In RBDO the performance mean is shifted to satisfy the reliability requirements and reduction of the variation is not the main concern. This is because in RBDO the probabilistic constraints at the tails of the distribution have to be satisfied to avoid any extreme events.
The characteristics of both the RDO and RBDO are included in the Design for Six-Sigma (DFSS) approach where both shrinking of the variation (PDF) and also the shifting of the PDF, away from the failure limit, are considered Duddeck (2007).
A comparison between RDO and RBDO is discussed in Duddeck (2007) and Kang

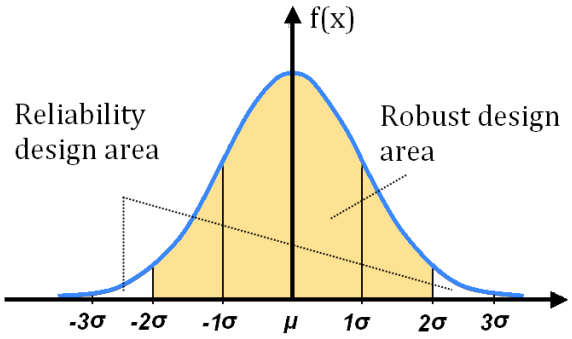

(a) PDF, reliability and robustness areas.

Sigma level	Probability of failure *P(f)*	Defects per million (short term)
± 1σ	3.17 x 10^{-1}	317400
± 2σ	4.54 x 10^{-2}	45400
± 3σ	2.7 x 10^{-3}	2700
± 4σ	6.3 x 10^{-5}	63
± 5σ	5.7 x 10^{-7}	0.57
± 6σ	2.0 x 10^{-9}	0.002

(b) Failure probability corresponding to sigma levels.

FIGURE 5.3 – Comparison between reliability design and robust design, Duddeck (2007).

(2005). In crashworthiness the extreme events are of little significance and the focus is on designs with reduced variations in performance, Figure 5.4. Hence RDO for crashworthiness studies is considered throughout this thesis.

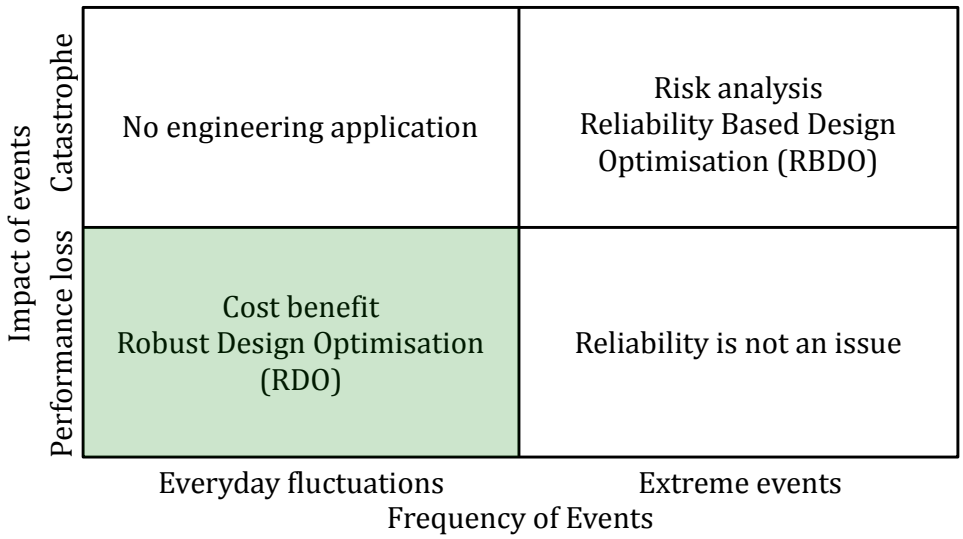

FIGURE 5.4 – Characteristics of RDO and RBDO, Padulo (2009).

5.5 Robust Design Optimisation (RDO)

The formulation of the objective and constraints is key to robust design optimisation. The optimisation strategy depends on the RDO formulation deployed. This is further discussed in the following section.

5.5.1 Problem Formulation

RDO strives for a design with optimal performance while keeping the variance of the performance to a minimum. The aim here is to formulate an optimisation that improves the mean performance of the design while reducing the performance variance. The mathematical formulation of the robust design optimisation presents the mean value of the response function instead of their nominal values. Moreover the standard deviations are used to define the objective functions and the constraints. Hence mathematically the robust design optimisation is a multi-objective approach where the objective mean and standard deviation are to be minimised.

$$\text{find} : \mathbf{x}; \quad \mathbf{x} \ \epsilon \ D \tag{5.1}$$

$$\text{to minimise} : \quad \mu(f(\mathbf{x})), \sigma(f(\mathbf{x})) \tag{5.2}$$

$$\text{subject to} : \quad \mu(g_i(\mathbf{x})) + n\sigma(g_i(\mathbf{x})) \leq 0 \quad (i = 1, 2, ..., l), \tag{5.3}$$

$$\sigma(h_j(\mathbf{x})) \leq \sigma^j \qquad (j = 1, 2, ..., m), \tag{5.4}$$

$$x_k^L \leq x_k \leq x_k^U \qquad (k = 1, 2, ..., n). \tag{5.5}$$

where $f(x)$ and $g_i(x)$ are the objective function and the constraint functions as formulated in deterministic optimisation, see Section 3.2.2. In equation (5.3) n represents the desired sigma level, usually $n = 2...3\sigma$ for robust design. In Equation

(5.4), $h_j(\mathbf{x})$ represents an additional constraint on the performance for which the standard deviation has an upper limit.
Due to the multi-objective character of RDO, the suitable optimisation strategy is to use a multi-objective optimisation algorithm. However the difficulty with this multi-objective approach is that there is no single optimum for all objectives. This is because often the objective criteria are conflicting with each other. Hence improving the performance of one objective has a performance reduction effect on another objectives. Therefore multi-objective optimisation provides a set of optimal solution known as Pareto-optimal solutions. Furthermore in multi-objective optimisation significantly large search space has to be explored to obtain a set of Pareto-optimal solutions. In crashworthiness this means simulation of many computationally expensive designs which is not ideal, see Marler and Arora (2009) for further reading. Due to this expensive nature, multi-objective optimisations are generally used with response surfaces, see Sinha et al. (2007). In RDO studies, different formulations have been used to avoid considering the multi-objective formulation, presented in the next section.

Objective Formulation

In RDO it is not always necessary to use a multi-objective formulation. For example when the objective is to reduce the mass of a structure, variability of this mass may not be as significant as variability of energy absorption capability of a structure. In cases where a true multi-objective formulation, as defined by Equation (5.2), is regarded, this is called objective robustness, Zaman et al. (2011).
In many publications, performance and robustness has been combined to a single response function. Here the weighed sum approach is the most commonly used method to translate the multi-objective formulation to a normalised single-objective formulation, see Equation (5.6), Zaman et al. (2011):

$$\text{to minimise}: \quad \alpha\frac{\mu(f(\mathbf{x}))}{\mu_0(f(\mathbf{x}_0))} + (1-\alpha)\frac{\sigma(f(\mathbf{x}))}{\sigma_0(f(\mathbf{x}_0))}, \tag{5.6}$$

$$0 < \alpha < 1.$$

Where μ_0 and σ_0 are the normalisation factors obtained from the initial design response. The normalisation removes the dependency on the size of μ and σ. The α value specifies the weight of the mean performance and its variance. Hence the trade-off between the two objectives can be decided depending on which one is the most important for the designer.
The formulation in Equation (5.6) is only a mean minimisation problem when $\alpha = 1$ and only a variance minimisation problem when $\alpha = 0$. The main issue with this formulation is the decision on the choice of the weighing factor α, Kang (2005). A use of this approach is found in Lönn et al. (2009).

Other alternative approaches that address multi-objective optimisation include min-max strategy. In min-max strategy the goal is to minimise the deviation of function values from the ideal reference point, see Azarm and Eschenauer (1993).

Constraint Formulation

The deterministic constraint formulation, in Section 3.2.2, is also translated to a non-deterministic formulation by including mean and deviation measures of the constraint responses. It is also known as feasibility robustness where, in the presence of uncertainties, the constraint conditions have to be satisfied Zaman et al. (2011).

$$\mu(g_i(\mathbf{x})) - n\sigma(g_i(\mathbf{x})) \geq \text{Lower limit}, \tag{5.7}$$

$$\mu(g_i(\mathbf{x})) + n\sigma(g_i(\mathbf{x})) \leq \text{Upper limit}. \tag{5.8}$$

Mostly one of the above formulations is used however in some cases both formulations are required.

Design Space Formulation

Variability is included in the RDO through the definition of random variables. They are usually related to the manufacturing and assembly tolerances, such as thickness or shape. Hence in the RDO the design variable randomness is represented via deviations of their geometrical dimensions. Equation (5.9) shows a design variable uncertainty formulation.

$$x_k^L + n\sigma_k^x \leq \mu_k^x \leq x_k^U - n\sigma_k^x/ \tag{5.9}$$

The variation of material parameters can also be treated in a similar way, which is not discussed here in detail because the thesis is focussed on shape modifications.
In this thesis the RDO formulation is not based on the multi-objective formulation where both the mean and the variance are minimised. Here the feasibility robustness is considered where the variations of the constraint responses are checked.

5.5.2 Performing Robustness Analysis

Generally in probability-based RDO for structural problems, the variability in objective and constraints are of importance. A straightforward approach to assess the robustness of a design is to look at the distribution of the outputs. The variability of the performance can be quantified by its deviation from the mean. Hence the standard deviation (e.g. sigma levels, $\pm 2\sigma$) of the design performance is used in this thesis to measure structural robustness.
The expected variability of the uncertain parameters needs to be defined to estimate

the variability in the performance. The uncertain parameters can be varied in several ways ; as a range (low and high limit), nominal value plus/minus a percent or delta variation around this value or through some levels (as in Taguchi's approach Beyer and Sendhoff (2007)). However a better approach is to model the distribution of the uncertainty variation if the information is available, see Section 5.3.
Assuming the distributions of the uncertainties are available, using a sampling method, see Section 3.5.1, a representative population is created using the distribution. Each of the individuals in the population are then computed to generate the observed outputs. A representative distribution is then fitted to the outputs to evaluate the design robustness through the calculation of statistical values such as mean, standard deviation, skewness and kurtosis, Figure 5.5. A probabilistic assessment can then be made to check if the design fulfils the requirements.
In addition to the statistical measures, the knowledge of the most important para-

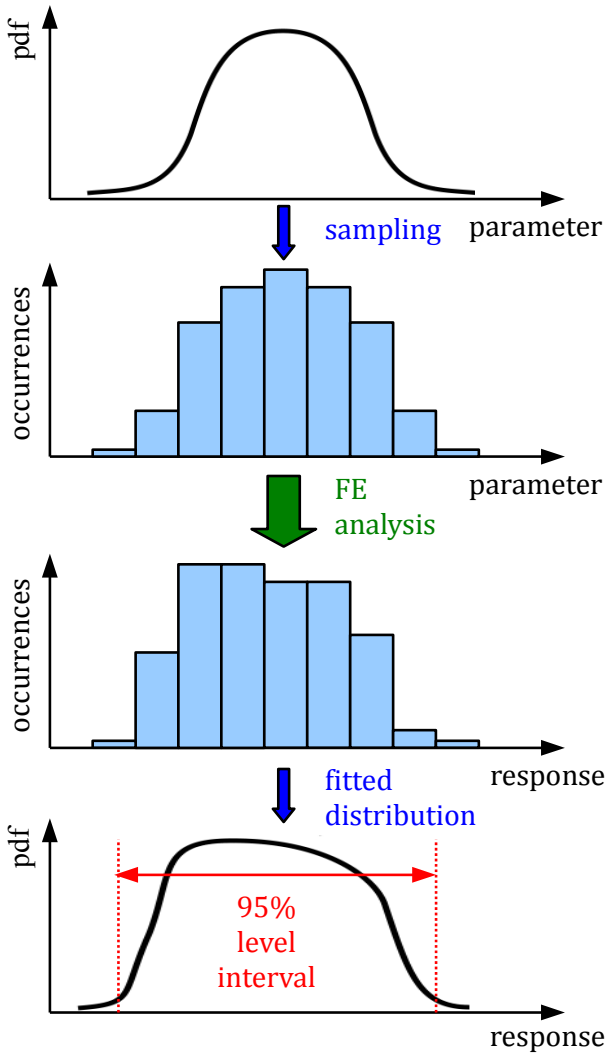

FIGURE 5.5 – An overview of the 95% probability approach, Hunkeler et al. (2013).

meters and the coupled effect of parameters to the outputs can be obtained through correlation matrix (linear/quadratic) and Principal Components Analysis (PCA) respectively, see Hilmann (2009). This information assists the engineer to know

what control factors can be adjusted to make a non-robust design robust.
A commonly used method for the assessment of robustness in crashworthiness is to use the 95% probability approach, Delcroix et al. (2007). A distribution is fitted to the observed outputs and a 95% probability interval [0.025 ; 0.975] (95% confidence interval or significance level of 0.05), is taken. Often a normal distribution can be assumed for the outputs and the intervals are then defined in-terms of sigma levels, $[\mu - n\sigma; \mu + n\sigma]$ where μ is the mean value, σ is the standard deviation of the output and n is the sigma level (generally $\pm 2...3\sigma$), see Figure 5.5.

Sampling for Robustness Analysis

A representative set of sample point has to be generated to fully model the uncertainty probability distributions. This may require a significant number of sample points depending on the problem in question and also the sampling approach used. This adds to an already computationally expensive RDO approach. Hence sampling techniques have been developed to reduce the required number of sample points while fully representing the probability distribution of the uncertainties. Some of the frequently used sampling approaches in crashworthiness design are presented in Section 3.5.1.
Commonly used stochastic sampling approach in crashworthiness include MCS and LHS. The minimum number of sample points, N, required for robustness analysis vary for the two approaches which is dependent on the number of input n_i and output n_o parameters. A recommendation is made in optiSLang (2011) where the minimum number of sample points for MCS is given by $N = (n_i + n_o)^2$ and for LHS $N = 2(n_i + n_o)$. To the author's knowledge, this is an empirical formula and still needs more rigorous mathematical investigations. A general approach is to match the required number of sample points to the type of problem at hand. For crashworthiness problem, which are generally complex, high number of sample points are required to consider noisy functions, non-linearity, number of design variables, crash stability issues, see Section 2.3.1. Also within crashworthiness the problem complexity vary, for example front crash is considered to be much more unstable due to bifurcation characteristics compared to side crash which is dominated by bending. Hence in this thesis simpler crash modes are considered to test different approaches to keep the number of sample points to a minimum.

5.6 Robust Design Approaches for Crashworthiness

Design robustness have been generally considered though three different approaches and they are termed as Taguchi's method (Design for quality), Sequential and Simultaneous RDO approaches. First the main principles are given. Then based on literature, their applicability for crashworthiness is discussed. Most of the other

more effective methods proposed in literature cannot be applied to crash problems due to its highly non-linear characteristics.

5.6.1 Taguchi's Design for Quality

Taguchi's method employs a special design of experiments technique (DOE), orthogonal array, to systematically vary and test different levels of control factors. Control factors are parameters that can be chosen and tuned by the designer to get optimal performance during optimisation. The columns of an orthogonal array indicate different control factors and their levels whereas each row represents an experimental run. The appropriate factor levels are established by the designer but normally a factor level of 2 or 3 is chosen Beyer and Sendhoff (2007).
For robust design, Taguchi's method uses inner and outer array approach, referred to as crossed array. The inner array contains the control factors and their levels. The outer array contains noise factors and their settings. Noise factors are parameters that are difficult to control and are sources of uncertainty, such as environmental conditions: temperature, pressure etc. This method systematically tests various combination of the control factor levels with combinations of noise factors being considered, see Lee and Bang (2006); Sun et al. (2011).
The mean and standard deviation for each row (each experimental run where the design is exposed to various noise factor levels) is calculated. Then a statistical analysis is made on this array, containing both mean and standard deviation, to find the design having best performance under the noise factor variations.
However, Taguchi's design for quality has been criticised in some aspects. The search for optimum design is dependent and limited by the factor levels. The method does not provide information regarding better solution beyond the factor levels. This limits the exploration of the full design space of an optimisation problem. The required number of experimental runs increase significantly with the number of control factors and noise factors, see Beyer and Sendhoff (2007). This is specially not suitable for RDO considering crash due to the expensive nature of crash evaluations.

5.6.2 Sequential RDO

This method is realised in two stages, in the first stage the optimisation study is carried out and the second stage is concerned with the robustness evaluation. For the latter, samples are generated around the optimal design using the uncertainty parameter distributions and the output distributions are analysed, see Section 5.5.2. This method is promising for robustness analysis of an already available or improved design and requires limited number of design computations. However this method is concerned with the robustness analysis of designs rather than searching for robust solutions since the start of the optimisation. Hence the optimisation is still for-

mulated as deterministic, see Section 3.2.2. Due to this formulation, the algorithm searches for optimal regions rather than robust regions of the design space.
Furthermore, usually the optimised designs are already pushed to the boundaries of the feasible design space. Hence these optimal designs may not exhibit robust behaviour since the uncertainties introduced to these designs may push the design performance in the infeasible region. Shifting the optimal design away from the boundary, towards the feasible region, or taking other sub-optimal designs that are away from the boundary may show robust behaviour. However the design performance is reduced making the design non-optimal, Figure 5.6, see Section 8.3.1 for further discussion.

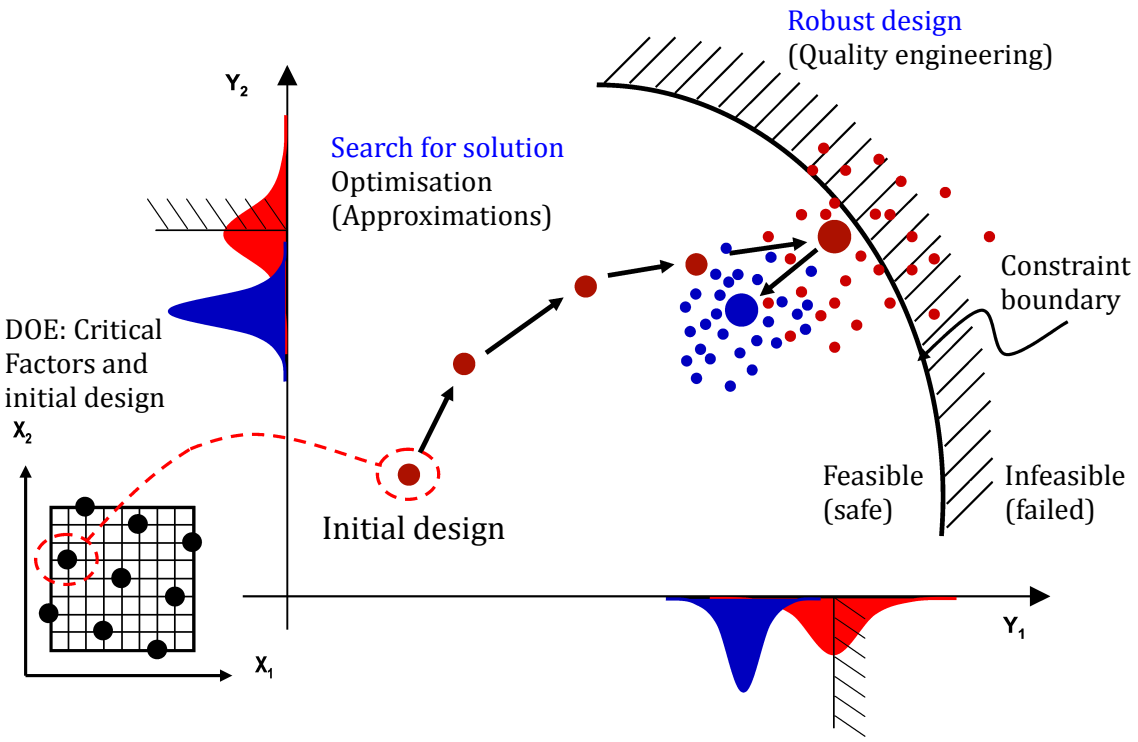

FIGURE 5.6 – Sequential robust design approach, Sippel et al. (2006).

5.6.3 Simultaneous RDO

This RDO approach, also known as parallel RDO or double loop RDO, works in a double loop. The inner loop is concerned with the robustness analysis of the designs and the outer loop performs the design optimisation. In a classical approach, the robustness of each optimisation design at each iteration is analysed, see Figure 5.7. For this the optimisation is formulated to improve the performance while reducing the performance variation in the presence of uncertainties, see Section 5.5.1. Since the RDO formulation is used from the start of the optimisation, the algorithm searches for robust regions of the design space.

This method is beneficial in assessing the robustness while optimising the designs at the same time. The final outcome of the study is an optimum design that is

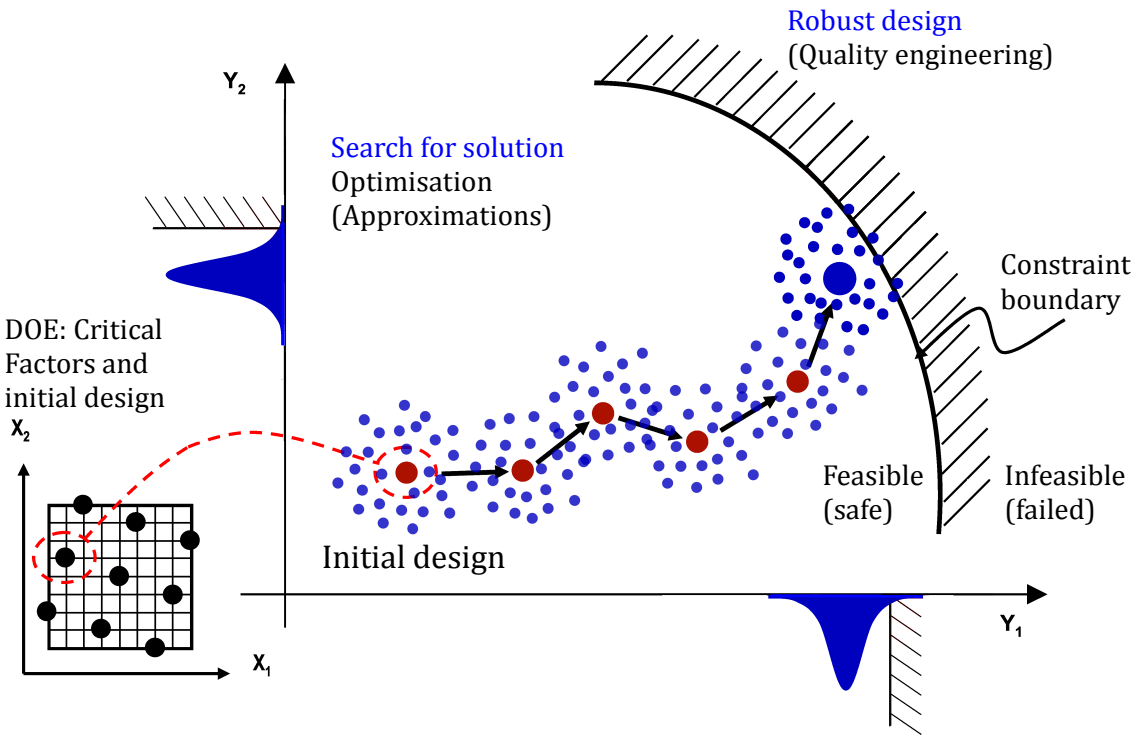

FIGURE 5.7 – Simultaneous robust design approach, adapted from Sippel et al. (2006).

insensitive to variations without the need of extra robustness analysis study of the optimum design. This method is however overshadowed by the number of design analysis (evaluation points) required for both optimisation and robustness analyses. It would be beneficial here to approximate the robustness at the start of the optimisation and use accurate robustness evaluations in the promising regions of the design space, to reduce the computational effort, as proposed in Chapter 8.

5.7 Robust Design for Crashworthiness

There have been very few studies that have included uncertainties in crashworthiness optimisation. One of the reasons is that the underlying computational effort is enormous. Since crashworthiness optimisation is already expensive, including robustness to the optimisation adds significantly to the computational effort. Most of the effective methods in literature cannot be applied to crash problems due to their highly non-linear characteristics.

A comprehensive survey on robust optimisation is presented in Beyer and Sendhoff (2007) while the particularities for crashworthiness are discussed in Duddeck (2007). In Redhe et al. (2004) different approaches for RDO are presented including RSM. A full car frontal impact problem to optimise the metal sheet thicknesses of the front rails using a multi-objective formulation is presented in Sun et al. (2011). The uncertainties considered include material parameters ; density, Young's modulus and

yield stress. The design objective is to increase the energy absorption and reduction the car weight. Taguchi's crossed array approach is used to perform the RDO.
In Koch et al. (2004) again the metal sheet thickness and material parameters are optimised for lateral impact. A multi-objective formulation is used to reduce the weight and its variance while considering dummy injury criteria. The uncertainties in barrier height and barrier impact position are included in the robustness analysis.
A front rail is optimised in Lönn et al. (2009) to maximise the mean and minimise the variability in energy absorption. The multi-objective formulation is translated to a single objective using the weighed sum approach, see Section 5.5.1. The position and size of the front rail trigger are used as the design variables. Geometric uncertainties are used as uncertain parameters.
Robust design considering uncertainties in shape parameters and impact conditions is addressed in Hunkeler et al. (2013). A sequential RDO approach is used to optimise a front rail followed by the analysis of robustness of the optimum design. Here the importance of shape parameter uncertainty is highlighted. Similar study is found in Hilmann and Paas (2006) where geometric parameters of a crash box are used for optimisation and robustness study.
Robust design of a knee bolster design considering both the sequential and simultaneous RDO approaches is presented in Zeguer et al. (2008); Stocki et al. (2007). Here shape and thickness parameters are considered for optimisation. For robustness analysis shape, thickness and knee impactor position is included. Other studies that have addressed design robustness for crashworthiness include the following, Acar and Solanki (2009); Lönn et al. (2011); Zhang et al. (2007).
From the literature, it is realised that RDO for crashworthiness has been mostly limited to small scale problems with few design variables and single components such as a front rail. The design variables are normally metal sheet thicknesses and uncertainties generally include impactor variations. Furthermore the implementation of the simultaneous RDO approach for robust design is overlooked. These limitations are mainly due to the computational requirement. Hence to account for this, studies have implemented RDO via RSM, see Lönn et al. (2011, 2009); Sun et al. (2011), which is further discussed below. In this study robust design approach is presented to optimise both the size and shape of the structure considering also the shape parameter uncertainty. Special attention is given on ways to reduce the computational effort.

5.7.1 RDO using Response Surfaces

The computational effort for RDO have been reduced by using response surface approaches. This section gives a brief discussion of the approaches that could be used for RDO via RSM, see Section 3.5.3 for RSM.
A crude approach is to use a global response surface for RDO. For this DOE is used

to generate sample points within the global (full) design space. Then a representative surface is fitted to the evaluated sample points. The idea here is to check the robustness of designs on the response surface without additional design analysis. Although the computational effort reduces significantly, the response surface quality is vitally important. Hence large number of sample points are required to generate the response surface for accuracy, Koch et al. (2004). This approach can be further improved by using an iterative approach. In the iterative process local response surfaces are created in a sub-region, of the full design space, which increases the quality of local response surfaces. For each response surface support points, robustness points are generated considering the noise variables via a DOE. Then robustness analyses of the support points are performed on the local response surfaces, see Section 3.5.4 for IRSM. Although this approach could be used for designs with smooth responses, for crashworthiness it may not be able to represent the true behaviour such as bifurcation, see Section 3.5.3. Furthermore, since the robustness analyses are performed on the response surface the sensitivity of the design may not be well represented due to the smoothness of the response surfaces. To better represent the robustness behaviour of designs, a dual response surfaces approach has been used for RDO, Sun et al. (2011). Similar to above, first a DOE generates sample points in the global design space. Then these sample points are analysed and robustness study is made for each design. From the robustness analyses mean (μ) and standard deviation (σ) values are obtained for each design. Then two response surfaces are created, one for μ and one for σ, see Figure 5.8. These responses are then used for optimisation Sun et al. (2011). An iterative implementation of this approach is discussed in Aspenberg (2011). Performing robustness analyses of each design at each iteration is computationally expensive. Hence an approach is presented in Lönn et al. (2009) where the stochastic variation of the noise variables are only generated once. This information is then re-used to analyse the robustness of all other designs in the optimisation.
Another approach, similar to above, is presented in Aspenberg et al. (2013). Here the difference lies in the creation of the μ and σ response surfaces. First sample points are generated in the global design space. Then, for robustness analyses, DOE is used to generate local sample points around each design points. Each of the local sample points are analysed and a local response surface is created (local to each design). Robustness analyses of designs are then performed on the local response surfaces. From the robustness analysis μ and σ value are obtained for each designs. Then two global response surfaces are created for μ and σ which are used for optimisation.

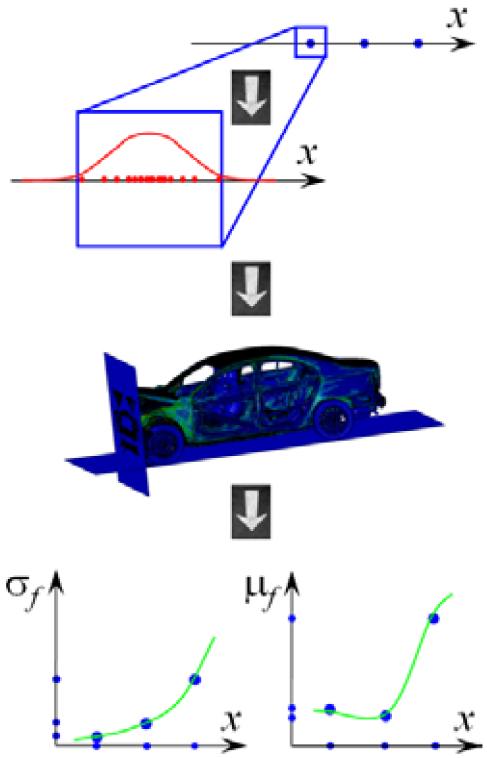

FIGURE 5.8 – Dual response surface approach to RDO, Aspenberg (2011).

PART III
Methods and Validations

Chapter 6

Shape Optimisation via SFE CONCEPT

6.1 Parameterisation with SFE CONCEPT

The success of shape optimisation significantly depends on the shape parameterisation used. Ideally, the number of possible shape configurations and the allowed shape modifications should be as large as possible. Also the adaptation of the parts to the modified geometry and the maintenance of the connections between parts are essential in cases with more complex structures. These parameterisation requirements can be fulfilled by SFE CONCEPT. In this chapter the essential features of SFE CONCEPT in the context of this thesis are presented[1], Rayamajhi et al. (2013b).

6.2 Parametric Modelling

SFE CONCEPT uses implicit parametric geometry models to realise shape changes, see Section 4.2.2. The main difference lies in the mathematical description compared to other tools such as CATIA, ProEngineer, SolidWorks or Siemens NX. The parametric SFE CONCEPT models are mainly based on three objects: points (influence points, IP), lines (base line, BL) and cross-sections (base section, BS). Complex geometries, such as joints and multi part connections, can be derived using these objects. Finally, parametric free form surfaces can be included.
The IPs are defined by the x, y and z coordinate values. All SFE CONCEPT object locations are determined by the IPs as they carry the global coordinate information. BL are created using two influence points. The location of the base line is modified by simply changing the coordinates of the IPs. Also the curvature of the base line can be modified by changing the tangents at the two IPs.

1. SFE CONCEPT version 4.2.5.2 is used.

The sections can be created either by using existing FE model sections as a template or a grid can be used to sketch a new section from scratch. Section IPs and segments are used to define a section shape, see Figure 6.1. Complex sections can be created by modifying the section IP locations, segment angles and curvature, connection location of the section lines or using multiple panels within one section.

The BL and base sections are used to create beams. A simple beam consists of two sections which can be of the same or different configurations. Complex beam geometry can be defined using several varying cross-sections along the beam length, see Figure 6.1; where a modified beam due to scaling of the two middle sections is shown. Since the beam is created using sections and one base line, any changes made to these objects vary the geometrical configuration of the beam, see Figure 6.2 depicting a modified section obtained via moved section IPs, Figure 6.2(a), and horizontal bend on the beam by changing the locations of the two middle sections, Figure 6.2(b).

A joint can be created at a connecting point between beams. Smooth connecting surfaces are created automatically between the beams using their cross-section lines. Once the joint is created, the joint surfaces adapt to any changes made to the beam shape, see Figures 6.3 and 6.5. The joint angle, curvature and location can also be used as parameters.

Surfaces are created using closed boundaries defined by lines. A flat surface is crea-

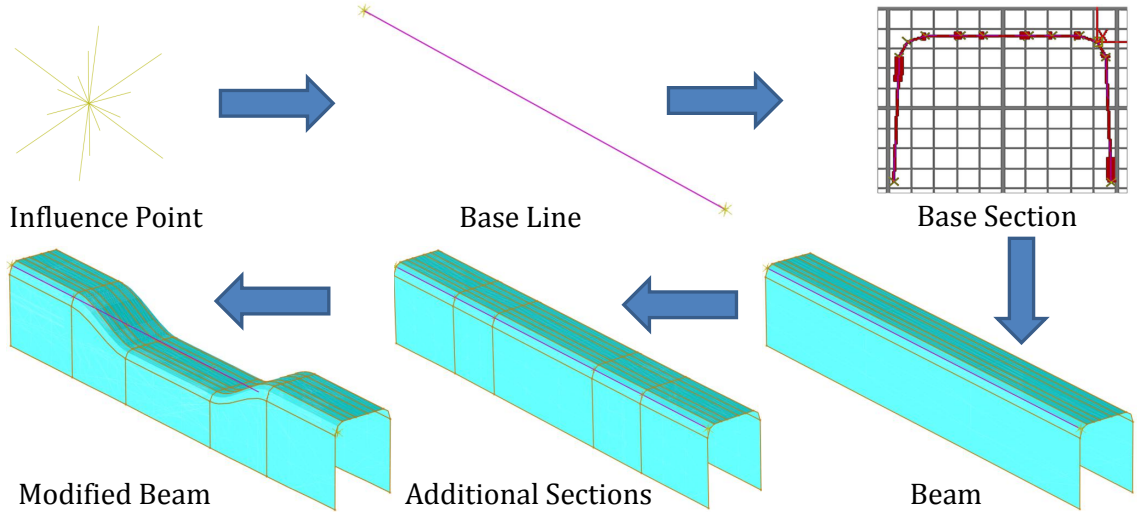

FIGURE 6.1 – Typical SFE CONCEPT shape variation based on two beam IPs, one BL and 12 cross-sectional IPs showing the transition from the original cross-section to the scaled cross-section.

ted for a boundary with straight lines; for a boundary with curved lines smooth curved surface is created, see Figure 6.3 where flat surfaces are created with the beam lines. Additional lines can be added to the surface for complex geometry. The surface can then be modified by changing the curvature of the boundary lines, the additional lines or both.

Main features that make SFE CONCEPT an ideal tool for optimisation include the

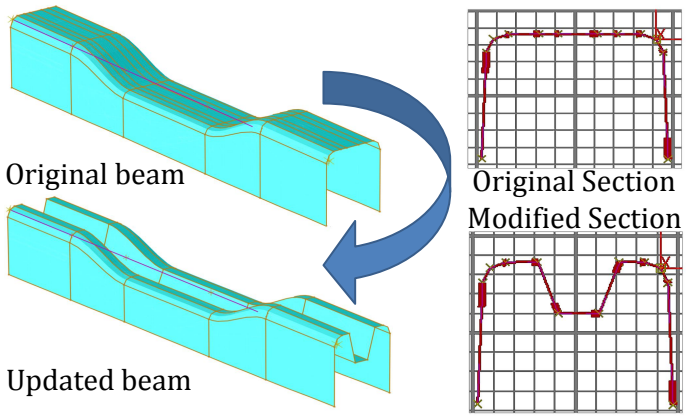

(a) Steps for section update resulting to modified beam shape.

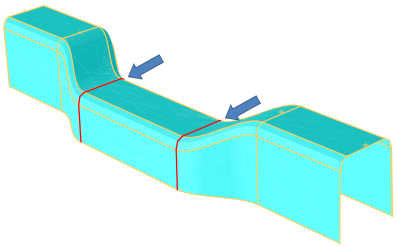

(b) Horizontal bend by changing cross-sections location.

FIGURE 6.2 – Typical SFE CONCEPT shape variation modifying a subset of IPs of the cross-section and cross-sections locations.

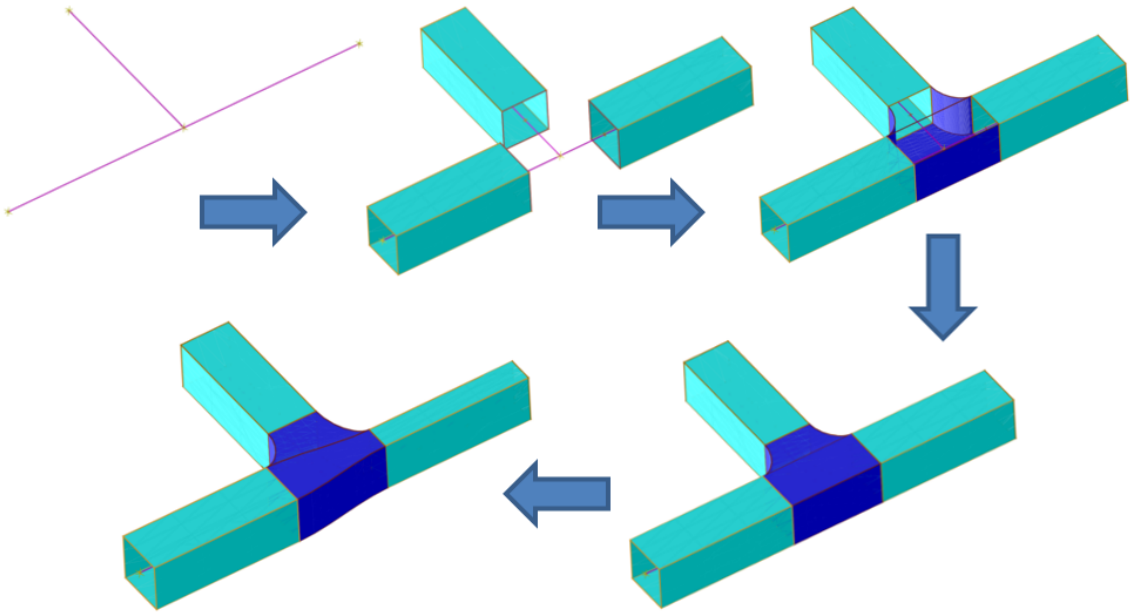

FIGURE 6.3 – Steps for automated joint creation and automatic adaptation to modified beam geometry, adapted from Hilmann (2009).

ability to realise large shape variations while maintaining the connection between adjacent parts, see Figure 4.3. Furthermore the modification of number of parts in a connection can be achieved due to its mapping technique, presented in the following sections. Since the mesh is only generated after shape modifications, the critical mesh distortion is avoided, which is a problem for some shape modification techniques, see Section 4.3.1. In cases where the results are mesh dependent, the re-meshing introduces jumps in the objective functions and constraints. Hence it is a challenge for optimisation algorithms. However this is not relevant for crash optimisation because it is known that crash simulations are not repeatable, specially when parallel computation is used. Contact bifurcations and numerical rounding errors also introduce the jumps in the objective functions and constraints without re-meshing. These are not addressed in this thesis.

6.3 Implicit Parameterisation via SFE CONCEPT

6.3.1 Mapping Technique

A mapping technique enables the definition of additional connections between different objects. Mapping means here projecting source objects to a target object such that the source is dependent on the target object. Both map object and map target can consist of one of the following objects ; point, line, section and surface. A point can be mapped to either one of the following: point, line, section or surface. A line can be mapped to another line or a surface and similarly a surface can be only mapped to another surface. If an object is mapped to a target, any changes made to the target will incur changes in the mapped object. However changes to the mapped object cannot be made independently of the target.

Point to Line Mapping

A general example of point to point and point to line map is presented here, the reader is referred to SFE CONCEPT (2009) for information on other map types. In Figure 6.4 point P is the map object and line AE is the map target. Various maps of point P to line AE can be made for a desired topological connection.

Map to furthest point: A point can be mapped to the furthest point of a line in a given direction, In Figure 6.4 point P is mapped to the furthest point (point A) of line AE in the negative x direction.

Map by direction: The desired direction for mapping can be chosen with the combination of x, y and z values. The direction of map is shown by an arrow, Point B in Figure 6.4.

Map target normal: This simply maps an object to a target in the normal direction. Point P is mapped to line AE at location C in Figure 6.4.

Map by parameter: A point can be mapped to a line by parameter (parameter of the line length) in terms of the location of the point on the line. The total length of the line is given as 1, in Figure 6.4 point P is mapped to point D with parameter 0.75 of the line AE.

Offset map: A mapping with offset distance in the x, y and z direction can be made between two points. In Figure 6.4 point P is mapped to point E, of line AE (without changing its y position, see point P') with an offset of (0, -3). This mapping is of special interest in this thesis for shape parameterisation. This is further discussed in Section 6.4.2.

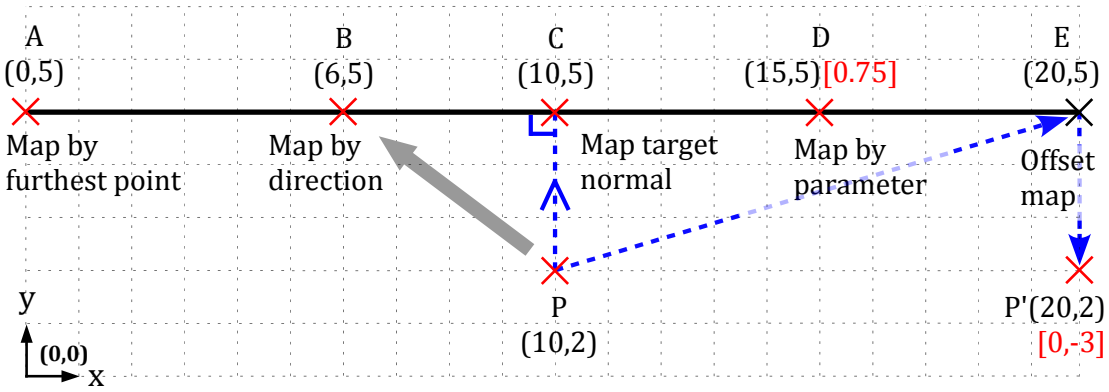

FIGURE 6.4 – Example of map types: IP to IP and IP to base line maps.

To highlight the mapping approach, one of the simplest examples (uses) of an IP (point) to line map is given in Figure 6.5. This example represents a topological joint connection between two beams. In Figure 6.5, beam B_2 is connected to beam B_1 by mapping the IPs and beam cross-section lines. IP_4 of beam B_2 is mapped to line L_1 of beam B_1 by parameter. The non-highlighted area represents the initial position of beam B_2 and joint, represented by IP_4 at 0.3 of line L_1. Once all the mapping, IPs and cross-section lines, are made the location of the joint can be simply modified by changing the location of IP_4 along line L_1, see Figure 6.5: IP_4' at 0.8 as new joint location. The beam B2 and its joint with B1 are defined to follow the change of IP4.

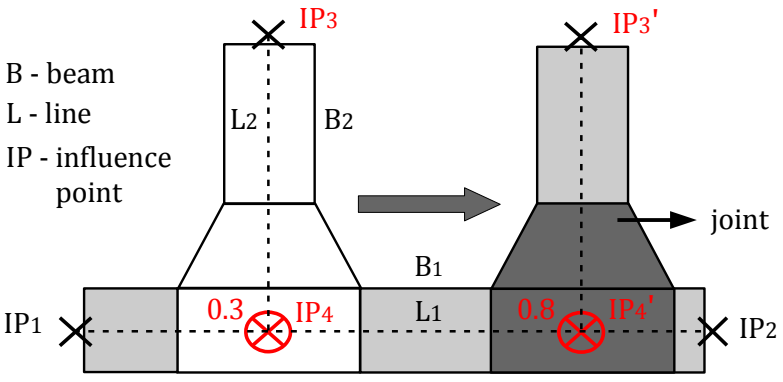

FIGURE 6.5 – Demonstration of IP to line mapping for topological joint connection.

Surface to Surface Mapping

Surface to surface mapping adds additional flexibility for the parameterisation of designs in SFE CONCEPT. This feature is specially beneficial for design parameterisation such that there are interchange and adaptation in the number of connecting parts, see Figure 4.3. A surface to surface mapping is presented in Figure 6.6 where a seat cross-member is mapped to the floor and rocker with two parts. When the cross-member moves from one surface (yellow floor and light green rocker) to another (green floor and blue rocker), the mapping information, multi flange and weld spot are automatically updated and the connectivity is maintained.
SFE CONCEPT also has a modular library feature where pre-optimised or new design features and design details can be stored for future use. It is important here that the mapping information between the design features should be pre-defined. Once the mapping is made it allows fast modification of designs by adding or removing design features and also a good collaboration between the design teams, see Figure 6.7 where the details such as beads and stamps are added to the design.

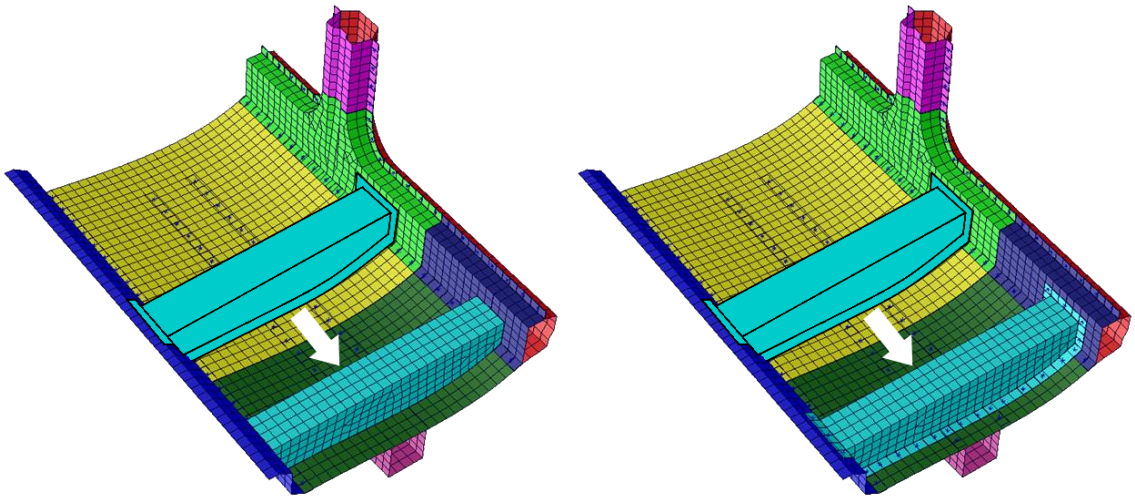

FIGURE 6.6 – Surface mapping and adaptation of multi-flange and weld spots, adapted from Zimmer (2006).

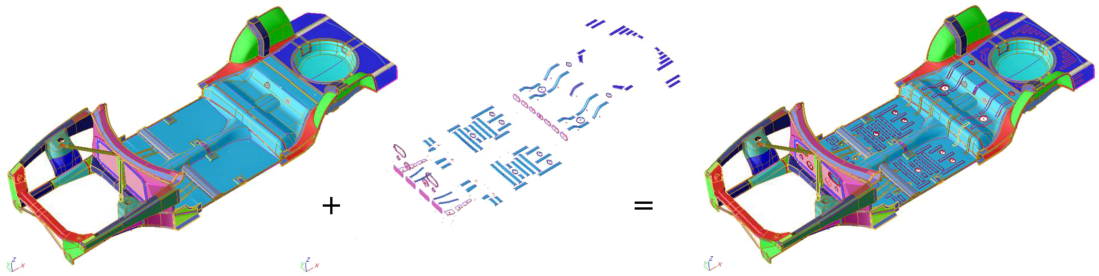

FIGURE 6.7 – Parametric details from the modular library, Zimmer et al. (2009).

FE CONNECT

This is a special application of the mapping technique. It is presented here since this feature is used later in the thesis. In crashworthiness study often only a small part of a large structure is considered for optimisation. Hence sub-models are used for optimisation to reduce the simulation time of the models, see Chapter 7. However in such approach it is important to maintain the interaction between the sub-model and the remaining model for the correctness of the sub-model results. It is therefore necessary to embed an updated parametric sub-model into the remaining, i.e. unchanged, FE model to obtain the updated interface conditions. In this approach, the parametric model is mapped onto the remaining FE model by a special feature in SFE CONCEPT, so-called "FE CONNECT".
The process to create this mapping is shown in Figure 6.8. First the FE model is imported into SFE CONCEPT. A parametric model is created close to the FE model boundaries. Additional connection sections are created in the FE model using the interface nodes. These section lines carry the information of the interface nodes of the FE model to connect the parametric model. BL are created between the FE sections and the parametric model sections to create closed boundaries. These closed boundaries are used to create filler surfaces for smooth transition of surface between the FE model and the parametric model.

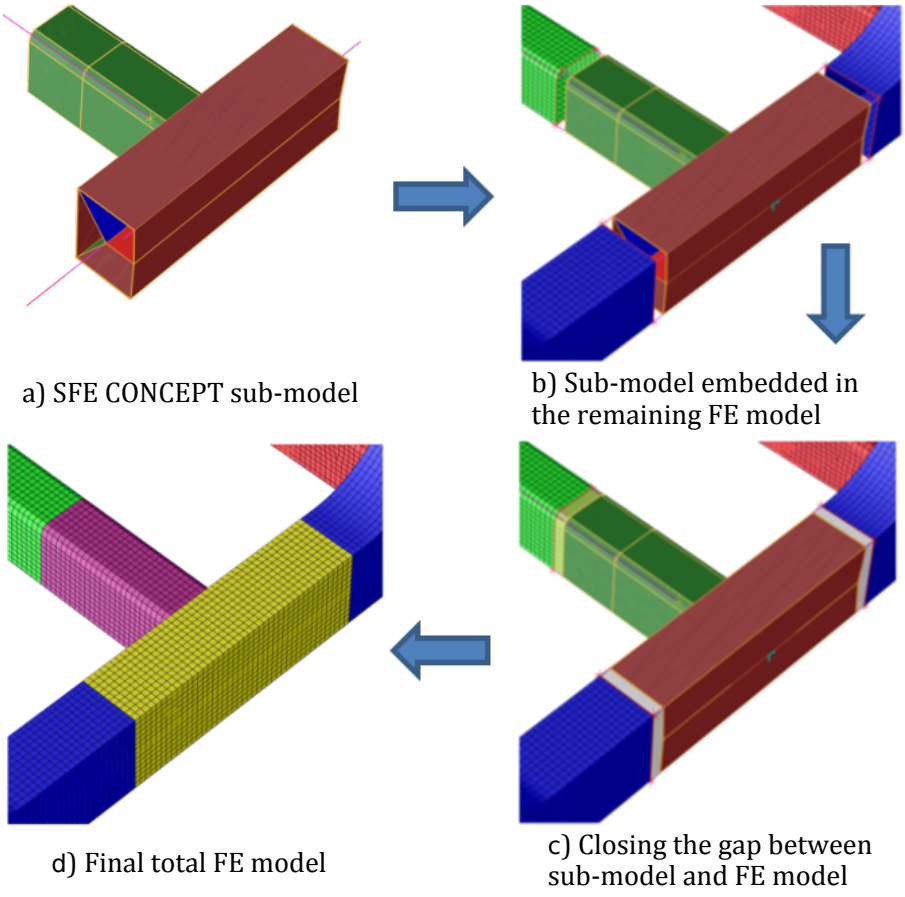

FIGURE 6.8 – Connecting parametric model to FE model.

6.4 Geometrical Compatibility

SFE CONCEPT has the capability to define design parameters both explicitly and implicitly which gives the user a great flexibility to define design parameters, see Section 4.2. This section presents now how these techniques and in particular the mapping approach can be used to avoid geometrically incompatible designs.

6.4.1 Dependent design parameters

Since some of the geometrical compatibility issues arise due to the dependency of parameters, it is crucial to define this dependency to avoid geometrical conflicts [2]. In a simple case where two parameters are dependent on each other, if the information of one parameter is known then the second parameter can be modified accordingly. Hence for simple cases (few shape parameters) the geometrical conflict can be avoided by simply defining dependent parameters. Also the ability to define dependent parameters is available in some of the optimisation tools, such as in optiSLang optiSLang (2011). To the authors' knowledge, from literature survey, this can be done by two approaches, presented in the next paragraph.

Dependent design parameter rules

Parameter dependency can be defined as simple or conditional. In a simple dependency, mathematical expressions are used whereas for conditional dependency, variables are calculated in-terms of some conditions such as if, then or else. A simple dependency case is shown in Figure 6.9(a) which represents a beam cross-section with two reinforcements with height A and B respectively. In Figure 6.9(a), H defines the design space for A, B and also B is dependent on A. Generally to remove a geometrical conflict the upper bound for A and B would be defined such that they do not cross the horizontal dotted line (allowing for maximum height configuration simultaneously for both A and B), see Figure 6.9(a) (left) where D (blue area) is the allowable space for parameter B. However in cases where A is small, the allowable space, D, for parameter B increases (red area, Figure 6.9(a), centre) but this extra space is not explored by parameter B due to the upper bound setting. Also if the design space, H, is changing (Figure 6.9(a), right) then parameter A is dependent on parameter H and parameter B is dependent on parameters A and hence H. In this case it gets even more difficult to assign the bounds for parameters A and B without reducing the design space. Hence for the dependent parameters (A and B) the design space is constantly changing depending on the driving parameter (in this case parameter H and A) and this has to be taken into consideration to explore more design configurations. To avoid overlapping, either B should be modelled as

2. Another compatibility issue is related to the outer design space due to presence of other components around the modified geometry, assembly of parts.

dependent on A or vice versa.

Parameter dependency for this case can be defined by simple mathematical expressions, see Equations (1 - 5). There, X and Y determine the position of parameter A and B depending on parameter H. Example: if $H = 10$, $X = 0.8$ and $Y = 1$; then $A = 8$, the allowable space for B is 2 and since $Y = 1$; $B = 2$. A geometrical configuration achieved from this parameter dependency setting (which cannot be achieved by bound definition) is shown in Figure 6.9(b).

$$\mathrm{A} = \mathrm{H.X} \tag{6.1}$$

$$\mathrm{B} = (\mathrm{H} - \mathrm{A})\mathrm{Y} \tag{6.2}$$

$$0 < \mathrm{X} < 1; \quad 0 < \mathrm{Y} < 1. \tag{6.3}$$

However the definition of dependent parameters with this approach becomes more

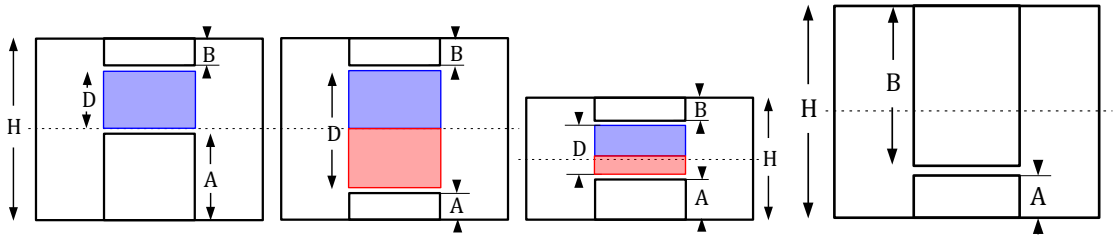

(a) Problem due to bound definition.

(b) A possible configuration by parameter dependency definition.

FIGURE 6.9 – Parameter dependency definition - simple problem.

difficult for complex design cases and also for a higher number of design parameters. A slightly complex design is shown in Figure 6.10(a) where the red boundary defines the outer design space and the blue lines represent the cross-section of a front rail. As parameters, the locations of the corners may be taken. The definition of parameter dependency becomes even more complex and tedious if the cross-section varies along the front rail beam. Here, the simple definition of mathematical dependencies between the design parameters becomes more or less impossible. Therefore the parameter interdependency definition is used to adopt designs in the upper and lower bound. For design with greater complexity an offset mapping technique can be used.

The parameter dependency for such complex problems can be better defined using so-called offset mapping techniques where physical objects such as IPs, lines are used to control the design geometry instead of mathematical expressions. This is explained in the following paragraph.

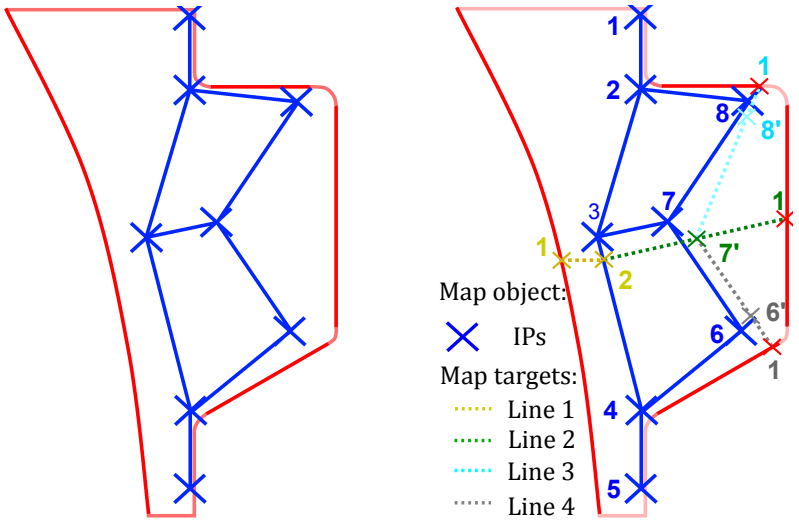

(a) A more complex cross-section (blue) within a design space (red) which is difficult to parameterise with simple mathematical expressions.

(b) The same cross-section now parameterised with the offset-mapping technique.

FIGURE 6.10 – Parameter dependency definition - complex problem, Hunkeler et al. (2010).

6.4.2 Offset Mapping

Offset mapping is a technique where the changes in design objects such as IPs, lines..., are controlled via so-called construction objects, see for example line L_1 and line L_2 in Figure 6.11. These construction objects are also SFE CONCEPT objects such as IPs, base lines, section segment lines but they are not part of the design. The information of these construction objects, such as length of section line, are used to change the design configuration. Such mapping technique can be used to control design variables to avoid geometrical conflicts. In the following sections this offset mapping approach is presented for a few parameterisation problems.

Cross-section Parameterisation

In Figure 6.11 one of the simplest offset mapping network (same parameterisation problem as in Figure 6.9) is presented to demonstrate the technique. Here the map targets are lines L_1 and L_2 and map objects are points (IPs) P_7-P_{10}. Points P_1 and P_2 of line L_1 are mapped to the design space boundary (black lines) in the normal direction (normal map, see Figure 6.5). Point P_4 of line L_2 is mapped to line L_1 at position P_3 by parameter (0.5 of line length L_1) and point P_5 is mapped to the design space boundary in the normal direction. Points P_9 and P_{10} of the upper reinforcement are mapped to line L_1 at position P_3 by an offset distance. Similarly points P_7 and P_8 of the lower reinforcement are mapped to line L_2 at position P_6 by an offset distance.

Due to the type of mapping network used, the position of lower (green) reinforce-

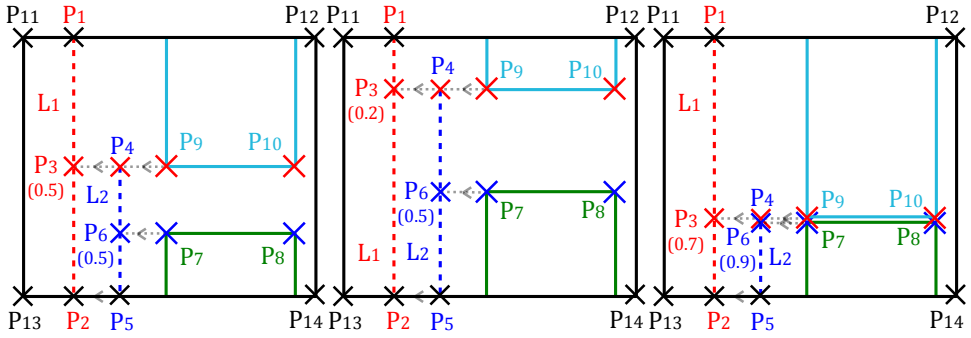

FIGURE 6.11 – An offset mapping network for cross-section shape - fixed design space.

ment is dependent on the position of upper (light blue) reinforcement. Since points P_9 and P_{10} are mapped to point P_3, the position of points P_9 and P_{10} (and hence the height of upper reinforcement) is controlled by point P_3, see Figure 6.11 (centre). Also since point P_4 is mapped to point P_3 and point P_5 of line L_2 is mapped to the boundary, the length of line L_2 increases in Figure 6.11 (centre). Now the points P_7 and P_8 of lower reinforcement have bigger allowable space for shape modifications. The overlap between the two reinforcements never exists because point P_6 can never exceed point P_3. This mapping network also works when the design space is changing as the offset mapping beams are mapped to the design space boundaries.
Another similar example is shown in Figure 6.12. The map target lines are mapped to the design space boundaries. The green and red map object IPs (points) are mapped to green and red map target IPs respectively. Here the aim is to keep the reinforcement within the design space when the design space is modified. In Figure 6.12 four different configurations and their respective parameter values are shown.
Also for the complex problem presented in Figure 6.10(a), the offset mapping net-

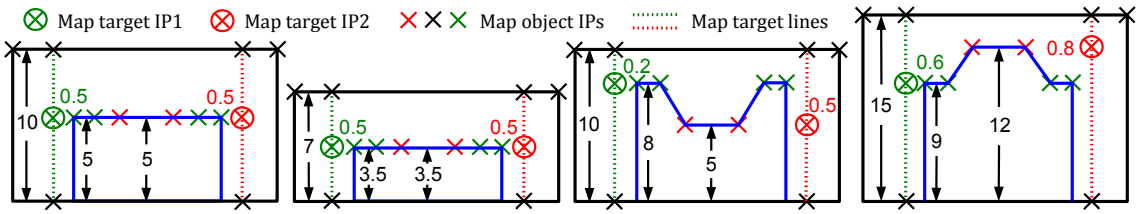

FIGURE 6.12 – An offset mapping network for cross-section shape - changing design space.

work is presented in Figure 6.10(b). For a beam with varying cross-section along the beam, different offset mapping network can be constructed.

Non-cross-section Parameterisation

For the non-cross-section parameterisation, with offset mapping technique, the crash box trigger parameterisation problem discussed in Section 4.4 (Figure 4.4) is

presented. In Figure 6.13, a crash box design (side view) with two triggers is shown. The aim here is to avoid conflicts between the two triggers when modifying their location along the crash box. In this example Line L_1 and L_2 are the map targets and points 9-24 (of the triggers) are the map objects. In Figure 6.13(a), point 1 of line L_1 is mapped to the edge line of the crash box (by parameter) at position 1'. Similarly point 2 of line L_1 is mapped to point 8 of crash box (normal map). Point 3 of line L_2 is mapped to line L_1 by parameter at position 3' and point 4 is mapped to point 8. Now all the points of the left trigger are mapped to point 1 (which is at location 1') and all the points of the right trigger are mapped to point 3 (which is at location 3'). Here the right trigger is dependent on the location of the left trigger. Similar to the previous example, the overlap between the two triggers never happens because point 3' cannot pass point 1', see Figure 6.13(b). Additional offset line networks can be added to control also the width and height of the triggers.

Another non-cross-section parameterisation is presented in Figure 6.14 where the

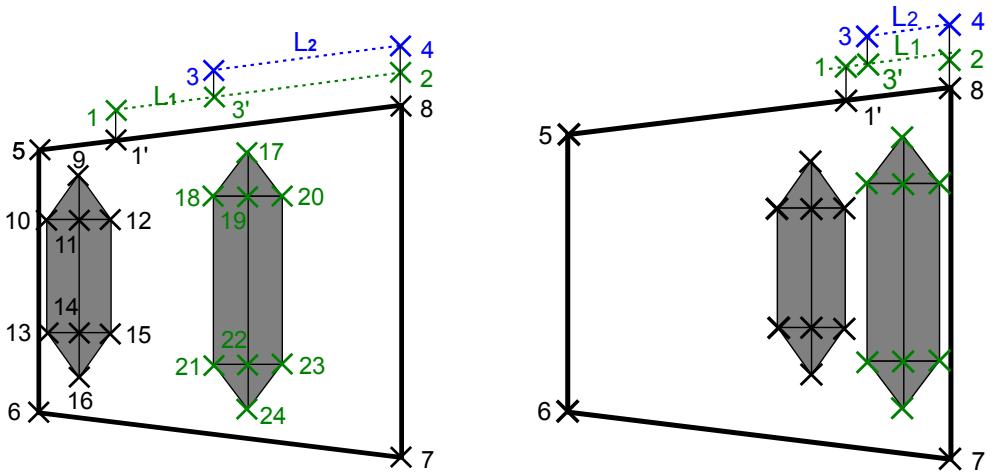

(a) Initial trigger setting.

(b) Modified trigger setting.

FIGURE 6.13 – Side view of a crash box with triggers and offset mapping lines.

mapping beam is green (not part of the design), red surface is the design space and blue is the structure to be modified. Three configurations are shown which are controlled by the two middle cross-sections of the mapping beam (green).

The offset mapping capability with the implicit modelling approach assists for grea-

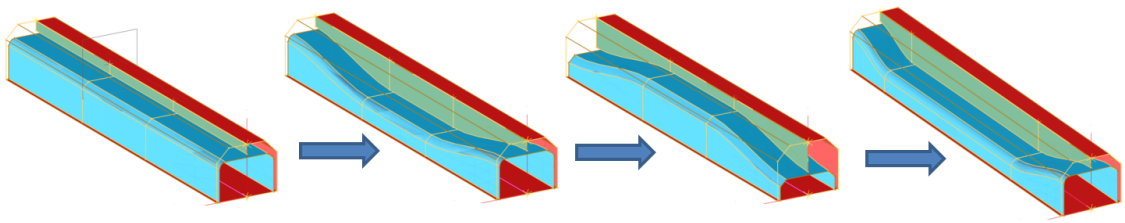

FIGURE 6.14 – Non-cross-section design modification (blue) with offset mapping beam (green) within the design space (red).

ter flexibility in shape parameterisation and to solve geometrical incompatibility issues. Although offset mapping technique can be used effectively to avoid geometrical conflicts often it cannot be used to resolve all the geometrical conflicts, specially in the presence of large number of shape variables, without reducing the design space. Hence the user has to select the most important conflicts that has to be avoided without reducing the design space. It is also a good practice to use both implicit and explicit design variables to achieve the desirable parameterisation.

6.5 Records of Shape Parameters

In SFE CONCEPT the way parameters are handled during an optimisation depends on the *Record* feature. First the decision has to be made regarding what design modifications are preferable. Then a *Record*/parameter name is set for the particular design variable. The *Record* function is activated with the start button. Any model modification made, when the *Record* is active, is saved to the *Record*/parameter name. The parameter *Record* is completed with the stop button.
A parameter value of zero is assigned to the original model, i.e. before any modifications, and a parameter value of 1 is assigned to the modified design. The modifications to the design, when the *Record* values are changed, can be viewed in the GUI window. Also the modification to an already defined parameter can be achieved simply by adding, removing or modifying entities from the records.

6.6 Batch Mode Process

SFE CONCEPT can be fully ran in batch mode from parametric model update to FE mesh generation. This feature is important for the realisation of an automatic closed optimisation loop, Figure 6.15. A typical batch script is shown in Appendix A.1.
Here the parametric model is loaded in SFE CONCEPT and updated with the new design variables. The updated model is saved and meshed with the required element size. A solver is chosen for the export of appropriate FE model and additional definitions such as spot welds. The model is then exported, in the chosen format, with the option of choosing only the required parts for export.

6.7 Optimisation Workflow

An optimisation loop is established here with three main components. SFE CONCEPT, SFE CONCEPT (2009), is used as the geometry controller and the mesh generation tool, RADIOSS, RADIOSS (2011), as the explicit finite element solver and optiSLang, optiSLang (2011), as the optimiser. optiSLang controls the op-

timisation loop (workflow) and uses optimisation algorithms to advance the process. optiSLang offers various functionalities such as sensitivity analysis, multi-objective and multi-criteria optimisation while its speciality lies in robust design optimisation and reliability based design optimisation. In-terms of optimisation algorithms it supports gradient based algorithms, population based algorithms (evolutionary, genetic and particle swarm) and response surface based optimisations (single surface or iterative approach).

For optimisation, variations in the geometry and other design attributes are recorded in SFE CONCEPT. The parameter bounds (allowed upper and lower bound of each parameter) are fed into the optimiser. Design geometries are created in SFE CONCEPT corresponding to the parameters generated by optiSLang. These designs are meshed in SFE CONCEPT and exported in RADIOSS format. The FE model is complemented by additional external FE definitions (external to SFE CONCEPT) such as material parameters and impactor models using scripts written in Perl. This compiled file is then analysed using RADIOSS and the responses fed back to optiSLang. Hence a loop is created as shown in Figure 6.15.

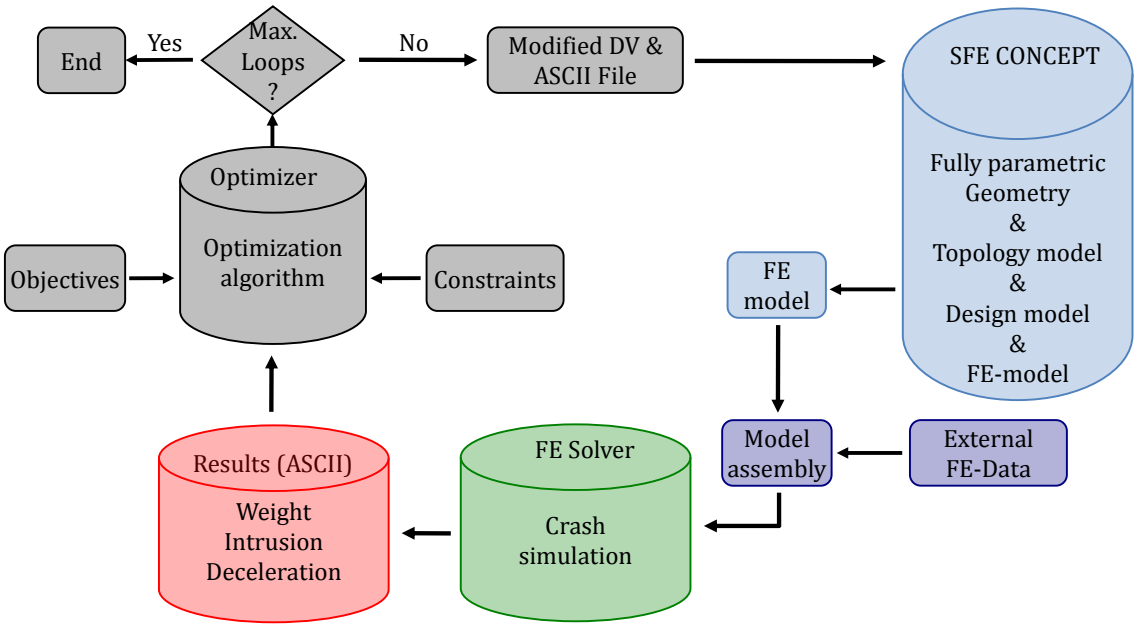

FIGURE 6.15 – Optimisation workflow, Volz et al. (2007).

6.8 First Validation: Bumper Beam

A first example is chosen to validate the parameterisation and optimisation approach. Because this is a rather simple case and does not reflect sufficiently well the industrial situation, a second example is presented which represents an industrial case with a very restrictive design space and shows clearly the necessity to find ways to reduce computational effort.

6.8.1 FE Model and Design

An initial geometry of the bumper system and a rigid impactor is created in SFE CONCEPT, see Figure 6.16. The bumper geometry is meshed with an element size of 10 mm (except the impactor) resulting in approximately 10,000 shell elements. A section is created on the crash box, at the impact side, to measure the axial forces. Three measuring grids are created at the inner surface of the beam which measure the maximum beam deflection in the x direction. The beam intrusion is measured using the displacement of the impactor. An average computational time for the model is 14 minutes, on a 4 core Intel Xeon E5410 2.33 GHz CPU, with an impact duration of 65 ms. The impactor mass is 1200 kg and the impact velocity is 15 kph in the x direction. This corresponds to the repair crash test, see RCAR (2011) for RCAR repair test. The front end module plates (stays) are fixed in all directions.

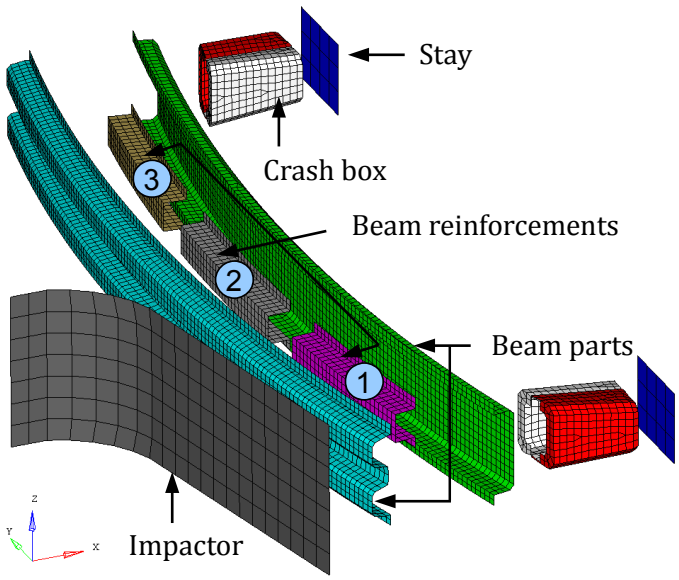

FIGURE 6.16 – Exploded view of the initial bumper design.

6.8.2 Design Space Definition without Geometrical Conflicts via Offset Mapping

The bumper design parameters are categorised into the beam and the reinforcement parameters. The parameterisation is motivated by industrial needs as discussed with the industrial partners[3]. In total there are 28 design parameters, 7 beam parameters and 3 reinforcements with 7 parameters which consist of shape, location and thickness parameters. For shape parameters, the cross-section control points are used to modify the shape, see Figure 6.17(a).

In Figure 6.17(a), coloured squares represent the cross-section shape control points

3. PSA Peugeot and Citroën.

of the beam and reinforcement. Similar coloured control points are used to define a parameter, for example red for parameter A (beam height). A control point with two colours means they are used to define two parameters, e.g. blue for parameter B and light green for parameter C. In Figure 6.17 the parameterisation of one reinforcement is shown ; the same parameterisation is used for the other two reinforcements. The position of the reinforcement is modified by changing the parameters L_1 and L_2 (reinforcement cross-section positions which define the reinforcement length) within a portion of the main beam, see Figure 6.17(b) for the design space for one reinforcement. The initial values and the bounds of the parameters are specified in Table 6.1.

The mapping network for the bumper beam and the reinforcement is shown in Fi-

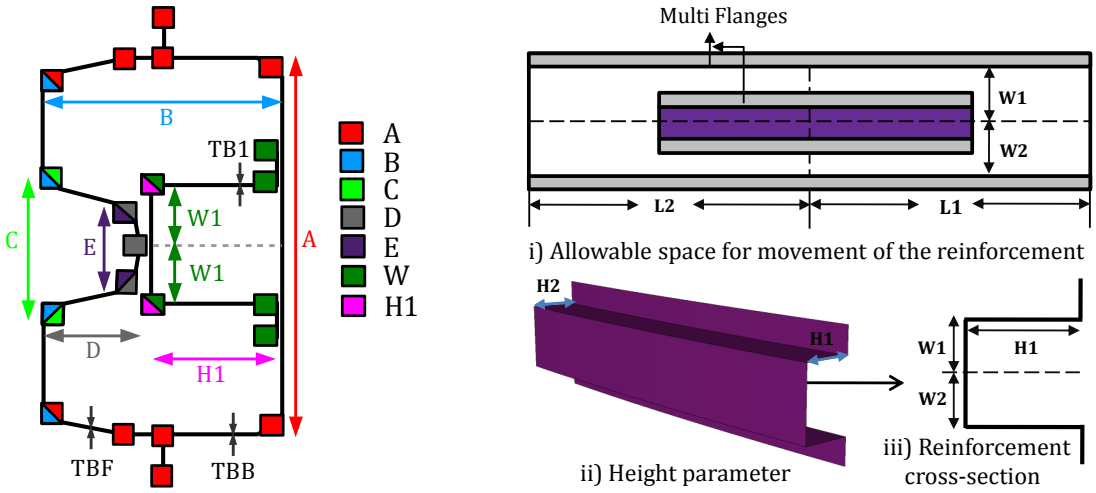

(a) Beam cross-section parameters - control points.

(b) Beam reinforcement parameters.

FIGURE 6.17 – Bumper beam and reinforcement parameterisation.

Units in mm	Beam parameters							Reinforcement parameters						
	A	B	C	D	E	TBF	TBB	B_1H_1	B_1H_2	B_1W_1	B_1W_2	B_1L_1	B_1L_2	TB_1
Upper bound	121	70	51	25	30	2.5	2.5	48	48	30	30	156	156	1.5
Initial design	101	64	35	20	26	1.5	1.5	48	48	20	20	131	131	1.0
Lower bound	93	59	19	3	18	1.0	1.0	20	20	10	10	31	31	0.5

TABLE 6.1 – Initial design parameters and parameter bounds for beam and reinforcement.

gure 6.18(a). In Figure 6.18(a) the outer design space (red boundary), beam cross-section lines (solid lines) and mapping lines (dotted lines) are shown. The principle approach to create such offset mapping network is presented earlier in Section 6.4.2.

For the presented design case, although there are various parameter conflicts, one obvious parameter conflict occurs between beam parameter D and reinforcement parameter H_1, see Figure 6.18(b)(left). Ideally both parameters should be allowed to have the maximum variability possible to keep the size of the design space. However this is difficult to define through the upper and lower limits, due to the parameter dependency. Here a offset mapping is made such that the allowed variability of parameter H_1 is dependent on the size of parameter D. Similarly the reinforcement widths, W_1 and W_2, are modified dependent on the size of beam height, parameter A.

Figure 6.18(b)(right), shows the possible maximum settings of parameter D and

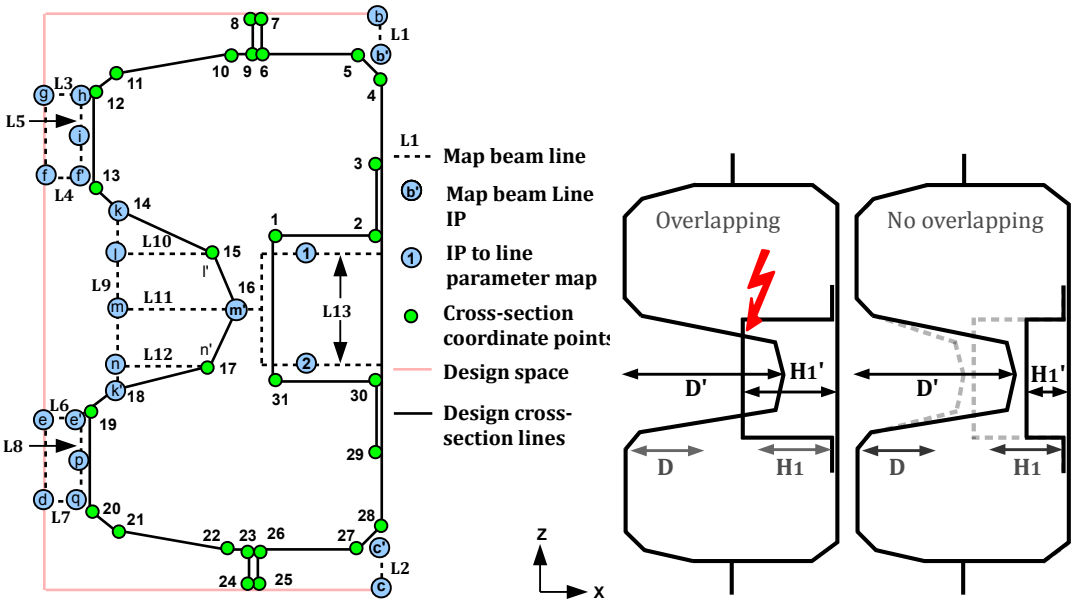

(a) Offset mapping network. (b) Parameter overlapping issue.

FIGURE 6.18 – Offset mapping network and an example of possible parameter conflict.

parameter H_1 through offset mapping. However this is not achievable through the upper and lower limit definition of the parameter since it over-constraints the design space for parameters D and H_1. The maximum setting of the parameters with bound definition are shown in Figure 6.18(b)(right) with dotted lines.

6.8.3 Optimisation Problem Definition

The optimisation is formulated considering the constraints on maximal force in the crash box, $F_{\max} = 140$ kN, maximum intrusion, $I_{\max} = 80$ mm, and maximal deflection, $D_{\max} = 85$ mm, at the impact end of the bumper. These constraints are applied such that the damage to the other structures such as front rail (plastic deformation), radiator, hood and lights are avoided. The initial bumper design violates all three constraints, see Table 6.2. Hence the initial bumper design is first

optimised with respect to the constraints to identify a feasible region and then minimised concerning mass. A commercial EA is used considering both recombination and mutation operator. The optimisation software used here is optiSLang, optiSLang (2011). Before the optimisation is performed a global sensitivity analysis is made to screen the most important design variables, see Tu and Jones (2003) for an screening approach. It is found that the beam parameters are more dominating than the reinforcement parameters (only some parameters of the reinforcement on the impact side are important). The results of the sensitivity study can be found in Section A.2(Appendix). Hence the optimisation is run in two stages. In stage I only the beam parameters are optimised and the reinforcement parameters are fixed. In stage II the optimisation of only the reinforcements is made (beam parameters fixed) using the optimum beam shape parameters from Stage I.

6.8.4 Optimisation Results

Optimisation Stage I

A design improvement is found after 111 finite element computations with a mass of 13.4 kg resulting in the increase in bumper system mass by 2 kg. Although there is an increase in mass the design is now feasible. The outputs of the optimum design from this stage are provided in Table 6.2. A comparison of the initial cross-section design (dotted lines) and the optimum cross-section design (solid blue lines) is shown in Figure 6.19(a).

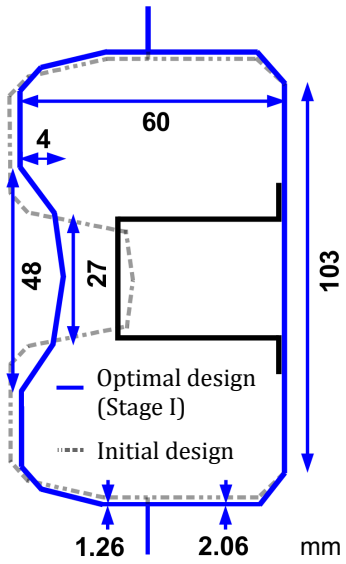

(a) Optimum bumper beam and reinforcement 1 cross-section shape.

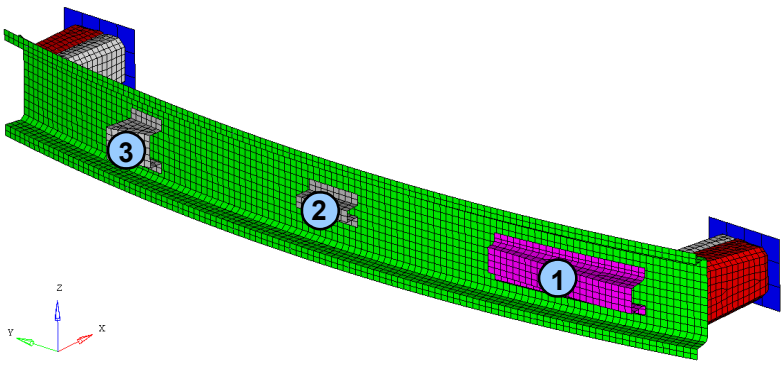

(b) Optimum reinforcement shapes and locations.

FIGURE 6.19 – Optimum bumper beam design.

Outputs	Mass (kg)	Max. section force (kN)	Max. deflection (mm)	Intrusion (mm)
Initial	11.4	168.3	90	85
Stage I	13.4	139.4	80	78
Stage II	12.8	134.1	81	80

TABLE 6.2 – Design outputs: start and improved designs (Stage I and Stage II).

Optimisation Stage II

It took 369 design evaluations to find the improved settings for the reinforcements due to the high number of design variables (21 reinforcement variables). The optimum shapes and locations of the three beam reinforcements are shown in Figure 6.19(b). There is a marginal improvement in the mass of the bumper system, see Table 6.2. Looking at Figure 6.19(b), an obvious result is that the size and thickness (1.20 mm) of the reinforcement (reinforcement 1) on the side of the impactor is more influential than the other reinforcements (reinforcement 2 and 3) further away from the impactor. Hence the parameter values for reinforcements 2 and 3 are at their minimum and could be removed from the design for this impact case. Also the cross-section configuration in Figure 6.19(a) (both beam and reinforcement cross-sections) would not be achievable using the upper and lower bound definition because of penetration, see dotted and solid black lines. This improved configuration is achieved due to offset mapping.

6.8.5 Conclusions

A method for shape optimisation using a parameterisation which avoids geometrical conflicts is presented in this section. For such problems, an offset mapping technique is proposed here. This enables that the geometry can be modified without conflicts maintaining the desirable large range of design variables. This type of parameterisation gives parameter settings for physically feasible designs with no surface penetrations and overlap. The parameterisation approach is successfully validated on a simple bumper design case to avoid geometrical compatibility issue.

6.9 Second Validation: B-Pillar Reinforcement

In this section a second validation case is considered for shape optimisation. The design case is very restrictive for shape variation and hence it is a challenge to parameterise the design without geometrical conflict.

6.9.1 FE Model and Design

An industrial half car FE model is provided to optimise the reinforcement of the B-pillar for lateral impact. The FE model and impact case is adapted to the in-house physical test that is performed to test the performance of the lateral structures [4]. The half car model is cut in the longitudinal plane of the vehicle. The model is composed only of the structures directly involved in the vehicle lateral stiffness: the B-pillar beam with reinforcement, roof and seat cross-members and the rocker with their corresponding reinforcements. Here the full floor panel, seats and the front and rear doors are not included in the model, see Figure 6.20(a).

In the physical model the metal sheets at the cut plane are welded to a rigid fixed plate. Similar boundary conditions are applied to the nodes in the FE model shown in Figure 6.20(b). The door hinge reinforcement is represented by a rigid tube welded between the two hinges. This reinforcement helps to distribute the forces between the upper and lower hinges.

The impactor is modelled as rigid. The offset in the y direction between the impactor structures, Figure 6.21 is set to obtain the desired sequence of loading and deformation of the B-pillar.

For the impact conditions, an impactor mass of 898 kg is used with an impact velocity of 14.4 kph in the y direction. The total impact energy is scaled here to take into account the energy absorbed by the missing structures such as doors and floor. The actual impact velocity is 50 kph for lateral impact in EuroNCAP test (www.euroncap.com).

The model is meshed with an element size of 10 mm resulting in 117,000 shell elements. The parts are assembled using spot welds which are modelled as linear spring elements without rupture. The total computation time for the model on a 4 CPU Xeon machine is about 10 hours with an impact duration of 90 ms.

6.9.2 The B-pillar Design

The model provided is in the late design phase with detailed and complex geometry, Figure 6.20(a). The B-pillar is an assembly of four parts ; the outer panel, the two reinforcements and the inner panel, see Figure 6.20(a). The reinforcement used in the vertical region is manufactured from a tailored welded blank with four transition zones with varying thickness from 1.2 mm to 1.8 mm, see Figure 6.20(a) reinforcement 1. There are six bolt connections ; four for rear door hinges and two for the front door beam reinforcement [5]. These bolt locations cannot be modified during optimisation. The reinforcements, inner panel and outer panel are assembled at the sill and the rocker through spot welds in a multi-flange configuration. The rocker

4. The design and impact case is from PSA Peugeot and Citroën.

5. This reinforcement is used for frontal crash to reduce the impact load imposed on the front door cross beams.

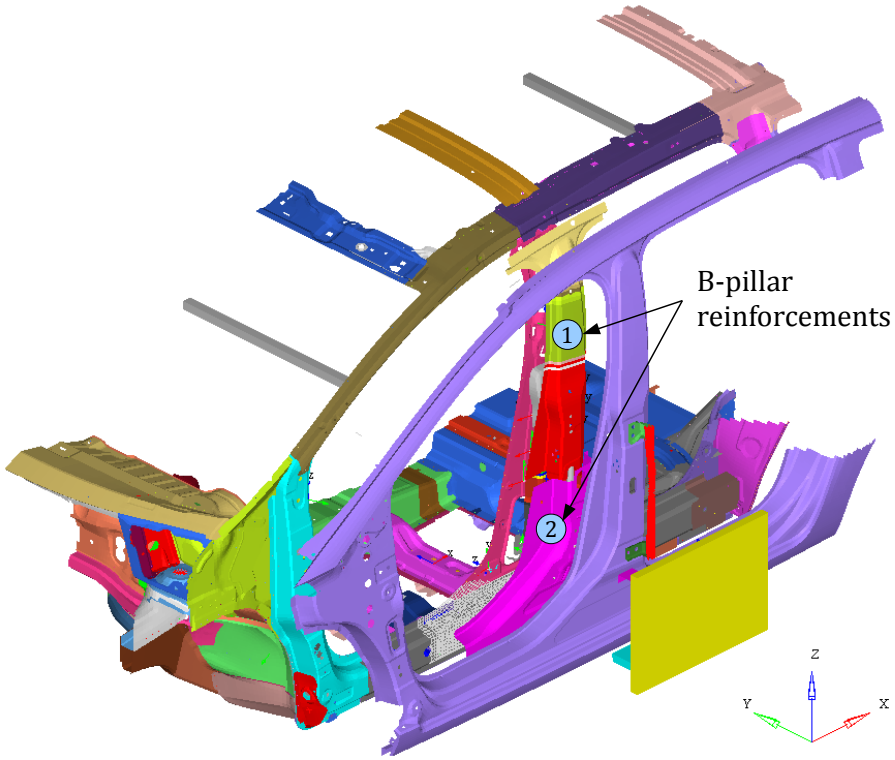

(a) An exploded view of the industrial model.

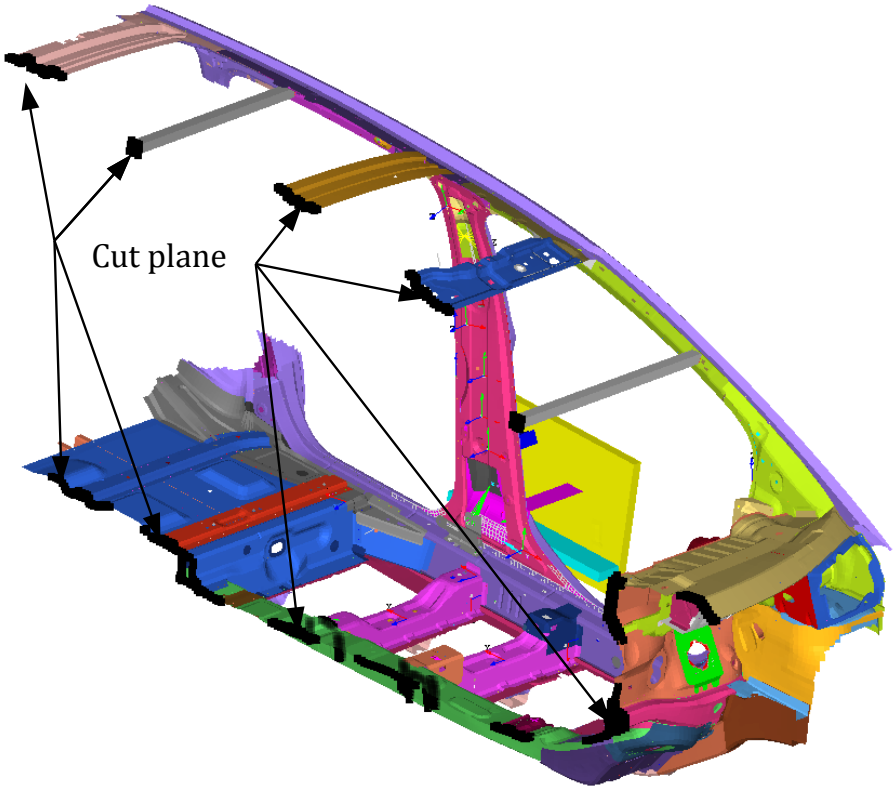

(b) Boundary condition applied to the cut plane.

FIGURE 6.20 – The lateral crash model.

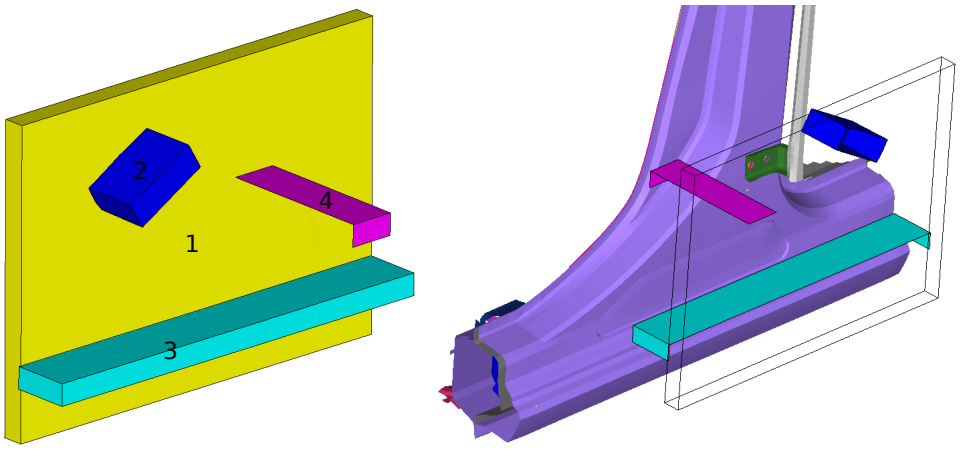

(a) Impactor structures offset. (b) Impactor location on the B-pillar.

FIGURE 6.21 – Impactor configuration.

also has three additional reinforcements in the impact region for energy absorption. Since the design space is very restrictive for optimisation, we first try to optimise the shape of the B-pillar reinforcements keeping it within the outer and inner panels (design space), see Figure 6.24.

Node	Non-parametric model		Parametric model		Intrusion diff. (|%|)
	Impact duration (ms)	Intrusion (mm)	Impact duration (ms)	Intrusion (mm)	
N1	64.5	170.0	70.8	182.3	7.23
N2	63.8	154.8	74.4	146.2	5.56
N3	63.1	118.3	73.9	120.1	1.52
N4	63.6	134.1	72.2	139.5	4.02
N5	63.7	144.6	72.4	139.5	3.5
N6	63.0	106.3	71.1	113.0	6.3

TABLE 6.3 – Comparison of the intrusion values at different locations along the B-pillar.

6.9.3 Modelling and Validation

The FE model is imported to SFE CONCEPT to use the geometrical details for parametric modelling. Here, the line curvature and the cross-sectional shapes of the beams are imported. Figure 6.22 shows the line curvatures, cross-section shapes and other modelling details obtained from the FE model. The multi-flange configurations are directly obtained from the FE model. For this, it is necessary to generate the parametric model as close as possible to the non-parametric FE model such that the optimisation results can be used later for the real design. To avoid a model with too many parameters, this re-modelling is performed here accepting smaller discrepan-

cies. For example the tailored blank variation of the thickness is neglected and the spot weld positions regularised. Due to these modifications, the parametric model has to be validated against the original model.

It is considered here to be sufficient to validate with respect to the deformation

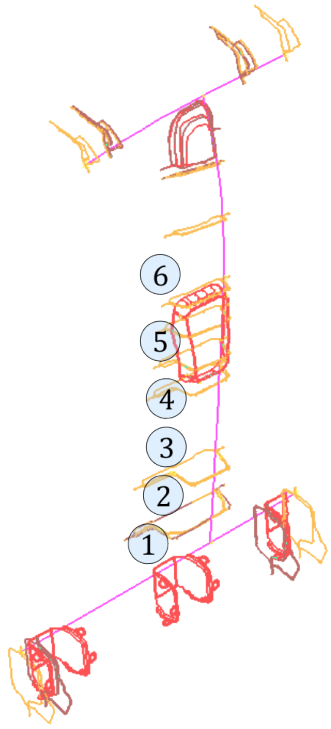

FIGURE 6.22 – Geometrical details used for B-pillar modelling and intrusion measurement node locations.

characteristics of the two models, although other characteristics are also assessed, such as plastic strain etc. To do this, the original B-pillar model is removed from the total model and the newly generated, parametric model is inserted using the FE CONNECT feature discussed in Section 6.3.1. This feature allowed for a smooth transition of geometry from the remaining FE model to the parametric model.

The intrusions at various locations along the B-pillar are compared. Table 6.3 shows the typical outputs from the two different B-pillar models and also the differences in the intrusion values. There is no significant difference in the intrusion values between the two models. The small differences can be explained by the simplifications mentioned above ; they will be accepted in the optimisation. More important is the difference in the times where the maximum deformations occur. The parametric model is in total slightly softer than the original version because of the manner how the tailored blank thickness variations are removed. Figure 6.23 shows the comparison of global and local deformation characteristics. Here global deformation refers to the bending of the B-pillar and local deformation refers to the localised deformation of structures. In Figure 6.23(a) the local deformations are highlighted in red.

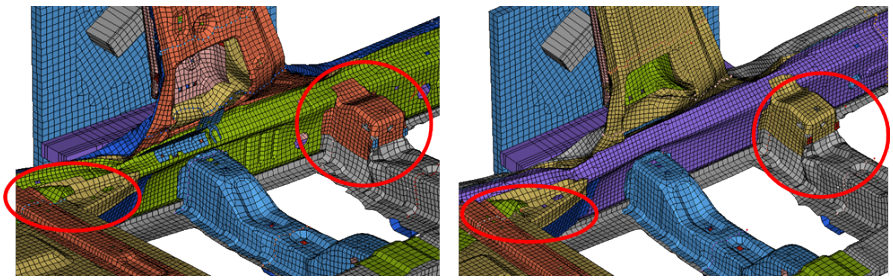

(a) Local deformation characteristics.

(b) Global deformation characteristic.

FIGURE 6.23 – Comparison of the deformation characteristics of the B-pillar at 80 ms ; left: Non-parametric B-pillar model ; right: Parametric B-pillar model.

6.9.4 Optimisation Problem Definition

The problem is set according to the industrial requirements to optimise, in the first place, the reinforcement of the B-pillar. The optimisation of the reinforcement is considered in terms of the shape and size parameters. The objective is to reduce the mass of the B-pillar. Also the allowable design space and the constraints are provided, presented in the following sections.

Design Space The design space provided is very restricted by the industrial requirements. The reinforcement should be within the outer and inner panels of the B-pillar, red boundaries (design space) in Figure 6.24(b). Other restrictions include the bolt locations for the rear door hinges and the frontal impact reinforcement for the front door cross beam, see red circles and lines in Figure 6.24(a). These restrictions define the limits for the shape parameterisation and variation. The remaining changes are: shape of the reinforcement in the top region and the region between the rear hinge bolt holes, see Figure 6.24(a).
Since the space between the outer and inner panels of the B-pillar is very limited, the potential to reduce the mass by the shape changes is not very high. This also

means the influence of the shape parameters to reduce the mass and increase the performance is very small.

Parameterisation The reinforcement sections at different locations along the B-pillar are used for parameterisation. The reinforcement is divided into 7 segments with 6 control points to change the shape, see Figure 6.24(b). Two grouped cross-sections (top and bottom of the B-pillar) are used which allows for shape change along the length of the beam, between the green arrow pairs in Figure 6.24(a). For each group, 5 shape parameters and 1 thickness parameter are assigned. Offset mapping is used to avoid geometrical conflicts and overlaps, see Figure 6.24(b) (dotted orange lines) for the offset mapping beam configuration. The allowable space for reinforcement shape modification and a possible reinforcement configuration is shown in Figure 6.24(b).

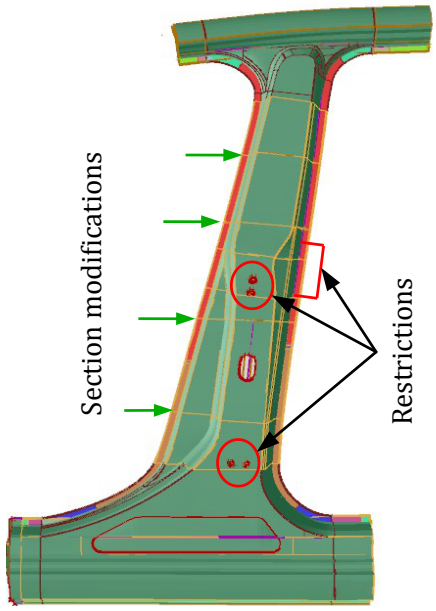

(a) Location of cross-sections where shape is modified and design restrictions.

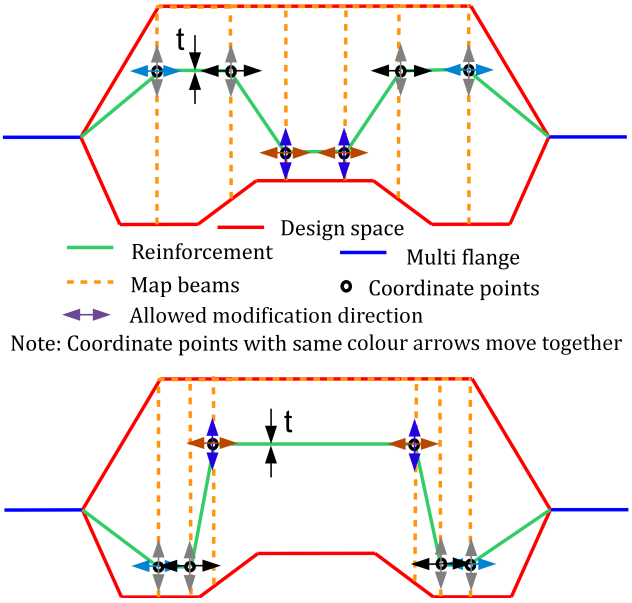

(b) Reinforcement control points, design space and a possible reinforcement configuration.

FIGURE 6.24 – Parameterisation of the B-pillar.

Constraints Two variables are monitored for the constraints, the intrusion of the B-pillar at various locations and the velocity of the intrusion points over time, t. These responses are used to monitor contact between the passenger and the structures and also for the minimum trigger time required for the side airbags to deploy. The measurement points are taken in the thorax (A), abdomen (B) and hip (C) region of a seated passenger, see Figure 6.25. Table 6.4 summarises the intrusion limits. The intrusion velocity of point A, B and C after 35 ms should not exceed 7.5 kph.

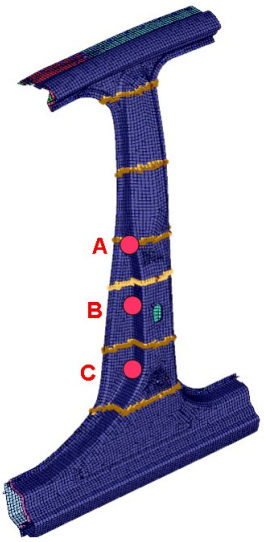

FIGURE 6.25 – Node location for the measurement of intrusion and velocity.

Node	Time (ms)	Intrusion (mm)
A	43	220
B	38	200
C	33	170

TABLE 6.4 – Intrusion limits for the three B-pillar regions.

Optimisation Algorithm and Workflow An EA, available in the commercial optimisation tool optiSLang, is used as the optimisation algorithm with 10 individuals in each generation. The approach here is to take a small population in each generation while using many generations (30 generations is the stopping criterion) to explore the design space. During each optimisation loop, the parameterised B-pillar is updated and embedded into the remaining FE model. Only the parameterised B-pillar is modified, the remaining structure stays untouched during the optimisation. Then the full structure lateral impact is performed.

6.9.5 Optimisation Results

Since the aim of this study is to validate the shape parameterisation technique, the optimisation is only run until sufficient improvements are achieved. This is the typical industrial situation also determined by the high computational effort for such a complex model. Figure 6.26 shows the geometry of the improved design after the first five generations (46^{th} design). Table 6.5 presents the comparison of outputs of the initial and the improved designs.

6.9.6 Conclusion

A B-pillar reinforcement optimisation is presented in this section. Again the offset mapping previously presented is successfully implemented to give a robust

parameterisation with no overlapping and penetrating designs. An improved design is obtained however the optimisation is stopped after 5 generations due to the high computational effort. This is $\approx$ 10 hours, on a 4 core Intel Xeon E5410 2.33 GHz CPU, for each simulation and hence $\approx$ 460 hours to get the improved design. Hence it is interesting to look at ways to reduce the computational effort for such complex and large models for optimisation. This becomes even more important for a double loop robust design optimisation where a large number of design analysis are required compared to a single loop optimisation. This is explored in the next chapters of this thesis.

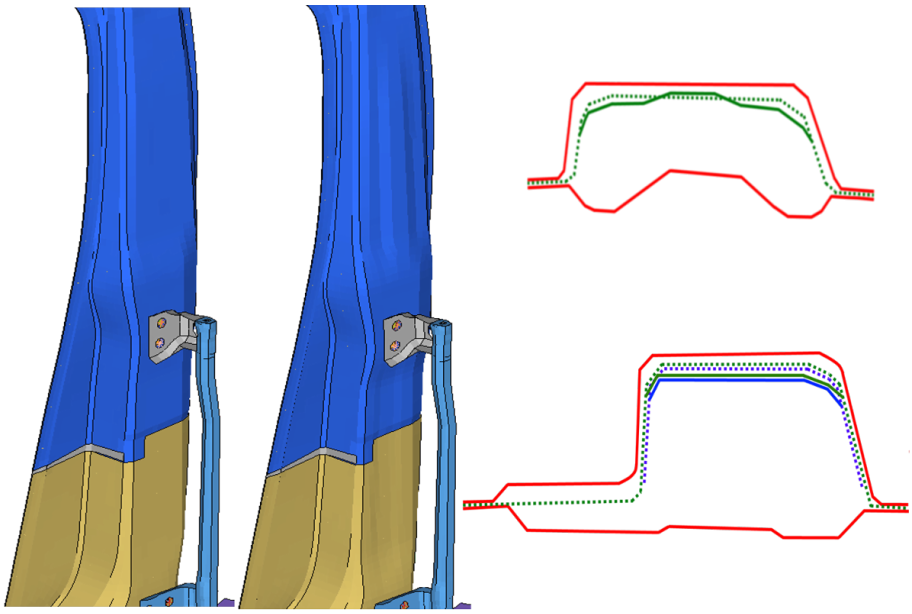

FIGURE 6.26 – Comparison of initial (left) and improved (right) B-pillar reinforcement geometry. The inserts show the cross-sections.

	Initial design			46^{th} design		
Mass (kg)	26.9			28.4		
Region	A	B	C	A	B	C
Intrusion (mm)	94	96	102	96	102	112
Velocity (kph)	4.3	7.9	8.4	6.4	6.9	7.2

TABLE 6.5 – Comparison of the responses of initial, where the velocity constraint are violated, and improved design.

Chapter 7

Computational Efficiency via Sub-modelling

7.1 Methods to Reduce Computational Effort

Recent studies for crashworthiness have been realised using more and more complex geometries and detailed finite element modelling. Such model complexity with the required high non-linearity (material, geometry and contact) leads to high numerical effort for simulation, which is in particular challenging for optimisation studies for industrial-sized problems with their high number of design variables, constraints and objectives, e.g. Duddeck (2008). Standard approaches have therefore only a restricted ability to explore sufficiently well the design space, which becomes even more crucial in cases where the robustness of the derived optima has to be assured (robustness in the means of insensitivity of the design with respect to inevitable fluctuations in design and noise variables). Nevertheless an approach where robustness analysis is included into the optimisation loop is necessary because the design is normally driven to the limits during an optimisation. The objective of this chapter is therefore to investigate methods to reduce computational effort for single simulations Rayamajhi et al. (2013a).

Some approaches used to reduce the simulation effort for crashworthiness studies include the following: Macro Element Method Takada and Abramowicz (2006), Multibody Modelling Sousa et al. (2008), Equivalent Static Loads Method (ESLM) Park (2011), sub-modelling Goodman et al. (2008). These approaches are best suited to certain type of problems ; e.g. Macro Element Method can be applied to early design phase ; ESLM gives a good approximation of responses through linear static analysis for non-linear dynamic systems, however this has some drawback when applied to shape optimisation, see Chapter 9. In general sub-modelling is, in the author's opinion, the best approach for the problem here. The application of all other methods listed above are restricted in this study due to the FE model provided from the industry. For example, in multi-body modelling the FE model is replaced by a multi-

body model obtained via the plastic hinge approach, see Sousa et al. (2008) and in the Macro Element Method the FE model is replaced by super-folding elements. Hence in these approaches usually the FE model is substituted with a simplified modelling. These approaches are therefore more suited to early design phase where the design details are not considered yet (like in the FE models). Hence here a method is needed to reduce the computational effort, which can be used even for very large FE models with industrial complexity.
In this section, the sub-model approach is discussed where the part of the total structure is extracted in which the optimisation is realised. Using just the sub-model to assess the improvements due to the change of design variables can be justified as long as the results are comparable to those of the full model. In fact the sub-model should represent the main tendencies of the total model with respect to design changes.

7.2 Sub-modelling vs Sub-structuring

Sub-structuring is the decomposition of a large model into several smaller models. Sub-structures are created by retaining the nodes at the interface boundary and eliminating the internal nodes, reducing the order of the mass and stiffness matrices. These boundary nodes retain the stiffness information of the sub-structure model. During optimisation large part of the structures remain unchanged, these unchanged structures can be isolated in a sub-structure avoiding repeated calculation of stiffness of that part. This approach is often used for NVH analysis, see for example Donders et al. (2010).
A sub-modelling method is useful where only a sub-region of a computationally expensive problem is of interest for the optimisation study. This means here the interest is in the optimisation problems where the design variables are only defined in a smaller part of the total model. This study region can have refined mesh for better accuracy compared to coarser mesh used for the remaining model.
For sub-modelling, first the interesting region for a required study is identified. A cut is made to separate this region (sub-model) from the remaining model. It is then crucial to consider the influence of the remaining model while using the sub-model for optimisation. This coupling of the sub-model and the remaining model (which remains unchanged during optimisation) is taken into consideration by applying Interface Conditions (ICs) to the sub-model at the cut sections (where the cut is made for the sub-model), see Figure 7.1. The ICs are obtained by the analysis of the full model which contains the sub-model. Generally the ICs at the boundaries of the sub-model are the imposed displacements applied to the interface nodes at the cut section. In the following part, an overview of the main studies, which used the sub-modelling approach for crashworthiness studies is given Chase et al. (2012).

7.3 State-of-the-art in Sub-modelling

Usually sub-models have been used for analysis and optimisation of component structures, such as bumpers, doors and B-pillar structures, see Hoppe et al. (2005); Marklund and Nilsson (2001); Song and Park (2006). A B-pillar optimisation study using sub-modelling approach is presented in Marklund and Nilsson (2001). The time histories of the nodal displacements and velocities at the cut-off sections are taken from the full car crash analysis and applied to the component model for optimisation. In this study, it is assumed that the ICs at the cut-off sections do not need an update during optimisation, which is not checked sufficiently well. Also the inclusion of velocity, at the interface, may not be required since the displacements history is already included. In Meister et al. (2005), lateral crash is studied again where the focus is on the performance of the side airbags. A sub-model is created with main structural components for lateral crash, the dummy and also the seat structure. Again the influence of the remaining structure is considered using the imposed displacements. A similar approach for the interface is used in Chase et al. (2012) and Goodman et al. (2008). In these studies a B-pillar structure and front rails are optimised respectively. Here displacements history is used as the ICs. Moreover, the ICs at the cut-off sections are updated during the optimisation due to the highly coupled sub-model and the remaining models .Depending on the interaction intensity between the remaining model and the sub-model, slight changes made to the sub-model, during optimisation, could influence the performance characteristics of the overall model.

In Bae and Huh (2012), structural improvement for lateral crash is made only considering the B-pillar structure for optimisation. The remaining structure is deemed to undergo rigid body motions with negligible deformation. Inelastic springs are used to model the effect of the remaining structure on the B-pillar. A slightly different approach is presented in Stein et al. (2012) where a lumped mass approach is used to represent the remaining structure for pedestrian impact. The sub-model (vehicle front structure) accuracy is increased by optimising the mass and inertia values such that the sub-model has similar prediction capability as the full model.

The sub-modelling approach is also implemented in several CAE packages such as Altair HyperWorks, HyperCrash (2013), ABAQUS, ABAQUS (2013) and LS-DYNA, Livermore Software Technology Corporation (2013). The sub-modelling creation process in these packages vary slightly. A box cut approach is implemented in ABAQUS and LS-DYNA, see Figure 7.1 whereas in HyperWorks nodes and elements are selected to create a section that defines the cut, see Figure 7.2. The displacements history at the section is saved from the full model analysis and imposed on the sub-model Altair HyperWorks (2012). This nodes and elements approach is also possible in ABAQUS and LS-DYNA.

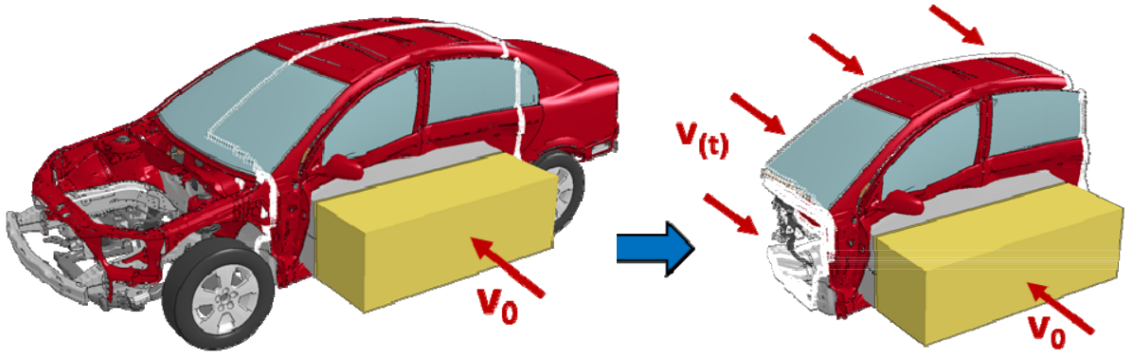

FIGURE 7.1 – Sub-model definition using box approach, Gutermuth et al. (2013).

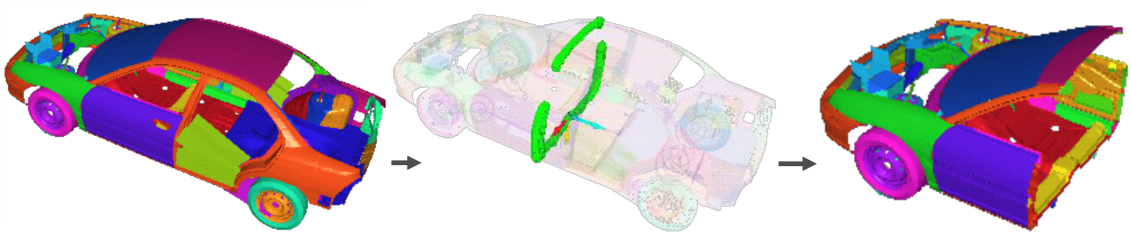

FIGURE 7.2 – Sub-model definition steps in Altair HyperWorks, Altair HyperWorks (2012).

Most studies that have optimised via sub-models have not considered the update of the ICs. This is specially important for crash because small design modifications made to the sub-model can effect significantly the coupling behaviour between the sub-model and the remaining model. Furthermore, from the literature, it is found that the displacements history represents sufficiently well the remaining model and has been frequently used. Hence later in this chapter a sub-model optimisation approach is presented where the displacements history is used as ICs which are updated during the optimisation.

7.3.1 Interface Conditions (ICs)

The ICs, applied to the sub-model cut-off sections, represent the influence of the remaining model on the sub-model. This is critical for the accuracy of the sub-modelling technique. In the literature this has been done in several ways such as rigid body model with concentrated mass at the interface, Stein et al. (2012), imposed displacements on the interface nodes, Marklund and Nilsson (2001), or deformable spring representation of the remaining model, Bae and Huh (2012). Also of importance during the optimisation is the update of the ICs. Since the structures are modified during the optimisation, the interaction between the sub-model and the remaining model also changes. This however depends on the coupling intensity of the sub-model and the remaining model, the impact condition and also the amount of design modification during optimisation.
With the use of spring and rigid body, the need to analyse the full model can be

avoided. However a good tuning of the stiffness to represent the remaining structure is required. Also the sub-model cut has to be made where there are very minimal effects of the impact in-terms of the deformation, i.e the remaining structures do not have any significant role in the impact case. For this the sub-model may have to be big, depending on the impact condition, reducing the computational advantage. The use of imposed displacements is easily implemented and the ICs update can be easily achieved. The update can be made by simply substituting the new sub-model into the remaining model. Here an additional full model analysis is required however this outweighs the importance of the sub-model accuracy during optimisation. Also the detailed local deformation close to the interface can be captured which may not be achieved with the use of other ICs representations. Recommendations to making sub-model cuts are presented in Section 7.4.

7.4 Recommendations for Sub-model Definition

7.4.1 Location of Cut

A sub-model whose parametric changes only slightly influence the changes in the ICs can be used. But for this sub-model cuts have to be made in locations which are further away from the region of local parametric changes. This leads to an increase in the size of the sub-model and therefore in computational time. Since the main advantage of using the sub-modelling technique is to reduce the computational time, having a larger/big sub-model also reduces this advantage. Ideally a sub-model should be:

(i) Small enough to reduce the computational time by some factor.

(ii) Big enough such that the influence of local parameter changes to the ICs is very small or negligible.

In this ideal case the update of the ICs during optimisation may not be required. However due to complex crash models this ideal case is highly unlikely. Hence an investigation has to be made to analyse the relationship between the ICs and the local parametric changes. Through this study the coupling between the parameters and the interfaces can be known and a decision can be made if the BCs update is required during optimisation, see Section 7.9.3.

Furthermore the location of the cut for the sub-model is important. If the cut is too close to the region where parametric changes are made then the influence of these parametric changes to the ICs is big. It should be also avoided to make cuts in regions with higher stress gradients or concentrations. This is because these regions are very sensitive to design changes and hence the ICs at these regions may not be stable (requiring many ICs updates during the optimisation). The location of the cut directly influences the stability/robustness of the ICs and hence the convergence of the sub-model optimisation.

7.4.2 Parameter Coupling

The sub-model cut should be made where the part that has to be modified during the optimisation is not shared between the sub-model and the remaining model. If this cannot be avoided then additional steps have to be taken. This means that the parameters common to sub-model and the total model have to be coupled in a certain manner. For shape and size optimisation, the thickness coupling can be maintained either by having a tailored blank formulation for thickness between the sub-model and the remaining model. For shape parameter coupling, intermediate sections can be placed in between the two parameter shapes of the sub-model and the remaining models. Although generally for shape coupling between the models post treatment may be required depending on the amount of changes on the shapes and the surface distortion. For topology changes, it should be assured that the main load paths between sub-model and total model are not influenced by them.
Such approach to deal with the parameter coupling may have an influence in the stability of the ICs. This is because the design modifications are also made close to the sub-model cut-off sections. Hence these problems have to be investigated further. In the studies presented in this thesis, these situations are avoided when creating the sub-model.

7.4.3 Impact Condition

The location of the cut is also influenced by the location of the impactor. In cases where the cut only includes a portion of an impactor in the sub-model, the impact condition (impact energy) should be scaled. This is due to the reduction of the impact area of the impactor and the structures. In addition, it should be assured that the impact sequence is maintained, i.e. the order of impacts on the sub-model should be equal to that in the total structure.

7.4.4 Validation of Sub-models

The sub-models have to be validated before they can be used for optimisation. A visual approach would be to compare the deformation characteristics, plastic strain etc. of the full model and the sub-model. Furthermore the deformation sequence can be observed such that the deformation modes are similar for both full and sub-model. More rigorous investigations can be made by comparing different curves such as displacement-time, energy (kinetic energy, internal energy), section forces etc. Time histories of specific nodes can be monitored and compared. From the author's experience, the interface regions between the sub-model and remaining model have to be thoroughly investigated. This is because the interface surface (and mesh) between the sub-model and full-model may not be smooth which may lead to stress concentrations.
Figure 7.3 shows the approximation quality of sub-models analysis which is in good

agreement with full model analysis. The computation time of the model is reduced by around 56%, Altair HyperWorks (2012). Hence optimisation using sub-models is advantageous to reduce the overall computational effort for crash optimisation and hence robust design optimisation studies where numerous computational runs are required.

7.5 Optimisation via Sub-modelling Approach

7.5.1 Motivation

The sub-model optimisation approach has a great potential given that the sub-model and the ICs are well defined. Although there are a few papers on sub-modelling, see Section 7.3, the consideration of sub-models for optimisation and the update of ICs during the optimisation is not found. In crash optimisation studies the use of sub-models, for highly coupled systems, are rarely discussed in the literature. The only comparable work found so far is realised by researchers at Red Cedar Technology Goodman et al. (2008), although the cases published are not carefully validated or documented. This is further discussed in the following sections.

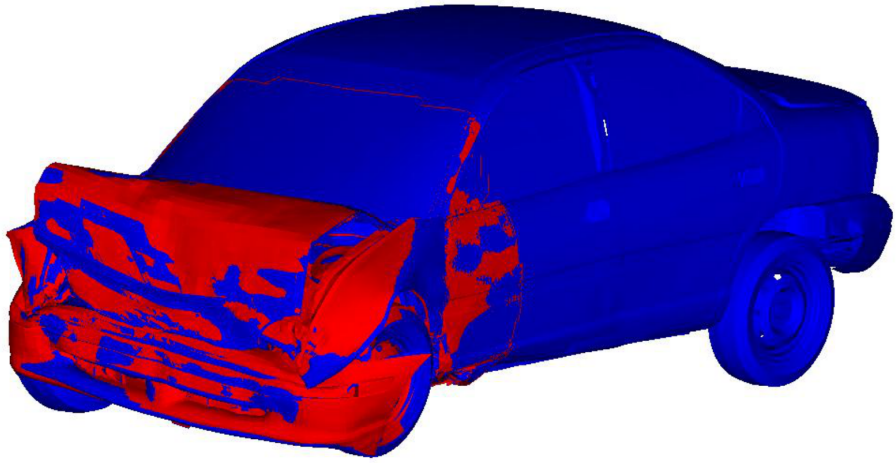

FIGURE 7.3 – Comparison of full model (blue) and sub-model analysis (red), Altair HyperWorks (2012).

7.5.2 Outline of the Basic Method

In this section, the sub-model optimisation methodology in Goodman et al. (2008) is presented. This is because the sub-model optimisation approach presented later in this chapter takes some inspiration from this work.
As shown in Figure 7.4, the sub-model is optimised with the initial ICs, obtained from initial overall model analysis, until a desired improvement is made (or until convergence). A relatively high number of sub-model (i.e. local) evaluations are

made during this step of optimisation. The optimisation is restarted each time the ICs on the sub-models have to be updated. Averill, Averill (2011), recommends 5-15 global iterations, i.e. interface updates. Hence 5-15 local optimisations are performed (depending on the problem).

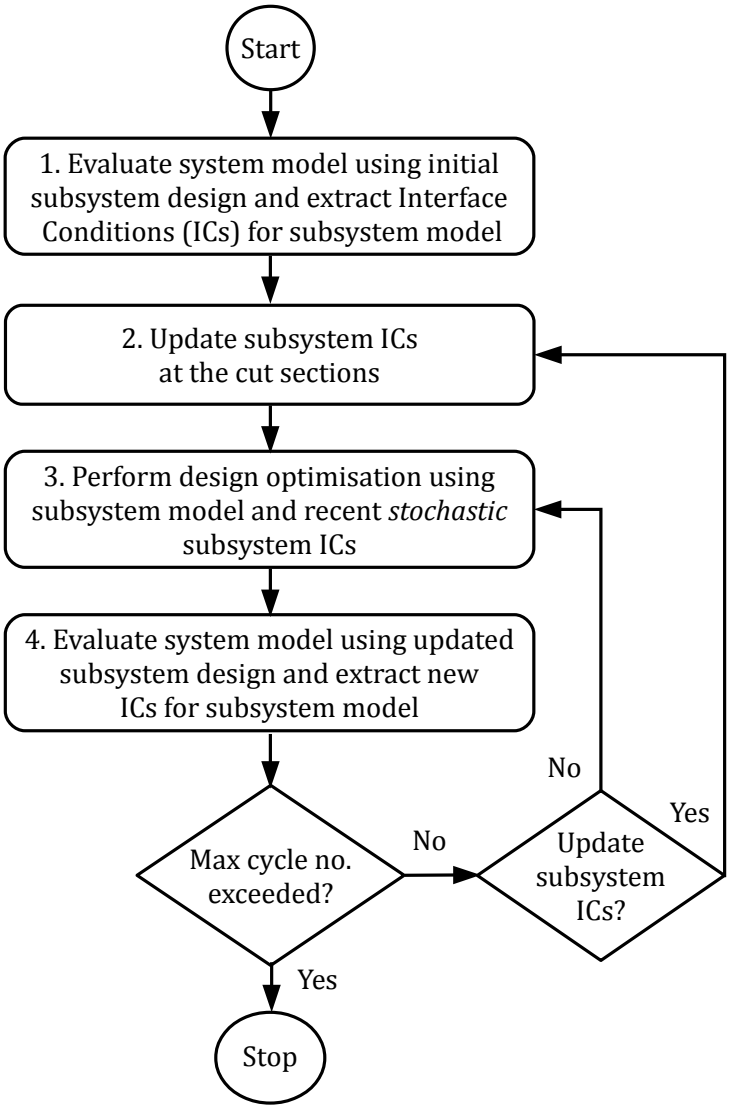

FIGURE 7.4 – Flowchart of sub-model optimisation approach used in Averill (2004).

This approach tries to find the optimal sub-model for certain criteria and - in addition - the associated ICs at which this sub-model exhibits optimal performance. In Goodman et al. (2008) it is stated that the performance of the optimisation can be improved by:

i. **Limiting local changes in the sub-model optimisation**
   The magnitude of ICs change, from one iteration to another, depends on the amount of modifications made to the design. Therefore the design change of the sub-model from one iteration to another should be kept small. This is because the current ICs will be wrong, requiring the ICs update, if the design changes are big. Hence small design modifications are made such that

the correctness of the ICs from one iteration to another is still retained. This approach has the disadvantage that the algorithm may get stuck in local minima due to the magnitude of design change. Also the optimisation convergence may take too long due to the small design changes.

ii. **Assuring robustness of the sub-model concerning variation of the ICs**
It is sometimes advantageous to perform a robust design optimisation on sub-model level where the uncertainty of the ICs are taken into account during optimisation by a stochastic variation of this set of ICs. The stochastic variation of the ICs also contributes to the robustness of the final optimum design in-terms of the ICs. The interface stochasticity is implemented by taking the weighted average of the ICs at two consecutive iterations. The interface variation does not carry any physical relevance since it is solely dependent on the design changes from one iteration to another, see for more details Section 7.5.3. Hence this is not considered in this thesis.

7.5.3 Discussion of the Basic Method

The information available from the literature mentioned earlier, Goodman et al. (2008), is not sufficient for implementation. Hence in this section the important particularities of the method, in the author's point of view, are discussed.

Optimisation Algorithm

The decision has to be made on either to continue with the running optimisation or start a new optimisation after the ICs update. If restarts of the optimisation are realised, whenever the ICs are updated, the overall convergence is not clear. Also the information of the associated sub-region, around where the latest optimum is found, may be lost when a restart is made. In addition, any previous evaluations will be useless as they are based on a different analysis model, in-terms of the ICs. If a continuous approach is implemented then an automatic ICs update criterion has to be used, discussed in Section 7.7.1. Making an update of the ICs during optimisation means inserting a discontinuity to the optimisation process, which challenges the optimisation algorithm. The convergence of the method can become questionable and rarely optimisation algorithms are adapted to these changes in the definition of the optimisation problem Sharp (2011). If successfully implemented, this approach is beneficial since the information of previous iterations is retained and used in future iteration. This could have better convergence characteristics compared to the start-stop optimisation strategy.

Robustness Considering Interface Conditions

For the robust design optimisation approach through sub-modelling, main sources of uncertainties can be categorised into three types

i. ***Test uncertainties***: The impact speed, impact mass, height, angle etc

ii. ***Manufacturing uncertainties***: Shape and thickness parameters and

iii. ***Interface uncertainties***: The uncertainty in the ICs

While the first two are discussed later in Section 5.2, the third uncertainty is discussed in the following paragraph.

Stochastic Interface The robustness of the optimised designs in terms of the ICs variability is important. Since the sub-model optimisation aims to find the improved design and its associated ICs at which the design exhibits this optimal behaviour. However if there is variability in the ICs then the design may no longer be optimal due to these variations. The sources of ICs variability can be linked to the variability in impact conditions and also the manufacturing uncertainties. The resulting performance variation of the designs, due to these uncertainties, depends on the sensitivity of the ICs to the design parameters and impact condition fluctuations. In Goodman et al. (2008), the variability in the ICs are not represented with sufficient detail. It is difficult to know the amount of variation to consider and also the number of variation analyses to be made.

The ICs are not addressed here since the focus is first to establish a sub-model optimisation approach. The ICs uncertainty can then be investigated in the future. Hence in thesis the robustness of the sub-models are considered with respect to the variations in categories (i) and (ii). from the literatures it is also realised that a sub-model optimisation approach is missing where the ICs are automatically updated without interrupting the optimisation.

7.6 Proposed Sub-model Optimisation Approach

From this section, and further, the sub-model optimisation approach developed in this thesis is presented. Here a continuous sub-model optimisation (as opposed to start/stop optimisation in literature, Goodman et al. (2008)) through an automatic ICs update criterion is proposed, see Section 7.5.3 for this choice. The algorithm considered here is the Iterative Response Surface Method (IRSM), explained in Sections 3.5.4 and 7.7.1. The sub-model optimisation approach is presented here considering the industrial lateral crash model, discussed in Section 6.9.1. A similar approach is used for the other sub-models described in Section 7.8.

7.7 Sub-model Optimisation Loop

For demonstration and discussion purpose, here a B-pillar sub-model is taken from a lateral crash structure. For further information on the full model and sub-model generation, readers are referred to Sections 6.9 and 7.9 respectively.
In the sub-model optimisation loop, the B-pillar (sub-model) geometry is optimised with the initial ICs. During the sub-model optimisation, the ICs will lose their correctness as long as they are not updated by a computation within the total model. Hence, the modified sub-model should be inserted, again after a certain optimisation phase, into the rest of the model to update the ICs. The corresponding ICs update and sub-model optimisation process are shown in Figure 7.5. The focus is set to perform the sub-model optimisation through continuous loop rather than the start-stop method implemented in Averill (2004). The next section discusses further the ICs update criterion and other specifics of the optimisation approach.

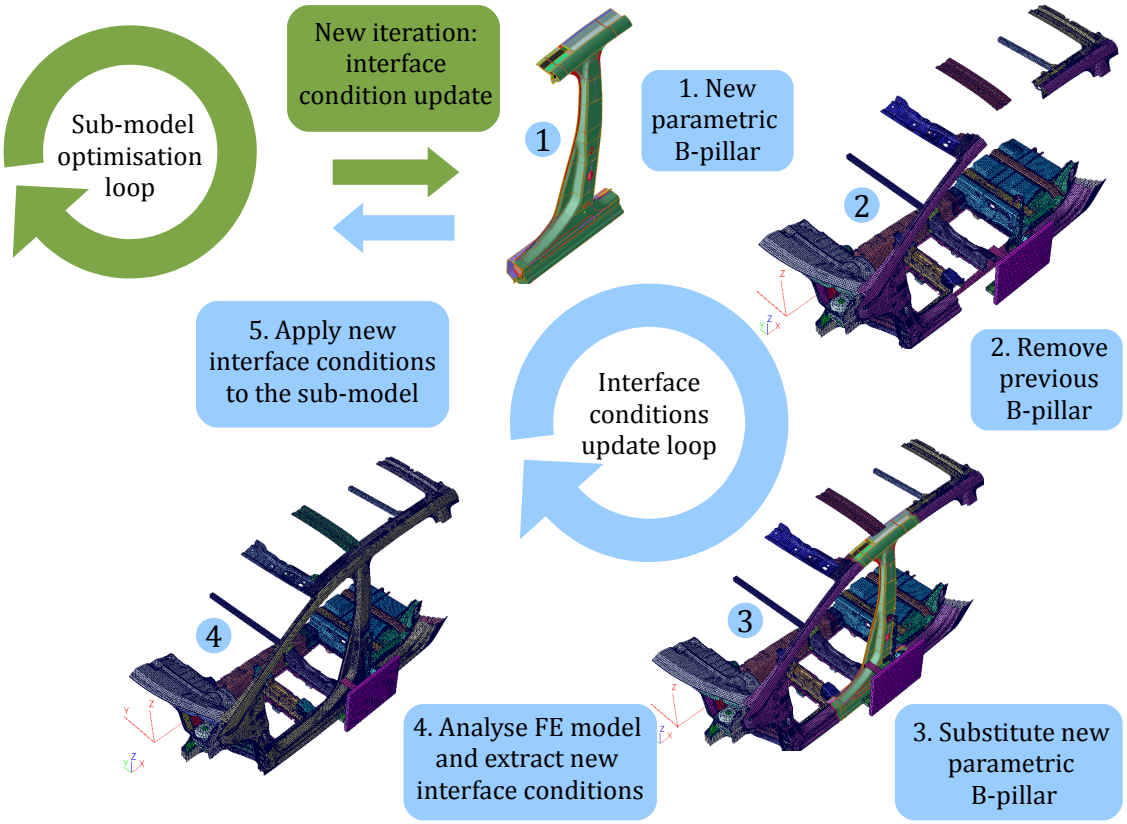

FIGURE 7.5 – Sub-model and ICs update loop.

7.7.1 IRSM for Sub-model Optimisation

7.7.2 Algorithm Requirements

The decision to use a continuous sub-model optimisation where the process is not interrupted by the update of the interface leads to certain requirements to be

fulfilled by the optimisation algorithm:

i. ***Interface conditions update criterion***: The use of a continuous sub-model optimisation loop requires a criterion to update the ICs at the sub-model sections. Hence the question of when and how to update automatically the ICs has to be addressed. The update has to be made such that the algorithm can handle this external influence and the algorithm should not be disturbed by the discontinuity introduced by changing the ICs.

ii. ***Information between iterations:*** Updating of the ICs may confuse the algorithm depending on when the update is made. If the update is made randomly at any point during the optimisation then within one iteration there are designs that are different in-term of the ICs. This makes the information within that iteration inconsistent. This random ICs update is problematic for RSM and IRSM since the response surfaces are generated using sub-models with different ICs.

   Also if there is information exchange between different iterations then again the designs in these iterations may be different due to the ICs update. Performing cross-over operations, as in GA, between these inconsistent designs from different iterations and the also carry over of designs (elitism) from one iteration to another will confuse further the algorithm and hence affect the convergence. Hence the update criteria has to be carefully considered keeping these situations in mind. To address this issue an ICs update approach, based on IRSM, is presented in the next section.

iii. ***Algorithm convergence:*** Convergence in-terms of both the design and associated ICs has to be obtained in the sub-model optimisation. These are interrelated because as the algorithm converges the design modifications get smaller. When the design modifications are small the update of the ICs is not required since the design modifications do not effect the ICs.

An optimisation algorithm that facilitates all of the above points needs to be considered for the continuous loop. Also this optimisation loop should be easily embedded in the overall RDO approach, presented in Chapter 10. Hence an IRSM is chosen as it is best suited to fulfil these criteria [1].

7.7.3 IRSM Discussion

In this section, the particularities of the IRSM necessary to adapt the general method to the sub-model optimisation are presented. For a general discussion on the IRSM please refer to Section 3.5.4. The general idea here is to update the ICs on the sub-models at each new iteration such that within one iteration the same ICs

1. The basic IRSM provided in optiSLang is modified here using external scripts.

are used. This removes the situation where the response surfaces are generated from designs with different ICs. Furthermore as the optimisation converges the sub-region size decrease, the quality of the response surfaces and also the sub-models increase, see Section 3.5.4. The quality of sub-models increase because the design modifications are reduced and hence the ICs are more representative of the full model. Further discussions on the use of IRSM are presented in the following paragraphs.

ICs Update Criterion

The ICs update criterion is based on each new iteration in the IRSM. At the new iteration, the sub-region is updated (depending on the optimum design at the previous iteration) and support points are generated around the centre point design of this sub-region. Here the centre point design of the new sub-region is the optimum design from the previous iteration. The ICs update is then made on the centre point design of the new iteration. Hence the update of the sub-region and that of the ICs are made at the same time. The ICs obtained from the full model analysis, using the centre point sub-model design see Figure 7.5, are used for all the sub-model designs within the sub-region. Therefore the response surfaces at each sub-region are generated from the sub-models with same ICs.

Sub-region Design Consistency

The IRSM method is proposed here since the only information passed from one iteration to the next is the sub-region optimum [2]. Because the update is made in the new iteration, the support points generated in the new sub-region use the same ICs. This removes the inconsistency in designs due to different ICs within one iteration, as discussed in Section 7.7.2.

Specific IRSM Settings Special features such as sample recycling and duplicate designs are used in optimisation algorithms to reduce the required number of design evaluations. These features should be switched off for better performance of the sub-model optimisation algorithm.

Sample Recycling Sample recycling is used to increase the response surface accuracy by taking the previously evaluated support points, that fall within the current sub-region, as additional support points to generate the response surfaces, see Figure 7.6. This cannot be used in this approach because designs from previous iterations are obtained with different sets of ICs. Hence if this option is used then the response surface will be created with inconsistent designs in-terms of the ICs.

2. In GA, since designs can move from one iteration to another, the designs within the iteration are inconsistent in-terms of the difference in the imposed ICs.

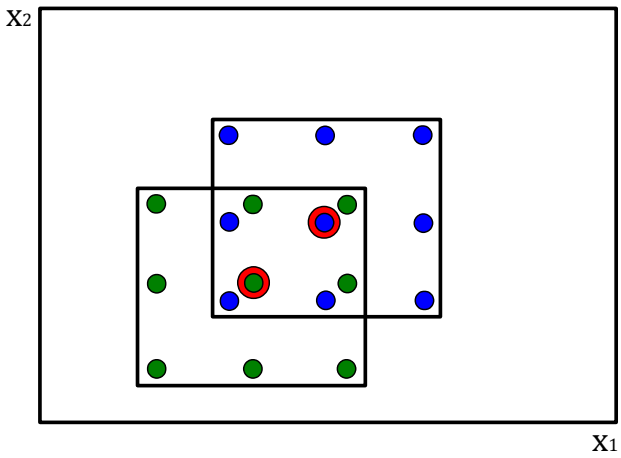

FIGURE 7.6 – An illustration of the sample recycling scheme.

Duplicate Designs Avoiding the analysis of duplicate design reduces the design analysis by using the responses of the previously evaluated design that has the same parameter setting as the currently required design. This cannot be used because although the designs are same in-terms of the parameters, they may be analysed with different sets of ICs.

Validation Step

At each centre point of the new iteration, the optimum design on the response surface from the previous iteration is validated with a full model simulation. Also since the updated ICs are applied to the new centre point, the design performance of this point is corrected with the updated ICs. This is crucial in terms of the convergence of the algorithm towards betters regions of the design space. The quality of the sub-model at each iteration is also observed by taking the difference between the full model responses and the sub-model responses.

Sub-region Size

The starting size of the sub-region plays a vital role in the correctness of both the response surface approximation and also the sub-model. If the sub-region is too large then the ICs, applied to designs far from the centre point, lose their correctness. Contrary to this, if the sub-region is too small then the algorithm could get caught in a local minima and also the convergence may take too long due to small changes in the design. Hence it is best to start with reasonable sized sub-region depending on the size of the design space.

Convergence

The IRSM convergence is assessed depending on the objective value and sub-region size from one iteration to another. Assuming a good direction of search is

made at the start of the optimisation, the convergence and hence, towards the end, the quality of the sub-model and the response surface increases. This is because the size of the sub-region decreases, which means that the density of points becomes higher improving the quality of the response surface. In-terms of the ICs, since the sub-region is small, the design modifications are also small. Hence the applied ICs to all the designs within this iteration are more correct compared to bigger sub-regions. Therefore towards the end of the optimisation the convergence is also achieved in terms of the sub-model design as well as the associated ICs.

Final Optimum

Ideally the final optimum is a point on a response surface and at the same time - because of the validation with a FE analysis of the sub-model - a point in the real design space. This is because the response surface optimum is validated, in the following iteration, with actual design analysis. However the final optimum can be a support point rather than a point on the response surface. In this case, specially, if this design is at the start of the optimisation it has to be validated with a full model analysis. This is because the response surface approximation at the start of the optimisation is generally poor and also the ICs do not represent well the remaining model. If this design does not perform well in the full model then an optimum point from the response surface can be chosen and validated, see Figure 7.7 for proposed optimisation loop.

7.8 First Validation: Rocker Reinforcement

Several validation cases are studied to test the proposed sub-model optimisation algorithm. In this section, validation on a simplified side crash structure is presented which is inspired from the CRASH-TOPO project, see CrashTopo (2012) for details.

7.8.1 Design Case

Full Model The design case is a simplified half side structure model with the end of cross-members fixed in all directions. The simulation time is around 10 minutes on a 4 core Inter Xeon E5410 2.33 GHz CPU. Three point masses are created, each with a mass of 100 kg at the free end of the rocker, see cyan beam sections in Figure 7.8 left. This is done to represent the effect of the missing structure at these sections.

Impact Conditions The impactor dimensions and impact velocity are obtained from EuroNCAP specifications, EuroNCAP (2011). In the EuroNCAP test, the car hits the pole and here the pole hits the car. The diameter of the impactor is 154

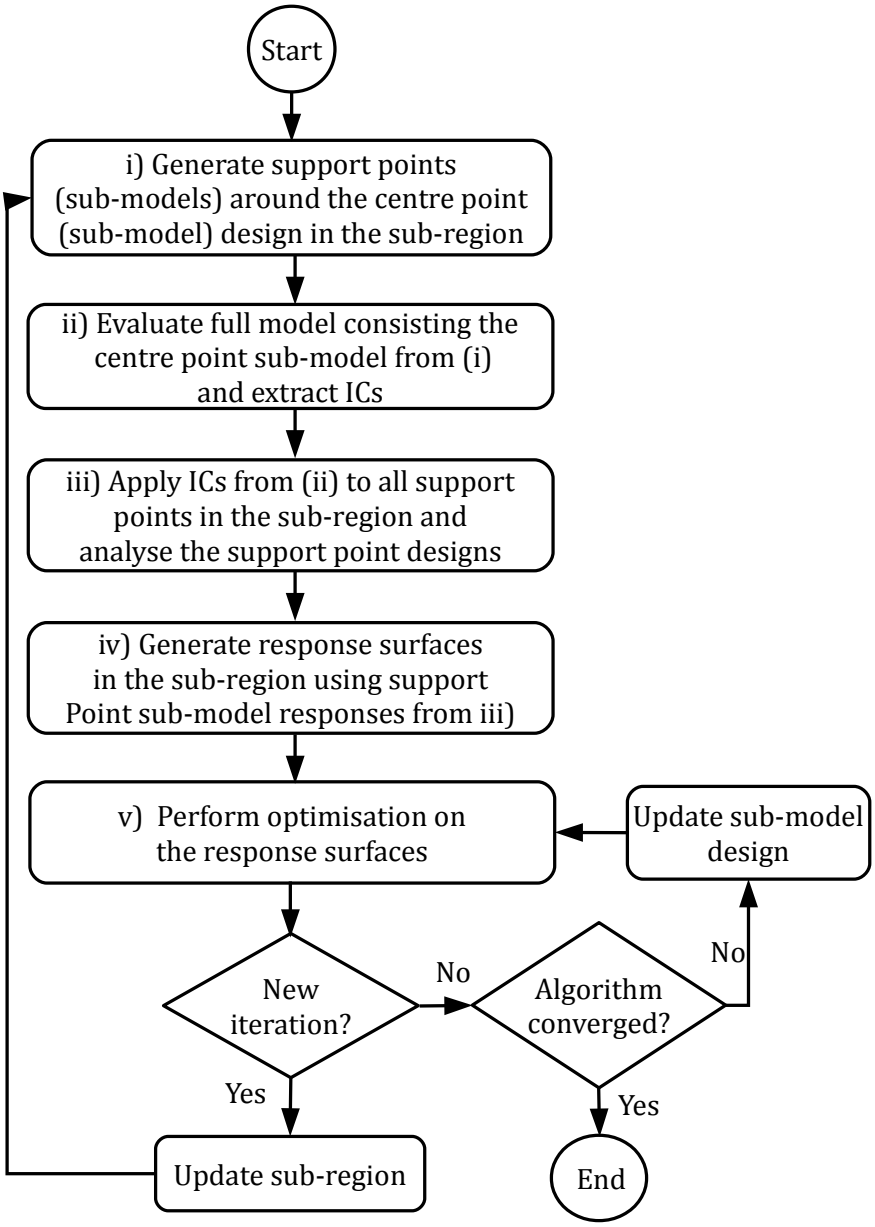

FIGURE 7.7 – Proposed sub-model optimisation loop.

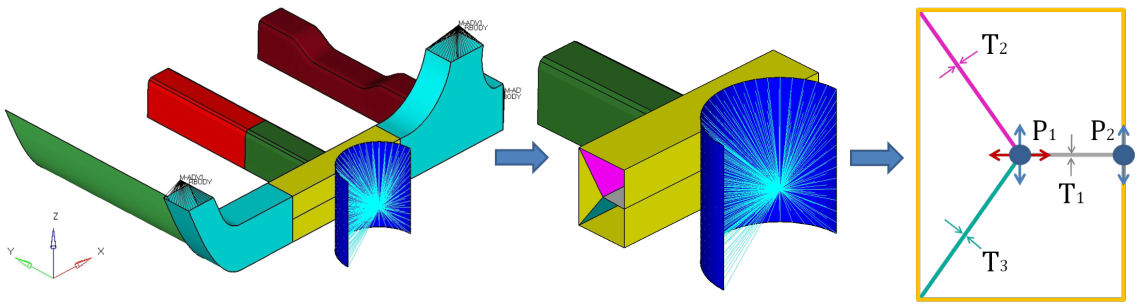

FIGURE 7.8 – Rocker design case and reinforcement parameterisation.

mm with a mass of 100 kg. The mass is reduced to scale the impact energy due to the missing structures. The impact velocity is 29 kph.

Sub-model The sub-model consists of the yellow and green parts, close to the impactor, of the full model, Figure 7.8 centre. The simulation time of this sub-model is around 3 minutes on the same machine. Only the yellow part of the rocker beam is reinforced with rib structures as appropriate for extrusion beams. The ICs are imposed on the cut sections of both the rocker and the cross member. Figure 7.9 shows the comparison of deformation in the y direction of the full model and sub-model. The sub-model deformation characteristics are in a good agreement with those of the full model. This shows the quality of the created sub-model.

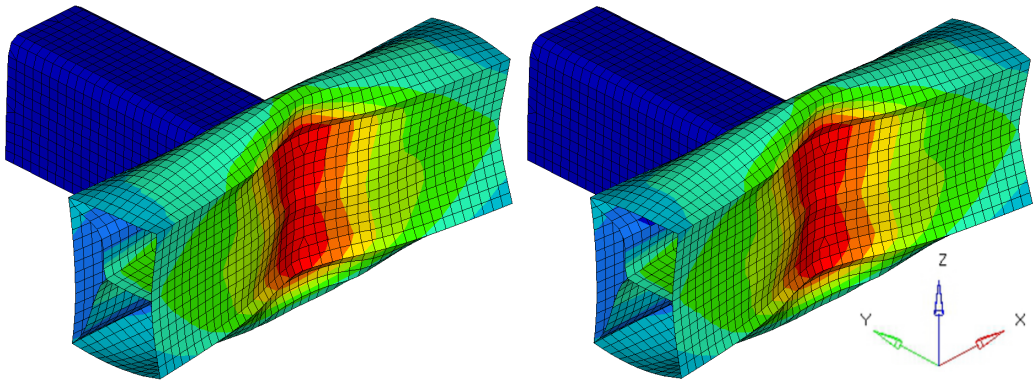

(a) Full model deformation characteristics, in the sub-model region. (b) Sub-model deformation characteristics.

FIGURE 7.9 – Comparison of global deformation characteristics of the full and sub-model.

Design Parameterisation The configuration and the thicknesses of the ribs are parameterised as these structures are not shared with the remaining structure, avoiding the parameter coupling issues mentioned in Section 7.4.2. The cross-section is parameterised with 5 design variables. In Figure 7.8 (right), the location of points P_1 and P_2 are modified together in the z direction (-50 mm ; +50 mm) and only point P_1 is modified in the y direction (-40 mm ; +40 mm). Also the thicknesses of the three ribs are modified independently, 0.5 mm $\leq t_{1,2,3} \leq$ 1.5 mm.

Objective and Constraint The optimisation objective is to minimise the mass while respecting the intrusion constraint, $I \leq 70$ mm, of the rocker, measured at a node next to the impactor.

7.8.2 Algorithm Settings

For the response surface in each sub-region, polynomial linear regression is chosen. This is due to the low number of support points required. It can also be argued

that the difference in approximation quality using 2nd or 3rd order regression compared to linear regression, considering the number of support points required, is not significant. Furthermore, the quality of the approximation increases as the sub-region size decreases towards the end of the optimisation. Linear D-optimal DOE (see Section 3.5.3) is chosen to generate 9 support points in the sub-region (1.5 × linear Koshal design, where linear Koshal = 6 optiSLang (2011)). This means at each sub-region there are 9 support points (and one additional evaluation for the validation of the previous response surface optimum). Hence the ICs are updated at the 11th, 21st, 31st... designs. For the starting design space range ; 100% and 50% of the full design space are tested. Here 100% means the full design space and 50% means half the size of the full design space which is calculated from the start centre point design.

7.8.3 Results and Discussion

The optimisation is started from a different reinforcement configuration to that shown in Figure 7.8 (right), see Figure 7.11(a).

With the 100% starting design space an improved design is found within 32 design evaluations. No design improvement is found after the 32nd design although the optimisation is allowed to run until the 11th iteration. Since the optimum is a support point design and not a response surface design [3], see Section 7.7.3, it is substituted back into the remaining model for validation. The intrusion at design 32 is overestimated by 6.1% (sub-model output = 69.7 mm compared to full model output = 65.7 mm). This is because at the beginning of the optimisation, since the sub-region is big (100% in this case), the support point designs are further away from the centre point design. This means that the designs within the sub-regions are very different, compared to the centre point design, due to the large design modifications. As a result, the ICs that are obtained from the full model analysis of the centre point design do not represent well the ICs of other sub-models within this sub-region. Hence it is better suited to find the optimum in the smaller sub-regions. This wrong interface information also affects the direction of the optimisation already from the beginning. This may have been the case here because no further optimum is found later in the smaller sub-regions. Hence it is more promising to start with a reasonably small sub-region depending on the size of the overall design space, see Section 7.7.3 for further discussion.

The 50% starting design space found an optimum after 102 design evaluations, Figure 7.10(a) design 102 ; 11th iteration in green. Again since this optimum is a support point design, it is substituted back into the remaining model for validation. This time the intrusion at design 102 is overestimated by 0.7% (sub-model output = 69.7 mm compared to full model output = 69.2 mm). This is because design 102 is

3. Only the response surface optimum is validated in the following iteration in the IRSM.

at a small sub-region where the response surface approximation is good, see Figure 7.10(b). Also the correctness of the ICs applied to the support point designs has improved which in-turn increases the quality of sub-model responses. A feasible design is found with a mass reduction of 5.3% compared to the start design, see Table 7.1. The final cross-section configuration is shown in Figure 7.11(b). Also to notice is the importance of the horizontal member of the rib. Since its thickness value has not been reduced to the minimum unlike the angled parts.

In-terms of the computational effort, in this example 111 design evaluations are

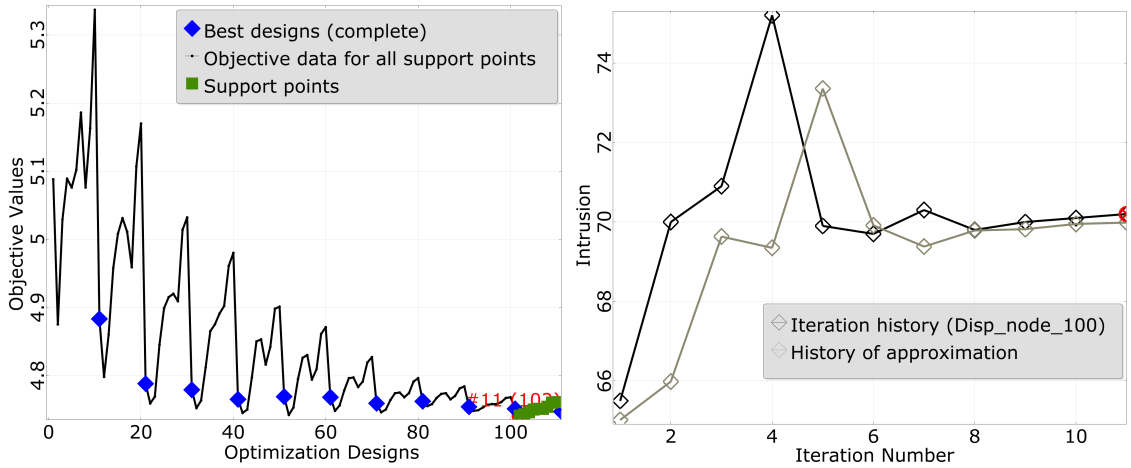

(a) Objective history of the support points.

(b) Constraint history at each centre point.

FIGURE 7.10 – Rocker sub-model optimisation history of the objective and constraint for the 50% case.

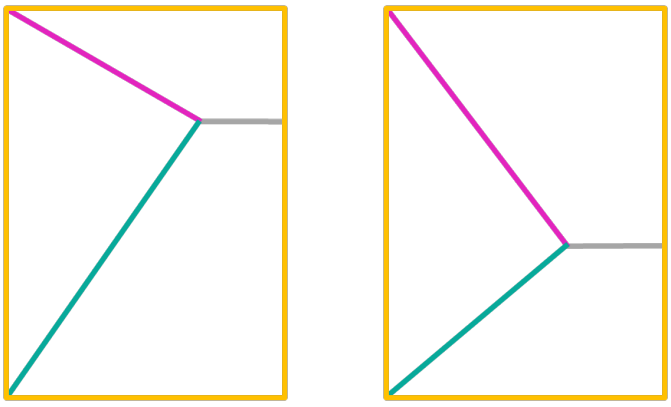

(a) Initial cross-section shape.

(b) Improved cross-section shape, 102nd design.

FIGURE 7.11 – Comparison of rocker cross-section shapes.

made in total to obtain the optimum design. However only 11 full model evaluations are required for the ICs update and the remaining 100 evaluations are made on the sub-model. A comparison of the computation time is given in Table 7.2. If only the full model is used for the optimisation then only 4 generations would be

	Initial design	102^{th} design
Mass (kg)	5.01	4.74
t_1 (mm)	1.3	0.86
t_2 (mm)	0.7	0.5
t_3 (mm)	0.9	0.5
Intrusion, I (mm)	70.7	69.2

TABLE 7.1 – Comparison of initial and improved rocker design.

	No. of full model eval.	No. of sub-model eval.	Total CPU time (h/cpu)	% of CPU time reduction
Full model opt.	111	0	74	0
Sub-model opt.	11	100	27.3	63.1

TABLE 7.2 – Comparison of optimisation time using full model or sub-model.

completed (since only 44 full model analysis can be made within this time). Also if a global response surface is created with only 44 support points then the quality of the response surface approximation would be poor.

7.9 Second Validation: B-pillar Reinforcement

For the design case, parameterisation and optimisation formulation of this validation case please refer to Section 6.9.1.

7.9.1 Sub-model Definition

The B-pillar sub-model is created keeping the full part that has to be optimised (the B-pillar reinforcement) and also the impactor within the sub-model. Also the sub-model cut is made where there are no stress concentrations and away from the impactor area and parameter changes. Other particularities of the method discussed in Section 7.4 are also considered when creating the sub-model. The B-pillar including the bottom and the top part are defined here as the sub-model, Figure 7.12. It has to be shown later that this sub-model is sufficiently large such that it is reasonable to assume that the interface values between the sub-model and the remaining model do not vary too strongly during optimisation. On the other-hand, the sub-model is small enough to increase numerical efficiency. The sub-model has a computational time of about 3 hours (on a 4 core Inter Xeon E5410 2.33 GHz CPU), which corresponds to a 70% reduction in the computational effort. This amount of reduction on a research computer is already significant and it can be assumed that this will be even more important in an industrial context.

The interface between the parametric B-pillar model and the remaining FE model is located at the sections where the FE B-pillar model is cut-out from the overall FE model to generate the parametric B-pillar model. In our study, the interaction

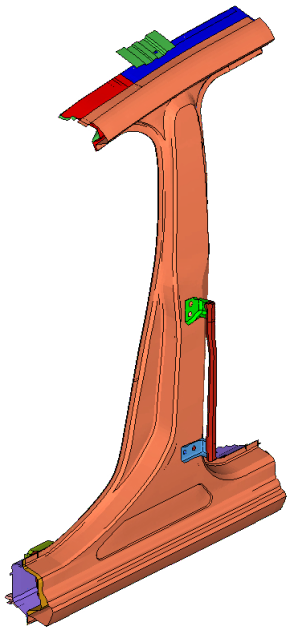

FIGURE 7.12 – Sub-model defined for B-pillar reinforcement optimisation.

between the remaining model and sub-model is taken into account using the imposed displacements on the nodes of the sub-model at the interface sections. These ICs are obtained from an initial simulation of the full model, in which an update parametric B-pillar has replaced the original B-pillar.

7.9.2 Sub-model Validation

The sub-model has to be validated against the full model for its deformation characteristics and other observed outputs. Several sub-models are created with modified design parameters and validated against the full model, see Section 6.9.4 for parameterisation. Table 7.3 shows the averaged percentage difference in the monitored output values (nodal displacement and velocity) between the different models and Figure 7.13 shows the global deformation for one validation case. It is important to notice both the local and global deformation characteristics of the sub-model which are in a good agreement. Although other observations are also made to validate the sub-models, as in Section 7.4.4, here only the node histories are considered. For the definition of the node location see Section 6.9.4. From Table 7.3, the difference in the responses is around 5% and can be deemed acceptable. However, after optimisation the sub-model has to be validated by inserting it into the remaining model.

7.9.3 Criterion for Interface Updates

As mentioned earlier, in Section 7.9.1, a coupling analysis is set up to get an idea about the interaction between the sub-model and the remaining model. This study gives an idea if the ICs update is required during the optimisation. This is not done

Node Location	Displacement (mm)		Diff. (%)	Velocity (after 35 ms)		Diff. (%)
	Full model	Sub model		Full model	sub model	
BASE (30 ms)	105	102	2.94	2.94	2.80	4.76
ABDOMEN (35 ms)	101	97	4.12	2.25	2.10	6.66
THORAX (40 ms)	96	94	2.13	1.75	1.62	7.42

TABLE 7.3 – Validation of outputs for the full and sub-model.

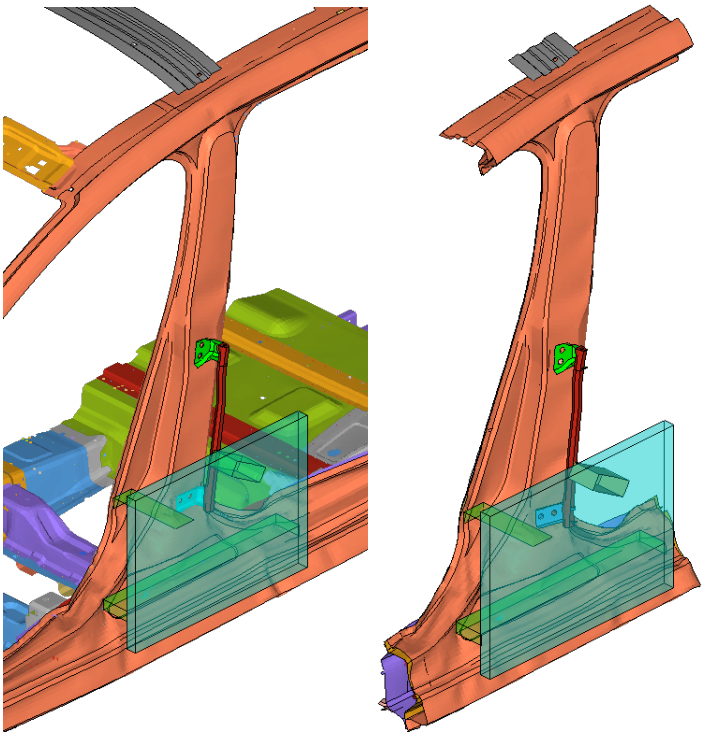

(a) Full model deformation. (b) Sub-model deformation.

FIGURE 7.13 – Comparison of global deformation characteristics.

for the previous validation case (rocker) because, here the design modifications are small and the sub-model cut interfaces are away from the design modifications (only the B-pillar vertical reinforcement). Therefore in this case the influence of the design modifications may be negligible and hence the ICs updated, during the optimisation, may not be required. This is tested via this study.

A total of 588 nodes are in the interface sections between the B-pillar model and the remaining FE model, see Figure 7.14. For this analysis only a reduced set of nodes are selected. For the four interfaces, only three nodes for each interface are selected from each flange layer. This is done for easy data handling for results analysis. If the results from these reduced set of nodes are not convincing then further addition of nodes can be implemented in the analysis. The images on the right of Figure 7.14 show the cut-out section geometries.

For this analysis, the computations on the overall model are required. Where modifications are limited to the B-pillar reinforcement. In total 12 design variables are

defined, 10 shape parameters and 2 thickness parameters. For a detailed description of the parameters see Section 6.9.4. The computation time for one simulation run is around 10 hours on a 4 core Intel Xeon E5410 2.33 GHz CPU. An ALHS is used to generate 60 designs, which is considered to be sufficient taking into account the high computational time. The B-pillar sub-model is defined with the same parameters as taken for the full model in Section 6.9.4. The response observed is the displacements of the selected interface nodes in x, y and z directions due to the change in design variables. The analysis took around 25 days to complete.

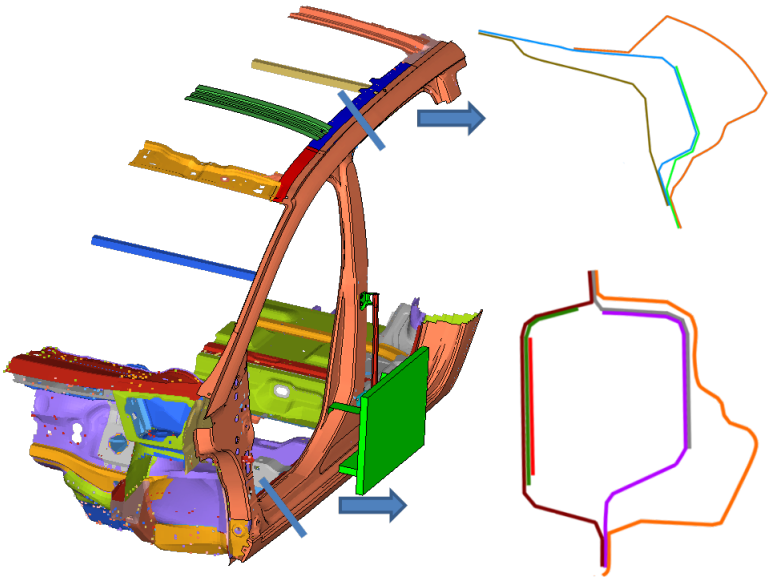

FIGURE 7.14 – Sub-model and remaining model interface section configurations.

Coupling Analysis Results

The influence of parameter changes on the interface nodes can be already analysed based on the selected number of samples. Hence no additional samples are necessary. The maximum node displacements are observed for the 60 designs. The distribution of each node displacements are summarised in Table A.3 (Appendix). Looking at the y and z displacement values in the table, there are moderate changes in the nodal displacements. This shows that the sub-model and the remaining model are moderately coupled to each other and hence an ICs update at the sub-model interface has to be made during the sub-model optimisation. Also to note is that these variations in the interface nodes are brought about by very small modifications in the parameter values (since the parameter ranges are not big). For the design with greater shape changes (future parameterisation), the coupling is likely to be even more intense hence the need for the ICs update.

7.9.4 Algorithm Settings

Again to reduce the number of support points, in each sub-region, polynomial linear regression is chosen. Linear D-optimal DOE (see Section 3.5.3) is used to generate 20 support points in the sub-region (1.5 × linear Koshal design, where linear Koshal = 13). This means at each sub-region there are 21 support points (20 DOE points, and 1 additional centre support point [4]). Hence the ICs are updated at the 23^{rd}, 45^{th}, 67^{th}... designs. The starting design space range is chosen as 50% of the full design space.

7.9.5 Results and Discussion

The initial B-pillar design does not respect all the constraints see Section 6.9.5. Hence the aim of the optimisation is to increase the performance of the B-pillar while reducing the mass.

An optimum is found after 200 design evaluations, see Figure 7.15(a) for the objective history. This design is validated by substituting it back into the remaining model. The design responses from this validation also satisfy the constraint since the response surface approximation at this point is good, see Figure 7.15(b). The mass of the optimum has increased by 5.6%. The optimum reinforcement shape of the B-pillar is shown in Figure 7.16 and the optimum design responses in Table 7.4. In-terms of the computational effort, in this example 199 design evaluations are made in total to obtain the optimum design. However only 9 full model evaluations are required for the ICs update and the remaining 190 evaluations are made on the sub-model. A comparison of the computation time is given in Table 7.5.

	Initial Design			46^{th} design		
Mass (kg)	26.9			25.4		
Region	A	B	C	A	B	C
Intrusion (mm)	94	96	102	95	105	112
Velocity (kph)	4.3	7.9	8.4	6.8	7.1	7.3

TABLE 7.4 – Comparison of initial and improved B-pillar reinforcement design.

	No. of full model	No. of sub-model	Total CPU time (h/cpu)	% of CPU time reduction
Full model opt.	199	0	7960	0
Sub-model opt.	9	190	2640	66.8

TABLE 7.5 – Comparison of optimisation time using full model or sub-model.

4. This point is the same as the previous response surface optimum validation point. Hence usually no additional evaluation is required. However since the "don't solve duplicate design" option is not used, see Section 7.7.3, this design is re-evaluated.

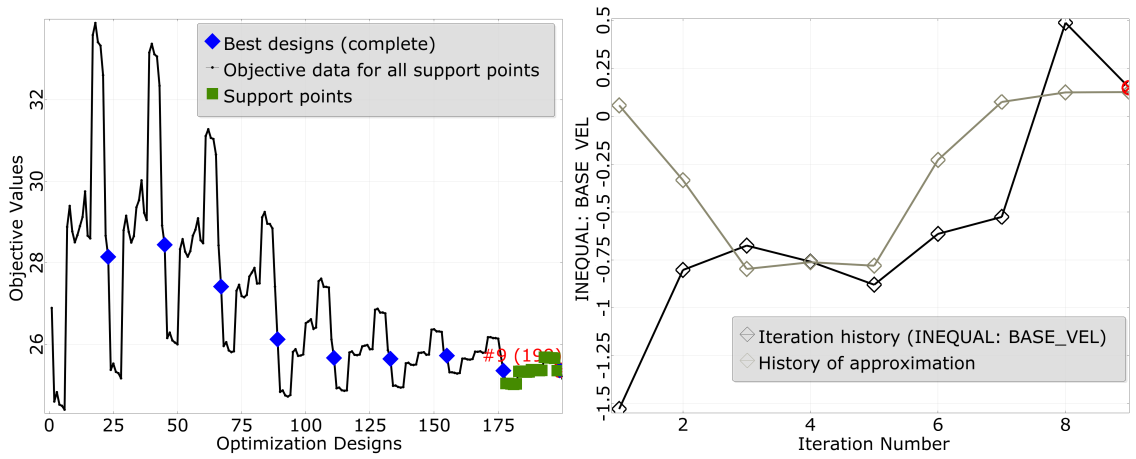

(a) Objective history of the support points. (b) Constraint history at each centre point.

FIGURE 7.15 – B-pillar sub-model optimisation history of the objective and constraint.

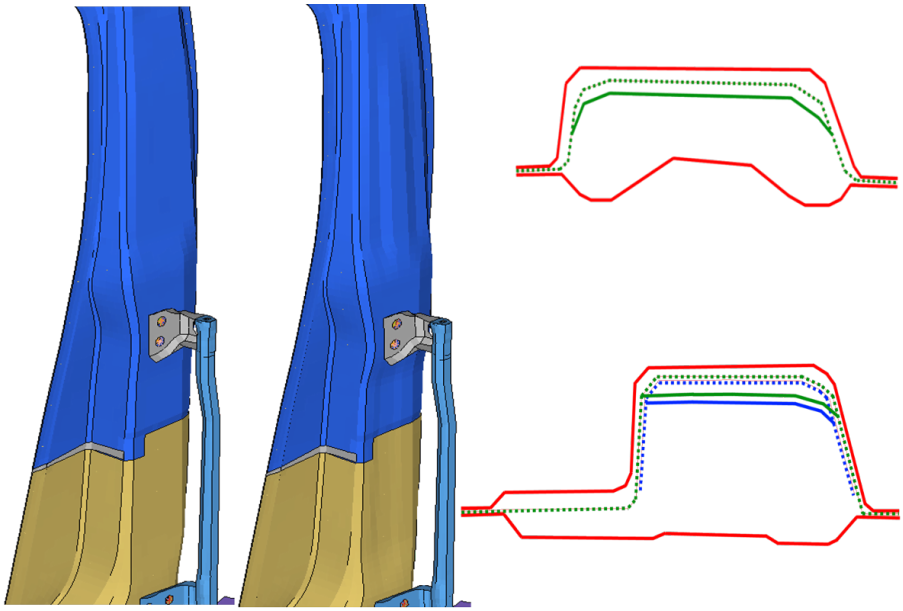

FIGURE 7.16 – Reinforcement optimum shape.

7.10 Conclusion

In this chapter sub-modelling approaches with the possibility to optimise using sub-models is presented. Some recommendations for sub-model creation are also discussed. An optimisation approach, of tightly coupled models, is presented which uses IRSM. To maintain the correctness of the sub-model, ICs that represent the effect of the remaining model are updated during the optimisation. Also some recommendation and discussion are presented for the implemented sub-model optimisation approach.
Two validation cases are used to test the implemented sub-model optimisation loop. Although an improved design is found in both cases, one of the important factor to consider is the start design range. In both cases significant amount of computation time is reduced when compared to the use of full models for optimisation

Chapter 8

Adaptive Parameter Sets for RDO

8.1 Introduction

Crashworthiness optimisation is already very demanding due to the expensive nature of crash simulation. Combining optimisation and robustness to formulate a RDO adds significantly to the overall computational effort, see Section 5.6. It is therefore interesting to investigate approaches to reduce the overall computational effort for RDO.

For robust design optimisation, the computational effort is determined by the following three aspects: (i) *time for the computation of a single crash event*, (ii) *time for the optimisation* and (iii) *the number of evaluations required for the robustness analysis of the optimisation designs*. For the first aspect, physical surrogate models such as sub-models or linear models obtained via the Equivalent Static Loads Method (ESLM), could be employed, see Chapter 7 and Chapter 9 respectively. The second aspect is concerned with the convergence of the optimisation. In this case the number of design variables can be reduced via design variable screening such that only the important design variables are included in the optimisation. This also depends on the performance of the optimisation algorithm, this is not further discussed in this thesis. Concerning the third aspect, the number of design evaluations can be reduced such that expensive robustness analyses are only made in interesting regions of the design space. In this chapter an approach to reduce the computation effort for the RDO in the third aspect is presented.

8.2 Motivation

Generally for RDO studies a double loop approach is more appropriate where robustness analysis is made for each optimisation point, see Section 5.6. This approach is relatively expensive due to the computational effort required for both the optimisation and robustness analysis. Also the effort is wasted when robustness analysis is made on optimisation points that are already infeasible. Hence the double loop

RDO approach can be adapted such that the robustness analysis is only made on the selected optimisation points that are both *feasible* and in a certain respect *optimal*[1]. Hence the general idea here is to perform the robustness analysis of designs in the interesting regions and avoid robustness analysis of designs in the unpromising regions of the design space. This gives rise to an adaptive parameter approach where the robustness parameters are only included in the interesting regions.

8.3 Proposed Adaptive Parameter Sets Approach

The general idea of this approach is to create a criterion that switches "on" or "off" the robustness analyses of designs. When the criterion is satisfied by an optimisation point, the robustness parameters are considered for robustness analysis. In contrast, if the criterion is not satisfied by an optimisation point, then no robustness analysis (the robustness parameters are excluded) is made for the optimisation point. Hence this approach is termed as adaptive parameter sets approach.
The approach is based on the outputs space such that the decision can be made for robustness analysis when the outputs approach the constraint boundary. It is difficult to implement this considering the inputs space since the parameter combinations that give designs near the feasible design space boundary are unknown. Similarly it is not easy to formulate the robustness analysis criterion depending on the objective values. Hence all the discussions presented in this chapter are based on the outputs space unless stated otherwise.
RDO method tries to find regions within the design space where the objective is minimum (or maximum) and also insensitive to unavoidable fluctuations in design and noise variables. In a constrained optimisation problem the design space is divided into feasible and infeasible space, see Figure 8.1. Promising solutions lie within the feasible design space. The designs in the infeasible region are of no significance, in-terms of robustness, since they have already failed to satisfy the performance criterion[2]. Hence the extra computational effort should not be spent on the robustness analyses of these infeasible designs. This however depends on the type of optimisation algorithm used, discussed in Section 8.4.
For the proposed RDO approach, the feasible design space is further divided into two regions ; the designs that are close to the feasible space boundary and the designs that are far away from the feasible space boundary, see Figure 8.1 feasible space divided by a green line. Since the optimisation normally tries to push the designs to the boundary of the feasible design space (Figure 8.1 red line), the sub-optimum solutions lie within this region. The interest here is on the designs that are optimal and robust hence the robustness analysis is only performed on these sub-optimal

1. Designs close to the boundary of the feasible design space.
2. However the information gathered through these designs help the algorithm to find better regions of the design space.

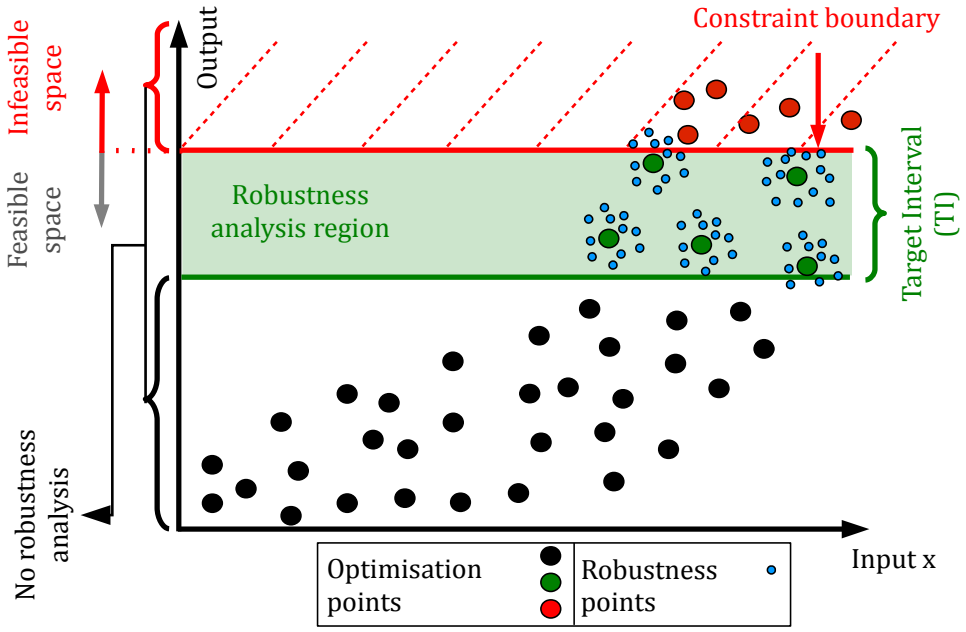

FIGURE 8.1 – TI definition for robustness analysis, for one input and output.

solutions, green region in Figure 8.1. However there is a small probability that the global robust optimum lies far off the boundaries. But it could be argued that a robust optimum cannot be easily judged if it is a local robust optimum or global robust optimum. Hence it is sufficient that an improved design is obtained that exhibits robust behaviour in the presence of unavoidable uncertainties.

To define this region, an offset of the constraint boundary is created, which is discussed more in detail in Section 8.5. The space between the constraint boundary and its offset is defined as the Target Interval (TI) for the robustness analysis, Figure 8.1. In most cases, it can be assumed that the robust optimum lies within T1 when it is carefully formulated. For the designs that are within the TI, robustness analysis is made whereas for designs that are outside the TI robustness analysis is approximated or avoided [3], see Figure 8.2 for the flowchart of this approach.

The optimisation is formulated to reduce both the mean (μ) and sigma (σ) of the objective and constraints. Although this formulation only comes into effect inside the TI, this formulation ensures that the optimisation algorithm searches for both optimal and stable regions of the design space. Also the designs outside the TI, where no robustness analysis is made, provide information to direct the algorithm to better regions with the evaluated optimisation values, see Appendix A.4.1.

This approach should reduce the computational effort for RDO significantly specially at the beginning of the optimisation where lots of designs may be infeasible or non-optimal (when the algorithm is still exploring the design space). Hence most of the robustness analysis will be performed only at the end of the optimisation when the algorithm has converged with most sub-optimal solutions (exploitation of

3. For designs outside the TI representative "dummy" robustness values are generated since this information is required formally by the optimisation algorithm, see Appendix A.4.1.

the better regions). Some important characteristics of this approach are discussed later in this chapter. The next two sections differentiate the proposed approach with other RDO approaches.

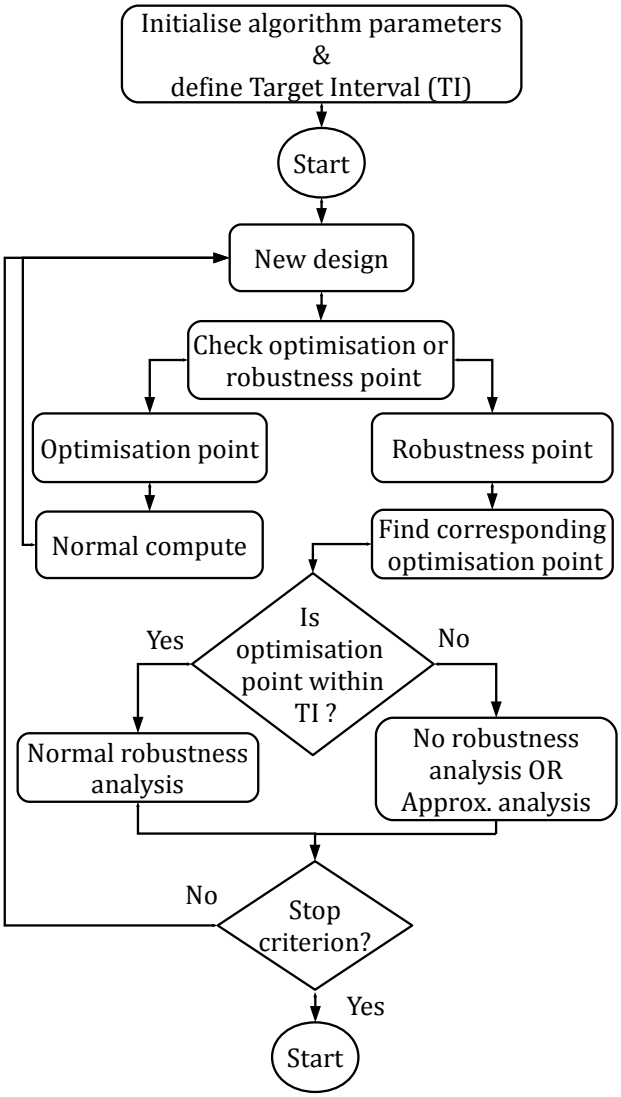

FIGURE 8.2 – Flowchart of the proposed RDO approach.

8.3.1 Sequential Approach

The sequential RDO approach is presented in Section 5.6.2. The main difference here is the RDO optimisation formulation itself. In the sequential approach the robustness analysis is performed, after a deterministic optimisation (where only the nominal values are of interest), on designs that are optimal. Hence the direction for the algorithm to search for stable regions in the design space is missing since the start. Also in the sequential approach the general idea is to analyse designs that are near the feasible space boundary in the hope to find a robust design. However generally these designs are already driven to the feasible design space and are not robust. Depending on the uncertainties included, designs far off the constraint boundary may have to be analysed for robustness. Generally how far off the constraint

boundary to perform the robustness analysis is not known, see Figure 5.6 in Section 5.6.2. Hence many robustness analyses may be required to find a robust design, see Figure 8.3 where the global robust optimum (blue) is missed as the search for robust optimum stops at the green point.

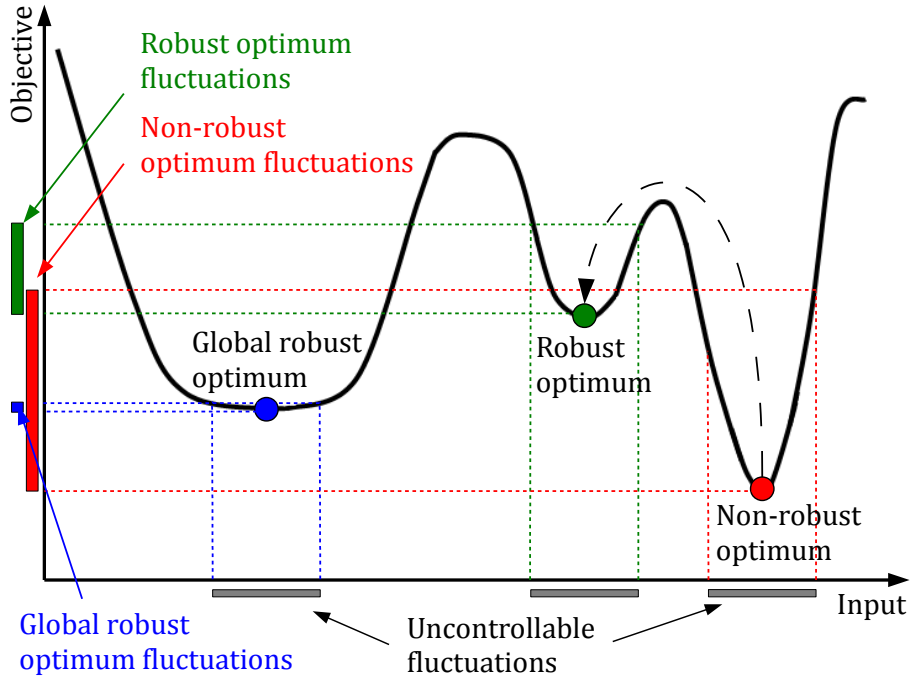

FIGURE 8.3 – One typical situation for Sequential RDO approach.

8.3.2 Adapted Sequential Approach

Another approach could be implemented taking the sequential approach one step further. Here a margin related to the constraint boundary is created. If this margin is selected carefully, the designs that are non-robust (designs too close to the feasible space boundary) are removed from consideration for robustness analysis. In this case the optimisation problem is over constrained where the feasible space is deliberately reduced, see Figure 8.4 where a 10% margin is adapted on the original constraint. Now the optimisation finds designs near the boundary of the newly employed constraint. These sub-optimal designs, at the boundary of this new feasible space, are more likely to be robust since these designs are already away from the real constraint, see green optimisation point in Figure 8.4. The problem here is to formulate a good size of the margin. Since this is a sequential approach, there is no direction for the algorithm to search for better regions in terms of robustness. An approach presented later in this chapter also creates a margin (offset) of the constraint boundary. However it is formulated as a simultaneous RDO approach where both optimal and robust designs are searched, see Section 5.6.3. In this approach the robustness of designs are evaluated within the interval between the margin and the constraint boundary.

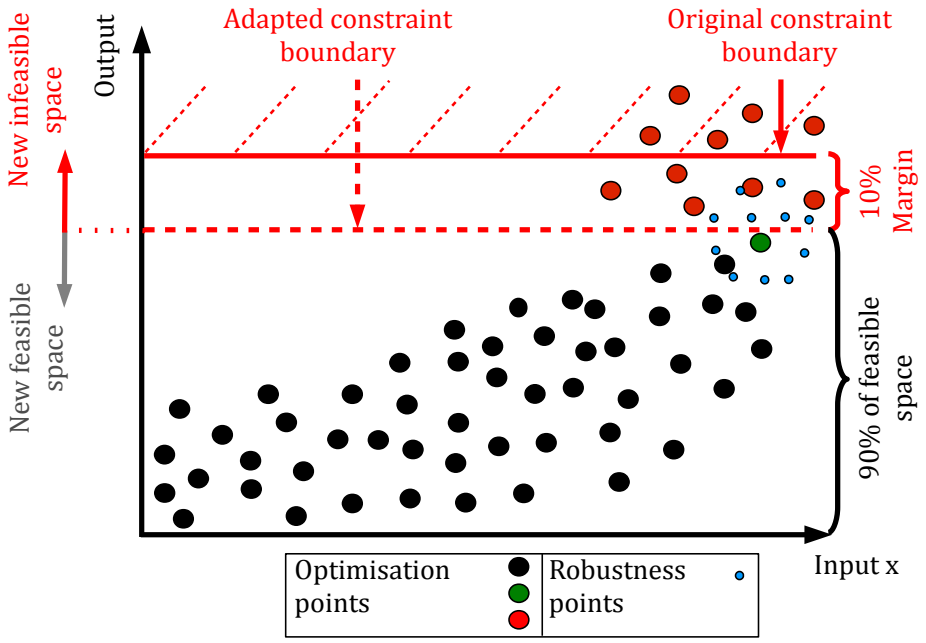

FIGURE 8.4 – An adapted sequential RDO approach.

8.4 Choice of Algorithm

The main requirement for an algorithm here is to be able to continue without the robustness information of points outside the TI. Since, for the implementation purpose, "dummy" robustness points are generated for each design outside the TI which are not computed and hence to do not contribute to the computational effort, see Appendix A.4.1. This limits the choice of the algorithm used.

Here response surfaces cannot be used easily since the information on the robustness of all the optimisation points is required to build the response surfaces for the mean (μ) and the standard deviation (σ). Avoiding the robustness analysis of designs outside the TI reduces the number of points used to generate these response surfaces (specially at the beginning of the optimisation since lots of designs may be outside the TI)[4]. As a result the quality of the generated response surfaces is significantly reduced. Therefore the proposed RDO approach, in this chapter, is investigated using a Genetic Algorithm (GA). An improvement to the approach presented in this chapter is presented in Chapter 9 which allows for the use of response surfaces for optimisation. This is because for designs outside the TI approximate robustness information of designs are made available via the use of ESLM. Since the robustness information of all the designs are available, the representative response surface for μ and σ can be generated.

The GA can still be used here since the "dummy" robustness information of designs

4. For implementation purpose "dummy" robustness points are generated for designs outside the TI. However using these "dummy" robustness points to build the response surfaces would be wrong as they do not have any physical meaning. Refer to Appendix A.4.1 for how these "dummy" robustness points are generated.

outside the TI is available. The idea is to direct the algorithm towards better regions of the design space using only the information of the optimisation outputs of designs outside the TI [5].

8.5 Target Interval (TI)

One of the most important aspects of this approach is the definition of the TI. Depending on the TI definition robust designs are found or missed. If a big TI is used then many designs fall within the TI which means many robustness analyses are required. This reduces the computational efficiency of the approach. If a small TI is used then, depending on how sensitive the design is, all the designs within the TI may be non-robust. This means that robust designs exist outside the TI. This robust design cannot be achieved since no robustness analyses are performed outside the TI. Hence the size of the TI significantly determines the performance of this approach. A TI should be defined such that it reduces the number of robustness analyses required and also contains the robust designs within it. The size of the TI should therefore be defined carefully. The next section proposes a way to determine the TI.

8.5.1 Size of TI

The size of the TI should be defined such that it accommodates the robust designs near the constraint boundaries. In addition, the activeness of the constraint and the size of output fluctuation should be considered. Here constraint activeness means how easily the constraint is violated. For a constraint that is not easily violated, a bigger TI has to be taken such the designs fall within this TI for robustness analysis. For an active constraint smaller TI should be defined because this constraint is violated more frequently which means there are many design close to the feasible-infeasible boundary. It should be avoided to evaluate robustness of the large number of designs, by taking a small TI, for computational efficiency.
Also the sensitivity of the designs to uncertainties has to be monitored to define the TI. This is because the defined TI should be able to accommodate both the optimisation point and also its robustness points (variations). Hence to get an idea of the variation in the responses due to uncertainties, a sensitivity analysis can be made with few designs. For this, first a representative sample points have to be generated in the whole design space. Then robustness analyses of these designs can be performed to get an idea of the responses variation. Since the approach here is based on the output space, it is difficult to generate a representative points in this space because relative inputs are required (which are not easily known). Although

5. The "dummy" robustness information do not play any role in directing the algorithm since the size of σ for all designs outside the TI is kept constant, see Appendix A.4.1 for further details.

the initially generated sample points may be well distributed in the input space, these points may be clustered in the output space, see Figure 8.5. Assuming that the points are also uniformly distributed in the outputs space, the following steps can be used to predict the required TI.

i. Generate m sample points in the input space.

ii. Generate n random robustness points around m points.

iii. Compute the standard deviation (σ) for each sample point m.

iv. Take the biggest σ value and define TI, Eqn (8.1), where R is for real robustness analysis.

$$\text{TI} > 2\sigma_R. \tag{8.1}$$

Here TI is defined to be greater than two times the biggest σ value because 2σ level is used for robustness analysis. Hence the TI should be able to accommodate the robust designs with this σ levels. However this initialisation step, to find the size of the outputs variation, may already be too expensive. Therefore experience or previous studies can be used to define the TI.

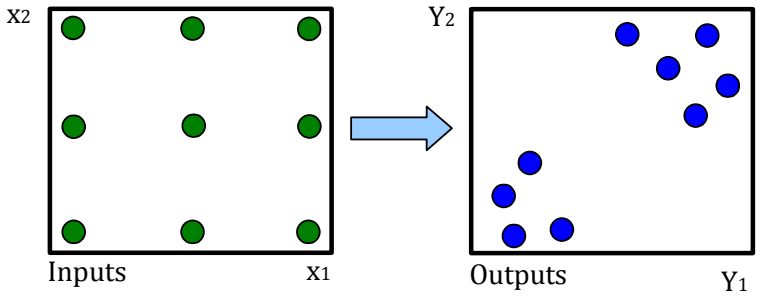

FIGURE 8.5 – Possible sample points distribution in the input and output space.

8.5.2 Number of TIs

For optimisation with multiple constraints either multiple TIs have to be defined or constraints can be combined using weighing factors where the most important (active) constraint would have the biggest weight. However the information on the important constraint is not available prior to the optimisation and also the weighing of these constraints is not straightforward. Hence it is easier to define multiple TIs, see Figures 8.6 and 8.7. If multiple TIs are defined, the size of the TIs are different for each constraint as explained in Section 8.5.1. The interesting question here is the decision on when to perform the robustness analysis. Two criteria can be used for the decision to perform robustness analysis.

i. If designs are in both the TIs then perform a robustness analysis, see dark green space in Figure 8.6 and green cube in Figure 8.7. This is a region where

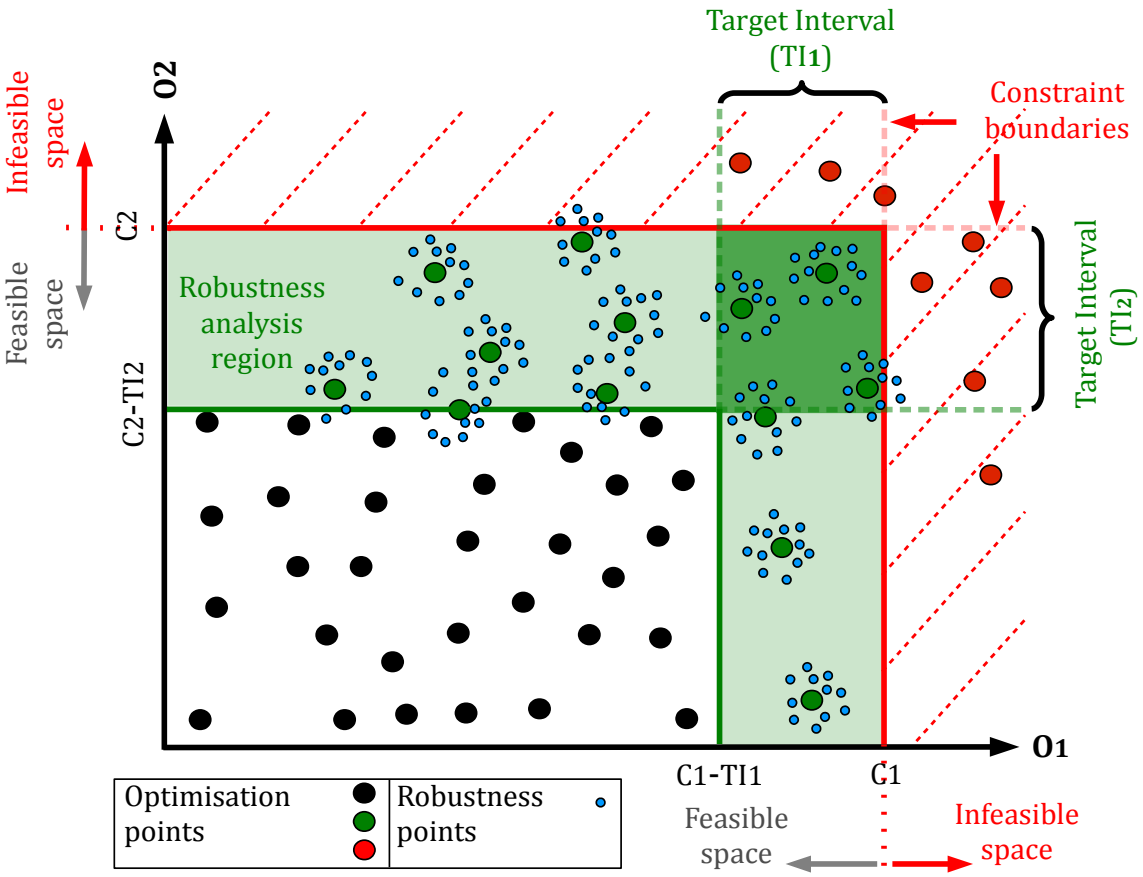

FIGURE 8.6 – TI definition for robustness analysis with two outputs.

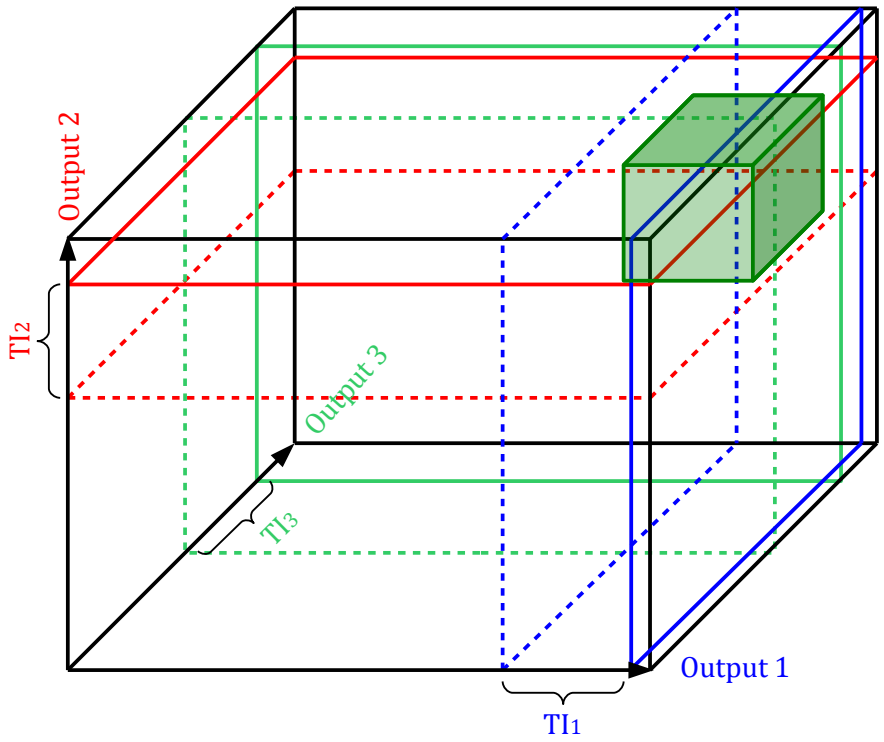

FIGURE 8.7 – TI definition for robustness analysis with three outputs.

the TIs overlap. For the case presented in Figure 8.6 this is formulated as:
if ($O_1 > C_1$ *OR* $O_2 > C_2$) $\rightarrow$ No robustness analysis.
if ($O_1 <$ C_1-TI_1 *OR* $O_2 <$ C_2-TI_2) $\rightarrow$ No robustness analysis.
else $\rightarrow$ perform robustness analysis.

ii. If designs are in the feasible design space and within one TI then perform robustness analysis, see light and dark green space in Figure 8.6. For the case presented in Figure 8.6 this is formulated as:
if ($O_1 > C_1$ *OR* $O_2 > C_2$) $\rightarrow$ No robustness analysis.
if ($O_1 <$ C_1-TI_1 *AND* $O_2 <$ C_2-TI_2) $\rightarrow$ No robustness analysis.
else $\rightarrow$ perform robustness analysis.

The formulation, for the decision to perform the robustness analysis or not, significantly affects the computational efficiency. For example the second formulation will require more robustness analyses as this criterion is easily fulfilled compared to the first criterion. However with the first formulation, if the TIs are not defined well then there may be very few designs within the TIs and these designs may not be robust.

8.5.3 Computational Advantage

In this approach the computational efficiency depends on the required number of robustness analysis. The size of TI plays a vital role here since the larger the size of the TI the more designs fall within this TI requiring robustness analysis. Hence the TI should be defined such that it is big enough to accommodate the robust designs and small enough such that it reduces the number of designs within the TI. Also the criterion for the robustness analyses decision is vital here, presented in Section 8.5.2. The computational advantage is also dependent on how quickly the algorithm converges (how quickly the algorithm gets into the TI). If the optimisation converges quickly then the robustness analysis has to be made for almost all designs in the following generations. This reduces the computational advantage that can be achieved through this RDO approach. Some ideas to increase the efficiency are presented in Section 11.2.3.

8.6 Validation Cases

For all the validation cases presented in this section, the 2σ approach is used for robustness analysis, presented in Section 5.5.2. Furthermore, the RDO formulation is not based on the multi-objective approach where both the mean and the variance are minimised. Here only the feasibility robustness is considered where the variations of the constraint responses are checked, see Section 5.5.1.

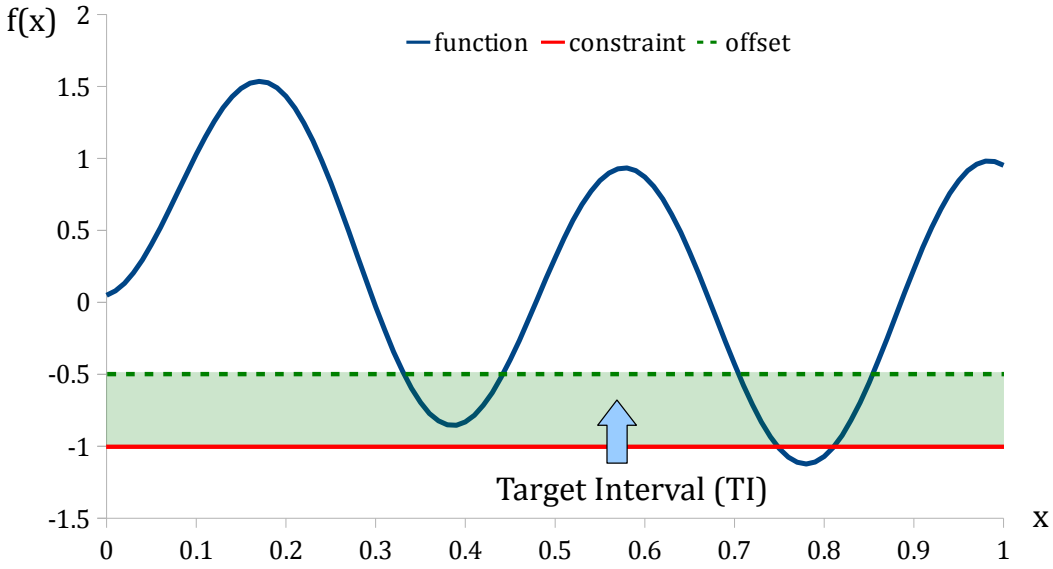

FIGURE 8.8 – Constraint offset and TI for a 1-D problem.

8.6.1 Analytical Test Functions

To test the newly implemented RDO approach, some analytical functions are used first, presented in the following sections.

Test Function 1

The first analytical test function is shown in Figure 8.8 given by Equation (8.2). The function has a global minimum at $x = 0.78$; $f(x) = -1.12$. However to really test the RDO approach the function is constrained at $f(x) = -1$. Due to this constraint the new optimum is now at $x = 0.39$; $f(x) = -0.8535$. The noise variable here is the variation in the input x with a standard deviation of $\sigma = 0.01$. The aim is to see if the modified RDO can find this new robust optimum. Different offsets are used to test if the size of the TI has any effect on the performance of the new RDO approach, see Figure 8.8 for an offset at $f(x) = -0.5$. Here robustness analysis is only made for designs within the TI. For the designs outside the TI, representative values are generated using the optimisation point values, see Section A.4.1.

A commercial GA available in optiSLang optiSLang (2011) is used as optimisation algorithm with 10 individuals in each generation. For robustness analysis, LHS sampling is used to generate 15 points, see Section 3.5.1.

$$f(x) = 2(x - 0.75)^2 + \sin(5\pi x - 0.4\pi) - 0.125. \tag{8.2}$$

The results with different TI size are given in Table 8.1. The first 7 runs are made without an offset to the constraint where the first run is made with normal RDO loop (real robustness analysis for all optimisation points). Most of the optimisation

runs are successful in finding the global optimum. Some of the runs that did not find the intended robust optimum at $x = 0.39$ have found similar robust optimum around $x = 0.7$ and $x = 0.8$, see grey highlighted cells in Table 8.1. The size of the TI, in this case, has no effect on the performance of the algorithm.

Run no.	TI		Start design	Optimum variable x^*	Design No.
	UB[1]	LB			
Normal	NA	-1	0.33	0.39	137
1	NA	-1	0.44	0.38	7
2	NA	-1	0.84	0.39	84
3	NA	-1	0.67	0.4	53
4	0	-1	0.94	0.39	64
5	0	-1	0.53	0.39	33
6	0	-1	0.63	0.39	58
7	-0.5	-1	0.13	0.39	52
8	-0.5	-1	0.33	0.39	41
9	-0.5	-1	0	0.41	38
10	-0.7	-1	0.83	0.83	59
11	-0.7	-1	0.35	0.72	10
12	-0.7	-1	0.36	0.39	37

[1] UB (Upper bound) and LB (Lower bound) represent the constraint and the offset.

TABLE 8.1 – Results for the modified double loop RDO runs of test function 1.

Test Function 2

The first analytical function is a general test to see if the global optimum of a constrained problem could be found. The second analytical function represents more the robustness test, see Equation (8.3). The function has 3 local and 1 global minima in the range of $x = [0, 4.5]$, see Figure 8.9. A constraint on the function is set at $f(x) = -3.6$ which eliminates the global optimum at $x = 4.2$. Hence now the global optimum is at $x = 3.3$. However, this optimum is narrower compared to another optimum at $x = 2.2$ and hence we expect this minima to be non-robust. This leaves a robust optimum at $x = 2.2$. The TI is defined by an offset at $f(x) = -1$. Again the noise variable here is the variation in the input x by $\sigma = 0.1$. The algorithm settings are the same as for the first test function.

$$f(x) = x\sin x^2. \tag{8.3}$$

Repeated tests are made with different starting points. The results of the different RDO runs for function 2 are listed in Table 8.2. The algorithm has managed to find

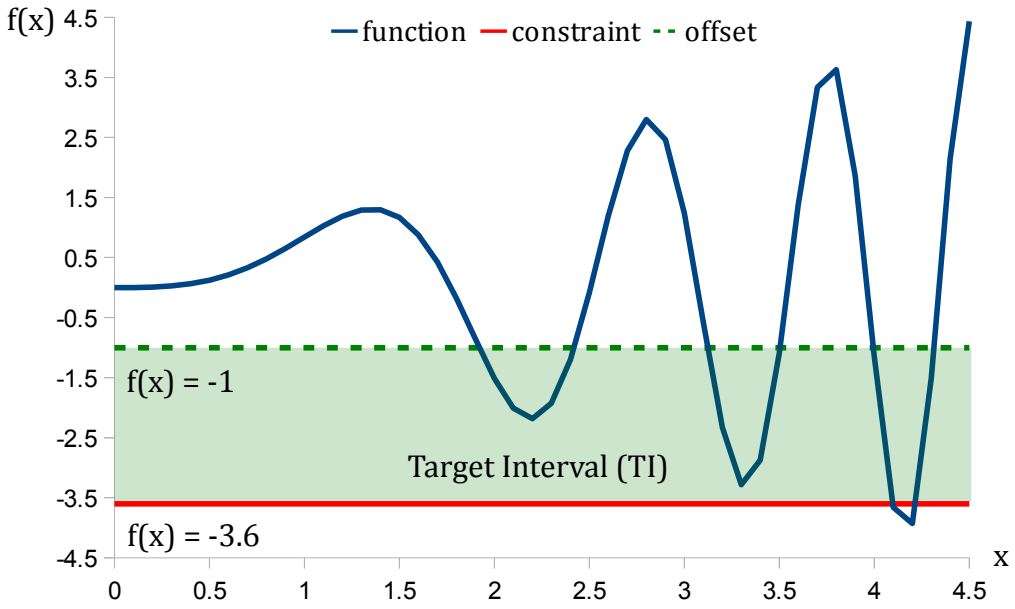

FIGURE 8.9 – A 1-D robust design analytic test function.

the robust optimum at $x = 2.2$ in most of the cases.

Run no.	TI		Start design	Optimum variable x^*	Design number
	LB	UB			
Normal	-3.6	-1	1.7	2.2	37
1	-3.6	-1	4.4	2.2	53
2	-3.6	-1	4.4	2.2	170
3	-3.6	-1	4.4	2.2	40
4	-3.6	-1	0	2.2	69
5	-3.6	-1	0	2.1	2
6	-3.6	-1	0	2.2	14

TABLE 8.2 – Results for the modified double loop RDO runs of test function 2.

Test Function 3

A Rastrigin function with reduced number of maxima and minima is used, see Equation (8.4). It is a multimodal function with a global optimum at $x_i = 0$; $f(\mathbf{x}) = 0$, see Figure 8.10(a). It is interesting to see how the newly implemented RDO approach performs for this demanding (multi-modal) case. Different TI (constraints), design space and inputs uncertainty are tested.

$$f(x) = An + {x_1}^2 - A\cos(\pi x_1) + {x_2}^2 - A\cos(\pi x_2). \tag{8.4}$$

Where $A = 10$, $n = 2$ (no. of design variables) and x_i = [-5.12,5.12].
For the first 3 tests, run no. 1-3 in Table 8.3, a constraint is applied at $f(\mathbf{x}) = 3.9$. This makes the global optimum infeasible, now there are 4 minima at $x_i \approx (\pm 1.95, \pm 0.015)$ where $f(\mathbf{x}) \approx 3.93$. For the variation in the inputs $\sigma_{x_i} = 0.05$ mm is used.

An offset is made at $f(\mathbf{x}) = 20$ to define the TI. For these runs, although the exact solutions are not found but solutions close to the stable regions are obtained, see Table 8.3.

In test runs 4 and 5, reduced design space and increased inputs variations are used.

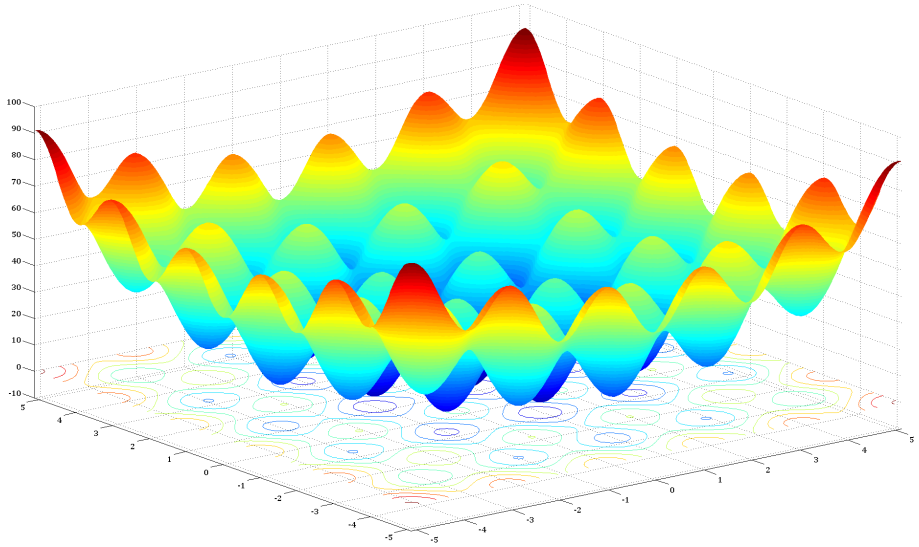

(a) 3D view of the Rastrigin function with 2 design variables.

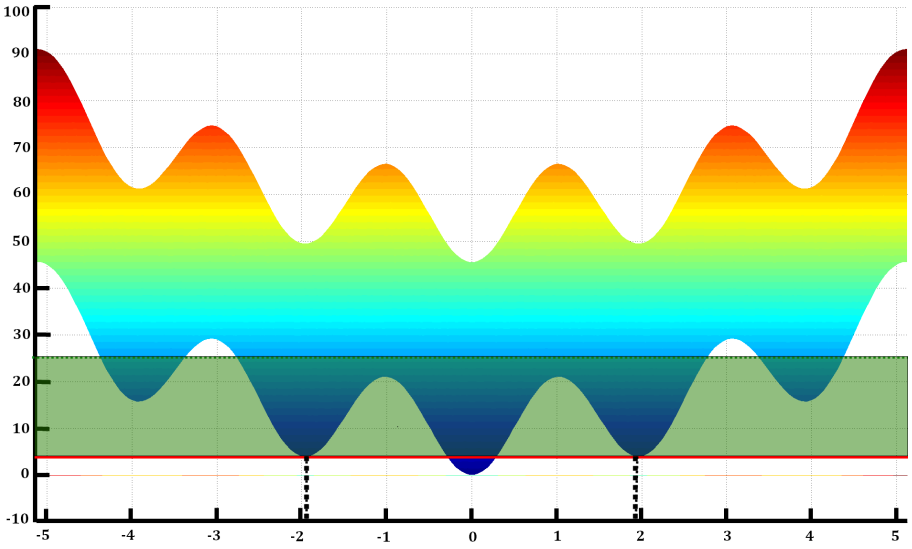

(b) Rastrigin function 2D view with Target Interval (TI) definition (green).

FIGURE 8.10 – Rastrigin function test case for the implemented RDO approach

Due to the new variations the region around $x_i \approx (\pm 1.95, \pm 0.015)$ is no longer robust. Hence now the more wider peaks at $x_i \approx (\pm 2, \pm 4)$ are stable regions for this uncertainty level. In both runs these regions are found with less number of evaluations due to the reduced design space.

For the remaining runs, a constraint is applied at $f(\mathbf{x}) = 4$, such that the global minimum and other minima at $x_i \approx (\pm 1.95, \pm 0.015)$ are made infeasible. Also the input variation is reduced to $\sigma_{x_i} = 0.05$ mm. Hence as expected, the algorithm finds the robust region around $x_i \approx (\pm 1.9, \pm 0.01)$.

Run no.	TI		Design space		Input	Optimum		$f(\mathbf{x})$	Design
	LB	UB	LB	UB	variation, σ_x	x_1	x_2		number
Normal	4	20	-5.12	5.12	0.05	1.8	-0.2	7.09	96
1	3.9	20	-5.12	5.12	0.05	-1.9	0.1	4.60	110
2	3.9	20	-5.12	5.12	0.05	-0.05	-1.91	4.17	123
3	3.9	20	-5.12	5.12	0.05	-1.87	0.11	4.92	107
4	4	20	-3	3	0.1	-2	-2	8	33
5	4	20	-3	3	0.1	1.8	2	9.15	37
6	4	20	-3	3	0.05	0.1	1.8	5.65	122
7	4	20	-3	3	0.05	-2.1	-0.2	6.85	67
8	4	20	-5.12	5.12	0.05	2	0.22	6.34	94
9	4	20	-5.12	5.12	0.05	-2.2	0.1	7.25	71
10	4	20	-3	3	0.05	-1.8	-0.1	5.65	41

TABLE 8.3 – Results for the modified double loop RDO runs of Rastrigin function.

8.6.2 Structural Validation Cases

It is not always easy to find benchmark problems to test the performance of optimisation approaches. Hence here simple problems (in-terms of impact case, parameterisation and number of design variables) are used for which the interpretation of results are easier. Two validation cases are presented here, a linear static torsion case and a crash case. These validation cases are chosen to take advantage of their simulation time.

Torsion Case

Design Case A metallic beam with dimensions 90 × 90 × 330 mm is used. The beam has U-type cross-section reinforced with rib structures, Figure 8.15. A static loading of 100 N per node is applied which creates both the torsion of cross-section and shear of the outer walls, see Figure 8.11(a). The material properties of the beam are: Young modulus, $E = 210$ GPa, Poisson's ratio, $\nu = 0.3$, density, $\rho = 8.34$ t/m^3. The material properties of the reinforcement are: Young modulus, $E = 2.3$ GPa, Poisson's ratio, $\nu = 0.35$ and density, $\rho = 1.45$ t/m^3. This test case is inspired from Hunkeler (2013).

Design Parameterisation The beam is parameterised such that the reinforcements change their locations. Only 2 parameters are used which are the location of the vertical walls (A) and horizontal walls (B). The maximum and minimum settings of the walls are presented in dotted red lines and dotted blue lines respectively, see Figure 8.11(b). For the uncertainty parameters, the location of parameters A and B are varied by $\sigma = 0.2$ mm and the force is varied uniformly by ± 4 N.

Objective and Constraint The objective is to reduce the mass of the beam. A constraint is applied such that the average maximum displacement, $d_{\max}$, of the

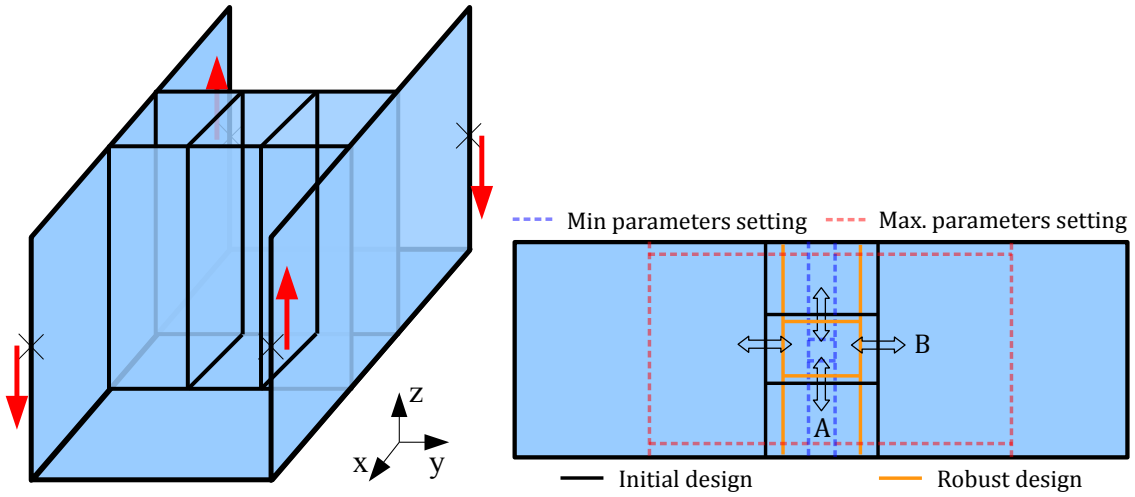

(a) Torsion load case.

(b) Reinforcement configuration of initial and final design.

FIGURE 8.11 – Torsion test case with rib reinforcement.

nodes (where the forces are applied) should not exceed 3.8 mm.

Algorithm Settings Again a general GA is used with 10 individuals in each generation. For the robustness analysis 15 individuals (generated using LHS) are used due to the quick analysis time. A TI is created by taking an offset of the constraint at $d = 3.4$ mm, see Figure 8.12.

Results and Discussion The initial rib configuration is a feasible design with average maximum node displacement $d_{\max}$=3.57 and mass = 827g. An improved robust design is found at the 8^{th} iteration, 81^{st} design, see Figure 8.12. The mass has been reduced to 820g, an improvement by 0.84 %. This improvement is not significant since thickness parameters are not included, which is always dominating. Also in this parameterisation case the mass is dependent on the length of the horizontal walls and hence parameter **B**. Figure 8.11(b) shows the initial and the robust rib design. Figure 8.12 shows the displacement history and the TI. Within the TI there are many designs that are in the feasible region however they are non-robust, see red dots within the TI in Figure 8.12.
The computational efficiency, to reach the robust optimum, is approximately 42% since out of the 1296 design evaluations (81 optimisation points + 81×15 robustness points), 555 robustness analyses are not required. This is because 37 designs out of the 81 optimisation designs are outside the TI that needed no robustness analysis.

Cantilever Beam

Design Case For test and validation purpose, a very simple impact case is used which is computationally cheap (simulation time $\approx$ 2 minutes). The beam is formed of two similar profiles which are laser welded together with a reinforcement inside

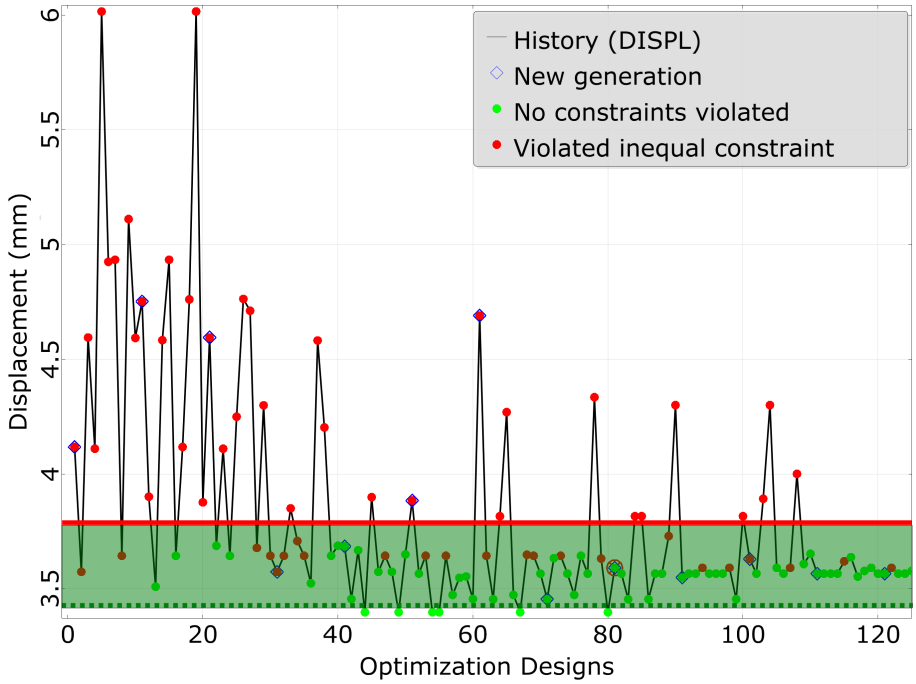

FIGURE 8.12 – Deflection response history and the TI.

the beam, Figure 8.13. The dimensions of the beam is 100 × 50 × 400 mm. A ball impactor is used with a mass of 80 kg and velocity of 8 kph. One end of the beam is constrained in all directions.

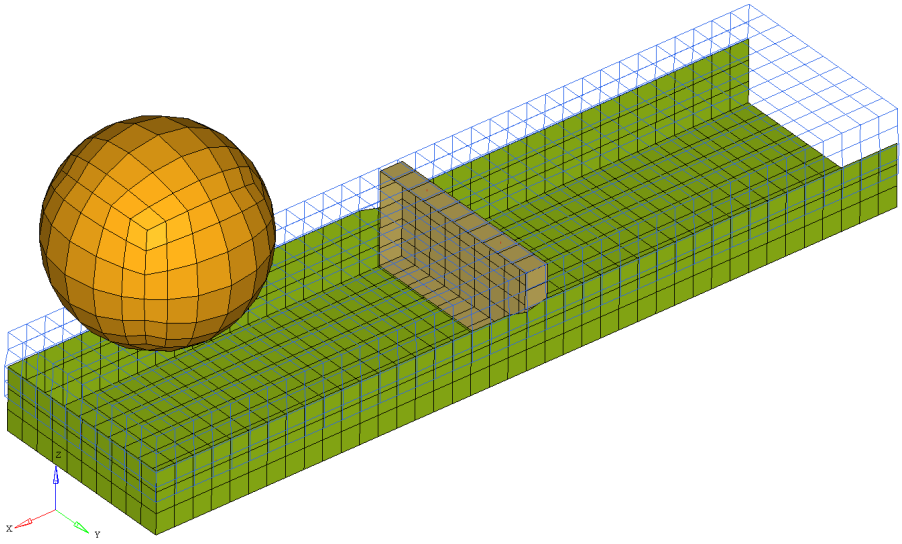

FIGURE 8.13 – A simple ball impact case.

Design Parameterisation The optimisation parameters are the thickness of the individual profiles, the reinforcement and also the position of the reinforcement. Table 8.4 presents the design variables and noise variable used in the RDO.

Objective and Constraint The objective is to reduce the mass of the beam while respecting the deflection constraint, $d \leq 30$ mm.

	Variable	Lower limit	Initial design	Upper limit	Distribution	Standard deviation
Design variables (mm)	P	100	200	300	normal	0.1
	t_{top}	0.5	1.0	1.5	normal	0.07
	t_{bottom}	0.5	1.0	1.5	normal	0.07
	t_{reinf}	0.5	1.0	1.5	normal	0.07
	Variable	Lower limit	Initial design	Upper limit	Distribution	Standard deviation
Noise variables	M_0 (kg)	79	80	81	uniform	NA
	V_0 (m.s^{-1})	2.124	2.224	2.324	uniform	NA

TABLE 8.4 – Design parameters and uncertainties included in RDO.

Initial design						Robust optimum					
Parameters				Outputs		Parameters				Outputs	
t_{reinf} (mm)	t_{bottom} (mm)	t_{top} (mm)	P (mm)	Mass (kg)	Deflection (mm)	t_{reinf} (mm)	t_{bottom} (mm)	t_{top} (mm)	P (mm)	Mass (kg)	Deflection (mm)
1	1	1	0	1.2	27.4	0.5	1.16	0.5	3	0.94	26.7

TABLE 8.5 – Results comparison of the initial and robust designs.

Algorithm Settings Here the same algorithm settings are used as for the torsion case, Section 8.6.2. An offset is created for the deflection at $d = 20$ mm, creating a TI with size 10 mm, see Figure 8.14.

Results and Discussion The optimum is found at the 14$^{\text{th}}$ iteration (149$^{\text{th}}$ design). Table 8.5 compares the parameters and the outputs of the initial and the optimum designs. The mass has improved by 21.7% due to the reduction in the thicknesses. Also for this case the position of the reinforcement is not significant. Figure 8.14 shows the deflection history and the TI used. It can be seen from Figure 8.14 that at the beginning of the optimisation many designs are outside the TI. This is because the optimisation algorithm is exploring the design space. However after the 4$^{\text{th}}$ iteration most of the designs fall within the TI, since the algorithm is at exploitation stage. As mentioned in Section 11.2.3, adaptive TI can be implemented to further reduce the computational effort, see Figure 8.14 blue dotted line for a proposed adaptation of the offset.

The computational efficiency, to reach the robust optimum, is approximately 29% since out of the 2264 designs (2249 + 15 robustness analysis points for the optimum), 660 robustness designs are not evaluated. This is because 44 designs out of the 149 optimisation designs are outside the TI.

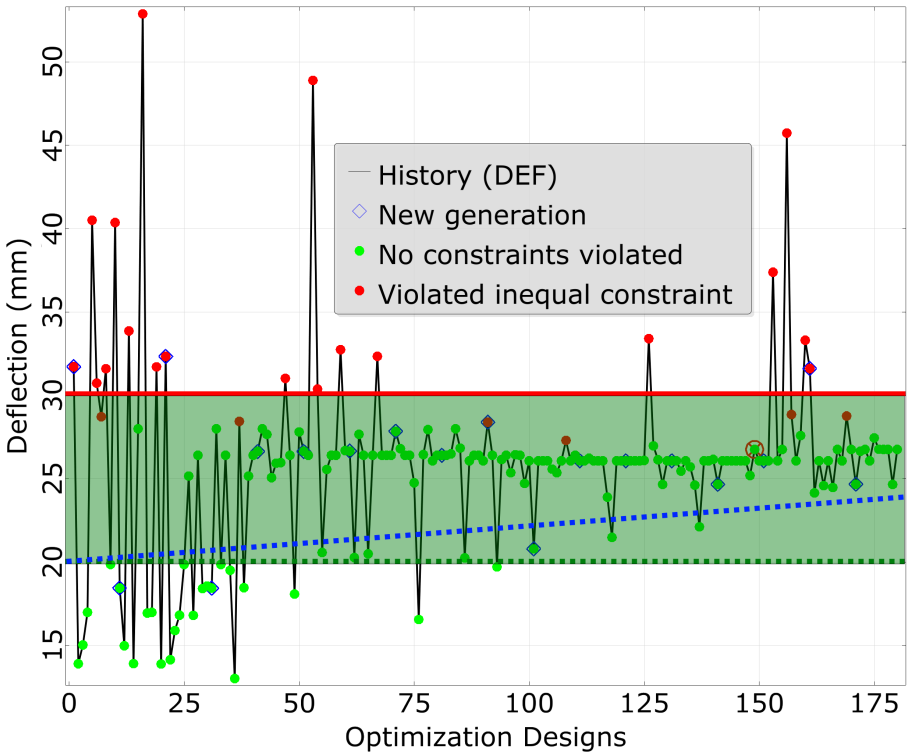

FIGURE 8.14 – Deflection response history and the imposed offset.

8.7 Limitations of the Approach

The approach presented here is limited due to the robustness analysis criterion (TI on output space). In some cases, since the TI is defined in the outputs space, the robust optimum is missed since it is outside the TI, Figure 8.15(a) and 8.15(b). In both cases, the robust design is not analysed with real analysis but "dummy" values are generated. Hence to avoid these situations either an additional robustness criterion has to be implemented (which is not easy to define) or in each iteration (generation) one or two best designs should be evaluated for robustness. This additional step should capture the robust designs that are outside the TI however this reduces the computational efficiency.

8.8 Conclusion

In this chapter an approach to reduce the computational effort for RDO is presented. The approach is based on searching for regions close to the feasible space boundary where there is a likelihood of finding robust designs. The approach is validated successfully for several analytical functions and design cases. However there are difficulties in this approach that have to be addressed before it can be applied to complex industrial problems.

Firstly the method is too dependent on the definition of the TI. If the TI is not well defined then the method fails, see Section 8.7. Generally it is difficult to define

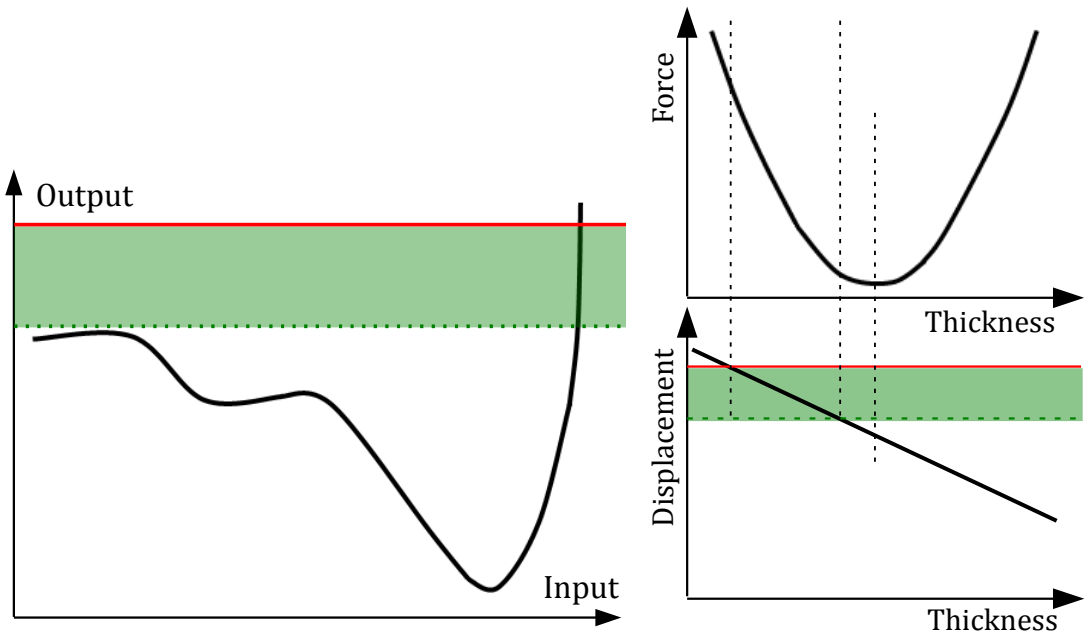

(a) TI far off the robust design. (b) TI not chosen carefully.

FIGURE 8.15 – Some functions where the approach misses the robust point.

the TI size and the generated "dummy" values for the robustness analysis of points outside the Target Interval (TI), see Appendix A.4.1.

Secondly it is difficult to judge the direction of the algorithm due to the missing robustness information of designs outside the TI. Due to this missing information the algorithm is directed towards regions of minima (algorithm only tries to reduce the nominal value without trying to reduce the variations). The information on the robustness is very limited to direct the algorithm since this is only available once inside the TI. Hence it is better to provide the algorithm also with the robustness information from the start of the optimisation. This could be done by using some approximation approaches, at the start, where the approximations are used to direct the algorithm towards better and stable regions and when these promising regions are found accurate solutions could be used.

Furthermore, designs that are slightly infeasible should also be included for robustness analysis. This provides the optimisation algorithm additional information regarding the parameter combinations that give infeasible solutions and also the robustness information of these infeasible designs. This additional information helps direct the optimisation algorithm towards robust regions of the design space.

Considering the discussions above, ESLM is investigated in Chapter 9 as an approximation approach for robustness analysis of designs outside the TI. The approximate robustness analysis via ESLM provides robustness information of all designs to assist the optimisation algorithm towards the boundaries of the design space where accurate robustness analysis of designs are made.

Chapter 9

Equivalent Static Loads Method (ESLM)

9.1 Introduction

Crash simulations through Finite Element Analysis (FEA) are computationally expensive due to the requirement to capture the true behaviour (time dependency and non-linearity) of crash events. However during RDO, it is not always required to evaluate the designs with full accuracy. See for example Redhe and Nilsson (2006) where multi-fidelity models are used for optimisation. Here mostly low fidelity models are used to explore the design space while few high fidelity models are used to correct the approximations. The main idea here is to divide the optimisation into two phases:

First phase: exploration of the design space with approximated evaluations,

Second phase: exploitation with more accurate evaluations.

At the first phase, only rough information is needed to guide the optimisation algorithm towards the promising regions of the design space. This can be achieved through some approximation approach such as ESLM see Kim and Park (2010). In the second stage, good and robust designs are identified with high-fidelity models. In the literature, approximate or low-fidelity models are often based on mathematical surrogate models (response surface methods), e.g. Kurtaran et al. (2002). They have some drawbacks: They require a high number of simulations, are often only applicable for a lower number of design variables and they might be only of acceptable quality in some sub-areas of the design space. Hence, in this thesis, an alternative approach is proposed, which is based on physical surrogates. More precisely, which replaces some of the non-linear and transient simulation by a set of linear static analyses. ESLM were already investigated for crash optimisations, Kim and Park (2010). Here, they are employed for the first time for robust design optimisation for crash.

9.2 ESLM State-of-the-Art

ESLM has been used in different studies for size, shape and topology optimisation due to its computational efficiency. It was first discussed in Choi and Park (2002) and Kang et al. (2001) where it is applied to linear dynamic cases. The design cases considered are circular cantilever beams and truss structures with cross-section dimensions as design variables. The method is further developed by the research group of Gyung-Jin Park, Hanyan University, Korea ; applications can be found in the field of crash, manufacturing etc Kim and Park (2010); Lee et al. (2013); Park (2011); Yi et al. (2011b). The ESLM is also implemented in commercial software such as Optistruct OptiStruct (2013) and GENESIS GENESIS (2012).

In this section the state-of-the-art of ESLM for crashworthiness with special focus on size and shape optimisation is presented. First, a crash box and a knee bolster design are optimised in Yi et al. (2011b) where the design variables are the thickness, the objective is the strain energy and the constraint is the displacement. In addition, a simplified front structure is optimised for pedestrian safety by the same authors discussing the difficulty to use the head injury criterion based on accelerations in a static simulation. The ESLM optimisation run is compared to a sequential response surface method (SRSM) and Kriging. It is concluded that ESLM has successfully found similar optimum as that from SRSM and Kriging by reduced number of non-linear analyses.

In Jeong et al. (2009) a vehicle frontal structure is optimised for the pendulum impact case. The design variables are 28 thicknesses of different parts. The optimisation is formulated to reduce the mass and constraints are the displacement, velocity and acceleration responses where the velocity and acceleration responses are calculated using finite differences from the displacement response. It is concluded that the ESLM is able to find improved solutions and the velocity and acceleration constraints are implemented successfully.

In Kim and Park (2010) an axially loaded cylindrical tube is studied for crash optimisation. The design variables considered are the radius and the thickness of the tube with mass as objective and displacement as a constraint. Since the design case is highly non-linear (plasticity, contact, buckling), the displacement response is very sensitive. To handle this buckling case, a move limit strategy is employed which progresses with only small changes in the design variables. Other applications of ESLM include manufacturing processes such as forging Lee et al. (2013) where shape variables are used, and vehicle roof crush where thickness variables are used Jeong et al. (2008) .

In total there is only a limited number of ESLM studies for crash optimisation, although the method is well exploited for other, simpler cases. Furthermore robustness is never considered via ESLM. In the next section the calculation of the ESL sets is

presented and the method is discussed in detail specially for crashworthiness.

9.3 Calculation of the ESL sets

The basic idea of the ESLM is to replace the computationally costly non-linear dynamic analysis with a set of linear static analyses. For this, first a non-linear dynamic analysis is made. Then load sets are generated, for all FE nodes, at each required time step using information from the non-linear dynamic analysis. These load sets are then used as multiple loading conditions that generate the same displacement effect as that from the non-linear dynamic analysis. The total number of load sets in ESL analysis is equal to the total number of time intervals at which the displacement fields are taken from the dynamic analysis to calculate the ESLs, see Figure 9.1. Since only linear static simulations are required, the computational cost for design analysis using ESL is very low compared to non-linear dynamic analysis. The derivation of the ESL sets is explained in the following via the simplified case of undamped dynamics.

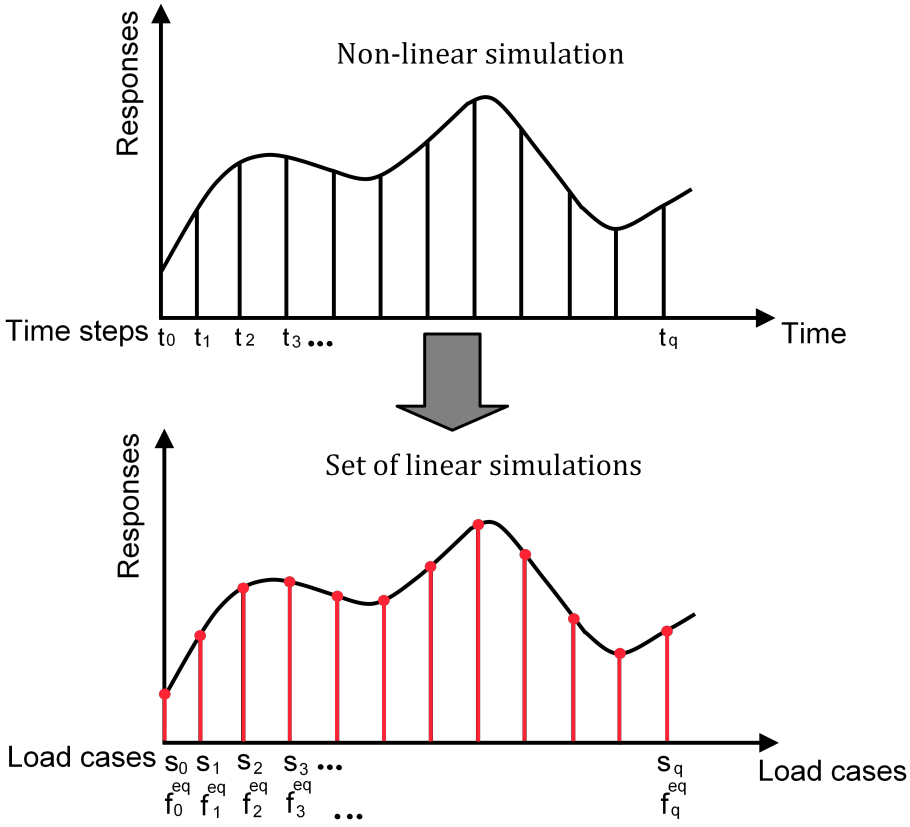

FIGURE 9.1 – Equivalent Static Load sets at different time intervals, Kim and Park (2010).

The equilibrium equation of an undamped structure is given as:

$$\mathbf{M}(\mathbf{b})\ddot{\mathbf{z}}_N(t) + \mathbf{K}_N(\mathbf{b}, \mathbf{z}_N(t))\mathbf{z}_N(t) = \mathbf{f}(t), \quad (t = t_0, t_1, t_2, ..., t_n). \tag{9.1}$$

$\mathbf{M}$, $\mathbf{K}$ are the mass and non-linear stiffness matrix respectively, $\ddot{\mathbf{z}}_N(t)$ is the acceleration, $\mathbf{z}_N(t)$ is the displacement and $\mathbf{b}$ is the design variable vector. Subscript N represents non-linear analysis, t is the time and n is the total number of time intervals chosen for ESLM. From Equation (9.1) the non-linear displacement $\mathbf{z}_N(t)$ can be calculated at each time interval t. The discrete displacement fields $\mathbf{z}_N(t_i)$ and the linear stiffness matrix $\mathbf{K}_L$ are used to calculate the ESLs at each time step, see Figure 9.1:

$$\mathbf{f}^{\mathbf{z}}_{eq}(s) = \mathbf{K}_L(\mathbf{b})\mathbf{z}_N(t), \quad (s = s_0, s_1, s_2, ..., s_n). \tag{9.2}$$

In Equation (9.2), subscript L represents linear static analysis and $\mathbf{f}^{\mathbf{z}}_{\mathrm{eq}}(s)$ is the s^{th} equivalent static load calculated at the i^{th} time interval. The evaluated ESL sets can now be used as external loads for linear static analysis via,

$$\mathbf{K}_L(\mathbf{b})\mathbf{z}_L(s) = \mathbf{f}^{\mathbf{z}}_{eq}(s). \tag{9.3}$$

From Equation (9.3), the linear displacement $\mathbf{z}_L$ can be calculated, which is identical to the non-linear displacement, $\mathbf{z}_N(t)$, from Equation (9.1).
The above process is used to calculate the ESL sets concerning displacement responses. The same process cannot be used to generate the stress responses due to the non-linear relation between stress and strain in the original system. Hence ESLs for stress response have to be calculated separately. This is not further discussed here since in this thesis only ESL for displacements are needed, see Kim and Park (2010) for further details.
Furthermore velocity $\dot{\mathbf{z}}_i$ and acceleration $\ddot{\mathbf{z}}_i$ responses are obtained using finite differences at the i^{th} time step, Jeong et al. (2009):

$$\dot{\mathbf{z}}_i = \frac{\mathbf{z}_{i+1} - \mathbf{z}_i}{\Delta t}, \tag{9.4}$$

$$\ddot{\mathbf{z}}_i = \frac{\mathbf{z}_{i+1} - 2\mathbf{z}_i + \mathbf{z}_{i-1}}{(\Delta t)^2}. \tag{9.5}$$

9.4 Optimisation using ESLM

The calculated ESL sets are used during the optimisation to reduce the evaluation time of the designs hence reducing the overall computational effort. This section presents the optimisation approach using ESLM with special focus on the displacement response.

The optimisation via ESLM is performed in two domains, design domain and analysis domain as shown in Figure 9.2. In the analysis domain the non-linear dynamic analysis is performed and the displacement field is extracted (for the required time steps). The ESL sets are generated using the displacement fields. Then the ESL sets are used as multiple loading conditions in the design domain for linear static optimisation and the design is updated. A loop is created that stops after some convergence criterion is fulfilled. Figure 9.3 shows the overall optimisation process using ESL sets which is further discussed in the following paragraphs.

1. First the cycle number ($k = 0$), initial design variables ($\mathbf{b}^{(k)} = \mathbf{b}^{(0)}$) and the convergence parameter (ε) are set.
2. Then a non-linear transient analysis is made on the design with $\mathbf{b}^{(k)}$. From this the non-linear displacement response ($\mathbf{z}_N(t)$) and the linear stiffness matrix ($\mathbf{K}_L$) (through linear analysis solver) are obtained, step 1 in Figure 9.3.
3. The ESL sets are calculated using the information from step 2.
4. The design analyses in the linear static response optimisation are made using the ESL sets, see step 3 and 4 in Figure 9.3.
5. When $k = 0$, the design is updated, non-linear transient analysis is made on the updated design and k is incremented by 1 . When $k > 0$ the convergence condition is checked. The convergence condition is the magnitude of design change from one iteration ($\mathrm{b}^{(k-1)}$) to another iteration ($\mathrm{b}^{(k)}$) and is given by the value, ε. If ε is satisfied the process is stopped else steps 1 - 4 are repeated. In this thesis the interest is to use ESLM for robustness analysis and not for optimisation. Hence only the steps (steps 1 - 3) in the blue region of Figure 9.3 are used.

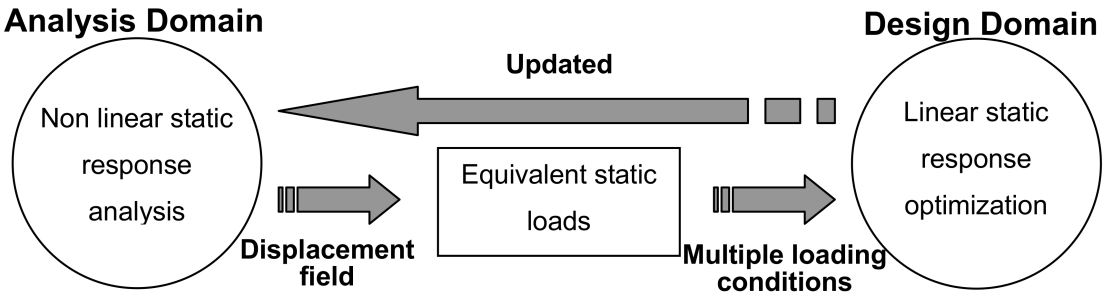

FIGURE 9.2 – Optimisation via ESLM: analysis domain and design domain, Park (2011).

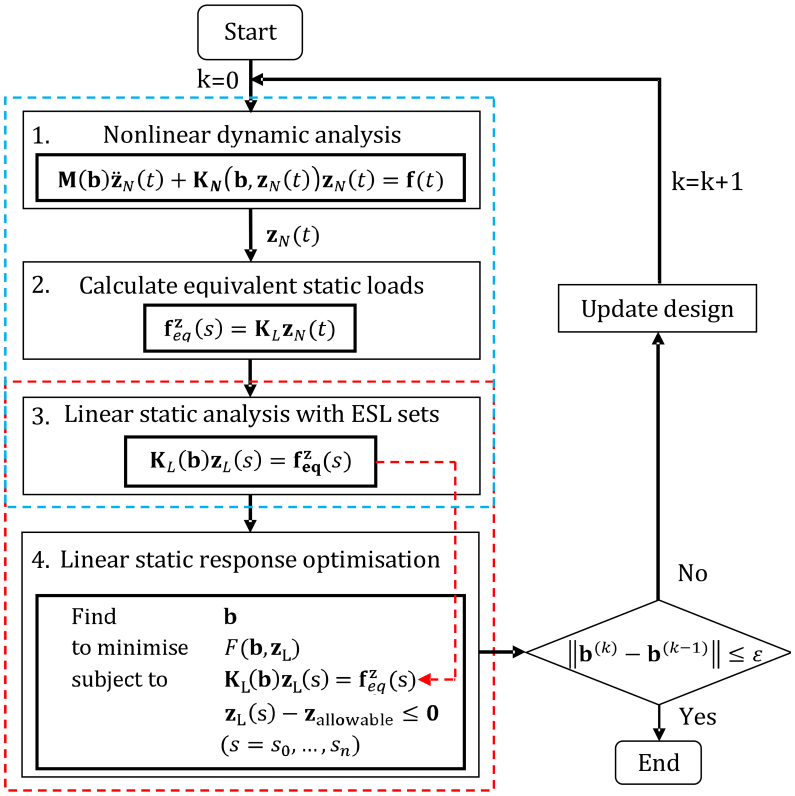

FIGURE 9.3 – Optimisation process using ESL sets considering displacement response, Park (2011).

9.5 Discussion of the ESLM

In this section the applicability of the ESLM for crashworthiness optimisation is discussed.

ESLM for Crash

The ESLM, when applied to crashworthiness studies, faces some challenges. This is because the linear static models have to capture the crash characteristics. During crash events large structural deformations occur in a very short period of time. This highly non-linear structural behaviour, such as contact, plasticity, buckling, cannot be fully captured by the ESLM. Similarly crash cases can also exhibit bifurcation behaviour due to stability or near contact situation where nearly the same designs (with non-linear dynamic analysis) give significantly different results. This cannot be modelled with the ESL approach, a new contact situation or a different buckling direction will not occur in the static analyses. The linear analyses are based on the stiffness matrix of the undeformed geometry while the non-linear analyses uses the deformed configuration.

It is therefore slightly questionable if the ESL optimisation can accurately replace the non-linear optimisation hence ESLM is presented here as an approximation approach to the non-linear dynamic analysis. The applications in this thesis concen-

trate therefore on crash cases, which normally do not show strong bifurcations etc. The more stable crash cases are related to bending, e.g. the low-speed impact onto a bumper or the lateral impact on the rocker.

Optimisation using ESLM

The first issue when using ESLM for optimisation arises because the sensitivities from the linear static analysis and non-linear dynamic analysis are different. Hence the sensitivities used in the linear optimisation might point in the wrong directions. The effect of this might be reduced by taking small steps and by updating more often the ESL. In Kim and Park (2010) validations were undertaken to show that at the last optimisation cycle, the sensitivity information from the linear response optimisation is comparable to that from linear dynamic response optimisation or non-linear static response optimisation. This statement should be taken with care, since it only looks at the very end of the optimisation when the convergence criterion is fulfilled. Hence the direction of the algorithm at the beginning might be different, which may lead to different regions of the design space. Also a profound analysis is missing for non-linear transient analysis. This is not further discussed here since ESLM is not used for optimisation in this thesis but only for robustness ; see, Kim and Park (2010), Shin et al. (2007) for further details.
The convergence of the algorithm can also be discussed in-terms of the design variable changes during optimisation. To keep the correctness of the initially generated ESL sets (in the analysis domain) the modified designs within the linear static response optimisation cannot be too different from the design for which the ESL sets are generated (move limit). Hence the exploration capability of the algorithm is limited and for highly non-linear cases the algorithm may get stuck in local minima. In linear response optimisation the contact non-linearity cannot be considered. Once the ESL sets are applied to the modified design there may be contact issues resulting into penetration. Hence in Yi et al. (2011a) the impenetrability condition between the potential contact surfaces is formulated as a constraint. The gap between the contact surfaces has to be greater than zero ($d_{gap} > 0$) for a design to qualify as a feasible design. Making the penetrating designs infeasible also means missing some good designs if contact is included.
Generally for crash optimisations time dependent responses are observed. However these responses cannot be considered in linear static response optimisation which limits the responses that can be studied. The velocity and acceleration responses in ESLM can be considered using finite difference approach, see Section 9.3. However these responses are simply an approximation from the linear displacement profiles.

Shape Optimisation using ESLM

It is specially difficult to handle shape parameters when ESLM is used for optimisation. This is because the load sets are defined at the nodes. The design changes during shape optimisation changes the location of the nodes. It is a severe problem specially if the designs are re-meshed since not only the nodes are moved slightly (node morphing) but they are at a completely different location in the geometry. In this case the loads are applied to the nodes at a completely new location giving unexpected deformations. For shape optimisation the question on where to apply the loads is important. In Figure 9.4 left, a beam is shown for which the ESL sets are generated. The length of the beam is increased and the ESL is applied to this modified beam, Figure 9.4 right. The question here is where should the ESL sets be applied ; only in the original portion of the beam (black load profile) or throughout the length of the modified beam (blue load profile). In the current ESLM the load is applied throughout the beam since the nodes are moved to the new portion of the beam. The correct approach would be, in most cases, to apply it only on the original portion of the beam. Hence load sets that are geometrically fixed would be more accurate, however this is difficult to implement since the loads are applied to the nodal locations.

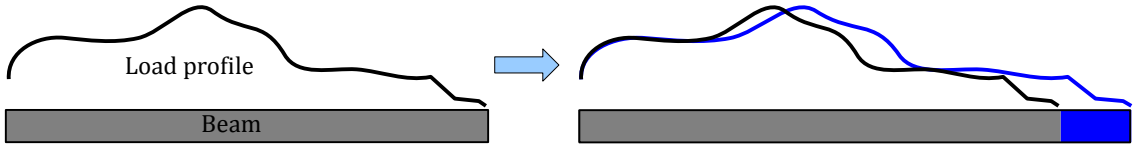

FIGURE 9.4 – Load definition issue for ESLM.

9.6 Proposed ESLM for RDO

As discussed in the previous part, the application of ESL for crash optimisation has some difficulties. Hence, this thesis explores how the described approach can be used for robustness analysis. This section presents therefore the implementation of the ELSM for robustness analysis during an optimisation. Here the ESLM calculation processes is implemented in MATLAB and automated to work with the existing optimisation loop, shown in Figure 6.15.

9.6.1 General Implementation

ESLM is used here, for the first time, for robustness analysis of designs during an optimisation. Taking advantage of the low computational time but considering its approximative character, it is an ideal approach to approximate robustness of designs at the regions of design space where accurate analysis is not required. Specially during the start of the optimisation ESLM can provide enough information

for the optimisation algorithm to progress to the robust regions of the design space. Hence in the approach presented here ESL computations are only used outside the Target Intervals (TI), see Section 8.5 and Figure 9.5. For the designs that fall outside the TI, ESL sets are generated. These ESL sets are then applied to their respective robustness points. Since the robustness points are small fluctuations of the optimisation point, the ESL sets generated from the optimisation points should still be valid when applied to the robustness points. Although exact responses cannot be obtained, good approximation of the responses can be achieved.

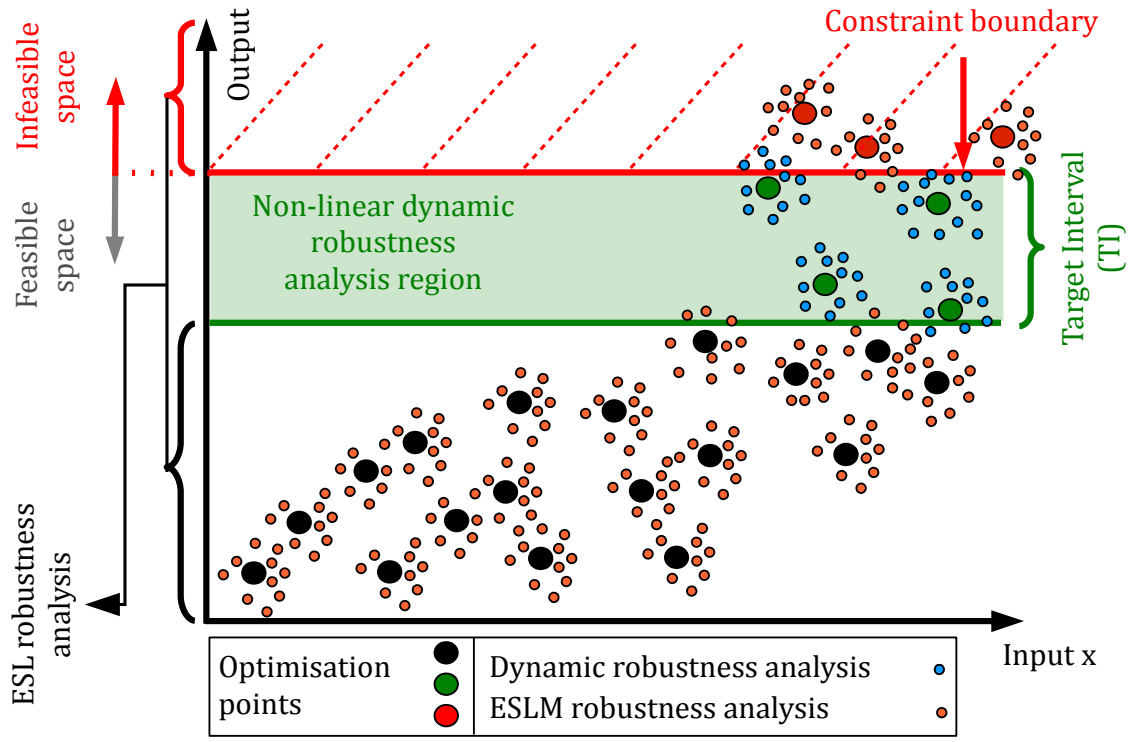

FIGURE 9.5 – Proposed robustness analysis with ESL outside the TI.

9.6.2 Shape Modification

In this thesis shape uncertainty is not considered, when using ESL, due to the re-meshing problem even when there are small shape modifications, see Section 9.5. This is not an approach limitation but an implementation limitation since this can be achieved by embedding a tool that can perform morphing for small shape changes (robustness points) and re-meshing for big shape changes (optimisation points).

9.6.3 Spot Weld Definition

It is difficult to formulate the weld spots together with ESLM since they have an influence on the stiffness matrix. To generate the ESL sets the correct product of the nodal displacement and the stiffness matrix element should be made. When the spot welds are included the ordering of the stiffness matrix is modified which makes

it difficult to generate the correct ESL sets. Since this is not a big part of the thesis it is not further investigated here.
To connect the different parts, spot welds are hence substituted with tied nodes. Tied nodes can be formulated between node to node or surface (group of nodes) to surface. It is more representative to use node to node ties at locations where spot welds exist however this is tedious to define. Also during the optimisation when there is a renumbering of the nodes due to re-meshing, the node to node tie definitions have to be automatically modified. Hence here surface to surface ties are used since the nodes in the surface definition are known even after renumbering of the nodes. An external script is used to automatically create the tie definitions, see Figure 9.9(a) surface to surface tie definition on the flange.
The tie definition is made by grouping the nodes as master or slave. The slave nodes are dependent on the master nodes. The stiffness elements of the slave nodes are excluded from the stiffness matrix. The slave nodes stiffness entries are represented by the master nodes stiffness. Hence the slave nodes are also removed from the nodes displacement list to generate the ESL sets.

9.6.4 Sub-modelling with ESL Analysis

In this section the implementation of sub-modelling with ESL analysis is presented. This is important since the idea is to use sub-modelling and ESLM for the overall RDO approach in Chapter 10. For this, first a non-linear dynamic analysis is made on the full model. From this the interface conditions (ICs) at the interface sections between the sub-model and the remaining model are extracted. These ICs are the interface nodes displacements at different time intervals, see Section 7.6 for further details. The generated ICs are then applied to the sub-model interface nodes and a non-linear dynamic analysis is made on the sub-model. From this sub-model analysis, the linear stiffness matrix ($\mathbf{k}_L$) and the non-linear displacements ($\mathbf{z}_N$) are extracted. The ESL sets $\mathbf{f}_e^{\mathbf{z}}q$ are then generated using $\mathbf{k}_L$ and $\mathbf{z}_N$. See Figure 9.10 for the sub-model analysis using ESL sets.
In this case both the translation and the deformation characteristics of the sub-model have to be captured. Here the translation characteristics are represented by the ICs at the sub-model interfaces and the deformation characteristics are defined by the ESL sets (since the impactor is removed). Since both the ICs and ESL definition are used, they have to be extracted from the same time step. Due to the formulation of the proposed approach, the performance of the ESL analysis is dependent on the sub-model quality. This is because the ESL sets are generated only after the sub-model analysis. Hence the quality of the sub-model is checked before the ESL sets are generated [1]. This dependency on the sub-model can be removed by explicitly calculating the ESL from the full model, removing the second step from

1. This is done by monitoring the outputs from the full model and the sub-model analyses.

Figure 9.6. However this is not done here as the main aim is to test the ESLM for robustness analysis. This could be implemented in the future.

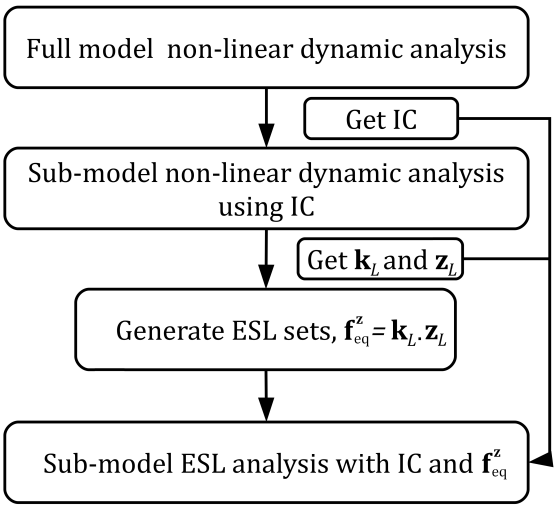

FIGURE 9.6 – Flowchart for sub-model analysis with IC and ESLM.

9.6.5 Robustness Analysis via ESLM

The purpose to use ESL in this study is to approximate the robustness of designs outside the TI. For these designs the optimisation points are still evaluated using non-linear dynamic analysis but the robustness points are evaluated using the ESLM. The idea here is to calculate the ESL sets from the optimisation point and apply these ESL sets to each robustness points of this optimisation point. Since the ESLs are only used for the robustness points, the limitations of ESLM, especially for large shape modifications for shape optimisation, are avoided. This is because the robustness points are designs with small fluctuations in the design and noise variables of the optimisation point. Since the design changes between the optimisation point and the robustness points are very small, the ESL sets can better approximate the responses. This is because the ESL sets are more correct since the ESLs are applied to the nodes that are not too far from their original position at which the ESL sets were generated. However one of the main issues to use ESL for robustness analysis is to consider the noise variables and specially the impact uncertainties. This is presented in the next section.

9.6.6 Impact Condition Uncertainties

Generally in RDO studies, the sources of uncertainty also include the variations in the impact conditions. Frequently considered impact conditions uncertainty include impactor mass, impact velocity, impact position and impact angles. Since the proposed idea is to use ESLM for robustness analysis, the impactor uncertainty cannot be easily considered for RDO. This is because it is difficult to generate ESL

sets that only represent the effect of the impact uncertainty. Also it is not ideal to generate a new set of ESL sets for each robustness point. In this section an approach is proposed to consider impactor uncertainty when using ESLM for robustness analysis. The general idea here is to separate the contribution of all the uncertainties (design variable fluctuations and noise variables) from the contribution of the design variables (nominal values) towards the generated ESL sets.

Initialisation

An initialisation is made where many ESL sets are generated that represent different uncertainty settings. For this an initialisation robustness analysis is made on a design point considering all the uncertainties. The ESL sets that represent just the uncertainties are obtained by taking the difference between the ESL sets of the design point and the robustness points. Hence the number of initialised ESL sets are equal to the number of initial robustness points. Once the ESL sets differences are created they are stored in an archive for later use during the optimisation. It is advantageous to have lots of robustness points in the initialisation such that almost all the uncertainty combinations are covered for which the ESL sets are generated. However this can only be achieved at a computational cost. Hence a good compromise has to be made between the computational cost and the number or initialised robustness points. The steps to obtain these initialised ESL sets are as follows ;

i. Evaluate an initial centre point design (A) and generate ESL sets (f_A).

ii. Evaluate (n) robustness points around the initial centre point (A) which represent (n) uncertainty parameter sets [2], see Figure 9.7 where $n = 6$.

iii. The ESL sets representing only the uncertainties are created using Equation (9.6), where f_{u_k} denotes the ESL sets representing only the uncertainties, f_k is the ESL sets of the k^{th} initialised robustness point and f_A is the ESL sets of the initial centre point (A).

$$f_{u_k} = f_k - f_A, \qquad k = 1, ..., n. \tag{9.6}$$

Optimisation

For the optimisation points outside the TI, the robustness points use the initially created ESL sets, f_{u_k}, that represent only the uncertainties. For the decision on which initially created ESL sets to use, a distance criterion is used. The general idea of the distance criterion is to test how far off a robustness point is from the centre point in-terms of each parameter. Depending on this the ESL sets that are more representative of the robustness point are chosen for ESL analysis. The steps to

2. This includes impact uncertainties and other uncertainty e.g. design variable uncertainty.

obtain the representative initialised ESL sets f_{u_k} for a robustness point are given as follows:

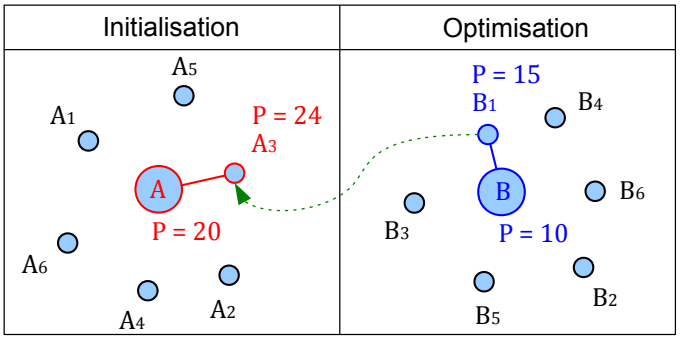

FIGURE 9.7 – Choosing initialised uncertainty ESL sets during RDO.

i. If an optimisation point (B) is outside the TI, generate ESL sets, f_B.

ii. For each robustness points (j) of the optimisation point (B);

1. Compare the uncertainty parameter values of robustness point j to the initially generated n uncertainty parameter values.
2. Find the minimum distance d between initial robustness point (n) and current robustness point (j) in-terms of the uncertainty parameter values. See Equations (9.7) to(9.9), where P is the uncertainty parameter, σ is the standard deviation of the uncertain parameter, z is the number of uncertain parameters and j is the number of robustness points for each optimisation point B, see Figure 9.7.
3. Take the ESL sets (f_{u_k}) of the robustness point (n) (that minimises the distance d) and add this to ESL set of optimisation point (B), f_B, see Equation (9.10).
4. Perform analysis of the robustness point (j) with the new ESL set, f_{new}.

$$AA_k = \left[\frac{P1_A - P1_{A_1}}{\sigma_{P1}} + \frac{P2_A - P2_{A_2}}{\sigma_{P2}} + \ldots \frac{Pz_A - Pz_{A_n}}{\sigma_{Pz}}\right] \tag{9.7}$$

$$BB_j = \left[\frac{P1_B - P1_{B_1}}{\sigma_{P1}} + \frac{P2_B - P2_{B_2}}{\sigma_{P2}} + \ldots \frac{Pz_B - Pz_{B_j}}{\sigma_{Pz}}\right] \tag{9.8}$$

$$\text{Distance } (d) = \min \ \|BB_j - AA_k\|; \quad j = 1, ..., l; \quad q = 1, ..., z \tag{9.9}$$

$$f_{new} = f_{u_k} + f_B. \tag{9.10}$$

Figure 9.7 shows an example where only one uncertainty parameter P is considered. Now lets consider that during the optimisation, design B is outside the TI hence robustness analysis should be made via ESLM. To obtain the initialised ESL sets (f_{u_k} that represents the uncertainties) for the robustness point B_1, initial robustness point has to be found that has similar uncertainty parameter values as B_1. B_1 has uncertainty value of $P = 5$ that is nearest to initialised robustness point A_3 which

has uncertainty value $P = 4$. Hence the initialised ESL sets f_{u_3} is used by robustness point B_1. The sum of load sets f_{u_3} and f_B is used to analyse the robustness point B_1.

Parameter Sets

There are few restrictions on parameter combinations using the proposed impact uncertainty approach. Due to the process by which the impact uncertainty ESL sets are calculated, shape parameters and impact uncertainty cannot be included together. This is because there is re-meshing after shape changes during the optimisation which changes the location of the nodes (re-numbering) and also the number of nodes. Hence when creating the new load sets, f_{new}, the number of nodes are different and hence f_{new} cannot be created.

9.7 Validation Cases

In this section some simple validation cases are presented to test ESLM for robustness analysis.

9.7.1 Simple Beam

To test the ESLM, first a simple design case is used as shown in Figure 9.8. The aim is to test the approximation capability of the ESLM when the design is slightly modified (only thickness modification). Few design evaluations are made with ESLM and compared to the results from non-linear dynamic analysis. From Figure 9.8 (a and b), it is already evident that ESLM has good approximation quality compared to non-linear transient analysis for the same design. Hence this is not shown in the figure for other designs (b-d), although the validations were made.

Model Description

A simple beam with dimensions 105 × 105 × 1000 mm is used with both ends of the beam fixed in all directions, see Figure 9.8. A pole impactor is used with a diameter of 100 mm and mass of 700 kg. The velocity of impact is 8 kph.

Results Comparison

In Figure 9.8 the maximum displacement of the beam in the y direction is presented. For visualisation purpose only four displacement contour values are shown. Figure 9.8(a) shows the displacement of the beam with non-linear dynamic analysis. From the non-linear dynamic analysis the ESL sets are generated. Designs in Figures 9.8 (b-d) are analysed using the ESL sets. The same design as in Figure 9.8(a) is analysed using the ESL sets, given in Figure 9.8(b). In this case the ESLM shows

good approximation quality for the displacement values. Also beams with modified thickness are analysed using the same ESL sets, Figures 9.8(c) and 9.8(d). The effect of the modified thickness on the displacement values is also captured when using the ESLM. This is especially important as the ESLM will be required to capture the effect of small design modifications during the robustness analysis.

9.7.2 Bumper Beam

As the second test case a design with multiple parts is chosen. The observation here is the spot welds definition to connect the different parts.

Model Description

The bumper design case used here is the same as that presented in Section 6.8.1. Here the spot welds are replaced by surface to surface tie definitions at the flanges, see Figure 9.9(a). The pendulum test case is used with the impact mass of 1643 kg and impact velocity of 8 kph, see UNECE (1980) for further test case description.

Results Comparison

Figures 9.9(b) and 9.9(c) show the maximum displacement in the x direction for non-linear dynamic analysis and ESL analysis respectively. For this case the results are exactly the same for the x displacement. Also the deformation characteristics in the flange region where tied nodes are defined in Figure 9.9(c) are the same as in Figure 9.9(b). Hence the tied node definitions can be used to represent the spot welds in ESL analysis.

9.7.3 Sub-model analysis via ESLM

Again a simple beam is used to test the analysis of sub-model with ESL analysis. Here the validation of the sub-model is also of importance, see Section 9.6.4.

Model Description

A pole impact is made on a curved beam with both ends fixed in all directions, See light red in Figure 9.10. The impactor has a mass of 500 kg, diameter of 100 mm and the impact velocity is 8 kph.

Results Comparison

Figure 9.10 shows the result comparison (displacement contour) of full and sub-model and also dynamic non-linear analysis and ESL analysis at different time steps. It can be seen from this figure that there is a good agreement between the full model

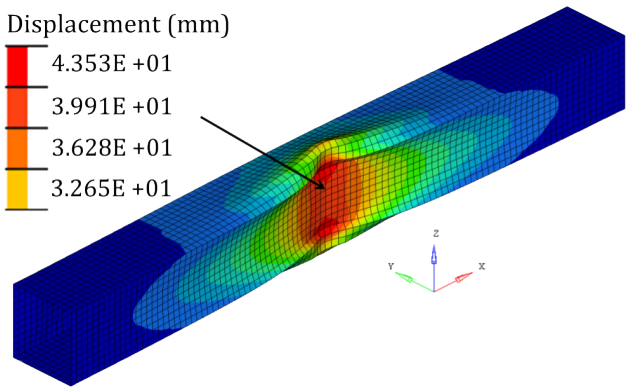

(a) Non-linear dynamic analysis, $t = 1.38$ mm.

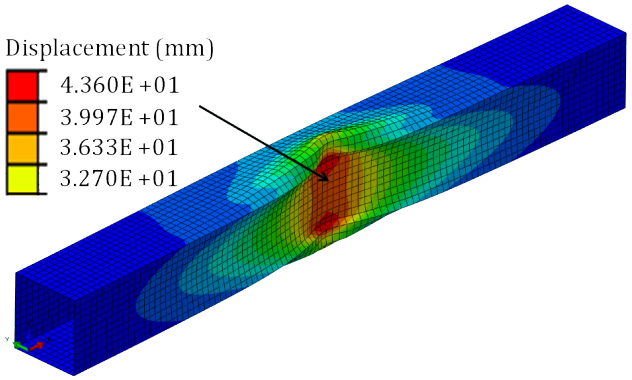

(b) Analysis with ESL sets from (a), $t = 1.38$ mm.

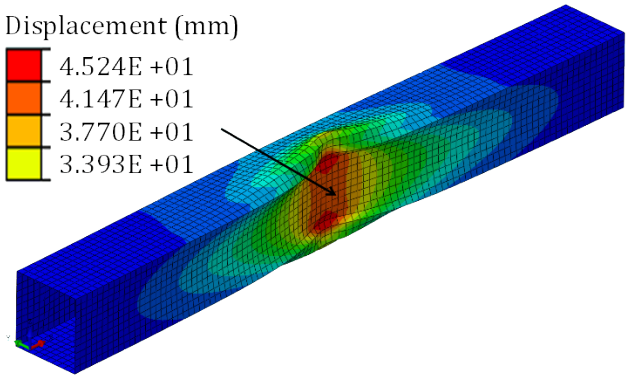

(c) Analysis with ESL sets from (a), $t = 1.33$ mm.

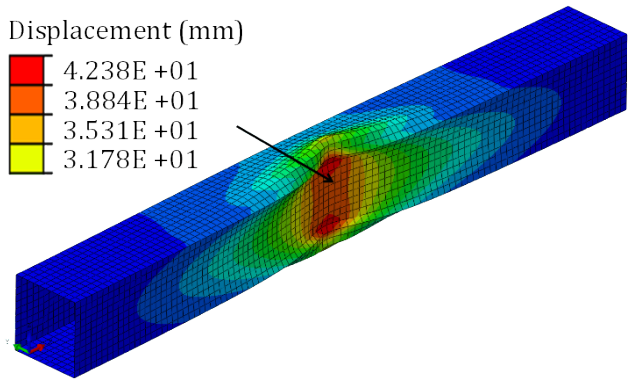

(d) Analysis with ESL sets from (a), $t = 1.42$ mm.

FIGURE 9.8 – Maximum displacement comparison of beams with different thickness, t.

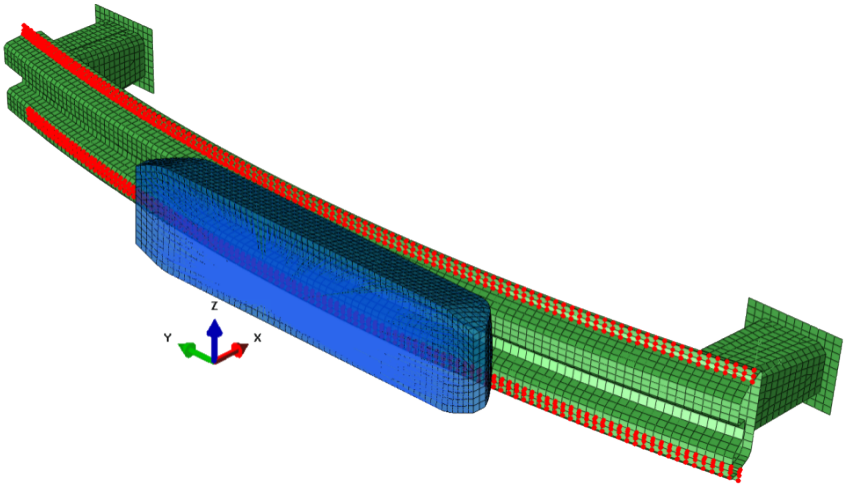

(a) Bumper impact case and spot weld formulation.

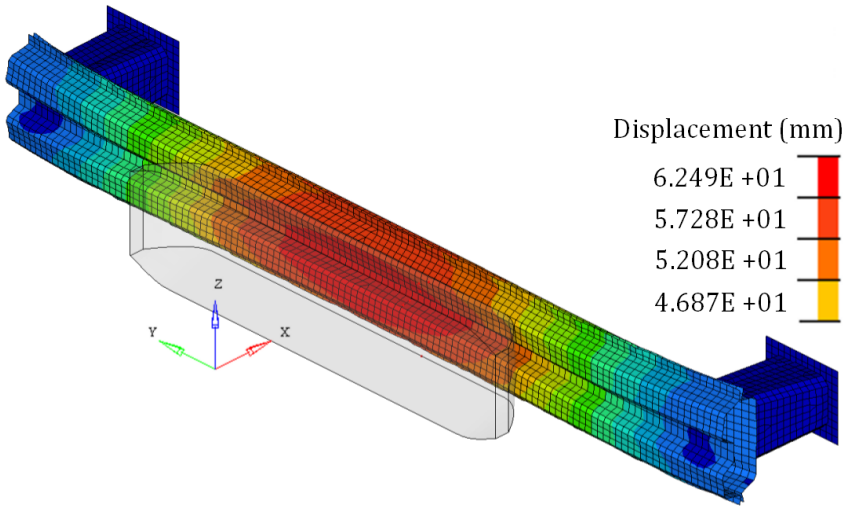

(b) Non-linear dynamic analysis.

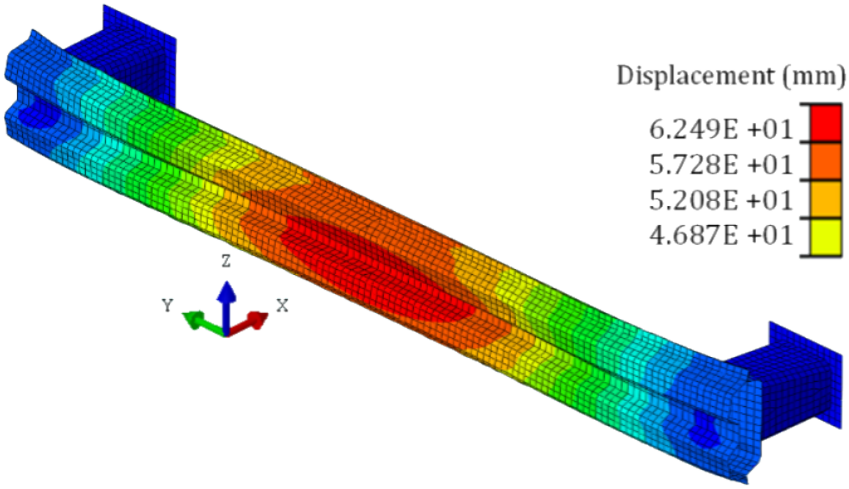

(c) Linear static analysis via ESLM.

FIGURE 9.9 – Bumper impact case and maximum displacement comparison.

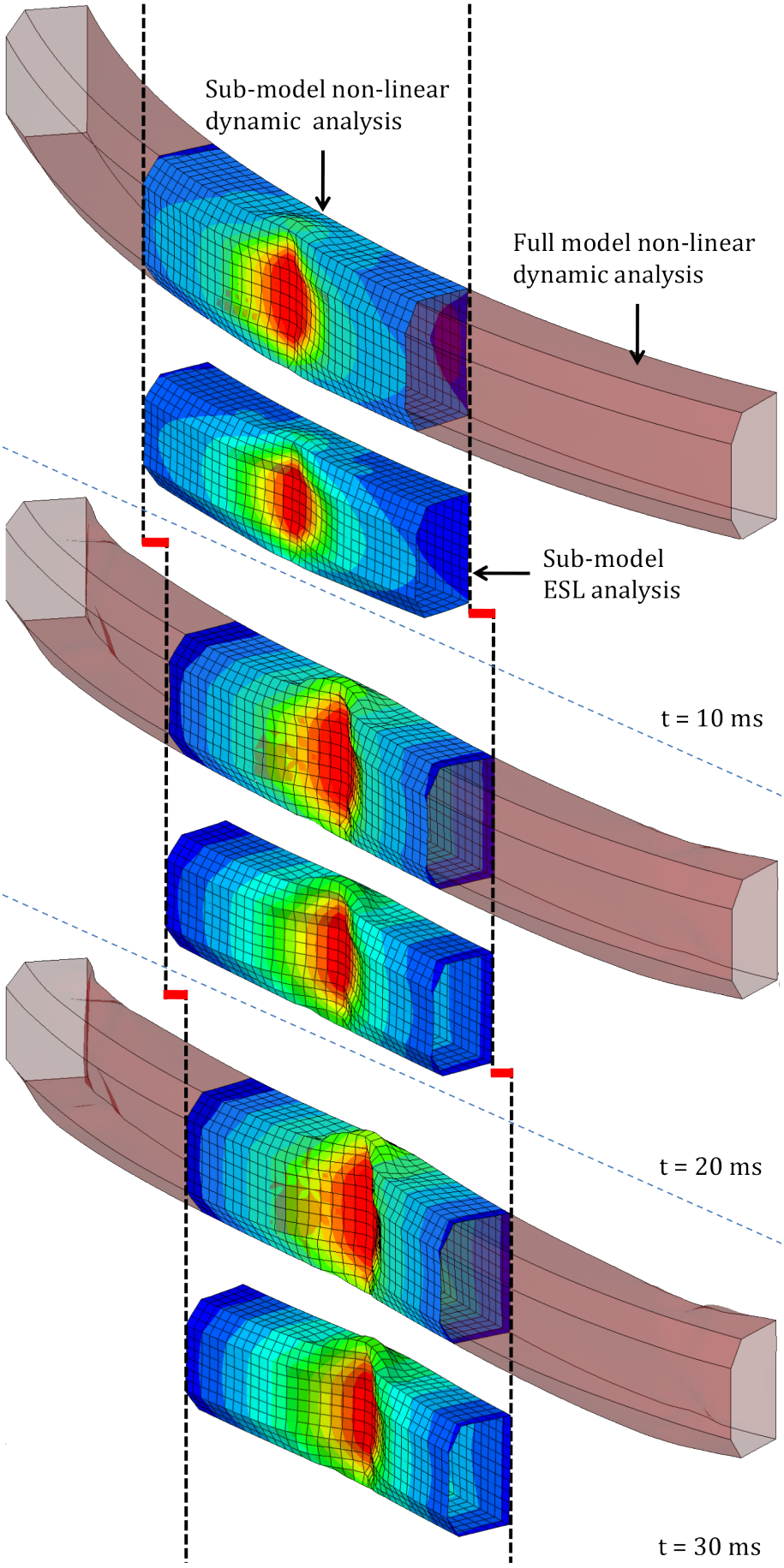

FIGURE 9.10 – Comparison of sub-model analysis using non-linear dynamic analysis and ESLM.

(red) and sub-model analysis, in all time steps, for which the results are superimposed [3]. Also there is a good approximation of the deformation characteristics using the ESL analysis. The slight difference between the sub-model analysis and ESL analysis is due to the difference in time step from which the figures are generated. In the ESL analysis both the deformation and also the translation of the sub-model are well represented, see red lines at each time step in Figure 9.10.

9.7.4 Robustness Analysis: ESLM vs Non-linear Dynamic

The ESLM implementation is successfully validated for some impact cases in the previous section. In this section the non-linear dynamic robustness analysis is compared to robustness analysis using ESLM. Here it is of interest to observe the robustness approximation of the designs when compared to the non-linear dynamic robustness analysis. Through this study the underestimate or overestimate of responses variation, via ESLM, can also be known.

Model Description

Figure 9.10 shows the model used in this study. The impactor has a mass of 500 kg, diameter of 100 mm and the impact velocity is 4 kph.

Study Formulation

The design to be analysed for robustness has a thickness of 1 mm. To keep this validation case simple, only thickness variation ($\pm$ 0.07 mm) is considered for robustness study. The observed response is the deflection of the beam measured at the centre of the beam. First non-linear dynamic robustness analysis is made by analysing 15 robustness points generated using the LHS. Then ESL sets are generated for the initial design. The same robustness points are analysed again by ESLM using the ESL sets. Then the variation on the output (deflection) is observed for both the analyses.

Results

The comparison of the deflection results from the two analysis approaches is presented in Table 9.1. From the table it is evident that even for this simple case the ESLM overestimates the output variation. In general this is not desirable. However since the idea is to use the ESLM for the robustness analysis of designs outside the TI, in the modified RDO loop, this is favourable for the approach. This is further explained in Appendix A.4.1.

3. Two results are shown at the same time, by overlapping the results, to show the difference.

Robustness analyses	Non-linear dynamic	ESLM
Minimum (mm)	20.26	19.83
Maximum (mm)	21.49	22.81
Mean (mm)	20.91	21.25
Standard deviation (σ)	0.375	0.937

TABLE 9.1 – Comparison of deflection variation via non-linear dynamic and ESLM.

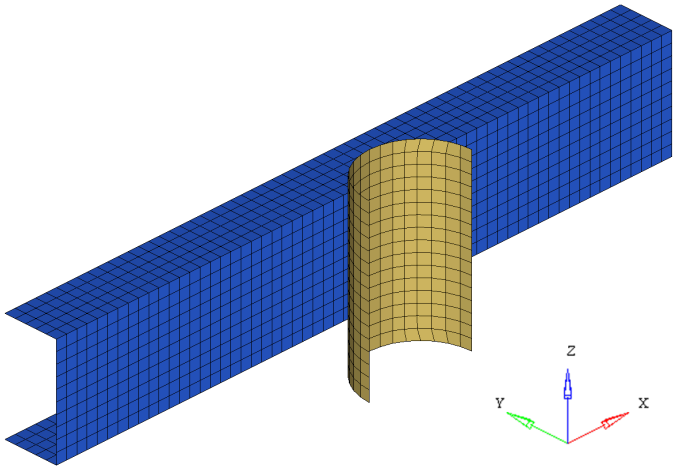

FIGURE 9.11 – Test case for robustness study using ESLM.

9.7.5 Impact Condition Uncertainties

In this section the proposed impact condition uncertainty approach presented in Section 9.6.6 is tested.

Model Description

The test case used here is the same as that shown in Figure 9.11.

Study Formulation

First a non-linear dynamic robustness analysis is made on a design with t = 1 mm (initial design) including the uncertainties in Table 9.2. The uncertainties considered are the thickness parameters (t), impact mass (M_0) and velocity (V_0) and impactor angles (δ_x, δ_y) and impactor position P. Two robustness studies are made, one with 20 sample points and another with 40 sample points generated using the LHS. From the analysed robustness points ESL sets are generated to represent the impact uncertainty, see Section 9.6.6 for more details. From this, two ESL sets initialisations are created, one with 20 impact uncertainty points and another with 40 impact uncertainty points. These two initialisations are used to test the effect of the number of sample points on the robustness analysis using ESLM considering impact uncertainty.

Another non-linear dynamic robustness analysis is made with 20 sample points generated using LHS. This robustness analysis is made on a design with t = 1.5 mm.

Noise variable	Distribution	Mean value	Standard deviation	Coefficient of variation, (%)
t (mm)	normal	1.5	0.07	0.14
Noise variable	Distribution	Mean value	Lower limit	Upper limit
M_0 (kg)	uniform	500	497	503
V_0 (m.s^{-1})	uniform	1.112	1.012	1.212
δ_x (°)	uniform	0	-1	1
δ_y (°)	uniform	0	-1	1
P (mm)	uniform	0	-1	1

TABLE 9.2 – Uncertainties included in the robustness analysis.

This design represents any optimisation point in the RDO. A robustness analysis is performed on the same design (t = 1.5 mm) with the same 20 sample points using ESLM considering impact uncertainty. The impact uncertainty is obtained from the initialised ESL sets. The idea here is to compare the robustness analysis via non-linear dynamic analysis and ESLM when considering impact uncertainty.

Robustness analyses	Non-linear dynamic	ESLM	
		20 Points	40 Points
Minimum (mm)	14.53	14.15	14.15
Maximum (mm)	16.18	16.57	16.88
Mean (mm)	15.47	15.23	15.51
Standard deviation (σ)	0.409	0.785	0.858

TABLE 9.3 – Comparison of response variation via non-linear dynamic and ESLM considering impact uncertainty.

Comparison of the Results

The response observed in this study is again the deflection of the beam. Table 9.3 shows the outputs from the robustness analyses. The variation of the response is again over-estimated when using ESLM for robustness analysis in both initialisation cases (20 or 40 points). The mean however is better approximated when using 40 initialisation sample points compared to 20 initialisation sample points. In a RDO the optimiser requires both the mean (μ) and sigma (σ) information. Since the ESLM is proposed for robustness analysis of designs outside the TI, it is crucial to better approximate μ. This is because the response surfaces are build using both μ and σ. The overestimate of the variation is acceptable as explained in Appendix A.4.1.

Limitations of the Implementation

In this section the impact uncertainty implementation is tested for robustness analysis via ESLM for designs outside the TI. Although the impact condition uncertainty is successfully validated for the simple case as shown in Figure 9.11, this is still an issues when used with a slightly more complex design case (multiple parts). The problem is mainly due to self or multiple part contact. This was validated by taking different design cases (similar to Figure 9.10 but including a reinforcement). Figure 9.12 shows a typical case of contact for the design case considered here. This occurs when the distance, d (Equation (9.9)), is large. This means that the difference between the uncertainty parameter of the robustness point and the closest initialised uncertainty parameter is large, see Section 9.6.6. As a result the initialised uncertainty ESL sets do not represent well the robustness point uncertainty parameters. In such case the robustness point is analysed with a ESL set that is non-representative of the robustness point. Hence this creates the contact issue and also gives a non-representative response of the robustness point.

This issue can be solved by taking more initialisation robustness points. However

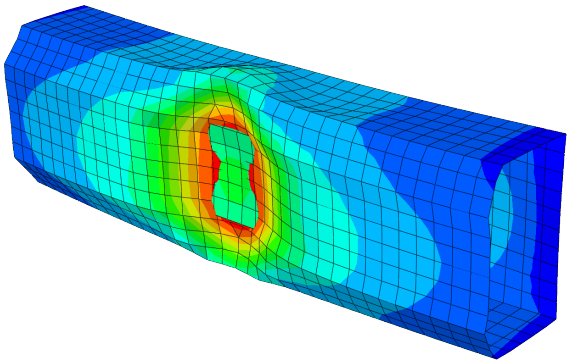

FIGURE 9.12 – Contact issue (penetration) due to impact uncertainties implementation.

this is not ideal for large industrial problems due to the computational effort. Also due to the implementation, the initialisation has to include almost all the uncertainty parameter combinations to avoid the penetration issue. Hence a new approach to consider impact uncertainty when using ESLM for robustness analysis has to be developed in the future.

9.8 Conclusion

In this chapter the ESLM for robustness analysis is presented and validated. An approach is considered to include impact condition uncertainties, via ESLM, which works by using the initially generated ESL sets. However, it is found that this approach is limited due to the contact issue that cannot be considered via ESLM. Hence for this implementation either a large number of initialisation points have to

be considered or an alternative approach has to be investigated.
Considering the requirement to use ESLM with sub-modelling within an overall RDO loop, this is also implemented and validated for a simple impact case. The validation cases give an indication that the ESLM can be used for robustness analysis.

PART IV
Overall Approach
&
Conclusion

Chapter 10

Efficient RDO via Approximation Approaches

10.1 Introduction

Generally in crashworthiness studies accurate solutions are used throughout the optimisation. However at the start of the optimisation, enough information to guide the algorithm towards better regions of the design space is of upmost importance. Hence approximation approaches could be employed, at the start of the optimisation, such that the computational effort is reduced while still providing the information for good optimisation direction. Then near the end of the optimisation, when the algorithm has already found better regions, more accurate evaluation approaches need to be employed. Through such approach computational effort can be reduced and hence large industrial models (model size, no. of design variables etc.) can be considered for RDO. In this section an overall approach is presented for an efficient RDO using physical surrogate models.

10.2 Proposed RDO Approach

The efficient RDO method presented in this section is based on the ideas developed in Chapter 8. The RDO approach is further enhanced here by embedding physical surrogate models; sub-modelling and ESLM. The overall computational effort is reduced hereby in-terms of:

(i) the simulation time of the optimisation designs by using sub-modelling and

(ii) robustness analysis time by using ESLM.

Both the sub-modelling and ESLM were already validated, in Chapters 7 and 9 respectively, and can be therefore used in the proposed RDO approach.

10.2.1 Optimisation Algorithm

There is a conflict in the choice of the optimisation algorithm. This is because for sub-model optimisation it is difficult to use GA or ES, see Section 7.7.2. Similarly for the proposed RDO approach in Chapter 8, IRSM cannot be used as discussed in Section 8.4. However, since the RDO approach is modified and ESLM is now used for robustness analysis of designs outside the TI, there is enough physical information to build the response surfaces using designs outside the TI. Hence IRSM can now be used in the proposed RDO approach and is chosen as the optimisation algorithm for the overall RDO approach. Response Surfaces used for RDO studies are presented in Section 5.7.1.

10.2.2 Description of the Approach

The RDO approach presented in Chapter 8 is modified due to its limitations discussed in Section 8.7. For the optimisation designs outside the TI, its robustness designs are analysed using ESLM, see Figure 9.5 in Section 9.6. For the designs inside the TI, robustness study is made through non-linear dynamic analysis. Furthermore the design optimisation is made using sub-models where the ICs on the sub-models are obtained from the full model analysis, see Section 7.6. Hence the overall approach is a combination of approaches presented in Chapters 7, 8 and 9.
Figure 10.1 shows the overall RDO loop where green represents sub-modelling related processes, blue represents ESLM related processes and red represents both sub-modelling and ESLM processes. Archives are created to store information, such as sub-model ICs and ESL sets, during the optimisation. For the archives, arrow-in means the use of information from the archive and arrow-out means update of the archive with new information. In the optimisation loop, Archive (A1) stores the ICs for the sub-models whereas Archive (A2) stores the ESL sets of designs. Both archives are updated during the optimisation. Archive (A1) is updated at the start of each new iteration whereas Archive (A2) is updated whenever an optimisation point is outside the TI. The algorithm is further discussed in the following paragraphs.

1. First the algorithm parameters [1] and TI are defined.
2. At the start of the optimisation process a new sub-model is created.
   2.1 If this sub-model is the centre point of a new iteration then the sub-model is substituted into the remaining model. The full model is analysed and new ICs are extracted. Archive (A2) is updated with the new ICs. See Section 7.7.3 for the update of the ICs at each new iteration.

1. Such as number of optimisation points per iteration and number of robustness points per optimisation point.

2.2 If the sub-model is within the current iteration then the process goes to step 3.

3. The sub-model is checked if it is an optimisation or robustness design [2].
   3.1. If it is an optimisation design then non-linear dynamic analysis is made on the sub-model with the most recent ICs from Archive (A2). The quality of the sub-model is also checked at this step [3]. Then a check is made if this optimisation point is within the TI.
      3.1.1. If it is inside the TI then the optimisation continues by creating a new sub-model design.
      3.1.2. If it is outside the TI then ESL sets are generated for this design and stored in Archive (A2). Also the quality of ESL analysis is checked at this step [4].
   3.2. If it is a robustness design then its corresponding centre point (optimisation design) is checked if it is inside or outside the TI.
      3.2.1. If it is inside the TI then dynamic non-linear analysis is made on the robustness design using ICs from (A2).
      3.2.2. If it is outside the TI then the robustness design is analysed using both the ESL sets, $f_{eq}^{\mathbf{z}}$ and the sub-model ICs from Archive (A1) and (A2) respectively. Refer to Section 9.6.4 for sub-model analysis via ESLM.
4. The stop criteria is checked to end the optimisation process. It is the maximum iteration number and parameter range and/or convergence test in-terms of the objective and parameter value change from one iteration to another. If the stop criteria is not fulfilled then the optimisation continues creating a loop.

10.2.3 Limitations of the Approach

The limitations of the approaches are mainly due to the ESLM used for robustness analysis. The main limitation for the study in this thesis is the exclusion of shape uncertainty. This is not an approach limitation but an implementation limitation as explained in Section 9.6.2. Also shape parameter and impactor uncertainties cannot be included together in the RDO (ESLM limitation) as explained in Section 9.6.6.

10.3 Validation Cases

In this section validation cases are presented for the overall RDO approach via physical surrogate models. First a simple curved beam is used to take advantage of

2. This depends on the algorithm settings, see Appendix A.4.2.
3. Responses difference between the full model and sub-model analyses.
4. Responses difference between the dynamic non-linear and ESL analyses.

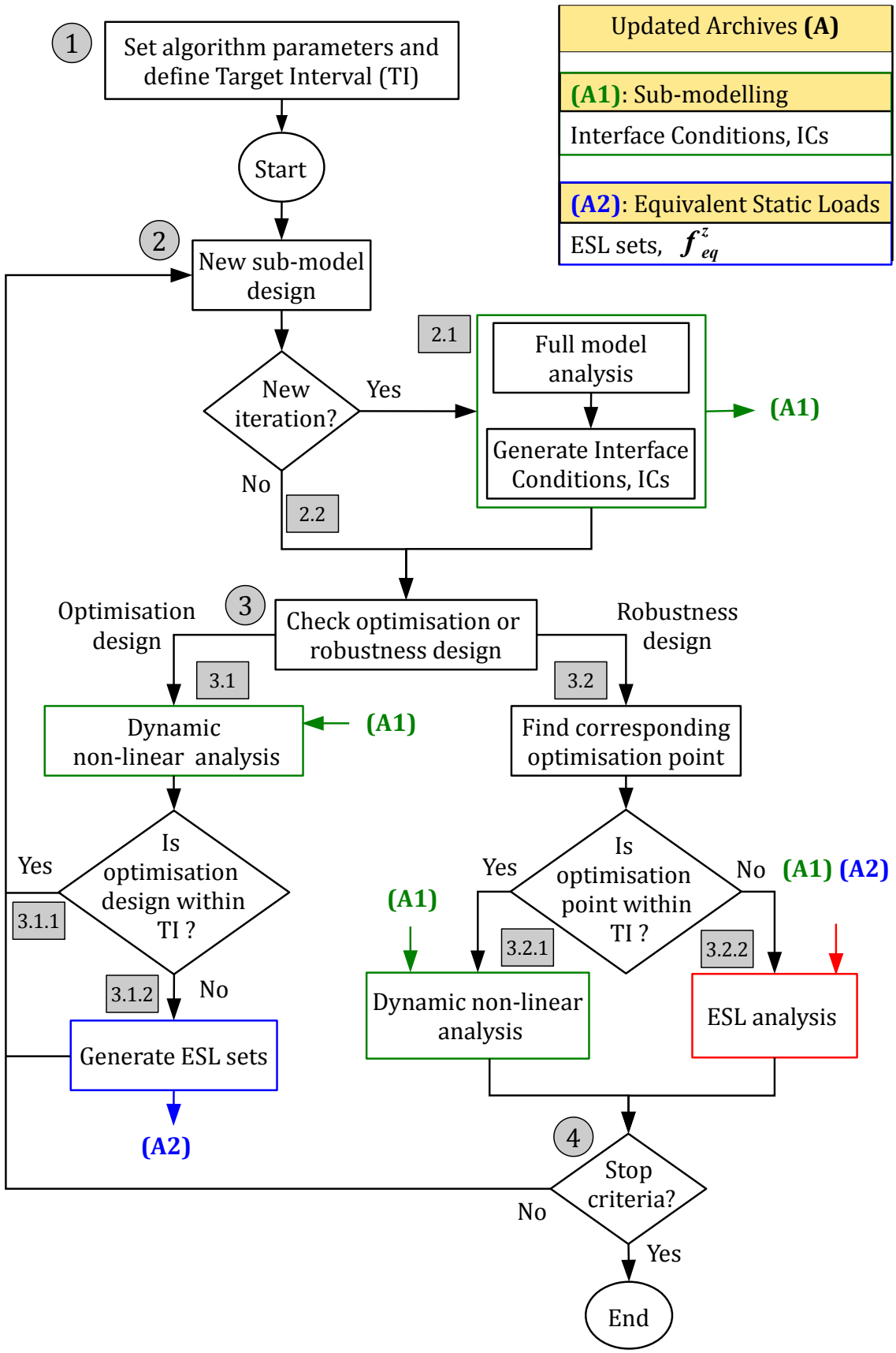

FIGURE 10.1 – Overall RDO approach using physical surrogate models ; sub-modelling and ESLM.

its quick analysis time. A slightly more complex model is then used as the second validation case where adaptive parameter sets are used in the RDO.

10.3.1 Simple Bending Case

A simple validation case is used considering shape and thickness parameters for optimisation. For robustness analysis only thickness uncertainty is considered, see 9.6.2 for this limitation.

Full Model

The design case is a simple curved beam with the two ends fixed in all directions. It has a C-section reinforcement that is connected to the beam using spot welds, see Figure 10.2 (left). The simulation time of the full model is around 3 minutes on a 4 core Intel Xeon E5410 2.33 GHz CPU.

Sub-model

A sub-model is created containing the parameterised reinforcement, Figure 10.2 (centre). The simulation time of the sub-model is around 2 minutes on the same machine. The sub-model, when analysed using ESLM, takes around 1 minute. This is due to the ESL sets calculation process and also the number of load sets calculated.

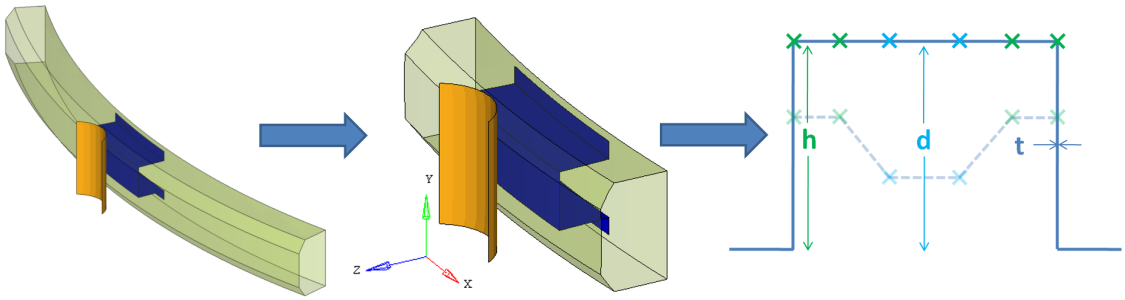

FIGURE 10.2 – Simple impact case to test the overall RDO approach.

Impact Conditions

A pole impact is considered with a diameter of 100 mm, mass of 500 kg and velocity of 4 kph.

Design Parameterisation

In this test only shape and thickness parameters are used in the RDO. For the robustness analysis only thickness uncertainty is used due to the issue with including shape uncertainty via ESLM, see Section 9.6.2. The reinforcement parameterisation

is shown in Figure 10.2 (right) where the green points are assigned to parameter h and the blue points are assigned to parameter d. The green and blue points move independently in the vertical direction. Also the reinforcement thickness t is included. In Figure 10.2 (right) dotted lines show a possible reinforcement configuration. The optimisation parameters are given in Table 10.1. The variation in the thickness uncertainty is $\pm$ 0.07 mm obtained from European Standards on laminate products Corus (2006).

	Lower bound	Initial design	Upper bound
h (mm)	50	70	84
d (mm)	30	70	84
t (mm)	0.50	1.00	2.00

TABLE 10.1 – Initial design parameters and parameter bounds for the reinforcement.

Objective and Constraints

The objective is to reduce the mass of the beam. The constraints are the displacement of the front, $d_f \leq 29$ mm, and the rear, $d_r \leq 16$ mm, in the middle of the beam. For the RDO, constraints are formulated as:

$$\mu_{d_f} + 2\sigma_{d_f} \leq 29 \text{ mm}, \tag{10.1}$$

$$\mu_{d_r} + 2\sigma_{d_r} \leq 16 \text{ mm}. \tag{10.2}$$

Algorithm Settings

For the response surface in each sub-region, polynomial linear regression is chosen. This is again due to the low number of support points required. Linear D-optimal DOE (see Section 3.5.3) is chosen to generate 6 support points in the sub-region (1.5 $\times$ linear Koshal design, where linear Koshal = 4). This means we have 7 evaluations at each sub-region (6 support points and one validation point of the previous response surface optimum). Hence the ICs are updated at the 8^{th}, 15^{th}, 22^{nd}... optimisation designs. For the robustness analysis 15 points, generated using LHS, are used due to the quick analysis time. The optimisation is started with 50% of the global design space for the correctness of the ICs within a sub-region, see Section 7.7.3.

Two TIs are defined due to the two constraints. An offset for each constraint is created at $d_f = 27$ mm and $d_r = 14$ mm. The OR formulation is used for the decision to perform robustness analysis using non-linear dynamic analysis or ESL analysis. This means that the optimisation designs have to fall within both the TIs for robustness analysis using non-linear dynamic analysis, see Section 8.5.2. If a design is outside any of the two TIs then robustness analysis of the design is made using ESLM. This

criterion reduces the number of non-linear dynamic analysis since limited number of designs satisfy this criterion.

Results and Discussion

The optimisation results are shown in Figures 10.3 - 10.5. A robust optimum design is obtained at the 9^{th} iteration, 60^{th} design, Figure 10.3(a). The optimum reinforcement shape and parameters are shown in Figure 10.4(a). The optimum design has a mass of 1.13 kg, a reduction in mass by 5.5%. Figure 10.5 shows the deflection history of both the front and rear of the beam [5] . It is evident from Figure 10.5 that the deflection constraint of the front of the beam drives the optimisation since it is violated more often compared to the rear deflection. This is because as the optimisation proceeds the thickness of the reinforcement has been reduced hence there is more deformation of the front of the beam and less deflection of the rear of the beam. Also the objective history trend can be explained by the thickness parameter since it is the most dominating. The objective increases at the start of the optimisation due to constraint violation and therefore increase in the thickness parameter. After about 20 designs the algorithm realises that the parameter combination evaluated so far increases the objective value. Hence it starts to search for parameter combinations (other end of the parameter bounds) that start to reduce the objective value from 20^{th} design onwards. Figure 10.3(b) shows the deformation history, at the front of the beam, at each iteration. The response surface approximation at the 9^{th} iteration is better than in the previous iterations due to the reduced sub-region size.

Also another significant observation is that the optimum is outside the TI for the

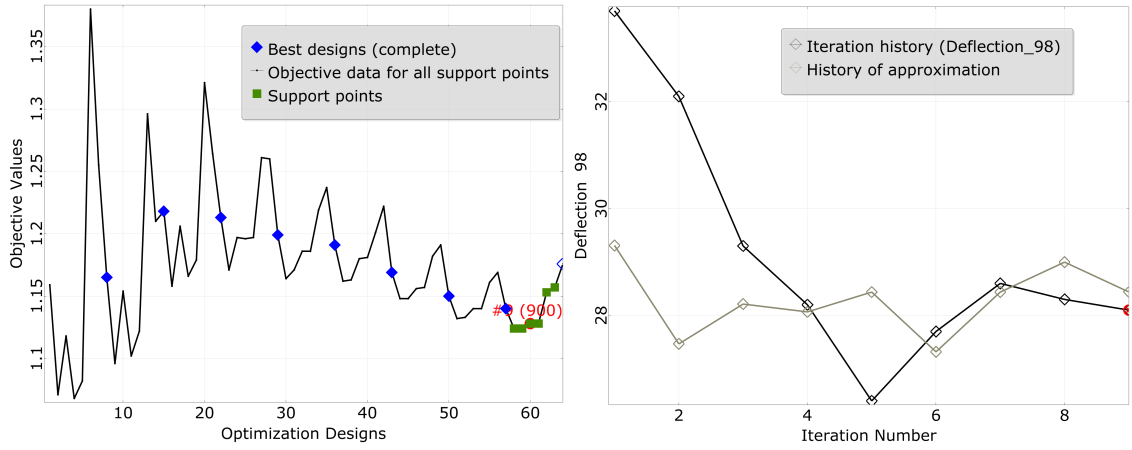

(a) Objective history of the support points. (b) Constraint history at each centre point.

FIGURE 10.3 – Optimisation history of the objective and driving constraint.

rear deflection response. Hence the optimum design is evaluated for robustness using

5. Deflection 98 and deflection 99 mean the deflection measured at nodes 98 and 99 respectively.

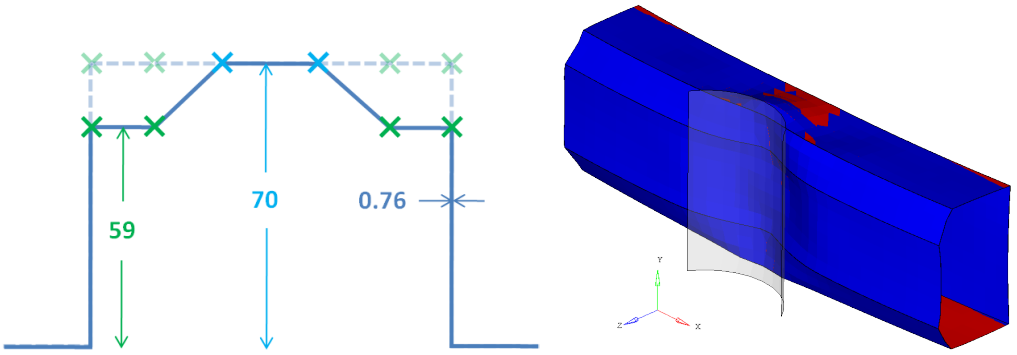

(a) Optimum reinforcement shape, mm.

(b) Validation of optimum design with updated ICs.

FIGURE 10.4 – Optimum reinforcement design shape and validation.

ESLM. Since it was shown earlier, Section 9.7.4, that the ESLM overestimates the responses variation, it can be considered safe to consider this design as robust [6].

Optimum Design Validation

Since the optimum is a support point design, a validation is required. This is because in IRSM only the response surface optimum at each iteration is validated, see Section 7.7.3. The sub-model optimisation may be erroneous because the sub-model may exhibit different behaviour due to the use of non-representative ICs, see Section 7.7.3. This is because the optimum design is evaluated using the ICs from a different design (ICs extracted from the iteration centre point design.). However since the design space is already reduced the optimum design should behave similarly with the updated ICs, see Section 7.9.5 for further discussion.
For the validation, the optimum design is substituted back into the remaining model and a full model analysis is made. New ICs are extracted from the full model analysis. The optimum model is then analysed using the updated ICs. Figure 10.4(b) shows the maximum deformation state of the optimum design with previous ICs (blue) and updated ICs (red). The deformation characteristics are very similar and the maximum difference in the deformation response is around 3%.

Computational Effort

The computational effort in this approach significantly depends on the TI definition. In this case, since two TIs are defined, the criterion on when to switch between non-linear dynamic robustness analysis and ESL robustness analysis is crucial for computational effort. In this case the OR formulation is used hence reduced number of designs are analysed using non-linear dynamic analysis. In fact in this case only four designs fall within both the TIs, designs 1, 10, 12 and 13. Table 10.2 presents

6. Non-linear dynamic robustness analysis can be made on this design for justification. This is not done here.

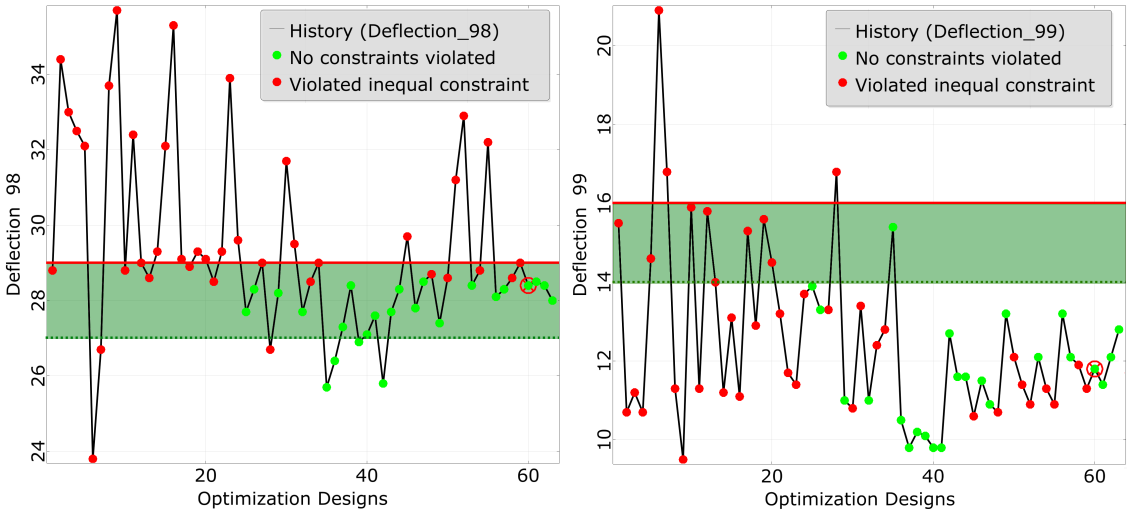

(a) Front deformation history.

(b) Rear deformation history.

FIGURE 10.5 – Deflection history of the beam and TI definition.

RDO	Analysis point	Analysis type	No. of analysis	CPU time (h/cpu)[2]	Total time
General approach[1]	Optimisation	Full model	63	12.60	201.6
	Robustness	Non-linear[3]	945	189.0	
New approach	Optimisation	Full model	9	1.80	77.2
		Sub-model[4]	63	8.40	
	Robustness	Non-linear	60	8	
		ESLM[5]	885	59	

[1] General RDO optimisation with IRSM without the use of sub-models and ESLM.

[2] CPU time divided by number of CPU cores.

TABLE 10.2 – Comparison of CPU time using general RDO and new RDO approach.

a comparison between general RDO approach, where full model non-linear dynamic analysis is used throughout the optimisation, and the new RDO approach. Compared to the general RDO approach the overall RDO computational effort is reduced by 61.7%.

Furthermore if the AND criterion was used then 39 designs fall within one TI. This also means the robust optimum would be analysed for robustness using non-linear dynamic analysis since it falls within the TI of the front deflection response, see Figure 10.5(a). Although the optimum would be accurately analysed for robustness, the computational efficiency would reduce due to the required number of non-linear dynamic analysis.

Conclusion

The overall RDO approach is tested on a simple design case considering shape and thickness parameters and thickness uncertainty. There is a significant saving on the computation time however the TIs in this case are not carefully defined. Hence the robust design is outside the TI and as a result analysed for robustness using ESLM.
Furthermore for larger industrial models the computational effort could be further reduced since the difference in computation time between non-linear dynamic analysis and ESLM could be very high. The same applies to full model and sub-model analysis where from an industrial model only a small part is used for optimisation.

10.3.2 Rocker Design Case

Design Case

The design case and impact conditions used in this validation are the same as presented in Section 7.8.1. The computation time of the sub-models via ESLM is around 1 minute. This is due to the reduced number of time intervals considered for ESL sets, explained in Section 10.3.2.

	Variable	Lower limit	Initial design	Upper limit	Distribution	Standard deviation
Design variables (mm)	P_z	-50	0	50	normal	1.0
	P_y	-40	0	40	normal	1.0
	t_1	0.5	1.0	1.5	normal	0.07
	t_2	0.5	1.0	1.5	normal	0.07
	t_3	0.5	1.0	1.5	normal	0.07
	Variable	Lower limit	Initial design	Upper limit	Distribution	Standard deviation
Noise variables	M_0 (kg)	98.5	100	101.5	uniform	NA
	V_0 (m.s^{-1})	7.91	8.06	8.21	uniform	NA

TABLE 10.3 – Design parameters and uncertainties included for RDO.

Design Parameterisation

An adaptive parameter approach is used here for the RDO. This is done to avoid using shape and impactor uncertainty parameters when using ESLM for design analysis. For designs outside the TI only the thicknesses are considered for optimisation and robustness analysis. For designs inside the TI, shape and thickness are considered for optimisation whereas for robustness analysis shape, thickness and

impact uncertainties are considered. The shape parameter variability is obtained from our industrial partners[7], thickness uncertainty from the European standard, Corus (2006), and impact uncertainty from the side pole impact protocol, EuroNCAP (2011). The parameter bounds and uncertainties are listed in Table 10.3. For the impactor uncertainty only impactor mass and velocity are considered since these are generally more dominating than for e.g. impact angle as preliminary studies have shown.

Objective and Constraint

The objective of the RDO is to reduce the mass of the rocker while respecting the intrusion constraint. The 2σ approach is used for the constraint for robustness analysis of designs, see Section 5.5.2. The constraint is formulated as:

$$\mu_I + 2\sigma_I \leq 62 \text{ mm}. \tag{10.3}$$

Algorithm Settings

For the response surface in each sub-region, polynomial linear regression is chosen. This is again due to the low number of support points required. This is enough as the quality of the approximation increases as the sub-region size decreases towards the end of the optimisation. Linear D-optimal DOE (see Section 3.5.3) is chosen to generate 9 support points in the sub-region (1.5 $\times$ linear Koshal design, where linear Koshal = 6. Hence the ICs are updated at the 11^{th}, 21^{st}, 31^{st}... designs. For the robustness analysis 15 points are generated using LHS, following the general rule in Section 5.5.2.
The optimisation is started with 100% of the design space range. Although it is argued in Section 7.9.5 that a smaller start design space is preferable for this approach (due to the correctness of the ICs), here the intention is to explore the full design space since the start of the optimisation. Gradient based approach is used as the optimisation algorithm on the linear response surfaces.
An offset to the constraint is created at $I = 58$ mm to define the TI, Figure 10.9. Hence the size of the TI is 4 mm. The decision on the TI size is made from previous optimisation results presented in Section 7.9.5.

Additional Settings

To assess the quality of sub-models and ESLM, validation cases are made and observed during the optimisation. For the sub-modelling case, at each new iteration the centre point design (optimum design from previous iteration) is substituted back into the remaining model and updated ICs are obtained. They are then used

7. PSA Peugeot and Citroën.

again to analyse the centre point design. The quality of the sub-model is assessed by observing the residual in responses between the sub-model analysis (via updated ICs) and full model analysis.
The ESL sets quality are assessed at each optimisation point outside the TI. The optimisation points outside the TI are first analysed via non-linear dynamic analysis. From this ESL sets are generated and the design is again analysed using the generated ESL sets. The responses from the two analyses are compared and the residual calculated.
Throughout this thesis the ESL sets are generated at certain time intervals from the start of the impact to the spring back. This requires more effort compared to few time intervals where the ESL sets are calculated and can be significant for larger design cases. Of interest are usually some critical time intervals where the responses are observed. However these critical time intervals shift during the optimisation due to the change in designs. Hence in this case during the non-linear dynamic analysis the time at maximum intrusion is obtained. Then several time intervals (± 5 time intervals) around this critical time step are used to generate the ESL sets.

Results and Discussion

The optimisation stopped after 13^{th} iterations with a robust design after 123 optimisation design evaluations. Figure 10.6 shows the support points at each iteration, the objective history of each support point and sub-region optimum on the RS (blue). The optimisation is started with feasible design hence at the first iteration the algorithm has found some feasible designs, see Figure 10.9. Then the algorithm explores other regions of the design space where mostly unstable regions are found until the 87^{th} design. Furthermore a trend is shown in Figure10.6 where at the start of the optimisation the algorithm searched for regions where the objective is reduced rapidly. However in this region the intrusion constraint is not satisfied, Figure 10.9. Now from the 4^{th} iteration the algorithm tries to find parameter combinations that satisfy the intrusion constraint. In doing so the objective increases. After the 8^{th} iteration the algorithm finds the parameter combinations that give feasible designs. Now the algorithm exploits this region of the design space and hence reduces the sub-region size. The optimisation stopped due to the sub-region size criterion. Figure 10.7(b) shows the driving shape parameter (vertical location of point P_1 and P_2, Section 7.8.1) and its bounds adaptation during the optimisation.
The optimum has a mass of 4.84 kg which is a reduction by 3.4% compared to the start design. Figure 10.6 shows the start and optimum designs. The most important member of the reinforcements is the horizontal member whose thickness has increased by 0.13 mm. Also the reinforcement has moved upwards in the vertical direction since the cross-member beam does not reinforce this region. The optimum is within the TI which means that it is assessed for robustness using non-linear dynamic ana-

lysis. From Figure 10.9 it can be seen that many designs violate the constraints, this is due to the demanding impactor mass and velocity uncertainty. Also many designs violated the constraint at the start of the optimisation as explained earlier and only 2 feasible designs fall outside the TI. It is also observed that the overestimate of the outputs variation still applies to this design case when using ESLM. In IRSM the quality of response surfaces increases as the optimisation converges

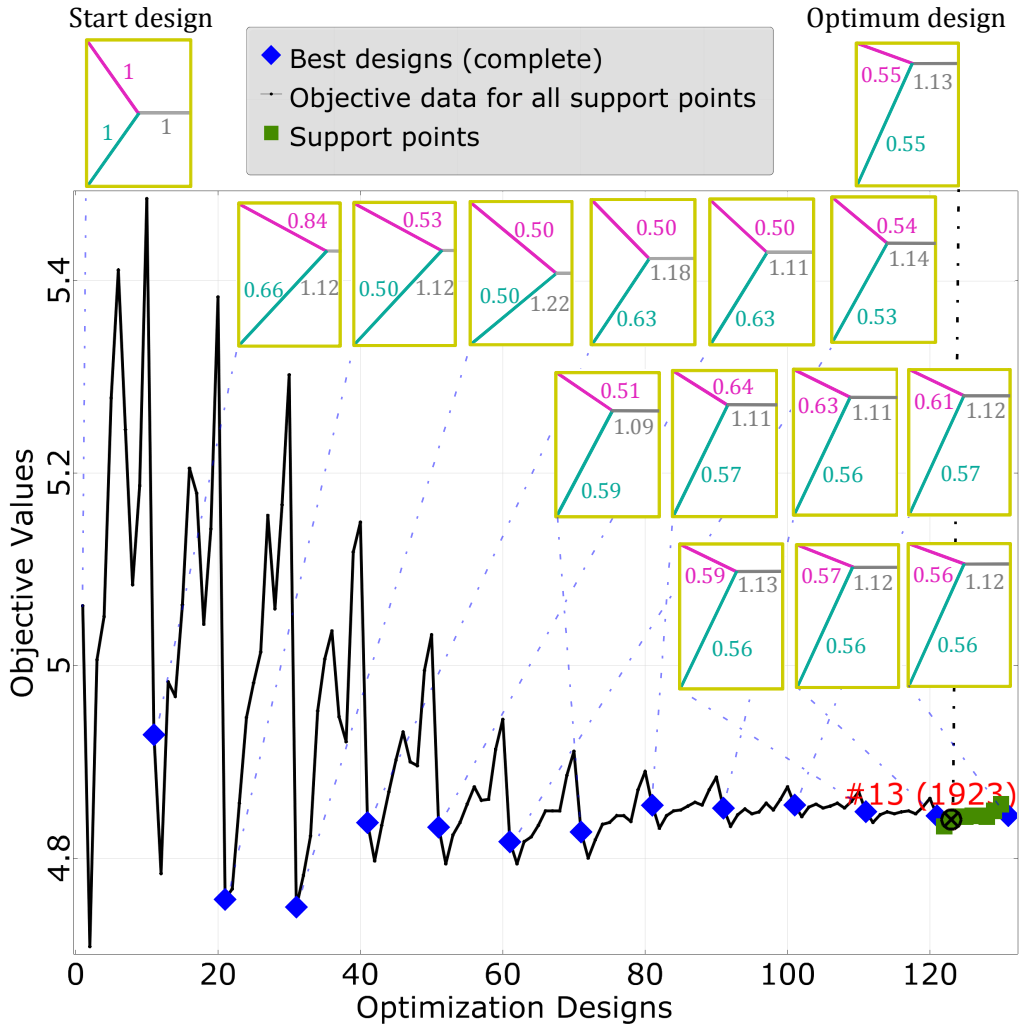

FIGURE 10.6 – Support point objective history and sub-region optimum designs.

since the sub-region size is reduced, see Figure 10.7(a). This also means that the quality of the sub-model increases. This is because the sub-region size is small which means the generated ICs from the centre point design is more representative of all other designs within this sub-region. The validation of the sub-models at each new iteration was also monitored. The optimisation was allowed to continue as the approximation quality was good. The same applied to the ESL analysis validation at each optimisation designs outside the TI.

Optimum Design Validation

The optimum found is a support point design hence this has to be validated using the updated ICs. Although 100% of the design space is used as the start

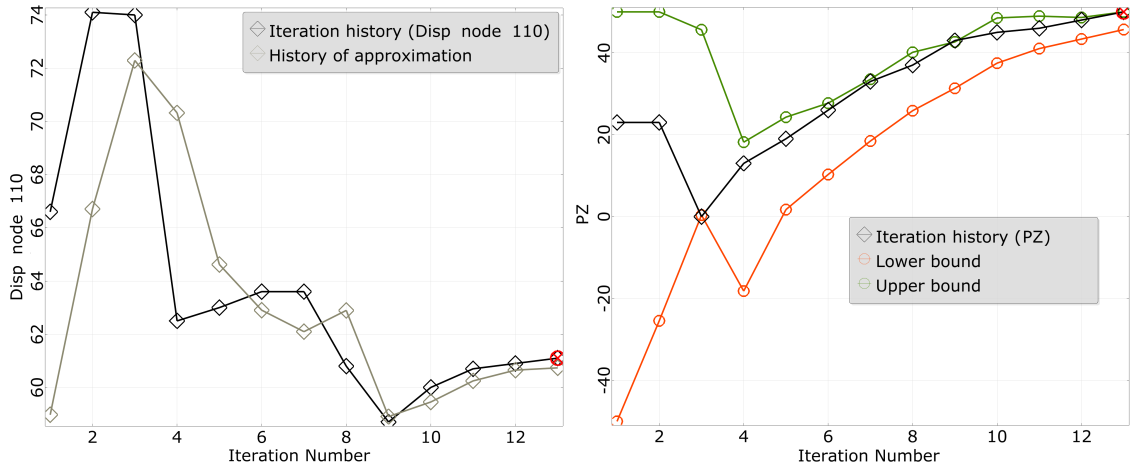

(a) Response history.

(b) Typical parameter history.

FIGURE 10.7 – Optimisation history at each iteration.

design space, the optimum is found at the later stage of the optimisation. This means that the ICs (obtained from the sub-region centre point) in this sub-region must be representative of the optimum design as explained in the earlier section. Hence we predict that the validity of the optimum should not be questionable. For validation purpose the optimum design is substituted back in the remaining model and updated ICs obtained. The optimum model is then analysed with the updated ICs. The behaviour of the optimum model in both ICs is similar. The validation is shown in Figure 10.8 where on the left the optimum model is analysed with previous ICs and on the right with the updated ICs.

Computational Effort

As stated earlier the computation efficiency depends on the TI definition. This is because for bigger TI definitions more designs fall within the TI that have to be analysed using the expensive non-linear dynamic analysis. In this case since the available information from previous optimisation run, Section 7.9.5, is used to decide the size of the TI, many designs are outside the TI and also the optimum is within the TI. The computational effort here can be discussed in terms of the number of sub-model and full model analyses used and also the number of design analyses made via non-linear dynamic analysis and ESLM.

In this example 131 (last design for the validation of the optimum at the last iteration) design evaluations are made in total to obtain the robust optimum design. However only 14 full model evaluations are required for the ICs update and the remaining 117 evaluations are made on the sub-model. Furthermore 75 designs fall outside the TI, which means $(75 \times 15 + 75)$ 1250 design evaluations are made using ESLM. Similarly 55 designs are within the TI and hence 880 design evaluations are made via non-linear dynamic analysis, see Figure 10.9. Table 10.4 summarises the computational effort and also compares it to the computational effort required using

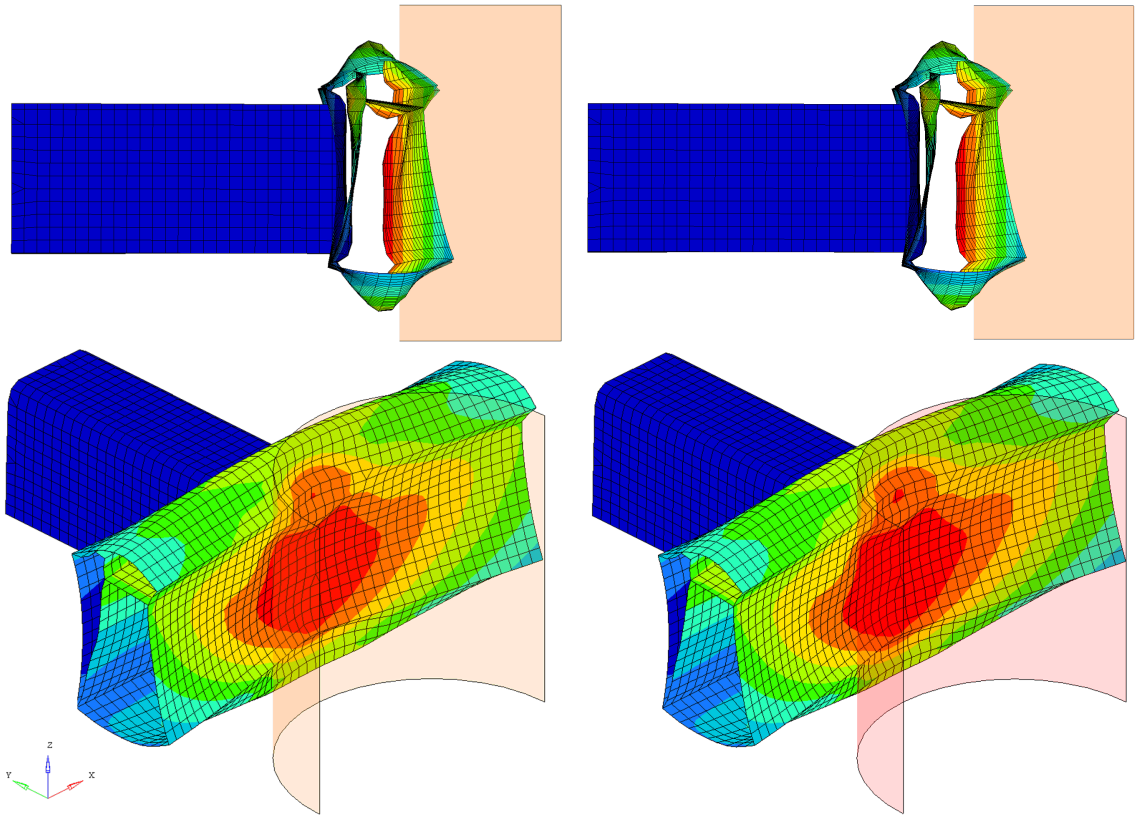

FIGURE 10.8 – Validation of the robust design with updated ICs. On the left optimum model analysis with previous ICs (ICs from the centre point design of the iteration where optimum design is found) and on the right with updated ICs.

general RDO using IRSM. The computational efficiency in this case is $\approx 61\%$ when compared to the general RDO run.

RDO	Analysis point	Analysis type	No. of analysis	CPU time (h/cpu)	Total time
General approach	Optimisation	Full model	131	87	1387
	Robustness	Non-linear	1950	1300	
New approach	Optimisation	Full model	14	9	275
		Sub-model	130	26	
	Robustness	Non-linear	825	165	
		ESLM	1125	75	

TABLE 10.4 – Comparison of CPU time using general RDO and new RDO approach.

Conclusion

In this section the overall RDO approach is successfully applied to a rocker design case. An adaptive parameter set is used where the designs outside the TI use thickness parameters and thickness uncertainty. For designs inside the TI, shape and thickness parameters are used for optimisation and impact uncertainty and design variable uncertainty are considered for robustness analysis. The robustness analysis via ESLM overestimates the responses spread in this case which can be deemed

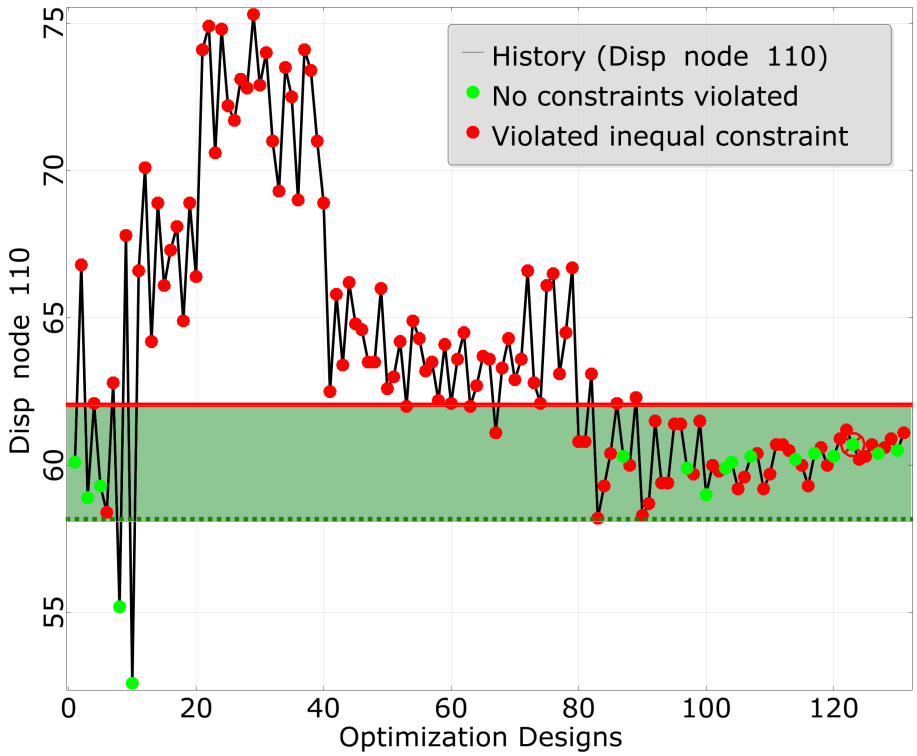

FIGURE 10.9 – Displacement history and TI definition.

as the effect of other uncertainties (impactor and shape) not included outside the TI. For the calculation of the ESL sets only critical time steps are chosen which is dependent on the time step at which the maximum intrusion occurs. This reduces the overall ESL loads calculation procedure and hence the ESLM analysis time. The computation efficiency for this design case is 61%.

Chapter 11

Summary and Future Work

11.1 Achievements

Shape Optimisation An approach is presented for shape parameterisation where the geometrical conflicts are dealt with efficiently during optimisation. The parameterisation approach is based on the offset mapping technique, available in the CAE package SFE CONCEPT. This approach gives robust shape parameterisations where problems arising from shape modification during the optimisation, such as surface penetration, overlapping and physically infeasible designs, are avoided.
The parameterisation approach is first applied to a shape optimisation of a bumper beam model. Here the geometrical conflict between the main beam and the reinforcements is avoided successfully. A more restrictive design space (for shape modification) is considered in the second validation case. Here the challenge remained in modifying the B-pillar reinforcement within the outer and inner panels.

Optimisation via sub-models To reduce the computational effort for optimisation of large industrial models, a sub-model optimisation approach is presented. A continuous optimisation loop is used where the coupling between the remaining model and sub-model is updated during the optimisation. This is because the coupling between the remaining model and the sub-model changes as the sub-model design is modified during the optimisation. Hence for the sub-model to approximate the correct behaviour of the overall model, the coupling between the models has to be updated. The sub-model optimisation is implemented via IRSM which also dictates the coupling update criterion.
Two validation cases are used, rocker reinforcement optimisation and an industrial B-pillar reinforcement optimisation. In both cases it is found that the sub-model optimisation has a real potential to reduce the overall computational effort for large industrial design optimisations.

Adaptive Parameter Sets for RDO A RDO approach is implemented where the robustness analysis is only made in the interesting regions, so called Target In-

terval (TI), of the design space. Only in this region the robustness analyses of the designs are assessed. For designs outside this region no robustness analysis is made. Hence it is termed adaptive parameter sets as the robustness parameters are only considered in the interesting regions of the design space. The idea here is to reduce the number of design analysis (no. of robustness analysis of designs) required for RDO studies.
This approach is validated via some analytical and simple physical test cases. However it is found here that the robust optima are not always within the TI. Hence in this case the definition of TI is very important and not easy to decide. To avoid this dependence of the approach on the TI definition, an alternative approach is introduced. This leads to the investigation of ESLM.

Robustness Analysis via ESLM To further enhance the modified simultaneous RDO approach, ESLM is tested and validated for robustness analyses of designs for the first time. The idea is to replace the expensive non-linear dynamic robustness analysis of designs with inexpensive linear static robustness analysis via ESLM. Robustness analysis via ESLM is performed for designs outside the TI in the modified simultaneous RDO. Furthermore since the overall RDO approach also implements sub-models for optimisation, design analysis via combined ESLM and sub-modelling is implemented.
Several cases are presented to validate both the ESLM and the combination of sub-modelling with ESLM. However difficulties are faced when considering shape variation and impactor uncertainties for robustness analysis via ESLM.

RDO via Approximation Approaches An overall RDO approach is implemented by combining the four approaches to reduce the required computational effort in RDO studies. In the proposed RDO approach, design optimisations are made using sub-models and robustness analyses are made using either non-linear dynamic analysis (for optimisation designs inside the TI) or ESLM (for optimisation designs outside the TI). The general idea here is to approximate the robustness of designs at the start of the optimisation (using ESLM) and use accurate robustness evaluations (via non-linear dynamic analysis) towards the end of the optimisation where the optimisation has already found interesting regions of the design space.
The validation is made first on a simple beam bending case where the reinforcement shape is optimised considering only the thickness uncertainties. In the second example, an adaptive parameter approach is employed due the limitation of ESLM to handle shape parameter and impactor uncertainties. For designs outside the TI only thickness parameters and thickness uncertainties are considered. Whereas for designs inside the TI, shape and thickness parameters are considered for optimisation and shape, thickness and impact uncertainties are considered for robustness analysis. It is found here that the computational effort is significantly reduced for RDO and this could be even more considerable for large industrial optimisations.

11.2 Future Work

The proposed approaches in this thesis are a work in progress and hence several areas are identified for further improvement of the overall RDO approach. Some of these areas are discussed here.

11.2.1 Shape Optimisation

Advanced Surface Mapping An improvement to the surface mapping algorithm in SFE CONCEPT has been identified. The advanced surface mapping should be able to map automatically one surface to another surface (the mapping information between the surfaces should be already defined by the user) when it is at a close proximity. When the surfaces move apart, increasing the distance between the surface, they should be automatically unmapped. Through this, a parameterisation case can be considered where the parts are either connected or not.

11.2.2 Optimisation via Sub-models

Automatic Interface Conditions Update For the further development of the approach one immediate area to investigate is the update criterion. At present it is dependent on the new iteration. This is not the best update criterion since the chance of missing an update point within the iteration is high (depending on the amount of parameter changes). Also making too many unnecessary updates can increase the computational effort due to the need of full model evaluations for ICs extraction. Therefore other measures for updates have to be implemented. The update of ICs at any point during the optimisation is questionable since it will create inconsistency of designs within a iteration, see Section 7.7.3.

Multi-band Interface Conditions For complex designs, such as the B-pillar, the use of band of interface nodes. For example 2 or 3 rows of nodes at the interface where the ICs are imposed. could be implemented This could improve the deformation characteristics of the sub-models as the band of rows would exhibit the rotation behaviour at the interface sections (which is not achieved by 1 row ICs). However this has to be further investigated.

Reuse Interface Conditions All the ICs generated during an optimisation can be stored in an archive. Then the representative ICs from the archive can be used for designs in the future generations[1]. Furthermore as the optimisation converges, in IRSM the sub-region size decreases, the design changes are small. Hence from some point during the optimisation the same ICs can be used where the ICs give a good approximation of all sub-models without any update.

1. Same ICs can be used for similar designs (designs with shortest distance in-terms of their design parameters).

11.2.3 Adaptive Parameter Sets for RDO

Computational Advantage In this approach the computational efficiency depends on how quickly the algorithm converges. If the optimisation converges too quickly then too many designs are to be analysed for robustness. Two approaches in the next sections are presented to avoid this.

Adapted Constraint An additional offset can be made very close to the constraint boundary to avoid robustness analysis of designs that are too close to the constraint boundary (similar to the adapted sequential approach, see Section 8.3.2). Since the designs that are too close to the constraint boundary often tend to be non-robust. This however depends on how sensitive the designs are to the fluctuations of the design and noise parameters. The new TI in this case is defined by the two offsets rather than the offset and the constraint boundary.

Adaptive TI As the optimisation algorithm converges, most of the designs fall within the TI. This means that the number of evaluations required at the end of the RDO increases with this approach. To address this issue, an adaptive approach to the TI can also be implemented. The adaptive approach changes the TI as the optimisation proceeds. Such adaptation of the TI helps to reduce the number of robustness evaluations at the end of the optimisation, see Figure 8.14.

11.2.4 Robustness Analysis via ESLM

Implementation The areas for further development of the approach are many. It is specially important here to implement mesh morphing of designs for robustness points to consider shape uncertainties. For this the shape fluctuations through the morphing approach has to be representative of the shape variations during the optimisation [2]. Recently this is possible with SFE CONCEPT where the re-meshing feature can be switched off.
For the implementation of the ESLM with sub-modelling the generation of the ESL sets can be made quicker by calculating directly the ESL sets from the full model, see Section 9.6.4 for more details.
To increase the accuracy of the deformation characteristics via ESLM, the stiffness matrix at each time interval could be computed to create the ESL sets, see Section 9.5. The inclusion of spot welds and also the refinement of the generated ESL sets in the critical time steps could further enhance the approach.

2. This means that the shape changes during the optimisation and the shape fluctuation in robustness points should be the same.

Space Mapping Another approach that could be implemented to increase the quality of analysis via ESLM is to use the space mapping technique. This technique has been applied previously, see Redhe and Nilsson (2006), where different fidelity models are used during an optimisation. In this thesis the ESL models and non-linear dynamic models are different fidelity models used during an optimisation. Hence via space mapping technique the responses from ESLM can be corrected to improve the approximation.

11.2.5 RDO via Approximation Approaches

Implementation The main limitations when using ESLM for robustness analysis here is the inclusion of shape parameters and impact uncertainty throughout the optimisation. Regarding the shape parameters it is just an implementation limitation, see Section 9.6. There is a bigger issue to consider the impact uncertainty, see Section 9.7.5. Hence a new approach has to be implemented to consider impact uncertainty via ESLM.
The overall RDO approach can be further enhanced by investigating a different criterion to switch the robustness analysis via non-linear dynamic analysis or ESLM.
Furthermore most application cases considered are simple for quick validation of the approaches. The next step would be to validate the approach on industrial designs case considering other responses (velocity, acceleration, stress etc.) in the optimisation.

Validations and Applications Further investigations and validations could be made on the approach using various benchmark test cases. Specially the application of the RDO approach to large industrial models such as the B-pillar is missing. It is also interesting to compare the RDO approach to some classical RDO approaches, however this is not straightforward.

Author's Publications

M. Rayamajhi, S. Hunkeler and F. Duddeck. Geometrical compatibility in structural shape optimisation for crashworthiness. *International Journal of Crashworthiness*, DOI:10.1080/13588265.2013.832720, 2013.

M. Rayamajhi, S. Hunkeler and F. Duddeck. Efficient robust shape optimization for crashworthiness. In *10th World Congress on Structural and Multidisciplinary Optimization*, Florida, USA, 2013.

S. Hunkeler, F. Duddeck, M. Rayamajhi and H. Zimmer. Shape optimisation for crashworthiness followed by a robustness analysis with respect to shape variables. *Structural and Multidisciplinary Optimization*, 48:367-378, 2013.

M. Rayamajhi, S. Hunkeler, F. Duddeck and M. Zarroug. Robust shape optimisation for crashworthiness via a sub-structuring approach. In *9th ASMO UK / ISSMO Conference on Engineering Design Optimisation*, Cork, Ireland, 2012.

M. Rayamajhi, S. Hunkeler and F. Duddeck. A Sub-structure Approach for Shape Optimisation for Crashworthiness. In *4th GACM Colloquium on Computational Mechanics*, Dresden, Germany, 2011.

Bibliography

ABAQUS (2013). ABAQUS unified FEA. http://www.3ds.com/products-services/simulia/portfolio/abaqus/.

Acar, E. and Solanki, K. (2009). System reliability based vehicle design for crashworthiness and effects of various uncertainty reduction measures. *Structural and Multidisciplinary Optimization*, 39:311–325.

Altair HyperWorks (2012). Radioss: Sub-modeling (cut approach). http://training.altairuniversity.com/wp-content/uploads/2012/08/RADIOSS_CRASH_CUT_V05.pdf.

Antoniou, A. and Lu, W. S. (2007). *Practical Optimisation: Algorithms and Engineering Applications*, chapter The Optimisation Problem. Springer, New York.

Arnout, S., Firl, M., and Bletzinger, K. U. (2012). Parameter free shape and thickness optimisation considering stress response. *Structural and Multidisciplinary Optimization*, 45(6):801–814.

Aspenberg, D. (2011). *Robust optimisation of structures - Evaluation and incorporation of variations in simulation based design*. PhD thesis, Linköping University, Sweden.

Aspenberg, D., Jergeus, J., and Nilsson, L. (2013). Robust optimization of front members in a full frontal car impact. *Engineering Optimization*, 45:245–264.

Au, S. K. and Beck, J. L. (2001). Estimation of small failure probabilities in high dimentions by subset simulation. *Probabilistic Engineering Mechanics*, 16:263–277.

Avalle, M., Chiandussi, G., and Belingardi, G. (2002). Design optimization by response surface methodology: application to crashworthiness design of vehicle structures. *Structural and Multidisciplinary Optimization*, 24:325–332.

Averill, R. C. (2004). Efficient shape optimisation of crashworthy structures using a new substructuring method. In *3rd German LS-DYNA Forum*, Bamberg, Germany.

Averill, R. C. (2011). Personal communication.

Azarm, S. and Eschenauer, H. (1993). A minimax reduction method for multi-objective decomposition-based design optimization. *Structural Optimization*, 6(2):94–98.

Bäck, T. (1996). *Evolutionary algorithm in theory and practice*. Oxford University press.

Bae, G. H. and Huh, H. (2012). Comparison of the optimum designs of center pillar assembly of an auto-body between conventional steel and AHSS with a simplified side impact analysis. *International Journal of Automotive Technology*, 13:205–213.

Bakr, M. H., Bandler, J. W., Madsen, K., and Sondergaard, J. (2001). An introduction to the space mapping technique. *Optimization and Engineering*, 2(4):369–384.

Bendsoe, M. P. and Sigmund, O. (2003). *Topology Optimisation: Theory, Methods and Applications*. Springer, Berlin.

Beyer, H. G. and Sendhoff, B. (2007). Robust optimization - A comprehensive survey. *Computer Methods in Applied Mechanics and Engineering*, 196:3190–3218.

Braess, H. H. and Seiffert, U. (2005). *Vieweg Handbuch Kraftfahrzeugtechnik*. Vieweg+Teubner Verlag.

Branke, J., Deb, K., Miettinen, K., and Slowinski, R. (2008). *Multiobjective Optimisation*. Springer, Berling, Germany.

Brecher, C., Klein, W., and Seiler, M. (2010). Parametric optimization of structural components considering geometrical restrictions. In *Proceedings of IV European Conference on Computational Mechanics*, Paris, France.

Breidenbach, A., Dams, R., Gerber, T., Reiter, L., Sikora, S., and Straube, O. (2009). Das incar-projekt. Technical report, ThyssenKrupp.

CARHS GmbH (2012). Safety Companion. Technical report, Alzenau, Germany.

Cavazzuti, M. (2013a). *Optimization Methods: From Theory to Design*. Springer, Berlin, Germany.

Cavazzuti, M. (2013b). *Optimization Methods: From Theory to Design*, chapter Design of Experiments, pages 13–42. Springer, Berlin, Germany.

Chase, N., Sidhu, R., and Averill, R. (2012). A new method for efficient global optimization of large system using sub-models - HEEDS COMPOSE demonstrated on a crash optimization problem. In *12th International LS-DYNA Users Conference*, Detroit, USA.

Chiandussi, G. and Avalle, M. (2002). Maximisation of the crushing performance of a tubular device by shape optimisation. *Computers & Structures*, 80:2425–2432.

Chiandussi, G., Bugeda, G., and nate, E. O. (2010). Shape variable definition with C0, C1 and C2 continuity. *Computer Methods in Applied Mechanics and Engineering*, 188:727–742.

Cho, Y. B., Bae, C. H., Suh, M. W., and Sin, H. C. (2006). A vehicle front frame crash design optimization using hole-type and dent-type crush initiator. *Thin-walled Structures*, 44:415–428.

Choi, W. S. and Park, G. J. (2002). Structural optimization using equivalent static loads at all time intervals. *Computational Methods in Applied Mechanics and Engineering*, 191:2077–2094.

Chuang, C. H., Yang, R. J., and Mallela, G. L. (2008). Multidisciplinary design optimization on vehicle tailor rolled blank design. *Structural and Multidisciplinary Optimization*, 35:551–560.

Corus (2006). Cold rolled uncoated and zinc or zinc-nickel electrolytically coated low carbon and high yield strength steel flat products for cold forming - tolerances on dimensions and shape. Technical Report EN10143: 2006, Corus Strip Products, UK.

Craig, K. J., Stander, N., Dooge, D. A., and Varadappa, S. (2002). Multidisciplinary design optimisation of automotive crashworthiness and NVH using response surface methods. In *9th AIAA/ISSMO Symposium and Exhibit on Multidisciplinary Analysis and Optimisation*, Atlanta, USA.

CrashTopo (2009-2012). Research project: Methodical and software-technical implementation of topology optimization for crash-stressed vehicle structures.

Delcroix, F., Stocki, R., Rutjes, N., and Happee, R. (2007). Methodologies and algorithms for robust optimization. Technical Report AP-SP72-011-D, APROSYS, Integrated Project on Advanced Protection System, SP7-Virtual Testing.

Department for Transport (2010). Reported road casualties Great Britain: 2009. Technical report.

Dietrich, T. (2013). *Neue virtuelle Methoden zur Integration einer numerischen Fußgängerschutz-Optimierung in den Entwicklungsprozess einer Motorhaube.* PhD thesis, Technische Universität München, Munich, Germany.

Donders, S., Pulymers, B., Ragnarsson, P., Hadjit, R., and Desmet, W. (2010). The wave-based substructuring approach for the efficient description pf interface dynamics in substructuring. *Journal of Sound and Vibrations*, 329(8):1062–1080.

Dorling, D., Newman, M., and Barford, A. (2010). *The Atlas of the Real World: Mapping the Way We Live*. Thames and Hudson.

Duddeck, F. (2007). Survey on robust design and optimisation for crashworthiness. In *Proceedings of 482nd EUROMECH Colloquium - Efficient Methods for Robust Design and Optimisation*, London, UK.

Duddeck, F. (2008). Multidisciplinary optimization of car bodies. *Structural and Multidisciplinary Optimization*, 35(4):375–389.

Eberhart, R. and Kennedy, J. (1995). A new optimizer using particle swarm theory. In *International Symposium on Micro Machine and Human Science*, Nagoya, Japan.

Eby, D. J., Averill, R. C., Goodman, E. D., and Sidhu, R. S. (2002). Shape optimization of crashworthy structures. In *Proceedings of 7th International LS-DYNA Conference*, Detroit, USA.

EuroNCAP (2011). *Pole side impact testing protocol, ver 5.2*. European New Car Assessment Programme.

EuroNCAP (2012). *Side impact testing protocol, ver 6.0*. European New Car Assessment Programme.

European Commission (1996). *Directive 96/79/EC of the European Parliament and of the council*. European Parliament.

Farkas, L., Canadas, C., Donders, S., Auweraer, H., and Schildermans, D. (2010). *Recent Advances in Optimization and its Applications in Engineering*, chapter Optimisation study of a parametric vehicle bumper subsystem under multiple load cases, pages 481–490. Springer.

Feuerstein, M., Witowski, K., and Müllerschön, H. (2008). Optimization of a crash management system considering multiple load cases using ANSA and LS-OPT. In *Proceedings of 7th LS-DYNA User Forum*, Bamberg, Germany.

Forsberg, J. (2002). *Simulation Based Crashworthiness Design - Accuracy Aspects of Structural Optimisation using Response Surfaces*. PhD thesis, Linköping University, Sweden.

Forsberg, J. and Nilsson, L. (2006). Evaluation of response surface methodologies used in crashworthiness optimisation. *International Journal of Impact Engineering*, 32:759–777.

Fradin, P. (2004). Passive safety of passenger cars by mégane series. In *European Automotive Safety Conference*, Bad Nauheim, Germany.

Frangopol, D. M. and Maute, K. (2003). Life-cycle reliability-based optimization of civil and aerospace structures. *Computers & Structures*, 81(7):397–410.

GENESIS (2012). *GENESIS v12.2, Quick Reference Manual*. Vanderplaats Research & Development, Inc, Colorodo Springs, Co, USA.

Georgios, K. (2007). Shape and parameter optimization with ANSA and LS-OPT using a new flexible interface. In *Proceedings of 6th German LS-DYNA Forum*, Frankenthal, Germany.

Georgios, K. and Dimitrios, S. (2009). Multi-disciplinary design optimization exploiting the efficiency of ANSA-LSOPT-META coupling. In *Proceedings of 7th European LS-DYNA Conference*, Salzburg, Austria.

Giunta, A. A., Wojtkiewicz, S. F., and Eldred, M. S. (2003). Overview of modern design of experiments methods for computational simulations. In *41st Aerospace Sciences Meeting and Exhibit - AIAA*, Reno, Nevada.

Goodman, E. D., Averill, R. C., and Sidhu, R. (2008). *Evolutionary Computation in Practice*, chapter Multi-level decomposition for tractability in structural design optimization. Springer, Berlin, Germany.

Gustafsson, E. and Strömberg, N. (2008). Shape optimisation of castings by using successive response surface methodology. *Structural and Multidisciplinary Optimization*, 35:11–28.

Gutermuth, A., Jung, U., and Pitzer, M. (2013). Komponenten-Berechnungsmodelle von Pkw-Karosserien. *ATZ - Automobiltechnische Zeitschrift*, 115(9):722–729.

Hilmann, J. (2009). *On the development of a process chain for structural optimisation in vehicle passive safety*. PhD thesis, Technische Universität Berlin, Berlin, Germany.

Hilmann, J. and Paas, M. (2006). Method for structural optimization and robust design based on genetic algorithms. *VDI-Bericht*, 1967(1):217–232.

Hoppe, A., Kaufmann, M., and Lauber, B. (2005). Multidisciplinary optimization considering crash and NVH loadcases. In *Virtual Product Creation*, Stuttgart, Germany.

Hunkeler, S. (2013). *Topology optimisation in crashworthiness design via hybrid cellular automata for thin walled structures*. PhD thesis, Queen Mary University of London, London, UK.

Hunkeler, S., Duddeck, F., Rayamajhi, M., and Zimmer, H. (2010). Robustness analysis and shape optimisation for crashworthiness of passenger cars with SFE

CONCEPT. In *8th ASMO UK/ISSMO conference on Engineering Design*, London, UK.

Hunkeler, S., Duddeck, F., Rayamajhi, M., and Zimmer, H. (2013). Shape optimisation for crashworthiness followed by a robustness analysis with respect to shape variables - example of a front rail. *Structural and Multidisciplinary Optimization*, 48:367–378.

HyperCrash (2013). *HyperCrash ver 12.0, User's Guide*. Altair Engineering, Warwickshire, UK.

Jansson, T., Nilsson, L., and Redhe, M. (2003). Using surrogate models and response surfaces in structural optimisation - with application to crashworthiness design and sheet metal forming. *Structural and Multidisciplinary Optimization*, 25:129–140.

Jeong, S. B., Yi, S. I., Kan, C. D., Nagabhushana, V., and Park, G. J. (2008). Structural optimization of an automobile roof structure using equivalent static loads. *Proceedings of IMechE. Part D: Journal of Automobile Engineering*, 222:1985–1995.

Jeong, S. B., Yoon, S., Xu, S., and Park, G. J. (2009). Non-linear dynamic response structural optimization of an automobile frontal structure using equivalent static loads. *Proceedings of IMechE. Part D: Journal of Automobile Engineering*, 224:489–501.

Johnson, M., Moore, L., and Ylvisaker, D. (1990). Minimax and maximin distance designs. *Journal of Statistical Planning and Inference*, 26(2):131–148.

Jones, N. (1997). *Structural Impact*. Cambridge University press, Cambridge, UK.

Jurecka, F. (2007). *Robust Design Optimisation Based on Metamodeling Techniques*. PhD thesis, Technische Universität München, Munich, Germany.

Kalagnanam, J. R. and Diwekar, U. M. (1997). An efficient sampling technique for off-line quality control. *Technometrics*, 39(3):308–319.

Kang, B. S., Choi, W. S., and Park, G. J. (2001). Structural optimization under equivalent static loads transformed from dynamic loads based on displacement. *Computers & Structures*, 79:145–154.

Kang, Z. (2005). *Robust Design Optimisation of Structures under uncertainties*. PhD thesis, Universität Stuttgart, Germany.

Kaya, N. and Öztürk, F. (2010). Multi-objective crashworthiness design optimisation of thin-walled tubes. *International Journal of Vehicle Design*, 52:54–63.

Kicinger, R., Arciszewski, T., and Jong, K. D. (2005). Evolutionary computation and structural design: A survey of the state-of-the-art. *Computers & Structures*, 83:1943–1978.

Kim, H. S., Chen, W., and Wierzbicki, T. (2002). Weight and crash optimization of foam-filled three-dimensional S frame. *Computational Mechanics*, 28:417–424.

Kim, Y. I. and Park, G. J. (2010). Nonlinear dynamic response structural optimization using equivalent static loads. *Computational Methods in Applied Mechanics and Engineering*, 199:660–667.

Kitayama, S. and Yamazaki, K. (2014). Sequential approximate robust design optimization using radial basis function network. *International Journal of Mechanics and Materials in Design*, 10(3):313–328.

Koch, P., Yang, R., and Gu, L. (2004). Design for six sigma through robust optimization. *Structural and Multidisciplinary Optimization*, 26:235–248.

Koshal, R. S. (1933). Application of the method of maximum likelihood to the improvement of curves fitted by the method of moments. *Journal of the Royal Statistical Society*, 96(2):303–313.

Kurtaran, H., Eskandarian, A., Marzougui, D., and Bedewi, N. (2002). Crashworthiness design optimisation using successive response surface approximations. *Computational Mechanics*, 29:409–421.

Lanzi, L. and Castelletti, L. M. L. (2004). Multi-objective optimisation of composite absorber shape under crashworthiness requirements. *Composite Structures*, 65:433–441.

Lee, J. J., Jung, U. J., and Park, G. J. (2013). Shape optimization of the workpiece in the forging process using equivalent static loads. *Finite Elements in Analysis and Design*, 69:1–18.

Lee, K. H. and Bang, I. K. (2006). Robust design of an automobile front bumper using design of experiments. *Proceedings of IMechE. Part D: Journal of Automobile Engineering*, 220(9):1199–1207.

Lee, S. H., Kim, H. Y., and Oh, S. I. (2002). Cylindrical tube optimization using response surface method based on stochastic process. *Journal of Materials Processing Technology*, 130-131:490–496.

Leiva, J., Watson, B. C., and Kosaka, I. (2007). A comparative study of topology and topometry structural optimisation methods within the genesis software. In *6th German LS-DYNA Forum*, Frankenthal, Germany.

Linzmeier, D. (2006). *Real-time detection of pedestrians from moving vehicle using thermopile and radar sensor fusion.* PhD thesis, University of Ulm, Stuttgart, Germany.

Livermore Software Technology Corporation (2013). LS-DYNA. `http://www.lstc.com/products/ls-dyna/`.

Lönn, D., Bergman, G., Nilsson, L., and Simonsson, K. (2011). Experimental and finite element robustness studies of a bumper system subjected to an offset impact loading. *International Journal of Crashworthiness*, 16(2):155–168.

Lönn, D., Fyllingen, O., and Nilsson, L. (2009). An approach to robust optimisation of impact problems using random samples and meta-modelling. *International Journal of Impact Engineering*, 37(6):723–734.

Looss, B., Boussouf, L., Feuillard, V., and Marrel, A. (2010). Numerical studies of the metamodel fitting and validation processes. *International Journal on Advances in Systems and Measurements*, 3(1-2):11–21.

Lu, G. and Yu, T. (2003). *Energy absorption of structures and materials.* Woodhead publishing Ltd, Cambridge, UK.

Marklund, P. O. and Nilsson, L. (2001). Optimization of a car body component subjected to side impact. *Structural and Multidisciplinary Optimization*, 21:383–392.

Marler, R. T. and Arora, J. S. (2009). *Multi-Objective Optimization: Concepts and Methods for Engineering.* VDM Verlag, Saarbrücken, Germany.

Mckay, M. D., Beckman, R. J., and Conover, W. J. (1979). A comparison of three methods for selecting values of input variables in the analysis of outputs from a computer code. *Technometrics*, 21(2):239–245.

Meissner, H. and Thiele, M. (2009). Integration of morphing and optimization with the CAx-Load case composer at AUDI. In *Proceedings of 7th European LS-DYNA Conference*, Stuttgart, Germany.

Meister, M., Theobald, A., Hülsmann, J., and Klein, M. (2005). Occupant safety simulation with submodel technique. In *18th Annual Worldwide ABAQUS Users Conference*, Stockholm, Sweden.

Möller, B. and Beer, M. (2008). Engineering computation under uncertainty - Capabilities of non-traditional models. *Computers & Structures*, 86:1024–1041.

Myers, R. H., Montgomery, D. C., and Andersson-Cook, C. M. (2008). *Response Surface Methodology: Process and Product Optimization using designed experiments.* Wiley, New Jersey, USA, third ed. edition.

Nohr, M. and Blume, K.-H. (2009). Crash adaptive vehicle structures and components. In *21st International Technology Conference on the Enhanced Safety of Vehicles (ESV)*, Stuttgart, Germany.

optiSLang (2011). *OptiSLang Ver 3.2.1, Documentation*. Dynardo GmbH, Weimar, Germany.

OptiStruct (2013). *OptiStruct ver 12.0, User's Guide*. Altair Engineering, Warwickshire, UK.

Owen, A. B. (1992). Orthogonal arrays for computer experiments, integration and visualization. *Statistica Sinica*, 2:439–452.

Padulo, M. (2009). *Computational Engineering Design Under Uncertainty: An Aircraft Conceptual Design Perspective*. PhD thesis, Cranfield University, UK.

Paik, S. H., Moon, J. K., Chung, S. W., Ji, K. H., and Kim, S. J. (2004). Investigation of instability in crash analysis on various computing environments. In *45th AIAA/ASME/ASCE/AHS/ASC Structures, Structural Dynamics and Material Conference*, California, USA.

Park, D. K., Jang, C. D., Lee, S. B., Heo, S. J., Yim, H. J., and Kim, M. S. (2010). Optimising the shape of a bumper beam section considering pedestrian protection. *International Journal of Automotive Technology*, 11(4):489–494.

Park, G. J. (2011). Technical overview of the equivalent static loads method for nonlinear static response structural optimization. *Structural and Multidisciplinary Optimization*, 43:319–337.

Picheny, V., Wagner, T., and Ginsbourger, D. (2013). A benchmark of kriging-based infill criteria for noisy optimization. *Structural and Multidisciplinary Optimization*, 48(3):607–626.

RADIOSS (2011). *RADIOSS ver 11.0, Reference Manual*. Altair Engineering, Warwickshire, UK.

Rayamajhi, M., Hunkeler, S., and Duddeck, F. (2013a). Efficient robust shape optimization for crashworthiness. In *10th World Congress on Structural and Multidisciplinary Optimization*, Florida, USA.

Rayamajhi, M., Hunkeler, S., and Duddeck, F. (2013b). Geometrical compatibility in structural shape optimisation for crashworthiness. *International Journal of Crashworthiness*, pages 1–15. DOI: 10.1080/13588265.2013.832720.

RCAR (2011). *Low-speed structural crash test protocol*, 2.2 edition.

Redhe, M., Forsberg, J., Jansson, T., Marklund, P., and Nilsson, L. (2002). Using the response surface methodology and the D-optimality criterion in crashworthiness related problems. *Structural and Multidisciplinary Optimization*, 24:185–194.

Redhe, M., Giger, M., and Nilsson, L. (2004). An investigation of structural optimisation in crashworthiness design using a stochastic approach. *Structural and Multidisciplinary Optimization*, 27(6):446–459.

Redhe, M., Nielsson, L., Bergman, F., and Stander, N. (2005). Shape optimization of a vehicle crash-box using LS-OPT. In *Proceedings of 5th European LS-DYNA Conference*, Birmingham, UK.

Redhe, M. and Nilsson, L. (2006). A multipoint version of space mapping optimisation applied to vehicle crashworthiness design. *Structural and Multidisciplinary Optimisation*, 31:134–146.

Rekveldt, M. and Labibes, K. (2003). Literature survey on in-vehicle safety devices. Technical report, TNO Automotive.

Rodriguez, J. F., Renaud, J. E., Wujek, B. A., and Tappeta, R. V. (2000). Trust region model management in multidisciplinary design optimization. *Journal of Computational and Applied Mathematics*, 124:139–154.

Rudenko, O., Schoenauer, M., Bosio, T., and Fontana, R. (2002). *Artificial Evolution*, chapter A multi-objective evolutionary algorithm for car front end design, pages 117–135. Springer, Berlin.

Ryberg, A. B. (2013). *Metamodel-Based Design Optimization*. PhD thesis, Linköping University, Sweden.

SAE International (2008). Automotive Engineering International. magazine.

Schneider, D. and Bucher, C. (2008). Efficient RDO using sample recycling. In *Weimarer Optimization and Stochastics Days*, Weimar, Germany.

SFE CONCEPT (2009). *SFE CONCEPT Ver 4.2.5.2, Reference Manual*. SFE GmbH, Berlin, Germany.

Sharma, N., Suthan, Collins, J., and Sharma, B. (2010). Multi-disciplinary optimization of a sedan using size and shape parameterization. In *11th International LS-DYNA Conference*, Detroit, USA.

Sharp, P. (2011). Personal communication.

Shin, M. K., Park, K. J., and Park, G. J. (2007). Optimization of structures with nonlinear behaviour using equivalent loads. *Computational Methods in Applied Mechanics and Engineering*, 196:1154–1167.

Sinha, K., Krishnan, R., and Raghavendra, C. (2007). Multi-objective robust optimisation for crashworthiness during side impact. *International Journal of Vehicle Design*, 43:116–135.

Sippel, H., Katzenberger, R., and Wiegel, T. (2006). Multi-objective robust design optimization using ENGINEOUS software package iSIGHT-FD. In *International Conference ERCOFTAC 2006*, Canary Islands, Spain.

Song, S. I. and Park, G. J. (2006). Multidisciplinary optimization of an automotive door with a tailored blank. *Proceedings of IMechE, Part D: Journal of Automobile Engineering*, 220:151–163.

Sousa, L., Veríssimo, P., and Ambrósio, J. (2008). Development of generic multibody road vehicle models for crashworthiness. *Multibody System Dynamics*, 19:133–158.

Stander, N. (2001). The successive response surface method applied to sheet metal forming. In *Proceedings of the First MIT Conference on Computational Fluids and Solid Mechanics*, Boston.

Stander, N. and Craig, K. J. (2002). On the robustness of a simple domain reduction scheme for simulation-based optimisation. *Engineering Computation*, 19:431–450.

Statistisches Bundesamt Deutschland (2011). Balance of accidents, 2008. `http://www.destatis.de/jetspeed/portal/search/internetresults.psml`.

Steer, K., Wirth, A., and Halgamuge, S. (2009). *Nature-inspired algorithms for optimisation*, chapter The Rationale Behind Seeking Inspiration from Nature, pages 51–76. Springer, Berling, Germany.

Stein, M., Schwanitz, P., and Sankarasubramanian, H. (2012). Unified parametric car model - A simplified model for frontal crash. In *12th LS-DYNA Forum*, Ulm, Germany.

Stocki, R., Rutjes, N., and Delcroix, F. (2007). Methodologies and algorithms for robust optimisation. Technical Report AP-SP72-0011-D, APROSYS.

Suhrer, A. (2013). *Generische Parametrik in der Simulation und Optimierung von Karosseriekonzepten*. PhD thesis, Technische Universität München, Munich, Germany.

Sun, G., Li, G., Stone, M., and Li, Q. (2010). A two-stage multi-fidelity optimization procedure for honeycomb-type cellular materials. *Computational Materials Science*, 49(3):500–511.

Sun, G., Li, G., Zhou, S., Li, H., Hou, S., and Li, Q. (2011). Crashworthiness design of vehicle by using multiobjective robust optimisation. *Structural and Multidisciplinary Optimization*, 44:99–110.

SuperLIGHT-CAR (2011). http://www.superlightcar.com/public/index.php.

Syberfeldt, A. (2009). *A multi-objective evolutionary approach to simulation-based optimisation of real world problems*. PhD thesis, De Montfort University, UK.

Takada, K. and Abramowicz, W. (2006). Macro element fast crash analysis of 3d space frame. In *SAE World Congress 2007*, Detroit, USA.

Tereshko, V. and Loengarov, A. (2005). Collective decision-making in honey bee foraging dynamics. *Computing and Information Systems Journal*, 9(3).

Tho, C. H. (2006). *Crashworthiness design optimisation using surrogate models*. PhD thesis, The University of Texas at Arlington, Texas, USA.

Thole, C. A. and Mei, L. (2003). Reasons for scatter in crash simulation results. In *NAFEMS Seminar*, Wiesbaden, Germany.

Toropov, V. V. (1989). Simulation approach to structural optimization. *Structural Optimization*, 1:37–46.

Tu, J. and Jones, D. R. (2003). Variable screening in metamodel design by cross-validated moving least squares method. In *44th AIAA/ASME/ASCE/AHS/ASC Structures, Structural Dynamics and Materials Conference*, Norfolk, Virginia.

UNECE (1980). *ECE R-42. Uniform provisions concerning the approval of vehicles with regard to their front and rear protective devices (Bumpers, etc.)*. United Nation Economic Commission for Europe, Geneva, Switzerland.

Volz, K. (2011). *Physikalisch begründete Ersatzmodelle für die Crashoptimierung von Karosseriestrukturen in frühen Projektphasen*. PhD thesis, Technische Universität München, Munich, Germany.

Volz, K., Frodl, B., Dirschmid, F., Stryczek, R., and Zimmer, H. (2007). Optimizing topology and shape for crashworthiness in vehicle product development. In *International Automotive Body Congress*, Berlin, Germany.

Wang, G. G. and Shan, S. (2007). Review of metamodeling techniques in support of engineering design optimization. *Journal of Mechanical Design*, 129(4):369–463.

Wang, H., Müllerschön, H., and Mehrens, T. (2005). Shape optimization of a crashbox using hypermorph and LS-OPT. In *Proceedings of 4th German LS-DYNA Forum*, Bamberg, Germany.

Will, J., Baldauf, H., and Bucher, C. (2006). Robustness evaluations in virtual dimensioning of passive passenger safety and crashworthiness. In *Weimarer Optimization and Stochastics Days 3*, Weimar, Germany.

World Auto Steel (2011a). Future steel vehicle - Overview report. http://www.worldautosteel.org/projects/future-steel-vehicle/phase-2-results, [Accessed: 9 Dec 2011].

World Auto Steel (2011b). Ultra light steel auto body programme. http://www.worldautosteel.org/projects/ulsab/ultralight-steel-auto-body-ulsab-programme/[Accessed: 11 Dec 2011].

Wu, H. and Xin, Y. (2009). Optimal design of the S-Rail for crashworthiness analysis. In *Proceedings of 2nd International Joint Conference on Computational Sciences and Optimization*, Hainan, China.

Wynn, D. C., Grebici, K., and Clarkson, P. J. (2011). Modelling the evolution of uncertainty levels during design. *International Journal on Interactive Design and Manufacturing*, 5:187–202.

Xu, F., Sun, G., Li, G., and Li, Q. (2013). Crashworthiness design of multi-component tailor-welded blank (TWB) structures. *Structural and Multidisciplinary Optimization*, 48:653–667.

Yi, S. I., Lee, H. A., and Park, G. J. (2011a). Optimization of a structure with contact conditions using equivalent loads. *Journal of Mechanical Science and Technology*, 25:773–782.

Yi, S. I., Lee, J. Y., and Park, G. J. (2011b). Crashworthiness design optimization using equivalent static loads. *Proceedings of IMechE. Part D: Journal of Automobile Engineering*, 226:23–38.

Yin, H., Wen, G., Hou, S., and Chen, K. (2011). Crushing analysis and multiobjective crashworthiness optimization of honeycomb-filled single and bi-tubular polygonal tubes. *Materials and Design*, 32:4449–4460.

Zaman, K., McDonald, M., Mahadevan, S., and Green, L. (2011). Robustness-based design optimization under data uncertainty. *Structural and Multidisciplinary Optimization*, 44:183–197.

Zarei, H. and Kröger, M. (2008). Optimum honeycomb filled crash absorber design. *Materials and Design*, 29:193–204.

Zeguer, T., Bates, S. J., Patten, S., Jones, R. D., and Toropov, V. V. (2008). Robust design optimization of an automotive knee bolster. In *49th AIAA/ASME/ASCE/AHS/ASC Structures, Structural Dynamics and Materials Conference*, Schaumburg, Illinois.

Zhang, M., Beer, M., Quek, S. T., and Choo, Y. S. (2010). Comparison of uncertainty models in reliability analysis of offshore structures under marine corrosion. *Structural Safety*, 32(6):425–432.

Zhang, Y., Zhu, P., and Chen, G. (2007). Lightweight design of an automotive front side rail based on robust design. *Thin-Walled Structures*, 45:670–676.

Zhang, Z., Liu, S., and Tang, Z. (2009). Design optimization of cross-sectional configuration of rib-reinforced thin-walled beam. *Thin-Walled Structures*, 47:868–878.

Zimmer, H. (2006). SFE CONCEPT CAE design: A key enabler in virtual product and vehicle development. In *AUTOSIM*, Lisbon, Portugal.

Zimmer, H. and Prabhuwaingankar, M. (2005). Implicitly parametric crash and NVH analysis models in the vehicle concept design phase. In *4th LS-DYNA Anwenderforum*, Bamberg, Germany.

Zimmer, H., Prabhuwaingankar, M., and Duddeck, F. (2009). Topology and geometry based structural optimisation using implicit parametric models and LS-OPT. In *7th European LS-DYNA Conference*, Salzburg, Austria.

Appendix

A.1 SFE CONCEPT Batch Script

Listing 1 – Example of SFE CONCEPT batch mode.

```
# SFE CONCEPT batch script to update model geometry and
# to generate analysis files.

# Load SFE CONCEPT model
CONcept LOAd ALL BINary <file>
CONcept REAlize NEW
# Set design variables to actual values
MACro MERge OVErwrite <file>
# Update the model
CONcept UPDate ALL
# Save the updated model
CONcept SAVe ALL BIN <filename>

# Set an element size
MESh SET ELEment LENgth 10
# Create Finitie Element mesh
MESh CREate NEW
# Setup FE-definitions, e.g. RADIOSS as solver
FEDef SET SOLver RAD
# Setup weld spot connections definition
FEDef SET WELd ROW_area SOLver
# Create FE-definitions
FEDef CREate FEDef ALL
# Create weld weld spot  connections
FEDef CREate WELd ALL

# Save FE-mesh, e.g. in RADIOSS format
FEM SAVe pid ALL RAD <filename>
# Save FE-definitions
FEDef SAVe FEDef ALL <filename>
# save weld connections
FEDef SAVe WELd ALL <filename>

# End SFE CONCEPT
CTRl STOp NOCheck
```

A.2 Bumper Beam Sensitivity Analysis

For the sensitivity analysis, 100 random designs are generated so that the computation time is reasonable and also to ensure that the correlation of inputs to outputs and parameter significance are visible. These designs are generated using the ALHS, see Section 3.5.1.

First the sensitivity analysis is done with the inclusion of all the beam and reinforcement design variables as listed in Table 6.1. However when analysing the results it is realised that the thickness parameters are dominating. This domination also suppressed the sensitivity of the design to other parameters. Therefore second sensitivity analysis is made excluding the thickness parameters. The linear correlation matrix of beam parameters and reinforcement parameters are shown in Table A.1 and Tables A.2 respectively.

The linear correlation matrix identifies the linear correlation between the inputs and outputs. From the matrix, it is evident that beam parameters are more dominating than the reinforcement parameters. The reinforcement parameters do not have significant influence on the responses. Hence the optimisation is run in two stages. For stage 1, only the beam parameters are taken for optimisation. The second stage considered only the reinforcement parameters using the optimum beam parameters from stage 1.

	A	B	C	D	E
Mass (kg)	75.20	38.20	-8.40	38.30	21.20
Force (kN)	43.80	25.20	-12.80	32.70	8.40
Deflection (mm)	52.70	-49.90	10.60	30.80	6.20
Intrusion (mm)	64.30	-61.50	25.50	4.40	1.50

TABLE A.1 – Linear correlation matrix, beam parameters (%).

	B1H1	B1H2	B1W1	B1W2	B1L1	B1L2	B2H1	B2H2	B2W1	B2W2	B2L1	B2L2	B3H1	B3H2	B3W1	B3W2	B3L1	B3L2
Mass (kg)	2.40	2.50	2.90	2.50	9.90	10.00	2.50	2.10	2.90	3.20	11.60	9.60	2.60	1.60	3.70	3.60	10.80	12.20
Force (kN)	-12.10	-11.40	6.30	8.40	-13.70	-8.30	-7.90	-5.20	9.50	4.60	-3.30	-2.90	-5.20	-4.50	-3.80	-2.50	7.90	6.00
Deflection (mm)	-17.20	-13.20	-9.40	7.20	-10.10	-9.50	-13.90	-9.40	-8.10	-7.70	4.20	-8.20	-2.60	2.70	7.90	7.10	2.40	2.00
Intrusion (mm)	-9.10	-11.50	7.60	8.30	-6.00	-5.10	-6.40	-8.80	-2.50	4.40	4.10	-1.70	0.30	-2.90	5.90	6.40	0.10	-1.30

TABLE A.2 – Linear correlation matrix, reinforcement parameters (%).

A.3 Coupling Analysis Results

Node	Min	Max	Initial value	Mean	Std.-Dev.	CoV	Skewness	Kurtosis	Mean shift
N11920X	3.95	5.93	4.57	4.91	0.48	0.10	0.10	2.60	0.35
N11920Y	5.89	8.40	7.31	7.02	0.57	0.08	0.73	3.27	0.29
N11920Z	-12.81	-7.21	-11.92	-10.14	1.42	-0.14	0.17	2.07	1.79
N97898X	0.20	1.31	1.01	0.82	0.25	0.30	-0.72	2.93	0.19
N97898Y	32.20	38.52	34.08	33.99	1.46	0.04	1.61	5.02	0.09
N97898Z	-6.32	0.77	-5.63	-3.32	1.85	-0.56	0.44	2.07	2.31
N87930X	-4.56	-1.28	-1.90	-2.21	0.71	-0.32	-1.51	5.03	0.31
N87930Y	5.16	11.51	7.91	7.46	1.58	0.21	0.62	2.49	0.45
N87930Z	24.89	39.12	27.11	31.96	4.33	0.14	0.07	1.72	4.85
N95361X	2.65	4.46	3.10	3.39	0.40	0.12	0.48	3.01	0.29
N95361Y	6.47	10.92	7.10	8.31	1.12	0.14	0.17	1.97	1.21
N95361Z	-4.49	-1.95	-3.57	-3.25	0.68	-0.21	-0.03	2.35	0.32
N63784X	6.27	9.63	7.75	8.00	0.74	0.09	0.06	2.96	0.25
N63784Y	23.26	28.22	24.05	25.54	1.25	0.05	0.11	2.27	1.48
N63784Z	22.95	31.01	26.47	27.99	2.10	0.08	-0.81	2.99	1.52
N85277X	5.61	9.10	6.90	7.41	0.81	0.11	-0.06	2.65	0.51
N85277Y	42.69	54.03	46.46	48.73	2.71	0.06	-0.52	2.54	2.27
N85277Z	21.95	31.91	25.99	27.60	2.06	0.07	0.08	2.99	1.61
N80953X	0.19	3.28	1.17	1.62	0.78	0.48	0.15	2.13	0.44
N80953Y	3.95	10.10	7.70	7.52	1.40	0.19	-0.23	2.29	0.18
N80953Z	-16.30	-4.63	-5.20	-8.38	2.93	-0.35	-1.02	3.29	3.18
N44076X	0.49	3.57	1.20	1.87	0.82	0.44	0.30	2.10	0.68
N44076Y	1.37	4.12	2.61	2.77	0.78	0.28	-0.08	1.80	0.16
N44076Z	-18.21	-4.79	-4.93	-8.88	3.50	-0.39	-1.01	3.23	3.96
N50947X	0.23	3.38	0.80	1.58	0.84	0.53	0.25	2.13	0.78
N50947Y	1.89	5.54	4.31	3.47	1.06	0.31	0.23	1.82	0.84
N50947Z	-17.45	-3.88	-4.23	-8.03	3.49	-0.43	-1.03	3.28	3.80
N90522X	-1.29	2.49	-0.57	0.45	0.95	2.13	0.12	1.96	1.02
N90522Y	3.34	8.08	5.98	5.98	1.20	0.20	-0.24	1.95	0.01
N90522Z	-19.25	-3.65	-6.35	-9.87	4.03	-0.41	-0.68	2.69	3.52
N100793X	-0.41	3.13	0.10	1.17	0.93	0.79	0.21	1.99	1.07
N100793Y	3.52	6.10	5.17	4.87	0.68	0.14	-0.15	2.11	0.30
N100793Z	-21.06	-6.54	-7.73	-11.38	3.81	-0.33	-1.04	3.25	3.65
N105670X	-0.33	3.12	0.24	1.29	0.88	0.68	0.06	1.94	1.05
N105670Y	0.88	3.52	3.13	2.23	0.68	0.30	-0.01	1.77	0.91
N105670Z	-17.97	-2.79	-4.23	-8.08	4.05	-0.50	-0.90	2.94	3.85

TABLE A.3 – Distributions of the selected node displacement values, in mm.

A.4 Adaptive Parameter Sets for RDO

In this section some specifics for the implementation of adaptive parameter sets, when considering "dummy" robustness values for designs outside the TI, are presented.

A.4.1 Dummy Robustness Values

Although no robustness analysis is performed for designs outside the TI, due to the RDO formulation, for the algorithm to continue the robustness information (μ and σ) of these designs are required. Hence for implementation purpose "dummy" robustness values are created for the designs outside the TI. These values are generated using the nominal value of the optimisation point and a constant sigma value. The generated values are uniformly distributed around the optimisation point. In a RDO the designs are ranked in-terms of both the mean (μ) and the sigma (σ) values. Here since the σ value is set to be the same for all the designs outside the TI, these designs are ranked depending only on the nominal values. This assists the algorithm to make decisions for design selections for future generations depending on real outputs rather than "dummy" outputs.
The size of the "dummy" sigma value plays a vital role for the robustness characterisation of the designs outside the TI. If the "dummy" sigma value is too big then in a situation where a design which is in the feasible space but outside the TI may have most of the robustness points ending up in the infeasible space making the design non-robust, see Figure A.1a. This is not correct since "dummy" robustness values are used. Also the "dummy" sigma value must be bigger than the true sigma values to avoid exchange of the designs at the offset boundary making the non-robust design robust. For example if at the boundary of the offset there are two designs; design A: outside TI and design B: inside TI whose objective values are similar. If design A has a smaller "dummy" σ value than design B (real robustness values), then design A may be taken as the robust optimum in comparison to design B. This is again not correct due to the use of "dummy" robustness values, see Figure A.1b. Hence a preliminary robustness study on some designs or experience can be used to assign "dummy" sigma value.
Also the distribution of "dummy" robustness outputs is important. They have to be well distributed around the optimisation point for correct characterisation of robustness, see Figure A.1c for bad distribution case of the "dummy" robustness values. Uniform distribution or normal distributions of "dummy" outputs around the design can be made.

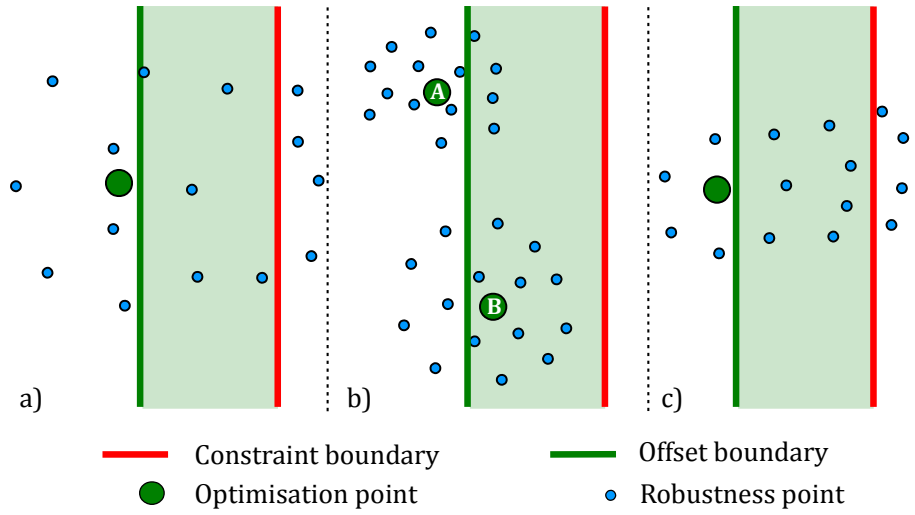

FIGURE A.1 – Different cases to consider for the "dummy" robustness values, σ.

Optimisation points, m: Design 1, Design 2 . . . . . , Design 10.

Robustness points, n: Design 11 . . . Design 25, ... , Design 146 . . . Design 160.

FIGURE A.2 – Evaluation steps and design numbering in optiSLang.

A.4.2 Implementation in optiSLang

The modified RDO is implemented in optiSLang by manipulating its double loop RDO algorithm using external script such as perl and batch file, see Appendix A.4.4. Before any scripts are written it is important to know how the double loop RDO in optiSLang works. It is specially important to know the order in which the designs are evaluated in order to create the "dummy" robustness values.
In optiSLang, the number of optimisation points m per generation and also the number of robustness points n per optimisation point are set. Then first the m optimisation points are evaluated followed by the evaluation of n robustness points per m optimisation points. The order of design numbering and valuation in optiSLang is illustrated in Figure A.2. Three scripts that are used to modify the double loop RDO are presented in the following Sections.

Command.bat

OptiSLang is provided with a command.bat file that controls the RDO workflow, see Appendix A.4.4. Same settings for m and n are made on the optiSLang RDO workflow and Command.bat [3]. The RDO run is then started in optiSLang setting the iteration number i to 1. Each new design point is categorised to either an optimisation point or a robustness point. This is done by checking the design number, d, using Equation (1) ; where n is the global design number and d is the design number

3. This is done to find the correct optimisation point to create "dummy" robustness values.

within one iteration.

$$d = n - (m + (m \times n))(i - 1), \tag{1}$$

$$1 \leq d \leq m + (m \times n).$$

If the design number, d, is less than m+1, it is an optimisation point else it is a robustness point. When the current design is an optimisation point then normal computation is made. If the current design is a robustness point then the corresponding optimisation point, s, of this robustness point is found by Equation (4). Command.bat then checks the folder, of this optimisation point, for an indicator file created by Output.pl, see Section A.4.4. If the folder does not contain the indicator file then normal robustness analysis is made through design evaluations else "dummy" robustness values are created using Dummy Output.pl script, see Section A.4.4. When the design number, d, is equal to $m+(m \times n)+1$, the iteration number is incremented by 1 and d is set to 1 (first optimisation point of the new iteration). The process is illustrated in Figure 8.2.

$$a = \frac{d - m}{n} + 1, \tag{2}$$

$$1 \leq a \leq m,$$

$$b = (d - m) - (a - 1)n, \tag{3}$$

$$m + 1 \leq b \leq m + (m \times n),$$

$$s = (m + (m \times n))(i - 1) + a. \tag{4}$$

Here a is the optimisation point and b is the robustness point within one iteration.

Output.pl

The first step in this RDO approach is to define the TI to categorise designs for real robustness analysis or "dummy" robustness analysis. To define the TI, an offset is created on each constraint boundary, see Figure 8.8 where the function is constrained at $f(x)$= -1 and an offset is made at $f(x)$= -0.5.
Each design is categorised into three groups ; infeasible solutions, feasible solutions within TI and feasible solutions outside the TI. This is done with the output.pl script that generates the output file required for optimisation, see Appendix A.4.4. The output.pl script generates all the outputs and checks if they are within the TI for each constraint. If the design is outside the TI, it generates an indicator file, in the current folder, to indicate that the design is not within the TI. The command.bat

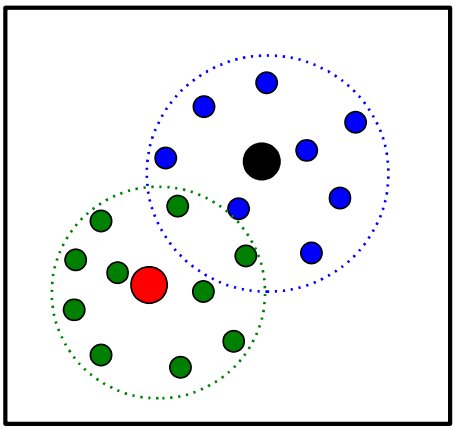

FIGURE A.3 – An illustration of sample recycling for robustness points.

script looks at each optimisation design folder for the existence of this indicator file, as mentioned in Section A.4.2.

Dummy Output.pl

If an optimisation point is outside the TI then "dummy" robustness values are generated using the Dummy Output.pl, see Appendix A.4.4. The output values of this optimisation point are used to generate the "dummy" robustness values which are uniformly distributed around this optimisation point. Dummy robustness points are generated using Equation (5).

$$d = O(a) + \frac{\sigma}{n}(b - (\frac{n}{2} + 1)). \tag{5}$$

Here $O(a)$ is the optimisation point output and σ is the standard deviation that represents the distribution of robustness points around the optimisation point, $O(a)$.

A.4.3 Special Algorithm Features

Special features such as sample recycling and duplicate designs are used in optimisation algorithms to reduce the number of evaluations required in RDO. These features should be switched off for better performance of the optimisation algorithm.

Sample Recycling

Sample recycling is used to reduce the number of design evaluations by using previously evaluated design responses close to the currently required design, Schneider and Bucher (2008), see Figure A.3 where the black optimisation point uses previously analysed 2 green robustness points. This cannot be used in this approach due to the generated "dummy" values for robustness. If these "dummy" values are chosen as the recycled samples then the evaluated robustness becomes incorrect.

Duplicate Designs

Avoiding the analysis of duplicate design reduces the design analysis by using the responses of the previously evaluated design that has the same parameter setting as the currently required design. This cannot be used because the generated "dummy" robustness values may be used by actual optimisation points or vice versa making the robustness evaluation incorrect.

A.4.4 Scripts

The scripts used for Function 1 (Figure 8.8) is provided here.

Command.bat

```
1
2  REM ****************************************************************
3  REM                                                                *
4  REM             Command.bat for modified double loop RDO           *
5  REM                                                                *
6  REM ****************************************************************
7  REM                                                                *
8  REM ******************** INITIALISATIONs *************************
9
10 REM size of initial population
11 set /a ini=0
12
13 REM size of population in each generation
14 set /a p=10
15
16 REM number of robustness points
17 set /a rob_no=15
18
19 REM total number of points in each generation
20 set /a t=160
21
22 REM Test whether optimisation point or robustness point
23 set /a k=11
24
25 REM Test for next generation
26 set /a g=161
27
28 REM ****************************************************************
29
30 REM set the current folder as the working folder.
31 set current=%CD%
32 REM reads the last four entery of the current folder.
33 set current=%current:~-4%
34 echo.%current% >design.txt
35
36 REM read the last digit on the current folder
37 set z=%current:~-1%
38 REM print the value of z to z.txt
39 echo %z% >z.txt
40 REM read the second last digit on the current folder
41 set y=%current:~2,1%
42 REM print the value of y to y.txt
```

```
43  echo %y% >y.txt
44  REM read the third last digit on the current folder
45  set x=%current:~1,1%
46  REM print the value of x to x.txt
47  echo %x% >x.txt
48  REM read the first value on current folder
49  set w=%current:~0,1%
50  echo %w% >w.txt
51
52  set /a n=w*1000+x*100+y*10+z
53  echo %n% >n.txt
54
55  if %n%==1 (echo 1 >"C:\Documents and Settings\exw309\Desktop\Toolbar\0\MAR WEEK 4\Mod_RDO\i.
56  copy "C:\Documents and Settings\exw309\Desktop\Toolbar\0\MAR WEEK 4\Mod_RDO\i.txt" .
57  set /p j=<i.txt
58  set /a i=%j%
59
60
61  set /a d=%n%-%t%*(%i%-1)
62  echo %d% >d.txt
63  if %d%==%g% (set /a i=%i%+1) & set /a d=1
64  echo %d% >d1.txt
65
66  echo %i% >"C:\Documents and Settings\exw309\Desktop\Toolbar\0\MAR WEEK 4\Mod_RDO\i.txt"
67  echo %i% >i.txt
68
69  if %d% LSS %k% (
70  goto normal_compute
71  ) else (
72  goto find_opt_rob_point
73  )
74
75  :normal_compute
76  REM echo >normalcompute.txt
77  REM **** COpy files and run simulation ****
78  copy "C:\Documents and Settings\exw309\Desktop\Toolbar\0\MAR WEEK 4\Mod_RDO\output.pl" .
79  call output.pl
80  goto END
81
82  :find_opt_rob_point
83  set /a a=((%d%-%p%)/%rob_no%)+1
84  echo %a% >a.txt
85
86  set /a b=(%d%-%p%)-(%a%-1)*%rob_no%)
87  echo %b% >b.txt
88
89  if %b%==0 (set /a b=%rob_no%) & set/a a=%a%-1
90  echo %a% >a.txt
91  echo %b% >b.txt
92
93  set /a f=%t%*(%i%-1)+%a%
94  echo %f% >f.txt
95
96  REM ******** Change numbers in brackets according to initialisations ********
97  REM                                                                          *
98  for /l %%k in (1,1,9) do if %f%==%%k echo 000%f%>t.txt
99  REM                                                                          *
100 for /l %%l in (10,1,99) do if %f%==%%l echo 00%f%>t.txt
101 REM                                                                          *
102 for /l %%m in (100,1,999) do if %f%==%%m echo 0%f%>t.txt
```

```
REM                                                                          *
for /l %%o in (1000,1,9999) do if %f%==%%o echo %f%>t.txt
REM                                                                          *
REM ***************************************************************************

set /p s=<t.txt
echo %s% >s.txt

if exist ..\Design_%s%\nocompute.txt goto dummy_values
goto normalcompute_1

:dummy_values
copy ..\Design_%s%\output.txt . /Y
ren output.txt opt_output.txt
copy /y "C:\Documents and Settings\exw309\Desktop\Toolbar\0\MAR WEEK 4\Mod_RDO\dummy.pl" .
if exist dummy.pl (call dummy.pl) else (echo nodummyoutput.pl found>nodummyoutput.txt)
goto END

:normal_compute_1
REM echo>normalcompute.txt
REM **** COpy files and run simulation ****
copy "C:\Documents and Settings\exw309\Desktop\Toolbar\0\MAR WEEK 4\Mod_RDO\output1.pl" .
call output1.pl

:END
@cls
```

Output.pl

```
#!/usr/bin/perl -w
open (OUT, ">output.txt");
open(FILE,"<design variable.txt");
while ($lines=<FILE>)
{
        if ($lines=~"^x")
        {
                $linea=$lines;
        }
        $x1=substr($linea,4,4);
        $a=2*($x1-0.75)*($x1-0.75);
        $b=(5*3.141593*$x1);
        $c=(0.4*3.141593);
        $d=0.125;
        $e=$b-$c;
        $f=sin($e);
        $y=$a+$f-$d;
}
        if ($y < -1)
        {
                open (OUTPUT, ">no robustness compute.txt")
        }
        if ($y > -0.5)
        {
                open (OUTPUT, ">no robustness compute.txt");
        }

        print OUT "y $y\n";
        print OUT "real optimisation values";
```

Dummy Output.pl

```
#!/usr/bin/perl -w
open (OUT, ">output.txt");

# ****************************************************************
# ******************** INITIALISATIONS ************************

# assign sigma value
$sigma=5;

# input number of robustness points
$rob_no=15;

# vlaue to spread the dummy outputs around the optimisation points.
$v=($rob_no/2)+1;

$int1=0;

# ****************************************************************

# current robust design number: value obtained from .bat run.
open (FILE1, "<b.txt");
while ($line=<FILE1>)
{
        $b=$line;
}
# print OUT "b\n";
# print OUT "$b";

open (FILE, "<opt_output.txt");
while ($lines=<FILE>)
{
        if ($lines=~"^y ")
        {
                $line1=$lines;
        }
}
        $line1=substr($line1,2,10);
        $y=$line1+($sigma/$rob_no)*($b-$v);

print OUT "y $y\n";
print OUT "dummy robustness values";
```